

Catalytic Approaches Towards Amidation of Unactivated Ester Derivatives

Nicola Caldwell

A thesis submitted to the Department of Pure and Applied Chemistry, University of Strathclyde, in part fulfilment of the regulations for the degree of PhD in Pure and Applied Chemistry.

I certify that this thesis has been written by me. Any help I have received in my research and the preparation of the report itself has been acknowledged. In addition, I certify that all information sources and literature used are indicated in the report.

Signed:

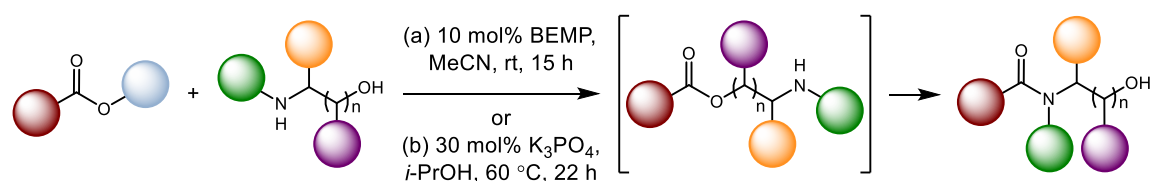
Date: June 2015

Abstract

Amide bond forming reactions are commonly encountered within a synthetic chemistry environment. Traditionally, a stoichiometric coupling reagent is employed to facilitate the condensation of a carboxylic acid and an amine. However, a number of disadvantages are inherent in this process, including by-product formation, poor atom economy, elevated cost, and variable yields.

An organocatalytic approach using *N*-heterocyclic carbenes (NHCs) would provide a more atom-economical route towards the synthesis of amides, addressing some of the issues outlined above. However, upon investigating anhydrous reaction conditions required for handling NHCs, a novel base-catalysed amidation manifold was identified. Catalytic amounts of base were found to mediate amidation of unactivated esters using amino alcohols in the absence of carbene catalyst.

Based on this initial observation, full optimisation of the base-catalysed amidation process was carried out using a combination of linear screening and Design of Experiments (DoE) techniques. Optimised conditions (Scheme 1a) were used to examine substrate scope, demonstrating that a wide range of products could be prepared using this methodology (53 examples, 40 – 100%), including oxazolidinone derivatives and medicinally-relevant compounds. Mechanistic investigations indicated formation of a transesterification intermediate, followed by intramolecular rearrangement to the more stable amide product.



Scheme 1: Novel methods for base-catalysed amidation of esters using amino alcohols

Subsequently, optimisation of a more sustainable base-catalysed amidation process (Scheme 1b) was carried out in order to address the green credentials of this reaction (16 examples, 42 – 100%). Additionally, by employing an alcohol additive to facilitate *in situ* formation of the activated ester species, the base-catalysed amidation methodology could be adapted to the direct synthesis of amide products (25 examples, 32 – 95%). Finally, several novel NHC systems were designed and evaluated for their ability to catalyse a direct amidation reaction.

Acknowledgements

I would firstly like to thank my PhD supervisor, Dr Craig Jamieson for giving me the opportunity to work on this project, and for his constant support and motivation throughout. It has been a privilege to be a founding member of the Jamieson group and I am extremely grateful to have been part of the journey!

I would like to acknowledge Dr Allan Watson for his helpful advice during the course of my PhD, and for his impact on the project as a whole. I am grateful to my industrial supervisor, Dr Iain Simpson, for his invaluable input to my research, and for his continued involvement and guidance throughout. I would also like to thank Peter Campbell and Frances Potjewyd for their contributions to this project; their efforts are greatly appreciated.

To my labmate and flatmate, Morag Watson, thank you for putting up with me and offering encouragement when I needed it! To all the members of the Jamieson and Watson groups who've made my PhD so enjoyable, thank you for your company and support, and for providing a constant source of entertainment! There was never a dull moment and it has been a pleasure working with you all.

Finally, to my family and friends, your love and support has made this all possible and I couldn't have done it without you. Thank you for always being there for me.

Abbreviations

ACS	American Chemical Society
ADHD	Attention Defecit/Hyperactivity Disorder
AMPA	α -Amino-3-hydroxy-5-methyl-4-isoxazole propionic acid
API	Active Pharmaceutical Ingredient
BEMP	2- <i>tert</i> -Butylimino-2-diethylamino-1,3-dimethylperhydro-1,3,2-diazaphosphorine
BMMP	1-(1-(1 <i>H</i> -Benzo[d][1,2,3]triazol-1-yloxy)ethylidene)pyrrolidinium hexachloroantimonate
Boc	<i>tert</i> -Butyloxycarbonyl
BOP	Benzotriazol-1-yloxytris(dimethylamino)phosphonium hexafluorophosphate
BTPP	<i>tert</i> -Butylimino-tri(pyrroldino)phosphorane
CDI	1,1'-Carbonyldiimidazole
CMC	Comprehensive Medicinal Chemistry
CNS	Central Nervous System
COMU	1-[(1-(Cyano-2-ethoxy-2-oxoethylideneaminoxy)-dimethylamino-morpholino methylene)] methanaminium hexafluorophosphate
CPME	Cyclopentyl Methyl Ether
DABCO	1,4-Diazobicyclo[2.2.2]octane
DBU	1,8-Diazobicyclo[5.4.0]undec-7-ene
DCC	<i>N,N'</i> -Dicyclohexylcarbodiimide
DCM	Dichloromethane
DIC	<i>N,N'</i> -Diisopropylcarbodiimide
DIPEA	<i>N,N</i> -Diisopropylethylamine
DMAP	4-Dimethylaminopyridine
DMC	Dimethyl carbonate
DMF	<i>N,N</i> -Dimethylformamide
DMSO	Dimethyl sulfoxide
DoE	Design of Experiments
d.r.	Diastereomeric ratio
ee	Enantiomeric excess
EPA	Environmental Protection Agency

E _T	Empirical polarity parameter
FTIR	Fourier Transform Infrared Spectroscopy
HATU	<i>O</i> -(7-Azabenzotriazol-1-yl)-1,1,3,3-tetramethyluronium hexafluorophosphate
HFIP	Hexafluoroisopropanol
HMPA	Hexamethylphosphoramide
HOAt	1-Hydroxy-7-azabenzotriazole
HOBt	1-Hydroxybenzotriazole
HOCT	Ethyl-1-hydroxy-1 <i>H</i> -1,2,3-triazole-4-carboxylate
H-PGDS	Human prostaglandin-D-synthase
HPLC	High Performance Liquid Chromatography
HYP	2-Hydroxypyridine
IMes	<i>N,N</i> -Bismesitylimidazolylidene
LCMS	Liquid Chromatography – Mass Spectrometry
2-MeTHF	2-Methyltetrahydrofuran
MOM-Cl	Chloromethyl methyl ether
m.p.	Melting point
MS	Molecular sieves
NCL	Native Chemical Ligation
N.D.	Not Determined
NHC	<i>N</i> -Heterocyclic Carbene
NHS	<i>N</i> -Hydroxysuccinimide
NMP	<i>N</i> -Methyl-2-pyrrolidone
NMR	Nuclear Magnetic Resonance
P ₁ - <i>t</i> -Bu	<i>tert</i> -Butylimino-tris(dimethylamino)phosphorane
PCA	Principal Component Analysis
PFP	Pentafluorophenol
pK _a	Acid dissociation constant
ppm	Parts per million
PyBOP	Benzotriazol-1-yloxytri(pyrrolidino) phosphonium hexafluorophosphate
PyBroP	Bromotri(pyrrolidino) phosphonium hexafluorophosphate
RME	Reaction Mass Efficiency
SCX-2	Strong cation exchange
SPPS	Solid Phase Peptide Synthesis

T1	First principal component vector
T2	Second principal component vector
T3P	Propylphosphonic acid solution
TBD	1,5,7-Triazabicyclo[4.4.0]dec-5-ene
TBME	<i>tert</i> -Butyl Methyl Ether
TFA	Trifluoroacetic acid
THF	Tetrahydrofuran
UV	Ultraviolet

Table of Contents

1	Introduction	1
1.1	Amide Bond Formation	1
1.2	Amidation Using Acyl Halides	2
1.3	Activating Agents	5
1.3.1	Carbodiimide-based Coupling Reagents	5
1.3.2	Uronium-based Coupling Reagents.....	8
1.3.3	Phosponium-based Coupling Reagents	11
1.4	Catalytic Approaches to Amidation.....	12
1.4.1	Boron-mediated Amidation	12
1.4.2	Metal-catalysed Amidation.....	17
1.4.2.1	Metal-catalysed Amidation of Carboxylic Acids.....	17
1.4.2.2	Metal-mediated Amidation of Esters	18
1.4.2.3	Metal-catalysed Amidation with Alcohols.....	21
1.4.3	Organocatalytic Amidation.....	24
1.4.3.1	<i>N</i> -Heterocyclic Carbene-catalysed Amidation Using Amino Alcohols.....	24
1.4.3.2	<i>N</i> -Heterocyclic Carbene-catalysed Amidation <i>via</i> Oxidative Processes.....	29
1.4.3.3	Nucleophilic Amidation Catalysts	33
1.5	Ligation Methods	35
1.5.1	Native Chemical Ligation.....	37
1.5.2	Staudinger Ligation	38
2	Project Aims.....	40
3	Results and Discussion.....	43
3.1	Synthesis of Analytical Construct.....	43
3.2	High Throughput Experimentation Using Known Carbene Systems.....	45
3.3	Preparation and Screening of a Model Carbene	49

3.3.1	Screening of Bases and Additives	50
3.3.2	Screening of Alternative Bases.....	52
3.4	Investigation of Reaction Conditions Using IMes.....	53
3.4.1	Investigation of Anhydrous Reaction Conditions	55
3.4.2	Further Investigation of Control Reactions	58
3.4.3	Exploring Alternative Ester Starting Materials	60
3.4.4	Mechanistic Hypothesis.....	61
3.5	Optimisation of Base-catalysed Amidation	63
3.5.1	Base and Solvent Screening	64
3.5.2	Optimisation of Reaction Conditions Using Design of Experiments.....	69
3.5.3	Examination of Substrate Scope for BEMP-catalysed Amidation.....	79
3.5.3.1	Investigation of Alternative Phosphazene Bases	84
3.5.3.2	Synthesis of Oxazolidinone Derivatives	85
3.5.3.3	Synthesis of Medically-relevant Compounds	88
3.5.4	Investigation of Mechanism for BEMP-mediated Amidation.....	91
3.5.4.1	Rearrangement of Ester.....	92
3.5.4.2	Competition Reactions	94
3.5.4.3	Further Investigation of Rearrangement	95
3.5.4.4	Altering Chain Length.....	97
3.5.5	Limitations of BEMP-catalysed Amidation	101
3.6	Development of a Sustainable Base-catalysed Amidation Process	103
3.6.1	Base and Solvent Screening	104
3.6.2	Optimisation of Reaction Conditions Using Design of Experiments.....	107
3.6.3	Examination of Substrate Scope for K ₃ PO ₄ -catalysed Amidation	112
3.7	Development of a Direct Amidation Method	115
3.7.1	Additive Screening	116
3.7.2	Base and Solvent Screening	118

3.7.3	Optimisation of Reaction Conditions Using Design of Experiments.....	119
3.7.4	Examination of Substrate Scope for Trifluoroethanol-catalysed Amidation	128
3.7.5	Mechanistic Investigations	133
3.8	Design and Synthesis of Bespoke Carbene Systems	136
3.8.1	Catalysts Designed to Facilitate a Dual Catalysis Mode.....	138
3.8.2	Pyrrolidine-derived Catalysts	152
4	Conclusions	157
5	Future Work	160
6	Experimental	162
6.1	General Techniques	162
6.1.1	Purification of Solvents	162
6.1.2	Purification of Reagents and Catalysts	162
6.1.3	Experimental Details	162
6.1.4	Purification of Products	163
6.1.5	Analysis of Products	163
6.1.6	Reversed Phase HPLC Methods.....	164
6.1.7	Normal Phase HPLC Method	166
6.2	General Experimental Procedures.....	166
6.2.1	Screening Reactions with Known Carbene Systems.....	166
6.2.2	Screening Reactions with Model Carbene System.....	167
6.2.3	Investigation of Reaction Conditions Using IMes	167
6.2.4	Optimisation of Base-catalysed Amidation.....	169
6.2.5	Optimisation of Sustainable Base-catalysed Amidation	170
6.2.6	Optimisation of a Direct Catalytic Amidation Method	171
6.2.7	Screening Reactions with Novel Carbene Systems.....	172
6.3	Results from Screening Reactions	174

6.3.1	Screening Reactions with Known Carbene Systems.....	174
6.3.2	Screening Reactions with Model Carbene System.....	175
6.3.3	Investigation of Reaction Conditions Using IMes	176
6.3.4	Optimisation of Base-catalysed Amidation.....	177
6.3.5	Optimisation of Sustainable Base-catalysed Amidation	180
6.3.6	Optimisation of a Direct Catalytic Amidation Method	182
6.3.7	Screening Reactions with Novel Carbene Systems.....	187
6.4	Characterisation Data for Isolated Products	191
7	References	262

1 Introduction

1.1 Amide Bond Formation

Amide bonds are ubiquitous in both naturally occurring and synthetic molecules. This important functionality constitutes the fundamental linking unit of amino acid monomers in proteins, which are essential for sustaining biological processes.

Amide bonds are also frequently observed in synthetic molecules; around a quarter of drug-like compounds contained in the Comprehensive Medicinal Chemistry (CMC) database in 1999 incorporated an amide motif as part of their structure.¹ Albeit slightly outdated, this study emphasises the clear prevalence of this functionality in a synthetic chemistry environment. Amide bonds are also featured in many top-selling pharmaceuticals such as those displayed in Figure 1.²

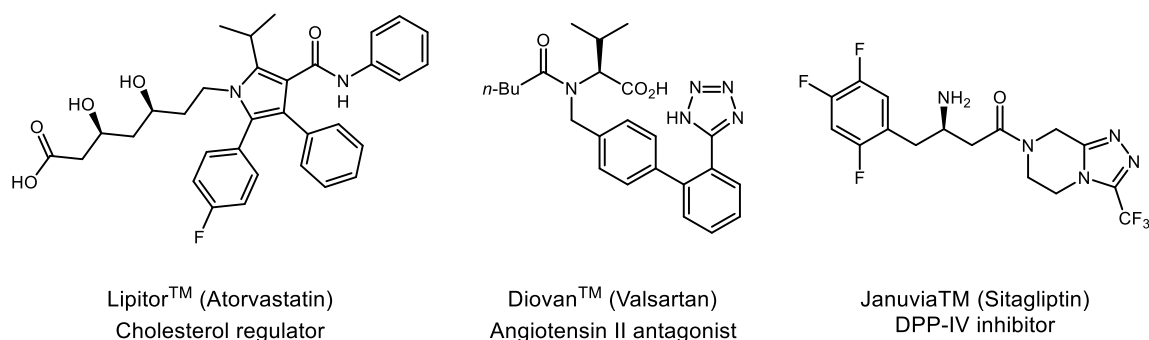


Figure 1: Examples of marketed drugs containing an amide motif

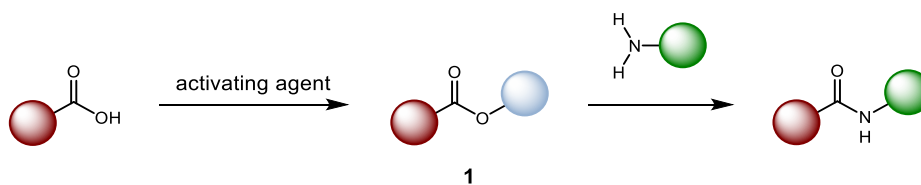
As a corollary of this, amide bond formation is the most commonly encountered reaction performed within a medicinal chemistry setting, as intimated in a recent study by Roughley and Jordan,³ which analysed reaction types employed during the synthesis of drug candidates, based on high impact publications from leading pharmaceutical companies (GlaxoSmithKline, Pfizer, and AstraZeneca). From this analysis, amide bond formation was the single most frequently performed reaction, comprising 16% of the total number of reactions reviewed.³

The popularity of this substrate class in small molecule drug discovery is presumably due to a number of favourable properties associated with amide bonds. Hydrogen bond donating and accepting capabilities associated with these motifs can enhance binding of small

Introduction - Amidation Using Acyl Halides

molecules to target receptors by enabling the formation of favourable interactions.² In addition, the chemical and metabolic stability of these systems is beneficial for drug candidates in order to improve bioavailability. The ready availability of starting materials, ease of handling and purification, and amenability to array chemistry⁴ facilitate straightforward access to amide containing compounds. This can be advantageous in a medicinal chemistry environment to evaluate structure-activity relationships (SAR) throughout a series of drug-like compounds.

As a consequence of all of the above, a range of amidation methods have been developed to expedite condensation of carboxylic acids and amines. The most widespread approaches involve conversion of the carboxylic acid to a more activated system (**1**) which will react readily with the amine coupling partner as illustrated in Scheme 2. Approaches to form the activated species are reviewed in subsequent sections.

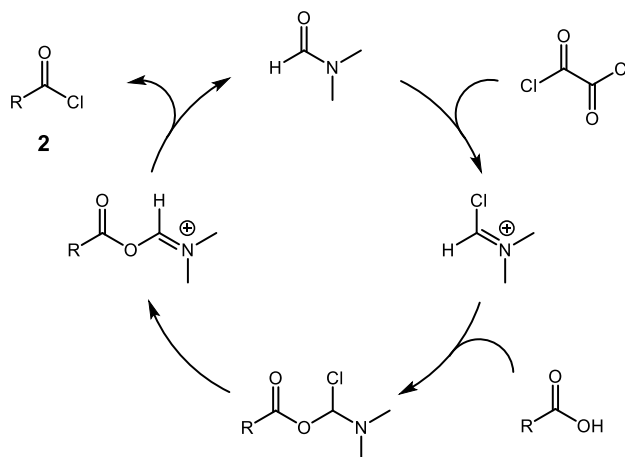


Scheme 2: Condensation of an acid and amine facilitated by an activating agent

1.2 Amidation Using Acyl Halides

Formation of the corresponding acyl halide is a relatively straightforward approach to activating the carboxylic acid starting material. Conversion to the acid chloride (**2**), for example, can be achieved using numerous chlorinating agents such as oxalyl chloride (COCl_2), thionyl chloride (SOCl_2), phosphorus oxychloride (POCl_3), and phosphorus pentachloride (PCl_5).⁵ Catalytic amounts of dimethylformamide (DMF) can also be employed to promote acid chloride formation,⁶ as shown in Scheme 3.

Introduction - Amidation Using Acyl Halides

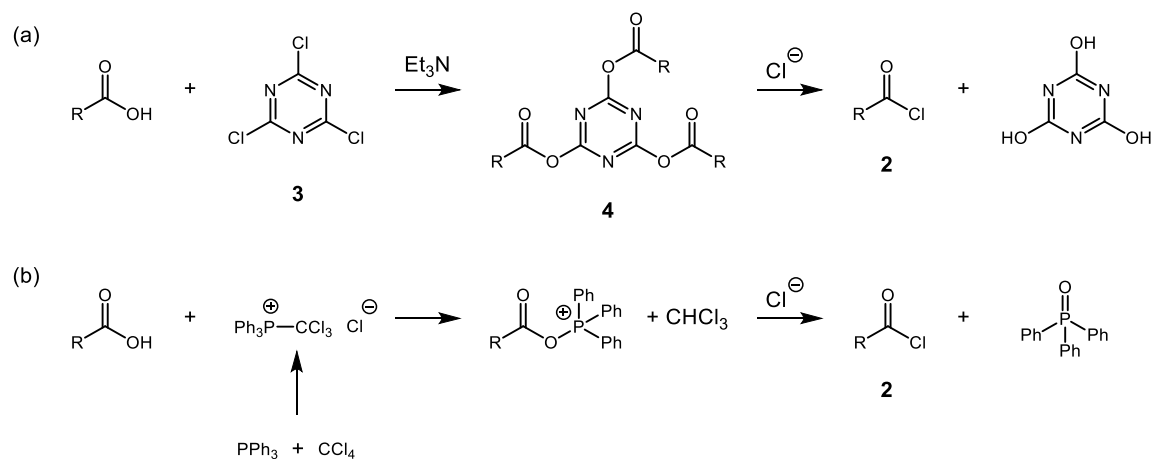


Scheme 3: Acid chloride formation using oxalyl chloride and catalytic DMF

Whilst this approach exploits the use of relatively inexpensive, commercially available starting materials, several inherent drawbacks are associated with the formation of acid chlorides. Indeed, a major disadvantage of employing chlorinating agents is the concomitant formation of HCl, which can be problematic when using acid-sensitive substrates such as Boc-protected amines. Several approaches have been developed which address the issues associated with HCl production (Scheme 4). For example, the use of cyanuric chloride (**3**) in the presence of base effects acid chloride formation whilst maintaining neutral pH (Scheme 4a).⁷ This reaction, proposed to proceed *via* a triacylated intermediate (**4**), requires only 0.33 equivalents of the chlorinating agent, minimising reagent use and by-product formation. The cyanuric acid by-product precipitates from the reaction mixture and can be removed by filtration, which is an added benefit when performing amidation on scale.

A complementary method employs triphenylphosphine and carbon tetrachloride to form the acid chloride, avoiding formation of HCl (Scheme 4b).⁸ A contemporary extension of this methodology utilises a combination of diethoxymethylsilane and bis(4-nitrophenyl)phosphate to perform *in situ* reduction of the triphenylphosphine oxide by-product to regenerate triphenylphosphine, allowing it to be used in catalytic amounts.⁹ However, although the issue of acid production is addressed through reagent selection in these cases, there are still safety concerns associated with the handling of chlorinating agents and related solvents, limiting the utility of these methods in synthesis.¹⁰

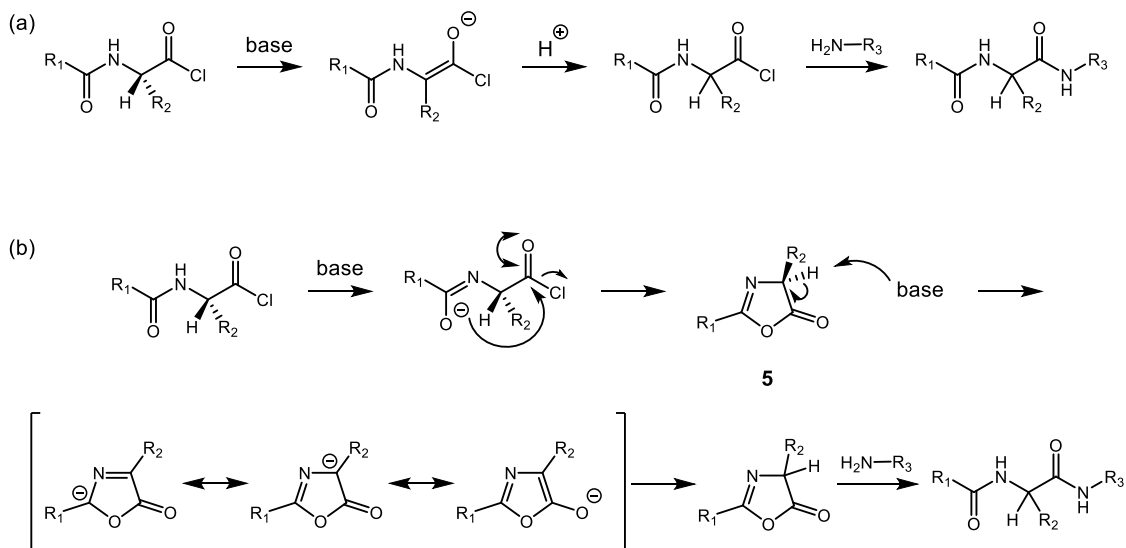
Introduction - Amidation Using Acyl Halides



Scheme 4: Chlorination methods avoiding HCl production using (a) cyanuric chloride, and (b) triphenylphosphine and carbon tetrachloride

In addition to the issues accompanying the use of chlorinating agents, and the concomitant generation of HCl, there are also drawbacks relating to the subsequent use of acid chlorides in synthesis. Amide bond formation *via* this process is normally performed in two steps, with the acid chloride being isolated prior to reaction with an amine. An organic base such as triethylamine or *N,N*-diisopropylethylamine (DIPEA) is commonly employed to neutralise any HCl formed, and prevent amine salt formation. However, the presence of base in the reaction mixture can cause issues with racemisation of chiral substrates, such as amino acids, due to the high reactivity of the acid chloride coupling partner. Racemisation can occur according to two principal mechanisms, as outlined in Scheme 5.¹¹ Enolisation (Scheme 5a) can occur by deprotonation at the α -position of the amino acid, leading to epimerisation. Alternatively, a base-mediated intramolecular cyclisation can occur (Scheme 5b), forming an oxazolone by-product (**5**). This intermediate, whilst still active towards amide formation, reacts only slowly with the amine coupling partner, so can be epimerised by exposure to base. Racemisation of starting materials by either of these processes leads to formation of products with reduced enantiopurity.⁵

Introduction - Activating Agents



Scheme 5: Mechanisms of racemisation by (a) enolisation, and (b) oxazolone formation

From consideration of the above, whilst acid chloride formation represents a facile approach to amide synthesis, a number of drawbacks are associated with this process. Accordingly, this has necessitated the development of more elegant methods to achieve this transformation, and a multitude of reagents have been designed which are more suitable for the formation of amide bonds.¹¹

1.3 Activating Agents

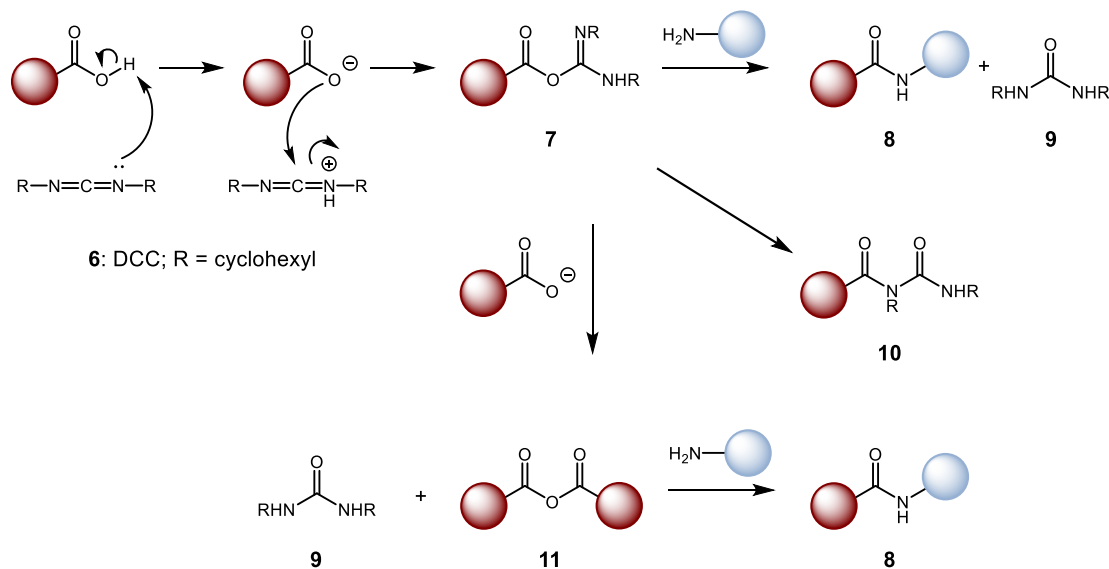
As stated above, due to the drawbacks associated with amidation *via* acid chloride formation, and the need for isolation of these species prior to reaction with the amine component, coupling reagents which facilitate *in situ* formation of an activated ester have become increasingly prevalent. A plethora of coupling reagents are now commercially available and widely used in both small molecule synthesis and peptide coupling.¹¹

1.3.1 Carbodiimide-based Coupling Reagents

The first coupling agents to be synthesised were carbodiimides, such as dicyclohexylcarbodiimide (DCC, **6**),¹² which promote amidation through the formation of an activated *O*-acylisourea intermediate (**7**).¹¹ Amide formation can proceed through interception of the *O*-acylisourea by the amine coupling partner (Scheme 6). Alternatively, reaction of the *O*-acylisourea with excess carboxylic acid starting material can result in the formation of a symmetrical anhydride species (**11**) which is also susceptible towards attack by the amine. Amidation *via* both of these pathways occurs with concomitant formation of

Introduction - Activating Agents

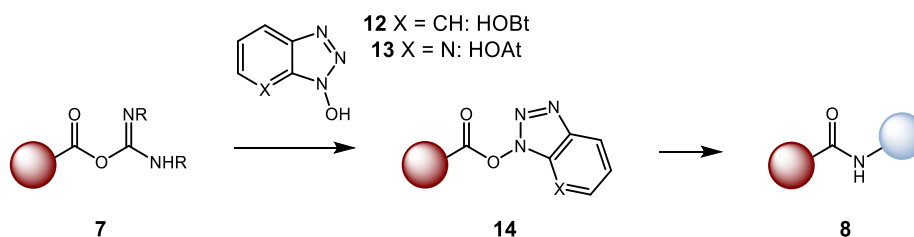
the corresponding urea by-product (**9**). Due to the high reactivity of the *O*-acylisourea (**7**), an additional unwanted side reaction can also occur, forming an *N*-acylurea by-product (**10**) via a rearrangement process.¹¹



Scheme 6: Mechanism of amide bond formation using carbodiimide coupling reagent

The superior reactivity of the *O*-acylisourea intermediate in this reaction manifold can also be problematic for chiral substrates, specifically amino acids, which have the potential to racemise via oxazolone formation as illustrated in Scheme 5.

A common solution to the issue of racemisation in this instance is the simultaneous use of an additive (Scheme 7). Hydroxybenzotriazoles react quickly with the *O*-acylisourea intermediate to form a second activated ester (**14**),¹³ which is not as susceptible to unwanted side reactions, helping improve the selectivity of this process. 1-Hydroxybenzotriazole (HOBt, **12**) has been shown to improve yield and lower racemisation during peptide coupling, compared to the use of a carbodiimide alone.¹⁴

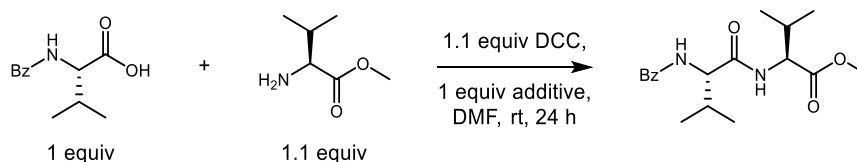


Scheme 7: Use of hydroxybenzotriazole additive

Introduction - Activating Agents

The related additive, 1-hydroxy-7-azabenzotriazole (HOAt, **13**), introduced by Carpino, has been shown to demonstrate superior efficiency compared to HOBt, reducing epimerisation levels further (Table 1).¹³

Table 1: Extent of racemisation using different hydroxybenzotriazole additives



Coupling Agent	Amount of DL-isomer (%)
DCC	61.5
DCC + HOBt	41.9
DCC + HOAt	14.4

Positional isomers of HOAt have been reported, however the 7-aza derivative (**13**) proved to be the most active. This is postulated to be attributable to a unique neighbouring group effect between the activated ester and the incoming amine, as shown in Figure 2. A hydrogen bonding interaction between the heterocyclic nitrogen and an amine proton is hypothesised to direct nucleophilic attack of the amine onto the activated ester (**15**), resulting in improved reactivity of this system compared to HOBt.¹³

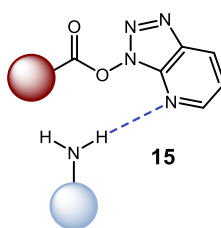
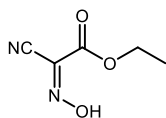


Figure 2: Neighbouring group interaction between HOAt-derived activated ester and an amine

Hydroxybenzotriazoles, and related derivatives, however, have been reported to exhibit explosive properties, which may limit their practicality in synthesis.¹⁵ More recently, oximes have been explored as innocuous alternatives. In a comprehensive study carried out by El-Faham, Albericio, and co-workers, ethyl 2-cyano-2-(hydroxyimino)acetate (Oxyrna, **16**, Figure 3) was found to display comparable reactivity to HOAt when used in combination

with diisopropylcarbodiimide (DIC) for peptide coupling reactions.¹⁶ Moreover, trial reactions proceeded with low levels of racemisation. Subsequent calorimetric tests were performed, with Oxyma demonstrating greater thermal stability compared to both HOAt and HOBt, indicating reduced explosive potential.¹⁶



16

Figure 3: Oxyma

In general, carbodiimide-based coupling reagents, when used in combination with an exogenous additive have been demonstrated to be widely applicable in amide bond formation. Recent advances to these systems, including the introduction of superior additives such as Oxyma, have led to good levels of reactivity and retention of stereochemical configuration at α -stereogenic centres.

Following on from the development of using reagent combinations to facilitate activation, newer generations of coupling reagents have been designed to combine the role of both coupling agent and additive in a single molecule, thus improving ease of handling and practicality.

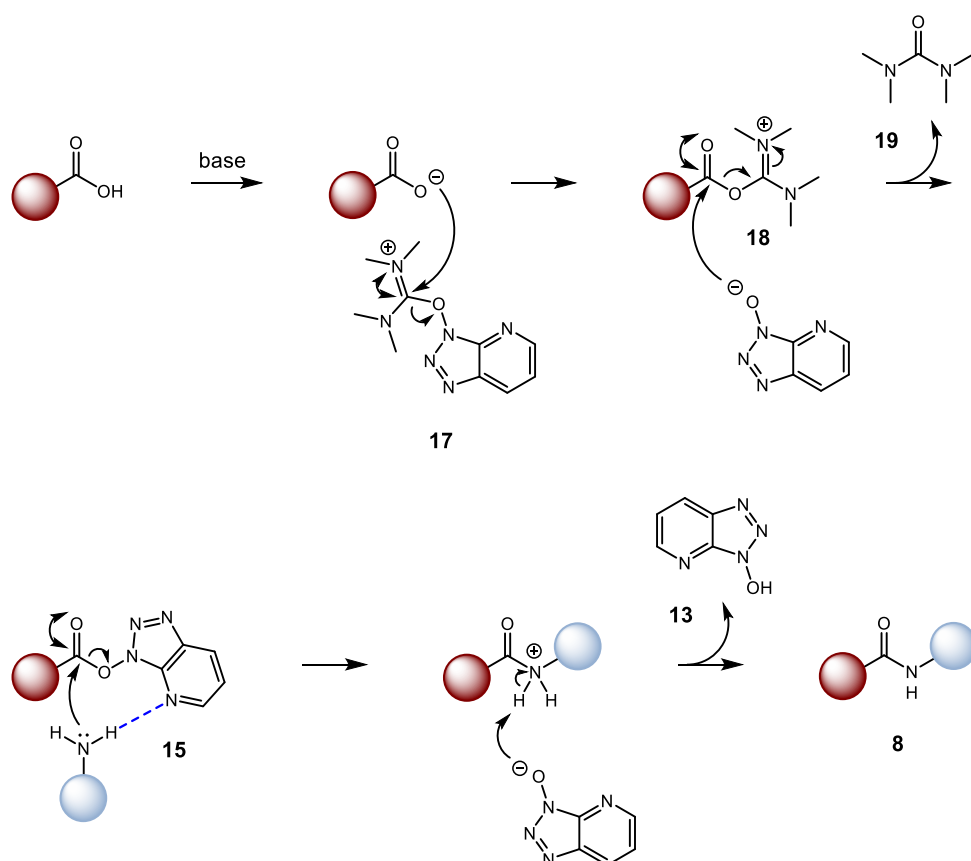
1.3.2 Uronium-based Coupling Reagents

Combined coupling reagents are currently the preferred method for achieving amide bond formation owing to their ease of handling, stability, and wide commercial availability. Accordingly, a palette of these systems now exist, many of which are structurally based on hydroxybenzotriazole or oxime-derived additives as discussed in Section 1.3.1.

As a consequence of their demonstrated efficiency in carbodiimide-mediated amidations, coupling reagents based on the structure of hydroxybenzotriazoles are amongst the most prevalent. Aminium/uronium salts such as *O*-(7-azabenzotriazol-1-yl)-1,1,3,3-tetramethyluronium hexafluorophosphate (HATU, **17**)¹³ are widely used, with hexafluorophosphate counter ions generally being preferred due to their increased solubility in organic solvents. Analogously to carbodiimide-mediated methods, the initial activation

Introduction - Activating Agents

mechanism associated with aminium coupling reagents involves reaction with the required carboxylate species to form an *O*-acylisourea intermediate (**18**, Scheme 8). This process liberates an HOAt anion, which can intercept the intermediate, forming a second activated ester species (**15**). A hydrogen bonding interaction between the heterocyclic nitrogen and the incoming amine then aids nucleophilic attack to form the desired amide product (**8**). Order of addition is crucial in this process as a potential side reaction can occur, forming a guanidinium by-product by direct reaction of the amine with the HATU coupling reagent.¹⁷

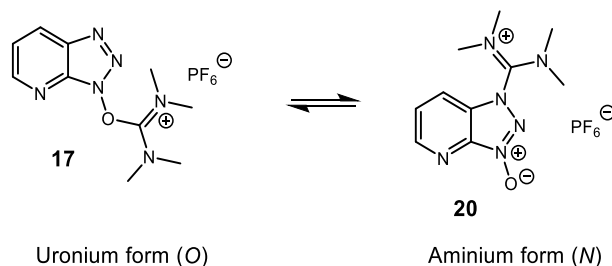


Scheme 8: Mechanism of HATU-mediated amide bond formation

Stoichiometric amounts of coupling reagent are necessary to effect this transformation, generating a stoichiometric amount of the corresponding tetramethylurea (**19**) and HOAt (**13**) by-products, which is a major disadvantage inherent in this process. Related considerations include poor atom economy and relatively high cost of the requisite reagents.¹⁸

The structural assignment of this type of coupling reagent (Scheme 9) has encountered a degree of debate in the literature as HATU was initially proposed to exist solely as the

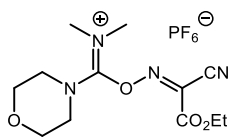
uronium (*O*) salt form (**17**) by analogy with previous systems.¹⁹ Subsequent X-ray crystallography studies by Carpino *et al.* have shown, however, that both the uronium and aminium (*N*) salt forms (**20**) of HATU can exist in the solid state and in solution. The structural form of this reagent is largely dependent on the method of preparation, with factors such as reaction conditions, base, and solvent influencing the resulting isomeric form.¹⁹



Scheme 9: Resonance forms of HATU

Evaluation of individual reactivities showed the uronium form to be considerably more efficient in the amidation process.¹⁹ Additionally, common organic bases used in amide coupling, such as triethylamine and DIPEA, were found to cause rapid isomerisation to the less reactive aminium form. Newer classes of reagents have been designed, which can only exist as the uronium form, thus alleviating problems associated with using the less reactive aminium species.¹¹

A pertinent example of improved reactivity as a result of constraining the structure to the uronium form is presented in the case of 1-[(1-(cyano-2-ethoxy-2-oxoethylideneaminoxy)-dimethylamino-morpholino methylene)] methanaminium hexafluorophosphate (COMU, **21**, Figure 4).²⁰ This coupling reagent, which incorporates Oxyma, demonstrated superiority over progenitor systems constructed from the hydroxybenzotriazole scaffold.²¹ This phenomenon is attributed by the authors to the fact that the reagent exists solely in the more active uronium form. Moreover, and as intimated previously, COMU benefits from reduced explosive potential due to the incorporation of the Oxyma-derived functionality as opposed to a hydroxybenzotriazole. Additional synthetic advantages of COMU-mediated amidation include a characteristic colour change upon reaction completion and increased solubility conferred by the morpholino moiety.²⁰



21

Figure 4: COMU

1.3.3 Phosphonium-based Coupling Reagents

A plethora of coupling reagents from other structural classes currently exist, the majority of which operate *via* a similar mechanistic pathway to that of HATU (Scheme 8). An example of an alternative class are phosphonium-based reagents (Figure 5).^{5,11,17} The earliest reagent of this type to be commercialised was benzotriazol-1-yloxytris(dimethylamino)phosphonium hexafluorophosphate (BOP, **22**),²² which suffered from limited use due to the release of the carcinogenic by-product hexamethylphosphoramide (HMPA). Future generations of phosphonium reagents such as benzotriazol-1-yloxytri(pyrrolidino) phosphonium hexafluorophosphate (PyBOP, **23**)²³ contain pyrrolidine groups to mediate this problem. As for uronium/amidinium reagents, the corresponding azabenzotriazole derivatives tend to be more reactive, and many HOAt-based phosphonium reagents exist. Halophosphonium analogues such as bromotri(pyrrolidino) phosphonium hexafluorophosphate (PyBroP, **24**),²⁴ which contain a halide leaving group, have also been found to be applicable to the formation of amide bonds.

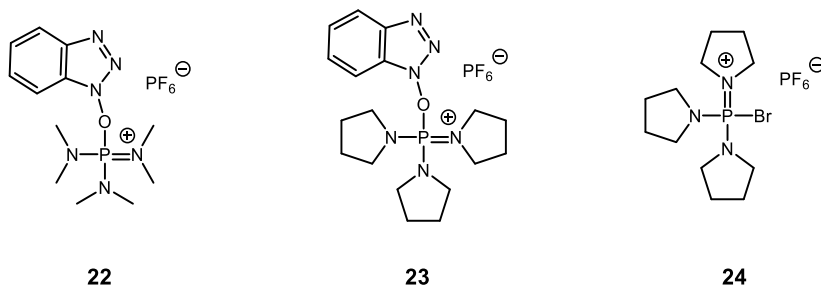


Figure 5: Common phosphonium-based coupling reagents

Based on the above, an extensive range of combined coupling reagents have been developed, which facilitate *in situ* formation of an activated carboxylate species. Selection of an appropriate system can be confusing as no single reagent is optimal for all substrates, and yields can be variable. For example, certain coupling reagents have been designed specifically for use in solid phase peptide synthesis or to suppress racemisation, limiting their

applicability to a targeted range of substrates. Overall, analysis of small molecule amide bond formations carried out on a range of medically-relevant substrates showed that there was no clear preference for a certain class of reagent.³ However, a comprehensive variety of coupling reagents are now readily available from commercial suppliers and can be easily handled under mild conditions, meaning that they are widely utilised in synthesis.

The major disadvantage of this approach towards amidation is the need for stoichiometric coupling reagent, resulting in the generation of equimolar by-products. Consequently, these reactions suffer from poor atom economy. An associated drawback is the fact that a number of commercially available coupling reagents can be relatively expensive, limiting their use on scale.

In general, whilst widely adopted as the preferred method for amide bond formation, this process is plagued with a number of disadvantages particularly in relation to reaction efficiency. Accordingly, recent attention has been directed towards the development of novel, catalytic approaches which address these major issues.

1.4 Catalytic Approaches to Amidation

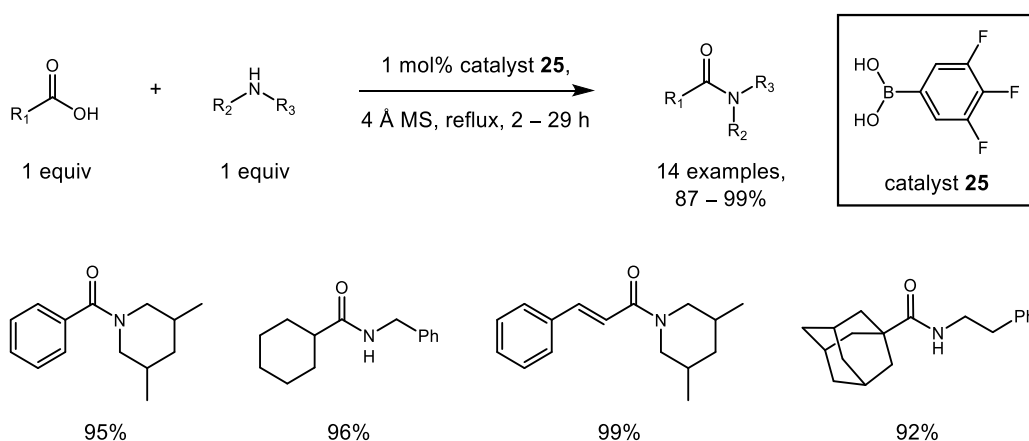
As discussed in Section 1.1, amide bond formation is the most commonly performed reaction in the pharmaceutical industry.³ However, preferred methods for the preparation of amides suffer from inherent drawbacks, most significantly the resulting formation of equimolar by-products. As a result, the American Chemical Society Green Chemistry Institute Roundtable, in collaboration with major pharmaceutical companies, highlighted ‘amide formation avoiding poor atom economy reagents’ as a crucial research area.²⁵ Development of catalytic methods would provide a more sustainable and efficient approach to amide bond formation processes and, hence, alleviate the issues associated with by-product generation and poor atom economy. Consequently, a number of catalytic approaches towards amidation have recently emerged in the literature.^{26,27}

1.4.1 Boron-mediated Amidation

Boron-based reagents have recently received increasing attention as an attractive alternative to the use of traditional amide coupling reagents.^{26,27} Yamamoto *et al.* were first to describe a catalytic protocol for boronic acid-facilitated amide bond formation (Scheme 10).²⁸

Introduction - Catalytic Approaches to Amidation

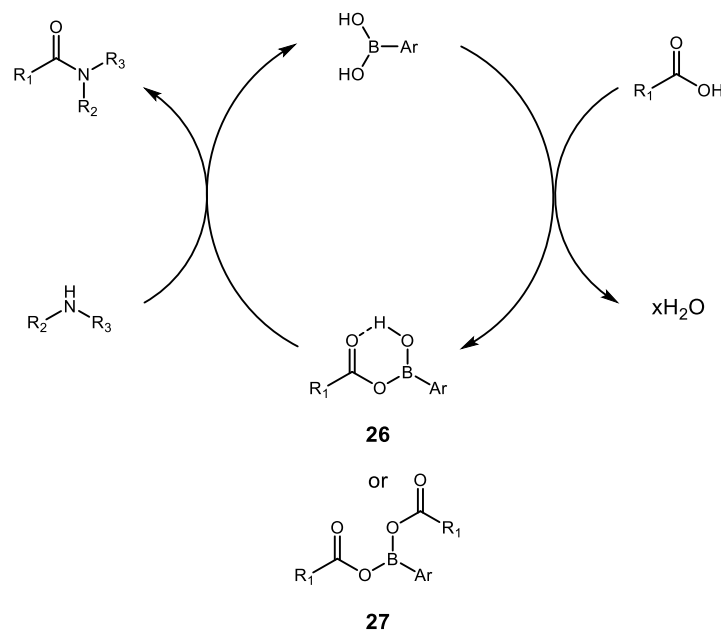
Electron-withdrawing substituents were used to tune the Lewis acidity of arylboronic acid catalysts, with 3,4,5-trifluorobenzeneboronic acid (**25**) proving to be the optimal system under the conditions investigated. A limited range of compounds were examined using this method, achieving excellent yields and low epimerisation levels for chiral examples. Sterically hindered acids such as 1-adamantanecarboxylic acid could be successfully coupled, and lactamisation was also reported using these conditions. However, high temperatures and prolonged reaction times were generally required which could potentially limit the utility of the methodology.²⁸



Scheme 10: Boronic acid-catalysed amide bond formation showing selected substrates²⁸

An important feature of this reaction is the inclusion of 4 Å molecular sieves to remove water generated during the condensation process. In the absence of molecular sieves, dramatic reductions in yield were observed due to hydrolysis of the proposed acyloxyboronic acid intermediate.²⁸ Although precise mechanistic details are the subject of some debate,^{29,30} it is believed that boronic acid-catalysed amidation proceeds *via* an acyloxoboronic acid species which acts as the active acylating agent (Scheme 11). Both mono-(**26**)²⁸ and diacyloxoboronic (**27**)³¹ acid intermediates have been proposed.

Introduction - Catalytic Approaches to Amidation



Scheme 11: Proposed mechanism for boronic-acid catalysed amide bond formation²⁹

Determination of the speciation of the boron catalyst has also been studied. Dehydration of boronic acids to the corresponding boroxine species is known to occur under anhydrous conditions.³² However, NMR studies showed that the free boronic acid was present exclusively, suggesting this is the active catalytic species in this reaction manifold.³³

Following on from this initial work, Yamamoto *et al.* evaluated a number of alternative boronic acids for their ability to catalyse the amidation reaction (Figure 6).³⁴ Pyridinium-based systems (**28**), for example, were found to display good reactivity. Interestingly, when this type of catalyst was used in a biphasic solvent system (ionic liquid/toluene), the amide product could be successfully extracted from the reaction mixture, while the catalyst remained in the ionic liquid layer. The catalyst/ionic liquid mixture could then be reused without noticeable loss of catalytic activity.³⁴ From a similar perspective, both Yamamoto³⁴ and Wang³⁵ have reported the design of resin-bound boronic acid catalysts, which allow for their filtration from the reaction mixture, and subsequent reuse. Although these methods represent an improvement over the original protocol, many of the catalyst systems employed require considerably forcing conditions to operate. Refluxing in high boiling point solvents is common in order to achieve good levels of conversion.

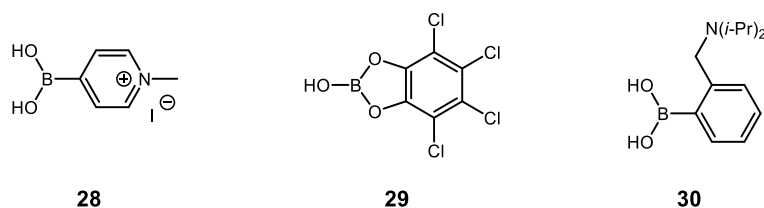
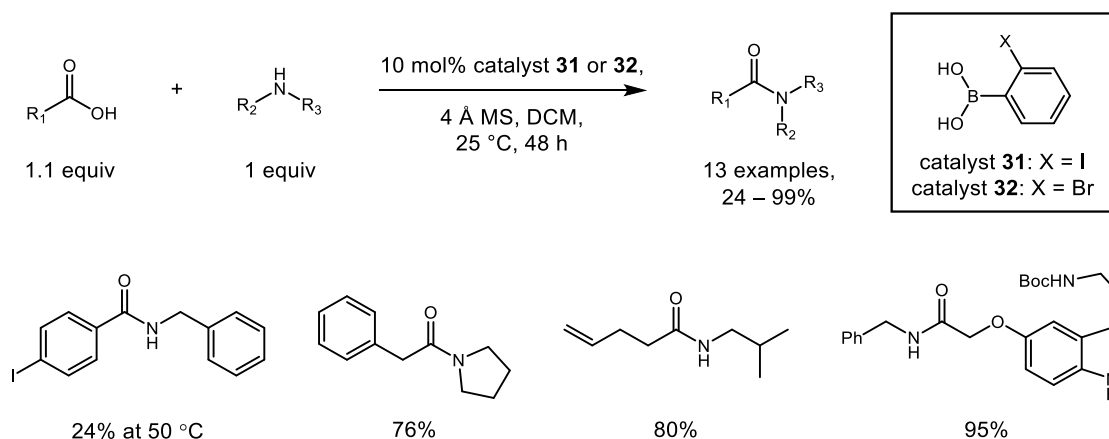


Figure 6: Alternative boronic acid catalysts^{34,36}

Novel catalyst systems such as chlorocatechol borane-derivatives (**29**)³⁴ and *ortho*-*N,N*-diisopropylbenzylaminoboronic acids (**30**)³⁶ have also been demonstrated to display enhanced reactivity in the amidation reaction, again at elevated temperatures.

More recently, Hall and co-workers reported a superior *ortho*-functionalised arylboronic acid catalyst capable of performing amidation at room temperature.³¹ A comprehensive evaluation of halo-substituted aryl boronic acids demonstrated *ortho*-iodophenyl boronic acid (**31**) to possess enhanced reactivity compared to previous systems. The utility of this catalyst, and the commercially available bromo-analogue (**32**), was subsequently assessed (Scheme 12), with most reactions proceeding at room temperature. Having stated this, some challenging substrates, such as aromatic carboxylic acids, required elevated temperatures (50 °C).³¹ Again, the addition of molecular sieves was critical to scavenge water from the reaction mixture. Alternative drying agents offered no further improvement to isolated yields.³³



Scheme 12: Room temperature boronic acid-catalysed amide bond formation showing selected substrates³¹

Subsequent optimisation studies described by Hall enabled the development of a second generation catalyst system (Figure 7), which incorporated an electron-donating group *para* to the iodine substituent (**33**).³³ It was found that increasing electron density on the iodine

Introduction - Catalytic Approaches to Amidation

adjacent to the boronic acid increased the reactivity of this particular catalyst, possibly due to the formation of a halogen-hydrogen bond with the boron-bound hydroxyl group in the proposed transition state (**34**).³⁰ Compared to the progenitor system (**31**), the electron-rich analogue (**33**) was applicable to the synthesis of a wider range of substrates, demonstrating reduced reaction times and improved yields (20 examples, 30 – 99%). Aliphatic and aromatic carboxylic acid and amine coupling partners could be successfully exploited. However, some heterocyclic carboxylic acids needed elevated temperatures (50 °C) and prolonged reactions (up to 48 hours).

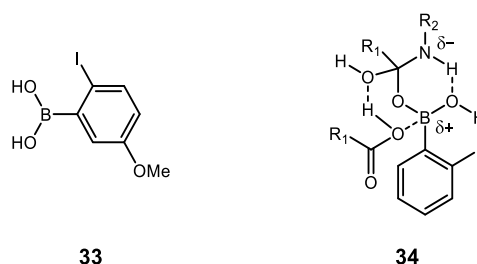


Figure 7: Hall's second generation boronic acid catalyst and proposed transition state formed during amidation reaction³³

Boronic acid-catalysed amidation offers a number of advantages over more conventional methods. Most importantly, as this approach does not involve generation of stoichiometric by-products, the atom economy of the amidation reaction is greatly improved. However, elevated temperatures and prolonged reaction times are needed in a number of cases. Furthermore, removal of water from the reaction mixture is essential to achieve suitable yields of products. More recently, Sheppard and Starkov have demonstrated the ability of simple borate esters such as B(OCH₂CF₃)₃ to promote amidation under milder conditions than those reported previously.³⁷ Reactions could be performed in acetonitrile at 80 °C without the need for strictly anhydrous reaction conditions or addition of an external dehydrating agent. Although super-stoichiometric amounts (two equivalents) of the borate ester were employed, it was found that products could be straightforwardly recovered after aqueous work up without the need for further purification. Subsequently, an elegant solid phase work up procedure was developed,³⁸ using commercially available resins to remove residual acid, amine, and borate ester reagent from the crude reaction mixture to furnish desired products in high purity. An extensive evaluation of the scope of this reaction was carried out, demonstrating that a diverse range of carboxylic acids and amines could be successfully coupled with 65 examples studied in total.³⁸ Trimethylborate was also found to

be effective in several cases, providing a more atom economical, commercially available alternative.^{37,38}

1.4.2 Metal-catalysed Amidation

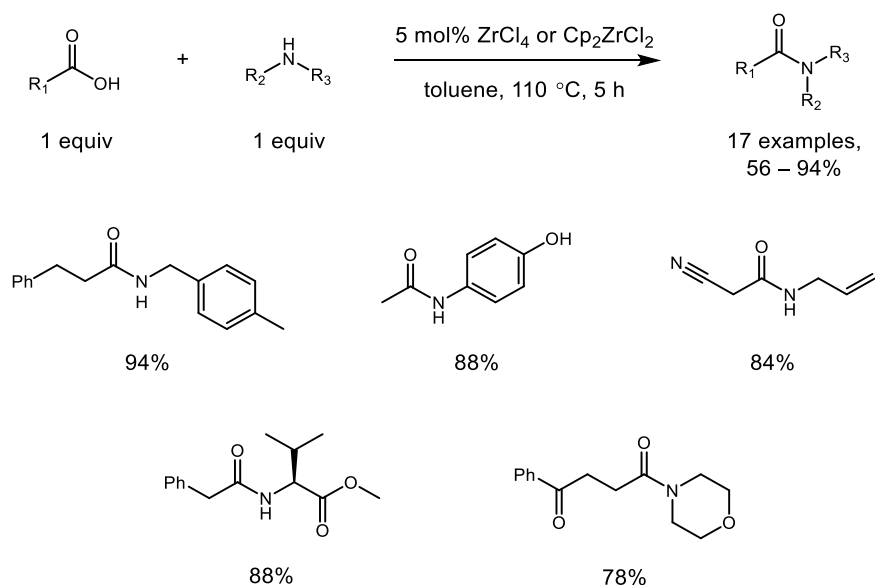
Direct amidation by condensation of a carboxylic acid and amine is inherently difficult due to the initial formation of a stable ammonium carboxylate salt. Conversion to the amide product can take place *via* thermal dehydration but extreme temperatures (>160 °C) are generally required.³⁹ However, slightly lower temperatures can be tolerated by performing the reaction in refluxing toluene, as demonstrated by Williams *et al.*, due to the fact that ammonium carboxylate salt formation is disfavoured in non-polar solvents.⁴⁰ Conventional amide bond forming methods utilising coupling reagents exploit the intermediate formation of an activated ester species which is more reactive towards the incoming amine. Similarly, boronic acid-catalysed amidation is facilitated by formation of an activated acyloxyboron species.^{28,31} An alternative approach involves the use of metal catalysts to achieve amide bond formation, either by enabling amidation of a carboxylic acid, or derivative thereof, or *via* an oxidative process using alternative starting materials such as alcohols.

1.4.2.1 Metal-catalysed Amidation of Carboxylic Acids

The ability of Lewis acids to expedite amide bond formation was reported as early as 1970 when stoichiometric amounts of TiCl₄ were used to couple a carboxylic acid and an amine.⁴¹ Since then, several Lewis acids have been shown to catalyse this transformation.

As part of their study of direct amidation, Williams *et al.* also assessed a number of metals for their ability to catalyse the transformation and a range of catalysts such as FeCl₂, CuBr, Ni(NO₃)₂, and TiCl₄ delivered full conversion to product in four hours.⁴⁰ Zirconium-based systems such as ZrCl₄ and Cp₂ZrCl₂ were especially effective, demonstrating increased reactivity with lower catalyst loadings, and furnishing complete conversion to a model substrate in reduced reaction times compared to the non-catalysed direct condensation process (Scheme 13).⁴⁰ These catalysts were trialled with a range of substrates, generally providing increased yields compared to non-catalysed reactions. However, elevated temperatures (110 °C) were still required and reduced reaction times were only observed for a small subset of examples reported.

Introduction - Catalytic Approaches to Amidation



Scheme 13: Zirconium-catalysed amidation showing selected substrates⁴⁰

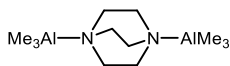
Concurrently, Adolfsson *et al.* also reported on the effectiveness of ZrCl_4 as a catalyst for amide bond formation.⁴² The use of molecular sieves enabled the reaction to proceed at lower temperatures ($70\text{ }^\circ\text{C}$) using catalyst loadings as low as 2%. The same authors have also demonstrated the suitability of $\text{Ti}(\text{O}i\text{-Pr})_4$ as an amidation catalyst under similar reaction conditions.⁴³

1.4.2.2 Metal-mediated Amidation of Esters

Even using Lewis acid catalysts, direct condensation of carboxylic acids and amines is challenging, with this process typically requiring elevated temperatures, extended reaction times, and active removal of water. Consequently, few practical methods for this transformation have been reported in the literature.⁴⁴ Carboxylic acid derivatives, such as esters, have therefore been explored as alternative starting materials for metal-catalysed amidation.

An early metal-mediated method for amide bond formation using ester starting materials was reported in 1977 by Weinreb and co-workers.⁴⁵ Treatment of the amine coupling partner with stoichiometric trimethylaluminium (AlMe_3) generated the corresponding dimethylaluminium amide which could be used directly in the amidation process or stored as a one molar stock solution. Subsequent reaction with a methyl ester formed the desired amide product in high yield (20 examples, 69 – 100%) with only gentle heating being

required (25 – 41 °C).⁴⁵ More recently, Woodward *et al.* employed DABAL-Me₃ (**35**, Figure 8), an air-stable adduct of 1,4-diazobicyclo[2.2.2]octane (DABCO) and AlMe₃, as an alternative reagent for this transformation. This reaction no longer needed to be carried out under an inert atmosphere, and did not require special handling of pyrophoric AlMe₃.⁴⁶

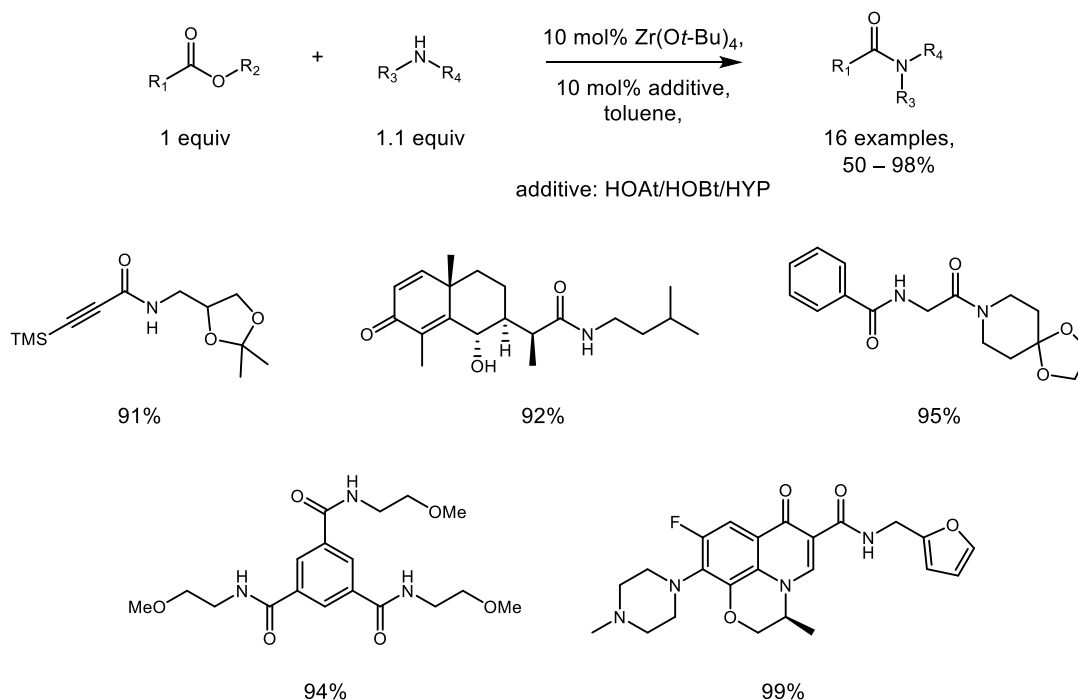


35

Figure 8: DABAL-Me₃

An effective example of metal-catalysed amidation using esters as substrates employs zirconium (IV) *tert*-butoxide (Zr(O*t*-Bu)₄) to convert simple ester starting materials to amides.⁴⁷ Common peptide coupling additives such as HOAt, HOBt and 2-hydroxypyridine (HYP), were screened in conjunction with the metal alkoxide catalyst, and found to significantly improve the yield of the product. The reaction was tolerant of a range of aprotic solvents without the need for concomitant removal of the alcohol by-product,⁴⁷ and could be carried out at room temperature or 60 °C for several substrates, although some more sterically hindered examples required elevated temperatures. A diverse substrate scope was examined to demonstrate the utility of this process and highly functionalised amides could be prepared successfully *via* this route, with selected examples displayed in Scheme 14. Functional groups capable of chelation with the metal catalyst, such as phenols, however, were not tolerated as substrates in this process.⁴⁷ In general, simple methyl or ethyl esters were employed, although the reaction was also demonstrated to proceed using benzyl, allyl, and butyl leaving groups.

Introduction - Catalytic Approaches to Amidation



Scheme 14: Zr(Ot-Bu)_4 -catalysed amidation of esters showing selected substrates⁴⁷

Subsequent mechanistic investigations indicated that the $\text{Zr(Ot-Bu)}_4/\text{HOAt}$ -mediated reaction progressed through the formation of a dimeric zirconium oxy-7-azabenzotriazolates species (**36**, Figure 9), which may help activate the amine through intramolecular hydrogen bonding, similarly to the neighbouring group effect observed with HOAt (Figure 2). Coordination of the ester starting material to the zirconium intermediate by breaking of a bridging Zr-O bond allows consequent reaction with the amine to deliver the desired amide product. This is in contrast to the authors' initial proposal that the additive facilitated *in situ* formation of an activated ester intermediate.⁴⁷

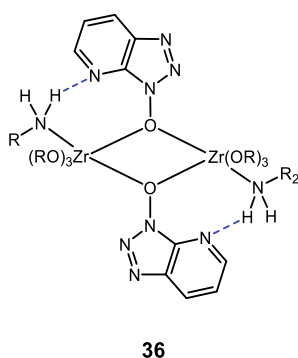


Figure 9: Zirconium-HOAt dimer intermediate⁴⁷

More recently, lanthanide-based catalysts have also been found to promote amidation of unactivated esters without the need for an accompanying additive. Lanthanum triflate ($\text{La}(\text{OTf})_3$) was shown to be an effective catalyst for this transformation, achieving high yields of amide products using low catalyst loadings (generally 1 – 5 mol%).⁴⁸ An extensive investigation of substrate scope (41 examples, 79 – 99% yield) was carried out to probe the wide utility of this amidation catalyst. Furthermore, the methodology could be successfully applied to the synthesis of a chiral bisamide ligand (**37**) and a soluble epoxide hydrolase inhibitor (**38**), synthesising these molecules in high yield without the need for stoichiometric coupling reagents (Figure 10).

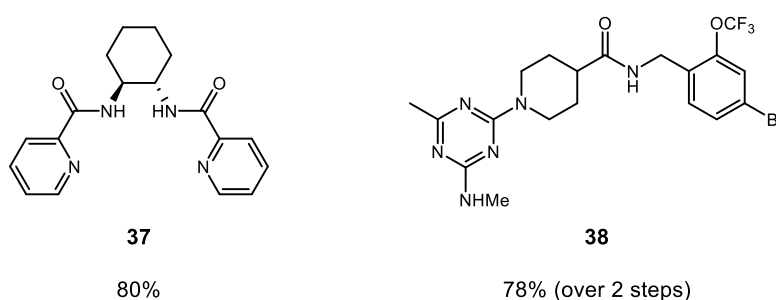


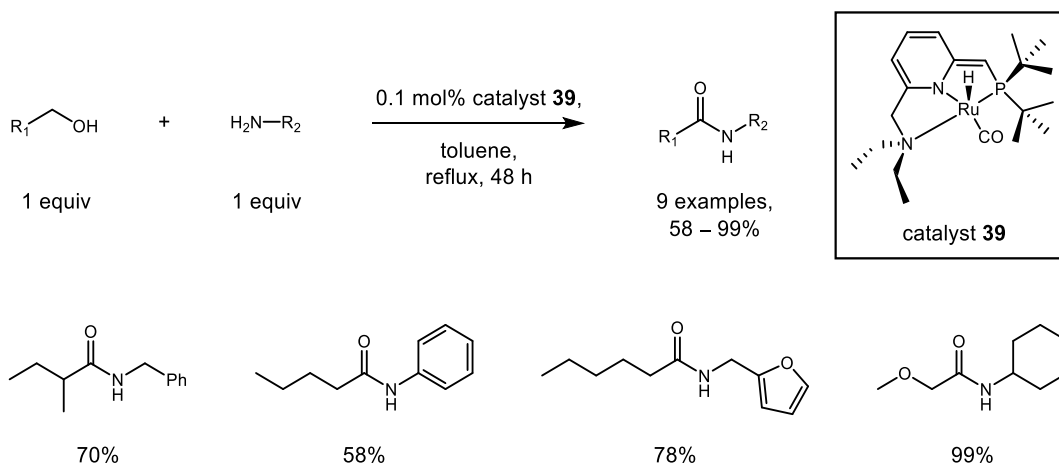
Figure 10: Applications of $\text{La}(\text{OTf})_3$ -catalysed amidation⁴⁸

Despite the wide applicability of this method to an extensive substrate scope, the major drawback of this process is the use of a rare earth metal catalyst. Limited resources of these metals exist which could lead to a potential shortage of supply in the future.⁴⁹ Alternative methods for the amidation of esters, avoiding the use of rare earth metals, would be more favourable from a sustainability perspective.

1.4.2.3 Metal-catalysed Amidation with Alcohols

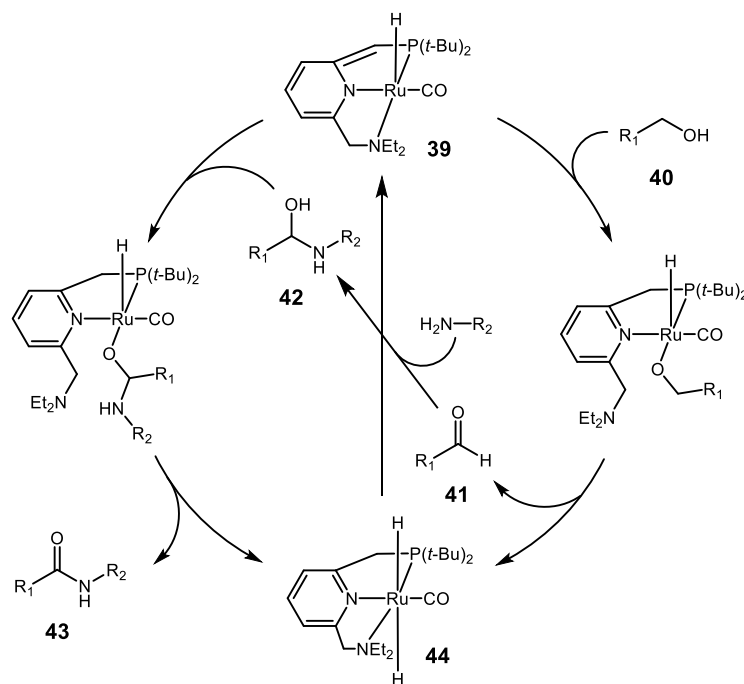
Alcohols have also been explored as alternatives to carboxylic acids in metal-catalysed amide bond forming reactions (Scheme 15). Pioneered by Milstein and co-workers, ruthenium pincer complexes have been exploited to facilitate amidation of alcohols *via* an oxidative process, producing hydrogen as the sole by-product.⁵⁰ Coupled with the fact that very low catalyst loadings (0.1 mol%) are sufficient to effect this transformation, this reaction represents a considerable improvement in atom economy compared to conventional amidation methods discussed previously (Section 1.3). Additionally, liberation of hydrogen gas is responsible for thermodynamically driving the reaction on an entropic basis.⁵⁰

Introduction - Catalytic Approaches to Amidation



Scheme 15: Ruthenium-catalysed amidation of alcohols showing selected substrates⁵⁰

Mechanistically (Scheme 16), complexation of the alcohol starting material (**40**) to the ruthenium catalyst (**39**) enables dehydrogenation to form the corresponding aldehyde (**41**). Reaction with the amine coupling partner is proposed to form a hemiaminal intermediate (**42**) which, upon complex with the ruthenium catalyst, can undergo β -hydride elimination to form the desired amide (**43**). Consequently, the known *trans*-ruthenium dihydride complex (**44**)⁵¹ is formed, which can eliminate hydrogen to regenerate the active catalyst species (**39**). Importantly, dehydrogenation of the hemiaminal intermediate appears to take place preferentially over dehydration to the corresponding imine. Hydrogenation of the imine would result in the formation of a secondary amine, which was not observed in significant amounts in this system. In the case of poorly reactive amine substrates, such as aniline, the aldehyde reacts with the alcohol starting material to form a hemiacetal intermediate and, consequently, generate an ester side product.⁵⁰



Scheme 16: Mechanism of ruthenium-catalysed amidation of alcohols⁵⁰

Overall, this reaction represents an original, efficient approach towards amide bond formation, which addresses the issues associated with poor atom economy of conventional methods. Slight drawbacks to this process include reduced yields with sterically hindered alcohol or amine starting materials and incompatibility of this reaction with secondary amine substrates.⁵⁰

Several successive reports have expanded upon Milstein's initial methodology. Other ruthenium catalysts have been developed which are also competent in performing this transformation (Figure 11). These include ruthenium diphosphine diamines (**45**),⁵² ruthenium thiocarboxamide complexes (**46**),⁵³ and *N*-heterocyclic carbene-based ruthenium catalysts (**47**).^{54,55} The latter were found to offer improved reactivity for secondary amine substrates compared to Milstein's original pincer-type complexes.⁵⁵ Simpler, commercially available catalysts such as dichloro(*p*-cymene)ruthenium (II) dimer ([Ru(*p*-cymene)Cl₂]₂) have also been successfully employed in combination with phosphine ligands, using 3-methylbutan-2-one as an external oxidant.⁵⁶ Alternative metal-catalyst systems have also been assessed for the amidation of alcohols. For example, Shimizu *et al.* have reported the use of a heterogeneous alumina-supported silver cluster (Ag/Al₂O₃) which can be removed from the reaction mixture by centrifugation and subsequently reused.⁵⁷

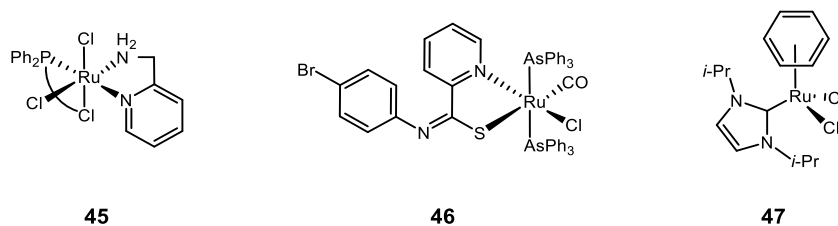


Figure 11: Alternative ruthenium catalysts for dehydrogenative amidation of alcohols

1.4.3 Organocatalytic Amidation

Metal-catalysed reactions are undeniably of great significance, and have been widely exploited in organic synthesis.³ Several, elegant metal-catalysed approaches to amide bond formation have been reported, as discussed in Section 1.4.2. However, organometallic reagents can be expensive, toxic, and sensitive to air and moisture. Furthermore, there are strict exposure limits for heavy metal residues in active pharmaceutical ingredients (APIs),⁵⁸ meaning that any residual traces must be adequately removed if metal-catalysed reactions are used in the synthesis of drug molecules. Palladium and ruthenium, for example, are classed as ‘metals of significant safety concern’, with maximum exposure limits of only 10 ppm for oral drug formulations.⁵⁸

Conversely, small organic molecules can be employed to catalyse a variety of reactions and are comparatively inexpensive and non-toxic. Conceptualised by MacMillan,⁵⁹ organocatalysis is a relatively new field of organic synthesis but has rapidly expanded over the last fifteen years to encompass a diverse range of transformations.^{60–62} Significantly, many small molecules are readily available as single enantiomers from the chiral pool, so there is a great deal of potential for use in asymmetric reactions. Indeed, several common organocatalysts, such as imidazolidinones, are derived from amino acids. Proline itself can be employed in a range of asymmetric transformations including aldol, Mannich, α -amination, and α -oxygenation reactions.⁶¹

1.4.3.1 *N*-Heterocyclic Carbene-catalysed Amidation Using Amino Alcohols

Based on the considerations outlined above, *N*-heterocyclic carbenes (NHCs) make ideal organocatalysts;^{63,64} many are commercially available or easily accessible *via* simple synthetic routes⁶⁵ and can be functionalised with chiral substituents in order to confer

Introduction - Catalytic Approaches to Amidation

enantioselectivity on the product. Importantly, due to their unconventional reactivity, they offer access to novel synthetic pathways.

NHCs are neutral compounds containing a divalent carbon atom which is adjacent to at least one nitrogen atom in a heterocyclic ring (Figure 12). The presence of inductively electron-withdrawing nitrogen atoms provides σ -stabilisation of the adjacent carbene centre. Simultaneously, π -stabilisation occurs through interaction of the nitrogen lone pair with the vacant p-orbital of the carbene. As a result of these complementary effects, NHCs behave as electron-rich nucleophilic species.

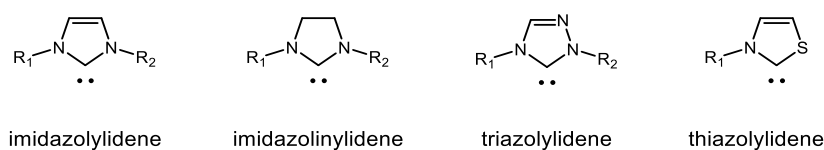
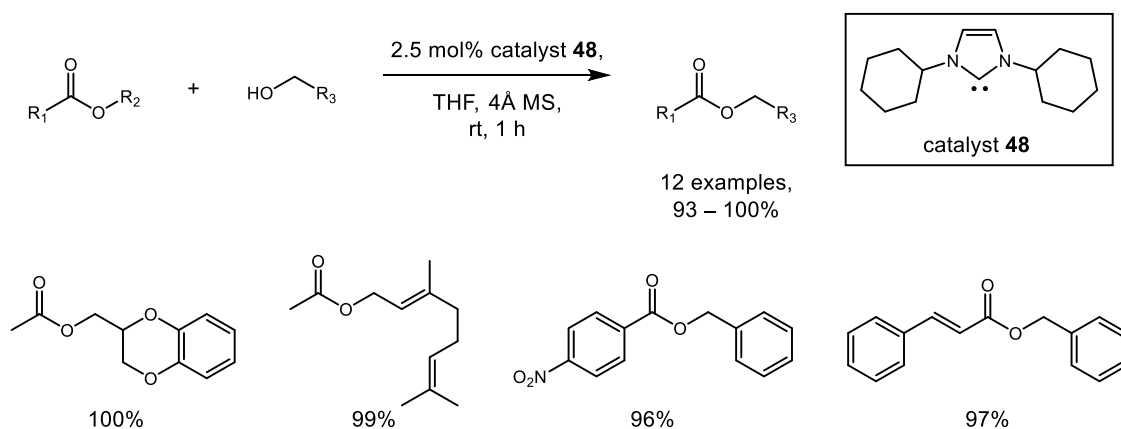


Figure 12: General structures of common NHCs

NHCs are well established as organocatalysts for transesterification reactions (Scheme 17). The scope of this reaction has been extensively studied and shown to be high yielding for a wide range of esters and primary alcohols.^{66–68} Generally, low catalyst loadings (as little as 0.5 mol%) and short reaction times (from 5 minutes) are sufficient to complete the transformation. However, given the reversible nature of the transesterification reaction, molecular sieves are usually required to remove the alcohol by-product from the reaction mixture and drive the equilibrium towards product formation.⁶⁷ Secondary alcohols are also tolerated but require slightly higher catalyst loadings (at typically 5 mol%).⁶⁹

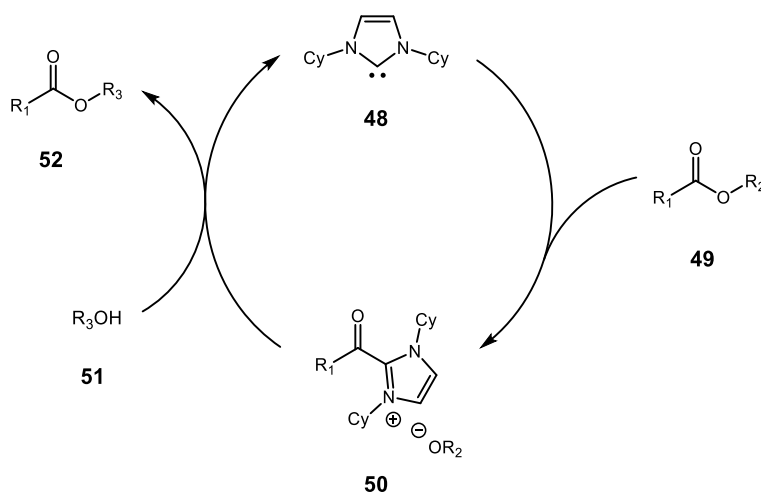


Scheme 17: NHC-catalysed transesterification showing selected substrates⁶⁷

Introduction - Catalytic Approaches to Amidation

The active NHC catalyst can also be generated *in situ* from the corresponding azolium salt, simplifying the process and avoiding the need to handle the free carbene, which can be sensitive to air and moisture. Results from this process are almost identical to those using the isolated carbene.⁶⁶

Mechanistically, it was initially envisaged that nucleophilic attack of the carbene catalyst (**48**) on the ester starting material (**49**) expels an alkoxide leaving group to form an acylimidazolium or Breslow intermediate (**50**). Reaction of this intermediate with the incoming alcohol starting material (**51**) forms the transesterification product (**52**) and regenerates the carbene catalyst (Scheme 18).^{66,70}



Scheme 18: Proposed mechanism for transesterification via an acylimidazolium intermediate

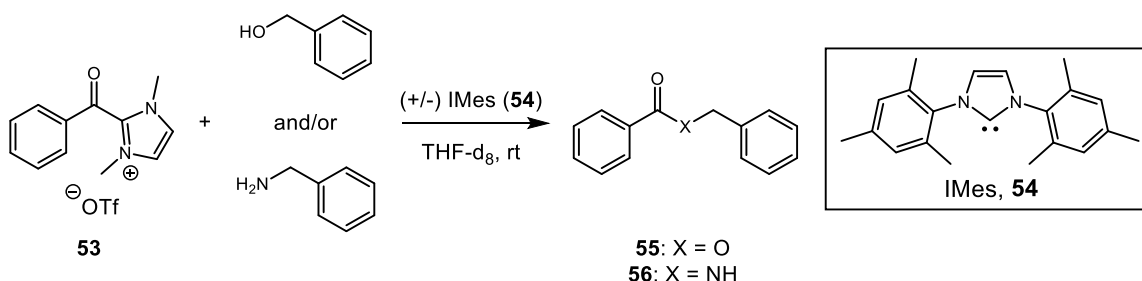
Based on the mechanism outlined in Scheme 18, it was reasoned that substitution of the alcohol nucleophile for an amine should allow facile access to the corresponding amide. However, direct amidation using NHCs has so far remained elusive; the majority of these processes exploit alternative starting materials and incorporate co-catalysts or redox processes.

Studer *et al.* have demonstrated that an acylazolium species of this type (**53**) is a competent acylating agent for benzylamine, resulting in smooth conversion to the amide (**56**) at room temperature (Table 2, Entry 1).⁷¹ Conversely, the acylation of benzyl alcohol required addition of the exogenous carbene, *N,N*-bismesitylimidazolylidene (IMes, **54**).⁷² No conversion to the corresponding ester was observed in the absence of IMes (Entry 2), and elevated temperatures were required for complete conversion in the presence of a catalytic

Introduction - Catalytic Approaches to Amidation

amount of IMes (Entry 3). Furthermore, competition experiments with both benzylamine and benzyl alcohol proceeded to form the ester product (**55**) chemoselectively in the presence of IMes catalyst (Entry 5). In the absence of IMes, a mixture of products were observed for competition reactions (Entry 4). As ester formation was shown to be unfeasible without the presence of exogenous carbene catalyst (Entry 2), the authors propose that the liberation of the free carbene upon amide formation is responsible for mediating esterification in this case.⁷¹ This evidence suggests that acylazolium formation is not the sole activation mode operating within this reaction manifold. If this was the case, amines should readily react in an analogous fashion to alcohols and alcohols should react with the acylazolium species without exogenous carbene.

Table 2: Selected results of chemoselective acylation⁷¹



Entry	Benzyl Alcohol (equiv)	Benzylamine (equiv)	IMes (equiv)	Yield of Ester 55 (%)	Yield of Amide 56 (%)
1	0	1.5	0	–	>99
2	1.5	0	0	0	–
3^a	1.5	0	0.2	>99	–
4	1.5	1.5	0	75	25
5^a	1.5	1.5	0.2	>99	0

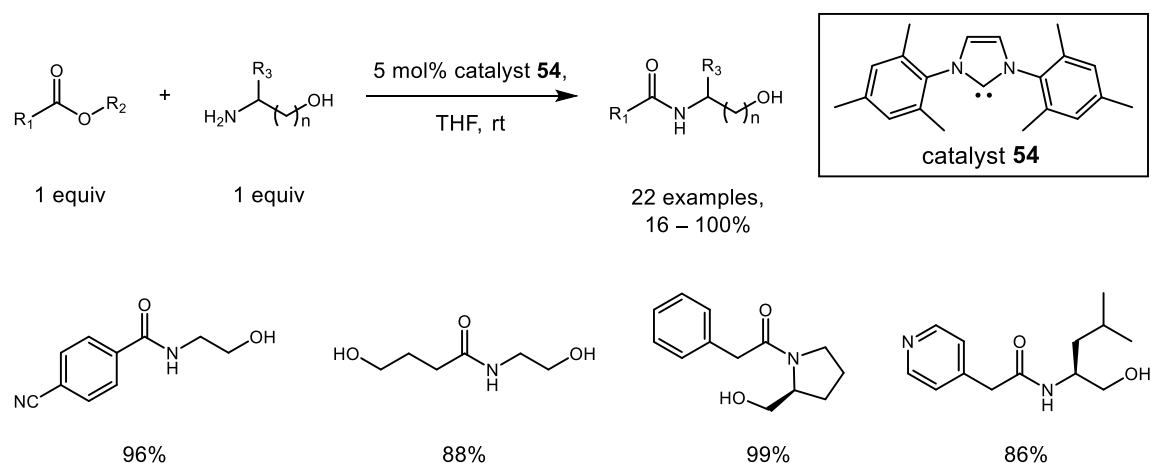
^aReaction performed at 60 °C

Computational studies on NHC-alcohol systems show a strong hydrogen bonding interaction between the carbene and an alcohol proton, resulting in lengthening of the OH bond by 0.03Å. A similar effect is not observed in the case of amines.^{71,73} This evidence suggests that alcohols undergo preferential activation by the carbene, increasing their

Introduction - Catalytic Approaches to Amidation

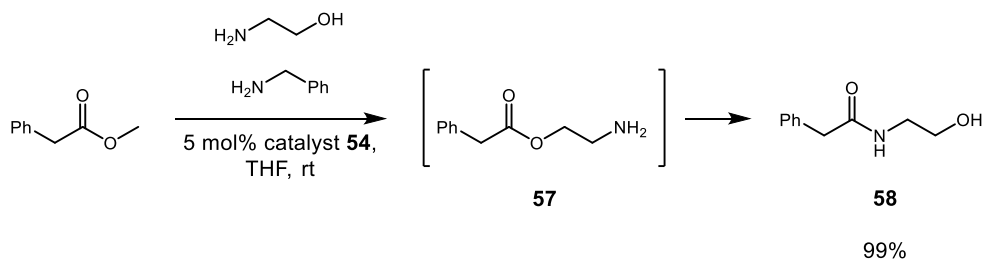
nucleophilicity and, hence reactivity in the initial transesterification process. Studer *et al.* propose a dual activation mechanism by the NHC catalyst – generation of the corresponding acylazolium intermediate and subsequent activation of the alcohol towards acylation.⁷¹

These computational results are in accordance with experimental data reported by Movassaghi and Schmidt who describe NHC-catalysed amidation of unactivated esters using amino alcohols (Scheme 19).⁷⁴ Under these conditions, a wide range of amides were formed in excellent yields.



Scheme 19: Amidation of unactivated esters using amino alcohols showing selected substrates⁷⁴

It is believed that direct amidation is not occurring in this instance, but rather that the reaction progresses *via* a transesterification intermediate (**57**), which then rearranges by *N-O* acyl transfer to form the more thermodynamically stable amide (**58**). In a competition reaction employing both ethanolamine and benzylamine, the amido alcohol (**58**) is formed in high yield but no benzylamine-derived amide product was observed (Scheme 20).



Scheme 20: Competition experiments with amines⁷⁴

The authors propose a similar activation mechanism to that established by Studer *et al.*, whereby the alcohol is preferentially activated towards nucleophilic attack by the NHC.^{74,75}

During the course of this investigation, a crystal structure was obtained of methanol in complex with IMes showing a hydrogen bonding interaction between the alcohol proton and the carbene centre (Figure 13), which is in agreement with the computational data reported by Studer *et al.*⁷¹ Further studies by Movassaghi and co-workers indicate complete deprotonation of more acidic alcohols, suggesting that for these systems, the NHC may be behaving as a base rather than a nucleophilic catalyst.⁷⁵

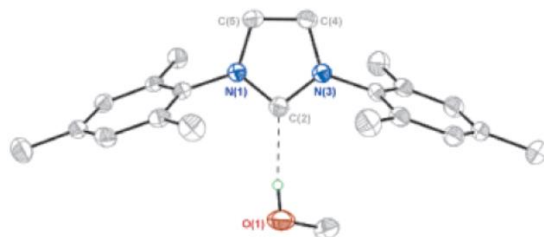


Figure 13: X-ray crystal structure of NHC-alcohol complex⁷⁴

NHC-catalysed amidation of unactivated esters using amino alcohols constitutes a mild amide bond forming process, simultaneously exploiting the increased reactivity of alcohols in the initial transesterification event, and the thermodynamic stability of the final amide product. Based on the available X-ray and computational data, it appears that alcohols are subject to initial activation by NHCs; an increase in the OH bond length upon complexation could enhance nucleophilicity and, hence, reactivity in this process. These data suggest preferential activation of alcohols compared to amines. However, the observation of an NHC-alcohol complex hints at the possibility of designing a superior second-generation catalyst system which could activate amines towards nucleophilic attack in a similar manner, facilitating a direct organocatalytic amidation method.

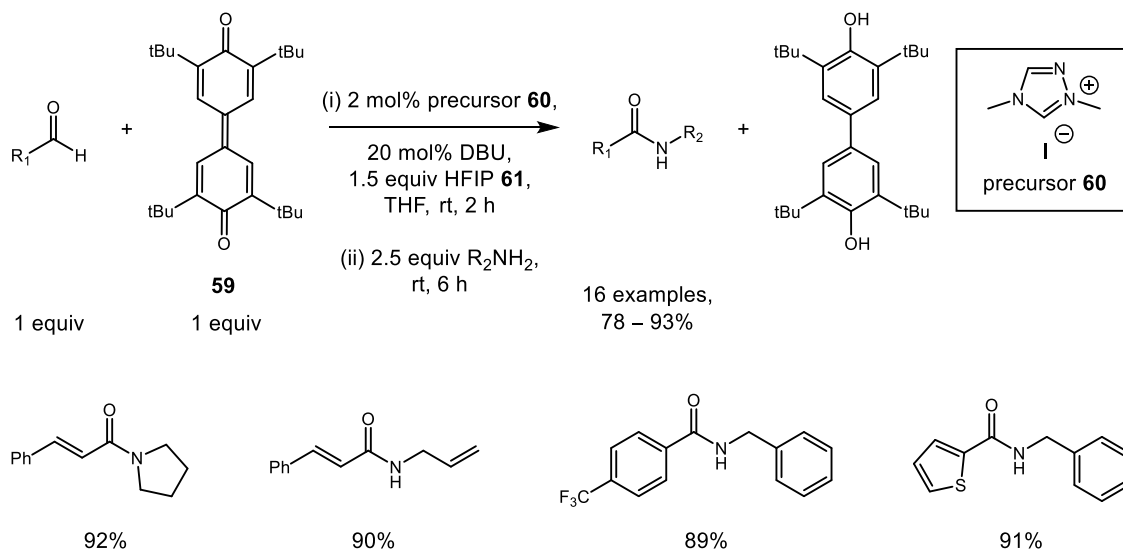
1.4.3.2 *N*-Heterocyclic Carbene-catalysed Amidation *via* Oxidative Processes

Alternative amidation methods using NHCs commonly exploit redox processes using aldehyde-derived starting materials. Amidation can either be achieved through the addition of an external oxidant, or *via* an internal redox process, employing starting materials with α -reducible functionalities.

An example of the former type of oxidative amidation, described by De Sarkar and Studer, uses a stoichiometric organic oxidant (**59**) in the presence of a simple triazolium-derived NHC (**60**) to perform amidation on α,β -unsaturated aldehydes (Scheme 21).⁷⁶ A

Introduction - Catalytic Approaches to Amidation

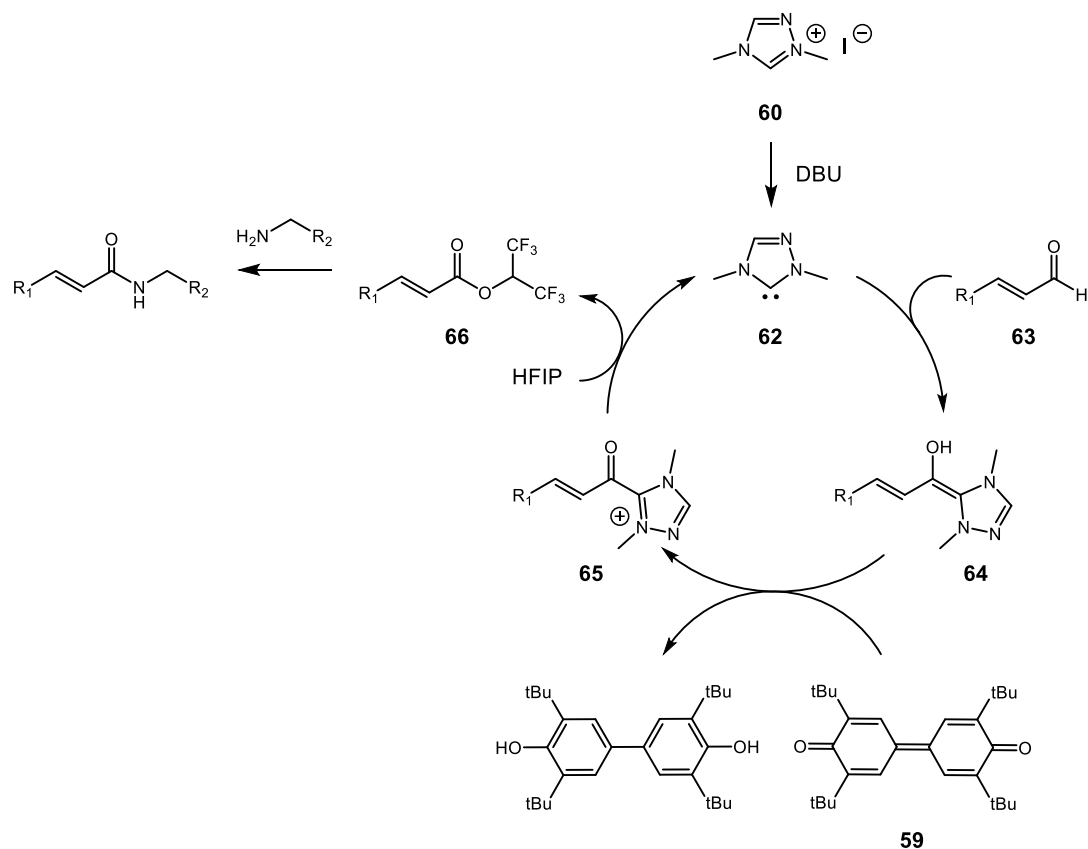
stoichiometric additive is also necessary to furnish high yields of amide products (13 examples, 78 – 93%), and optimisation efforts showed that hexafluoroisopropanol (HFIP, **61**) was competent in this capacity.



Scheme 21: Oxidative amidation of α,β -unsaturated aldehydes using an external oxidant showing selected substrates⁷⁶

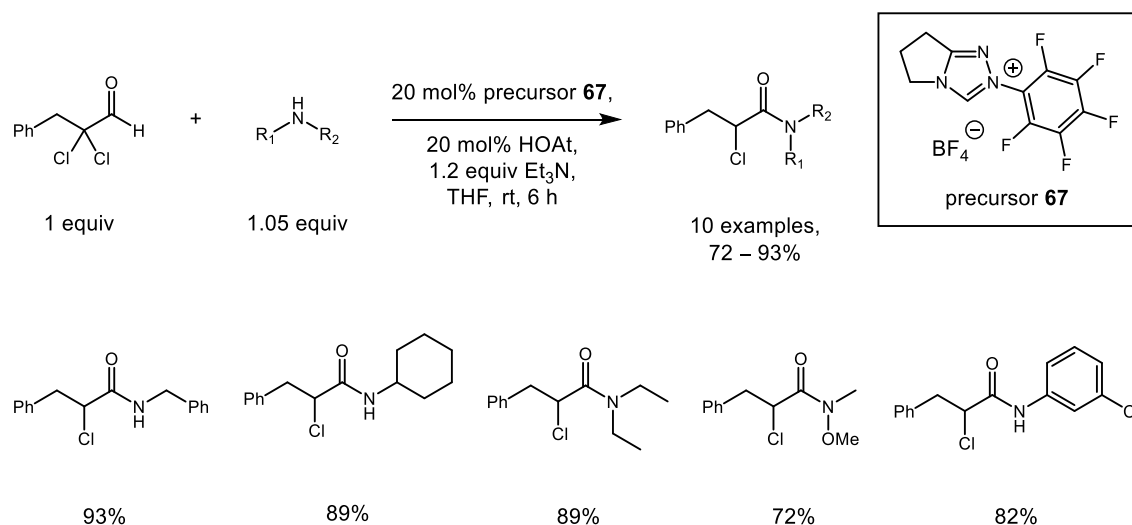
The active carbene catalyst (**62**) in this process is generated *in situ* by deprotonation of the triazolium salt precursor (**60**) by DBU (Scheme 22). Nucleophilic addition to the α,β -unsaturated aldehyde starting material (**63**) forms a Breslow intermediate (**64**)⁷⁷ which is re-oxidised by the external oxidant (**59**) to form an acylazolium intermediate (**65**). The authors propose that HFIP reacts with the acylazolium intermediate to provide a hexafluoroisopropyl ester intermediate (**66**) which they believe is the active acylating species in this reaction.⁷⁶

Introduction - Catalytic Approaches to Amidation



Scheme 22: Mechanism for oxidative amidation using an external oxidant⁷⁶

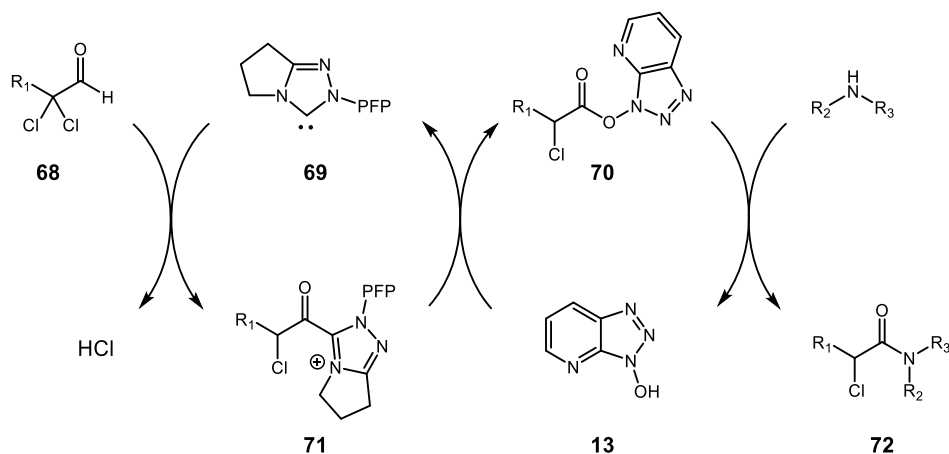
An alternative approach to oxidative amidation uses starting materials that are susceptible to internal redox reactions, eliminating the need to add an external oxidant. For example, Rovis and Vora have reported an amidation method using α -haloaldehydes in the presence of a pentafluorophenyl-substituted triazolium pre-catalyst (Scheme 23).⁷⁸



Scheme 23: Oxidative amidation of α -haloaldehydes showing selected substrates⁷⁸

Introduction - Catalytic Approaches to Amidation

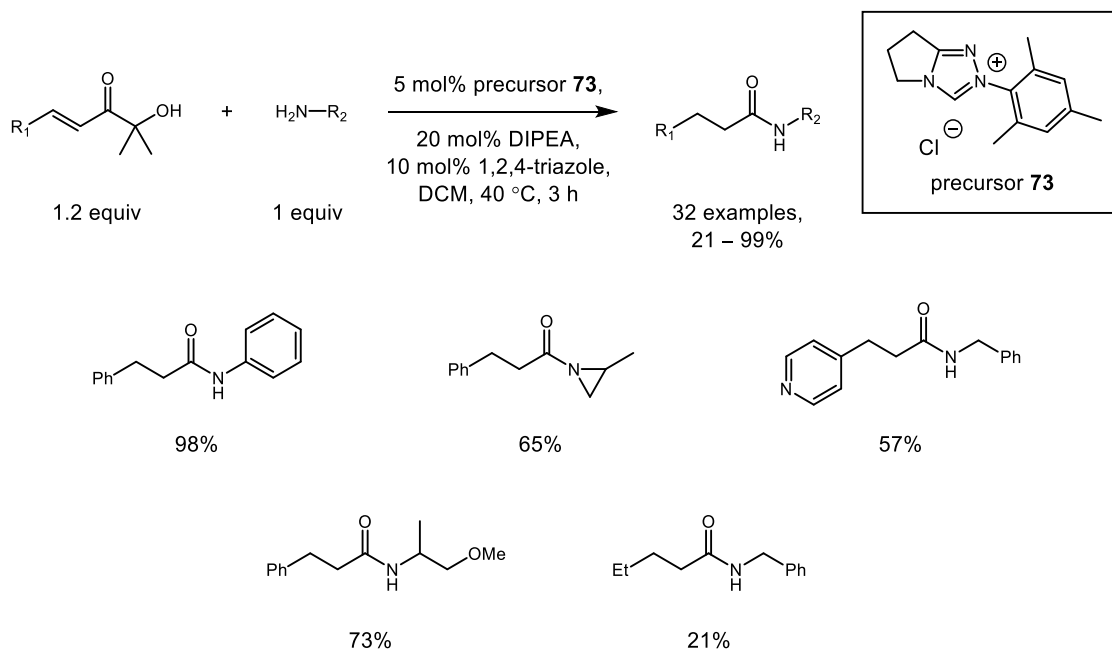
As with the example outlined by Studer (Scheme 21), an external additive is also required to promote the reaction. The authors highlight a range of additives capable of facilitating this transformation, although HOAt is favoured, furnishing a small substrate set (9 examples) in good to excellent yields (72 – 89%).⁷⁸ A dual catalytic cycle is proposed for this reaction in which HOAt is involved in a relay shuttle (Scheme 24). Similarly to the process involving an external oxidant, nucleophilic addition of the carbene (**69**) to the aldehyde (**68**) forms a Breslow intermediate. In this case, however, oxidation is facilitated by elimination of a chloride leaving group from the α -position of the carbonyl group to form the azolium intermediate (**71**). HOAt (**13**) intercepts the azolium intermediate to form a second activated ester species (**70**). Upon reaction with the amine to generate the desired amide product (**72**), HOAt is regenerated allowing it to be used in catalytic quantities, in standard loadings for an organocatalytic process.



Scheme 24: Mechanism for oxidative amidation *via* an internal redox process⁷⁸

A second, complementary example of internal oxidative amidation is presented by Bode and co-workers, using α' -hydroxyenone starting materials (Scheme 25).⁷⁹ These species are employed in an attempt to avoid issues with competing imine formation which is sometimes observed when using α,β -unsaturated aldehydes. Amide bond formation in this example is accomplished using a triazolium-derived NHC precursor (**73**) and a triazole additive, using lower catalyst loadings than those previously reported by Rovis (Scheme 23).⁷⁹

Introduction - Catalytic Approaches to Amidation



Scheme 25: Oxidative amidation of α' -hydroxyenones showing selected substrates⁷⁹

Elimination of acetone as a benign leaving group enables oxidation of the Breslow intermediate to the corresponding acylazolium intermediate. In this case, 1,2,4-triazole forms a second activated ester species, as detected by NMR studies, which performs the acylation reaction.⁷⁹

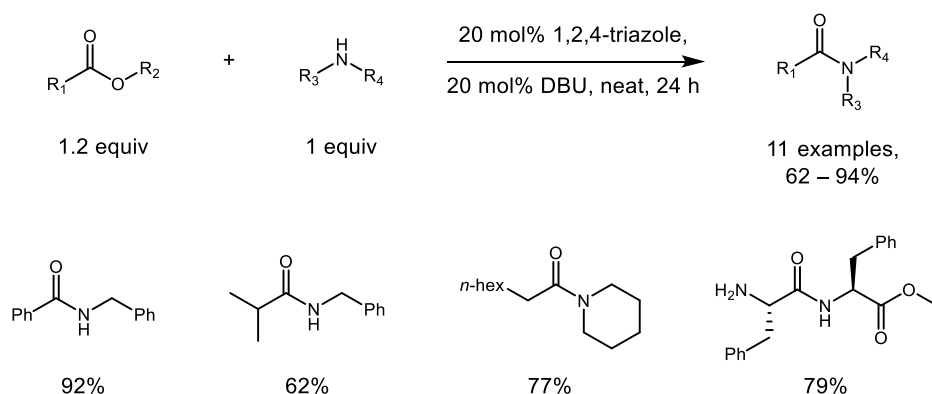
In summary, oxidative amidation processes exploit the unique reactivity of NHCs to facilitate amidation *via* the formation of a Breslow intermediate. However, to perform this reaction directly with aldehydes requires the addition of a stoichiometric oxidant to complete the catalytic cycle (Scheme 22), resulting in a considerable erosion in atom economy. Otherwise, starting materials containing an α -reducible functionality are utilised which are not readily available and must be synthesised by other routes prior to the amidation reaction. Moreover, the presence of an additive is almost always required to facilitate this transformation.^{76,78,79} These drawbacks have necessitated the design of novel, more synthetically accessible organocatalytic amide bond forming processes.

1.4.3.3 Nucleophilic Amidation Catalysts

Organocatalytic amidation methods which do not proceed *via* NHC catalysis are somewhat underrepresented in current literature. However, a handful of methods exist which enable amidation of unactivated esters by nucleophilic catalysis. A notable example was reported by Yang and Birman, employing catalytic quantities of 1,2,4-triazole (Scheme 26).⁸⁰ An

Introduction - Catalytic Approaches to Amidation

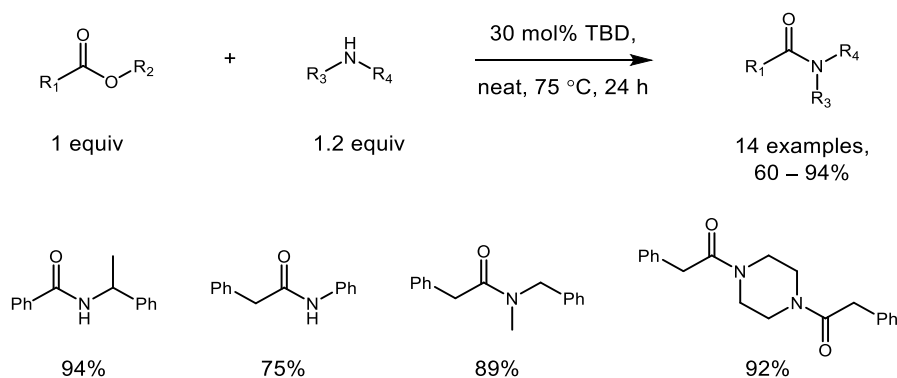
equimolar amount of DBU is required to generate the corresponding triazole anion which is capable of reacting with simple ester starting materials to form an activated carboxylate system. Reactions in the absence of base are unsuccessful.⁸⁰ This process makes use of commercially available starting materials and relatively inexpensive catalysts, contrary to the analogous NHC-mediated method developed by Bode (Scheme 25).⁷⁹ However, extended reaction times and elevated temperatures of up to 95 °C are necessary for the majority of substrates. Furthermore, the substrate scope elucidated by this method is fairly limited with respect to the amine coupling partner.



Scheme 26: Amidation of unactivated esters using a triazole catalyst showing selected substrates⁸⁰

A similar organocatalytic approach was developed by Mioskowski *et al.* using 1,5,7-triazabicyclodec-5-ene (TBD) to facilitate amidation of esters under solvent-free conditions (Scheme 27).⁸¹ TBD was found to be an active nucleophilic catalyst for amide bond formation, having previously been shown to be more effective than NHCs at catalysing transesterification reactions.⁸² Compared to the previous process using a combination of triazole and base, TBD-catalysed conditions appear to be applicable to a wider range of substrates, including aniline and secondary amines.⁸¹

Introduction - Ligation Methods



Scheme 27: Amidation of unactivated esters using TBD showing selected substrates⁸¹

Additionally, TBD-catalysed amidation has been demonstrated to be applicable on pilot-plant scale, representing a major advantage over conventional coupling reagent-mediated amidation. Multikilogram quantities of a human prostaglandin-D-synthase (H-PGDS) inhibitor (**74**) were prepared by Sanofi using TBD-amidation as the key step to couple the requisite ester and amine intermediates (Figure 14).⁸³ It was estimated that this strategy resulted in a saving of around \$2,400/kg due to the elimination of processing steps compared to the original discovery route.⁸³

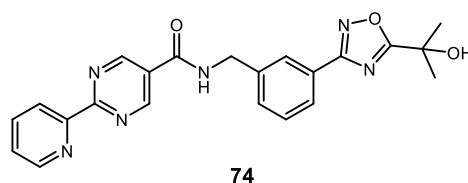


Figure 14: H-PGDS inhibitor synthesised by key TBD-catalysed amidation step⁸³

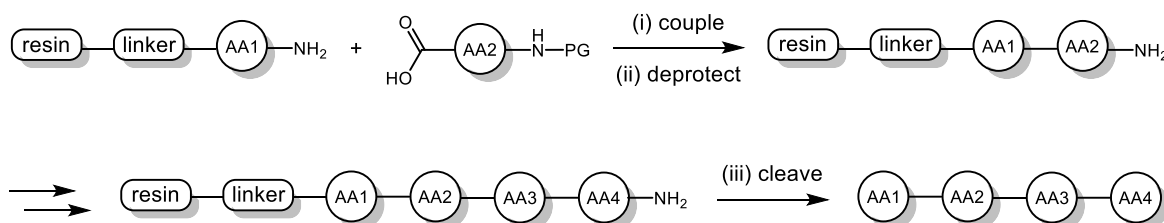
Based on the limited examples presented, organocatalytic amidation of simple ester starting materials appears to offer a range of advantages which warrant further investigations in this area. These include: ready availability of starting materials, improved atom economy, and lower associated costs. However, further elucidation of substrate scope is necessary to fully probe the utility of this approach towards amide bond formation, as well as investigating the potential to lower catalyst loadings of typically 20%.

1.5 Ligation Methods

Several recent advances have been made in the area of catalytic amidation, including boron-mediated, metal-catalysed, and organocatalytic approaches. However, the notable examples discussed have all concerned the application of these methods towards amide bond

formation in small molecules. Amide bonds are also an extremely important functionality in peptides, comprising the fundamental linking unit of amino acid monomers.

Currently, the most appropriate technique for assembling long chain peptide sequences is solid phase peptide synthesis (SPPS). Pioneered by R. B. Merrifield in 1963, this methodology addressed practical issues such as solubility and purification which accompanied solution-phase coupling processes.⁸⁴ As illustrated in Scheme 28, the C-terminal of the first amino acid in a desired peptide sequence is immobilised on a solid support *via* a covalent linker. A peptide chain is then constructed sequentially by stepwise amine deprotection and coupling of additional amino acid residues using conventional coupling reagents. Orthogonal protection strategies are employed and concomitant cleavage from the resin releases the newly synthesised peptide. The major advantage of this method is that the solid-supported peptide can be filtered and washed to remove by-products and unreacted starting materials.⁸⁴ This avoids the need to isolate and purify the peptide at every stage of the synthesis. SPPS has been widely established as a robust technique; the ability to automate this process has enabled straightforward access to long chain peptides.⁸⁵



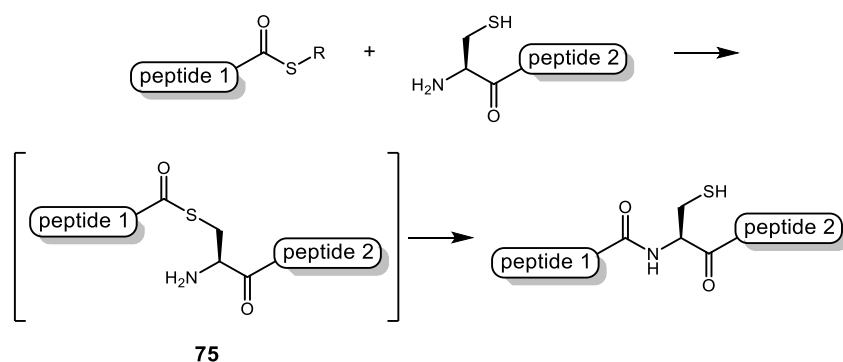
Scheme 28: Solid phase peptide synthesis⁸⁴

Although this innovative strategy has revolutionised peptide synthesis, there are several inherent drawbacks. Amino acid starting materials and coupling reagents must be used in excess to ensure high yields for each coupling step as any remaining unprotected amine could be reactive in future coupling steps, leading to the formation of by-products. As an added precaution, residual unreacted amines are subjected to a ‘capping’ procedure with acetic anhydride to render them inactive towards coupling. Also, as discussed in Section 1.3, common amide coupling reagents suffer from poor atom economy. However, super-stoichiometric amounts are required for SPPS (usually five equivalents),⁸⁶ resulting in an extremely inefficient process.

Contemporary methodologies which tackle these highlighted issues are limited. However, several chemoselective ligation methods have recently emerged which are of particular utility for the construction of longer target sequences.

1.5.1 Native Chemical Ligation

Native chemical ligation (NCL) was first described by Kent and co-workers in 1994, and involves the reaction of a C-terminal thioester with an N-terminal cysteine residue (Scheme 29).⁸⁷ This process proceeds via an initial transthioesterification event to form a thioester-linked intermediate (**75**), which undergoes spontaneous intramolecular rearrangement to form a native peptide bond at the ligation site. An exogenous thiol catalyst is also used to form more active thioester starting materials and to prevent oxidation of the cysteine residue to the corresponding disulfide. Aryl thiols were found to be particularly effective in this capacity.⁸⁸



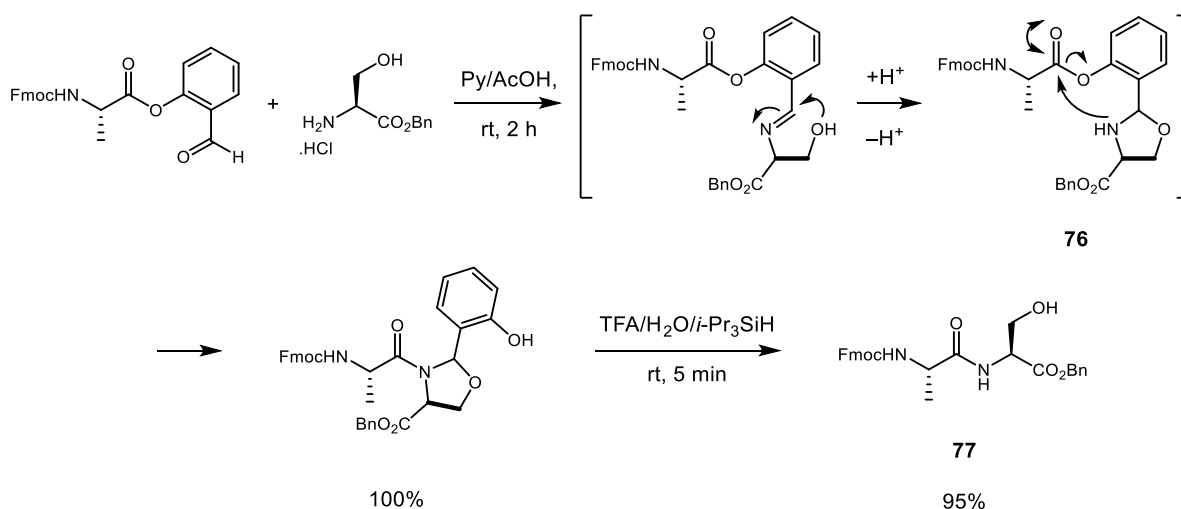
Scheme 29 Native chemical ligation⁸⁷

NCL represents a mild, chemoselective method for synthesising peptides but is reliant on the presence of a cysteine moiety to enable the initial transthioesterification reaction. However, not all proteins contain cysteine residues at the desired site of ligation. One solution is to employ cysteine residues to enable the ligation process then perform a subsequent desulfurisation reaction to generate an alanine residue at that position. Both metal-⁸⁹ and radical-based^{90,91} desulfurisation techniques have been reported.

Serine and threonine residues have also been investigated for their applicability towards ligation processes (Scheme 30). Recently, Li *et al* have exploited *O*-salicylaldehyde esters as starting materials in a chemoselective ligation reaction using alcohol-containing amino acids. Imine formation followed by cyclisation generates a pseudoproline intermediate (**76**)

Introduction - Ligation Methods

which can take undergo *O* – *N* acyl transfer to form an amide bond. Subsequent deprotection of the hemiaminal functionality releases the coupled product (**77**) in excellent yield.⁹² The drawback of both ligation approaches, however, is the need to prepare the *C*-terminal modified peptides, which can be difficult.

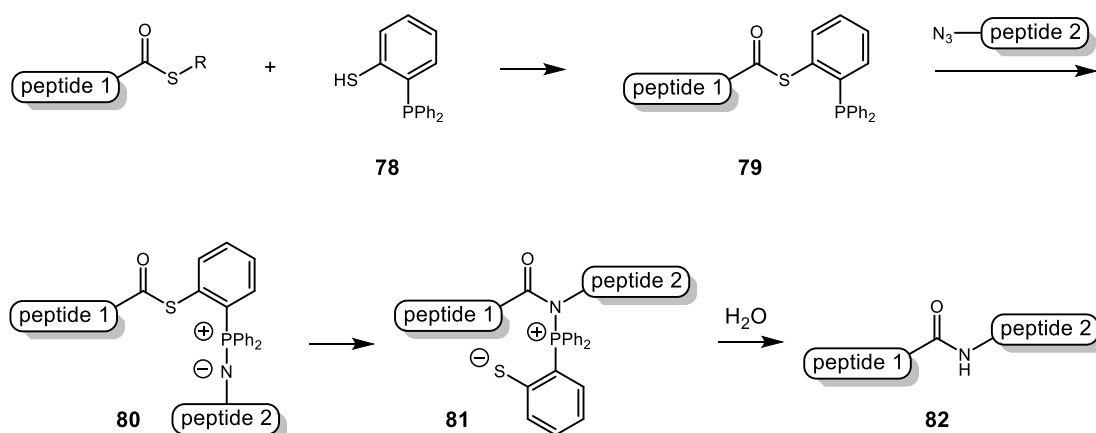


Scheme 30: Chemoselective ligation using serine residue⁹²

1.5.2 Staudinger Ligation

A complementary ligation method makes use of a Staudinger reaction to couple a *C*-terminal thioester and an azide (Scheme 31).^{93,94} This chemoselective method does not require the presence of a particular amino acid residue, so has the potential to be applied to the synthesis of a wider range of peptide derivatives. In this process, a phosphinothioester (**79**) is formed by transthioesterification using *ortho*-phosphinobenzenethiol (**78**). A Staudinger reaction of the phosphinothioester with an azide provides an iminophosphorane (**80**) which can rearrange *via* a six-membered transition state to form an amidophosphonium salt (**81**). Subsequent hydrolysis of the amidophosphonium salt releases the amide product (**82**) and generates a phosphine oxide by-product.

Introduction - Ligation Methods



Scheme 31: Staudinger ligation⁹³

As the phosphonium moiety is removed, so-called ‘traceless’ Staudinger ligation, unlike NCL, does not require further functional group interconversion after the coupling reaction. Additionally, as this process is highly selective, protection of amino acid side chains is not required. However, yields are modest, and the phosphinothiol suffers from poor aqueous solubility, meaning that further optimisation is needed for full application of this method in peptide synthesis.

In summary, a number of contemporary methods have emerged which address some of the issues associated with traditional amide bond formation using coupling reagents. The development of catalytic approaches has resulted in a significant improvement to the atom economy of this reaction. Boron- and metal-catalysed approaches represent alternative methods for the formation of amide bonds without the generation of stoichiometric by-products. Organocatalytic amidation also offers a potential advantage over traditional amidation processes, without the need to employ rare or toxic metals. Lower associated cost, reduced toxicity, and improved ease of handling make this approach a favourable alternative for atom economical amide bond formation. Additionally, several elegant chemoselective ligation processes have been developed, which are suitable for the preparation of peptide derivatives. However, as discussed previously, inherent disadvantages are associated with each of these methods. Therefore, although significant advances in the area of catalytic amidation have been reported in recent years, there is still scope to improve on certain aspects of this transformation. Development of improved methods for the synthesis of amides represents an attractive research area which could offer significant benefits over those developed previously.

2 Project Aims

As discussed in Section 1.1, conventional methods for the synthesis of amides using coupling reagents suffer from a number of substantial drawbacks, such as poor atom economy, by-product formation, cost of reagents, and poor selectivity. Against this background however, amide bonds are an extremely important functionality in both biological and synthetic molecules. Indeed, amide bond formation is extremely prevalent in the pharmaceutical industry owing to the favourable properties associated with this functional group and, consequently, amides are encountered in a number of marketed therapeutics.^{1,3} Therefore, the inherent inefficiency and waste generation associated with traditional amidation methods is a significant issue, particularly when these reactions are performed on scale. As a result, the American Chemical Society's Green Chemistry Institute have highlighted amidation as a key research area that requires the development of more appropriate synthetic routes to address the problems outlined.²⁵

Accordingly and as discussed previously, a number of catalytic amide bond forming methods have emerged in recent years, including boron-^{28,31,37} and metal-catalysed^{40,42,47,48,50} processes (Sections 1.4.1 and 1.4.2). Several elegant examples have been presented which represent considerable improvements to this process in terms of efficiency and by-product formation.

Organocatalytic amidation is another attractive approach which offers significant benefits over traditional amidation methods, without the need to use rare or toxic metals. In particular, *N*-heterocyclic carbenes have been established as competent organocatalysts in recent years, having been utilised for a diverse range of reactions, including asymmetric synthesis, transesterification, and condensation reactions.⁶³ Notably, NHC-catalysed transesterification has been demonstrated to be a mild, high yielding reaction that can be applied to a wide set of substrates (Scheme 17).⁶⁶⁻⁶⁹ The extension of this methodology to the synthesis of amides has received considerable attention, with Studer,⁷⁶ Rovis,⁷⁸ and Bode⁷⁹ reporting amidation using NHCs in the presence of a co-catalyst or external oxidant. However, these contemporary methodologies have so far not allowed for the direct amidation of simple unactivated esters, and commonly employ somewhat bespoke starting materials which are not often readily available.

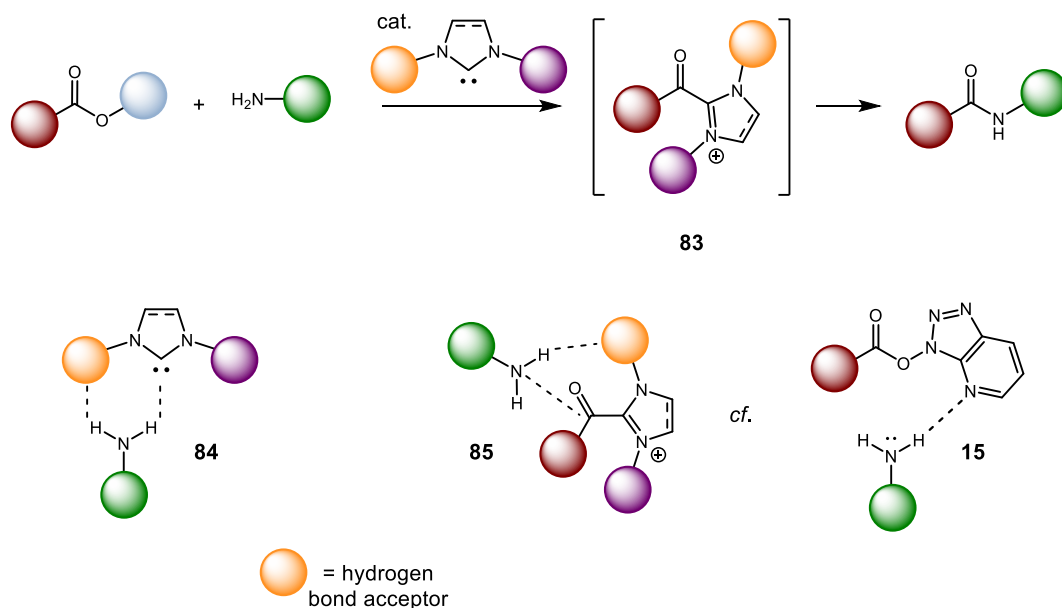
Project Aims

In an attempt to address these issues, Movassaghi has reported NHC-catalysed amidation of unactivated ester derivatives using amino alcohols (Scheme 19), although this process is believed to proceed *via* an initial transesterification reaction.⁷⁴ Subsequent rearrangement of the ester intermediate results in formation of the more thermodynamically stable amide product. Competition reactions with amines failed to generate any of the corresponding amide product (Scheme 20), indicating that the alcohol functionality was essential for the reaction to progress. During the course of this study, an interesting hydrogen bonding interaction was observed between the carbene catalyst and an alcoholic proton (Figure 13).^{74,75} Simultaneous computational studies reported by Studer showed significant lengthening of the OH bond when complexed to the carbene.^{71,73} These experimental and computational data suggest that the NHC is activating the alcohol towards nucleophilic attack under this reaction manifold. No similar amine activation was observed with the catalyst system studied, but it is conceivable that an appropriate NHC could be designed which is suitable for this purpose.

Based on these initial observations by Movassaghi and Studer, the aim of this project was to design a new generation of NHC catalysts that were capable of activating amines in a similar manner to that previously observed for alcohols. This could enable direct amidation of unactivated esters through enhancement of nucleophilicity of the amine component, representing an extremely attractive transformation which has so far remained elusive.

As discussed, the formation of a hydrogen bond with the carbene catalyst appeared to be a critical factor for delivering increased reactivity. Therefore, catalyst design in the first instance would focus on developing NHC systems which were capable of hydrogen bonding with the amine partner (Scheme 32). To enable enhanced activation, it was believed that incorporation of a hydrogen bond acceptor substituent on the NHC could provide a second interaction with the incoming amine. This type of catalyst could allow access to a dual activation pathway by performing initial amine activation (**84**) and subsequently directing nucleophilic attack onto the proposed acylazolium intermediate (**85**) *via* a neighbouring group effect similar to that observed with the common peptide coupling additive, HOAt (**15**).¹³

Project Aims



Scheme 32: Rationalisation of catalyst design

In accordance with the computational results reported by Studer,^{71,73} *in silico* data would be generated for all proposed catalysts in order to assess their suitability for the activation of amines. As it appeared that an increase in bond length upon complexation with the carbene was an important indicator of enhanced reactivity, this parameter would be investigated as a preliminary means of prioritising all proposed systems. In this way, novel systems could be evaluated in a high throughput manner and consequently selected for synthesis.

Following the design and synthesis of novel catalysts, screening reactions would then be performed to assess their capability for effecting amide bond formation. Any promising systems would then be advanced to further stages of reaction optimisation and investigation of substrate scope.

3 Results and Discussion

3.1 Synthesis of Analytical Construct

Previous work by Movassaghi has demonstrated that general NHC structures such as IMes are not adequate for performing direct amidation of unactivated ester derivatives,⁷⁴ suggesting that a specialist system would be necessary to facilitate this transformation. However, prior to the design and screening of novel catalysts, it was necessary to confirm if known carbene systems were competent catalysts in this reaction manifold. It was deemed important to examine IMes, and other commercially available NHCs in our own hands in order to assess their efficiency at catalysing a model amidation reaction. Having extensively investigated known systems, attention could then turn to developing alternative catalysts which had been specifically designed for use in direct amide bond formation.

In order to evaluate and potentially rule out known systems, a high throughput screening array was planned. Anticipating that the evaluation of a large number of NHC catalysts would require a robust screening protocol, a model ester was selected for use in the amidation reaction (Figure 15). This type of substrate was based on an analytical construct described by Andrews and Ladlow.⁹⁵

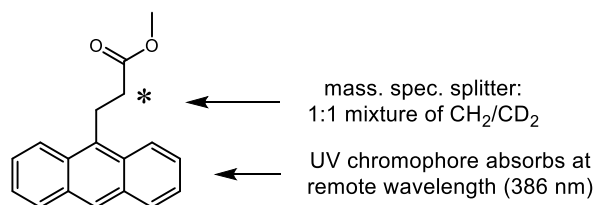


Figure 15: Features of analytical construct⁹⁵

A number of favourable properties are associated with this system which aid detection of the corresponding amide product. Since HPLC was considered to be the most rapid way to analyse a large number of reactions, it was important to be able to detect even low concentrations of product. The presence of an anthracene moiety which absorbs UV light at a remote wavelength (386 nm) enables facile monitoring of starting materials and/or products by HPLC. Furthermore, as this type of analytical construct was specifically designed to have a response factor equal to one, conversions can be calculated from the ratio

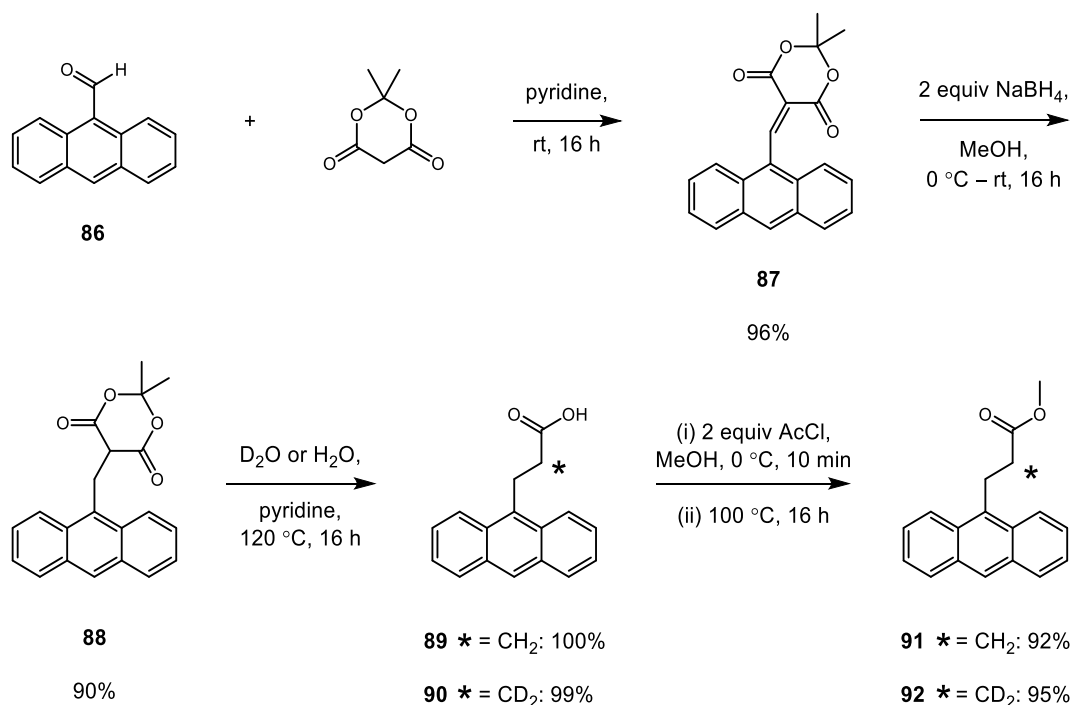
Results and Discussion - Synthesis of Analytical Construct

of peak areas allowing direct quantification of product without the need for prior HPLC calibration or the use of an internal standard.

Another beneficial property of this system is that it consists of an equimolar mixture of both protonated and deuterated esters. This mixture of isotopes functions as a 'peak splitter' during mass spectrometry analysis. A characteristic doublet can be observed for any starting materials or products which incorporate this functionality, again allowing for facile identification of any molecules of significance.

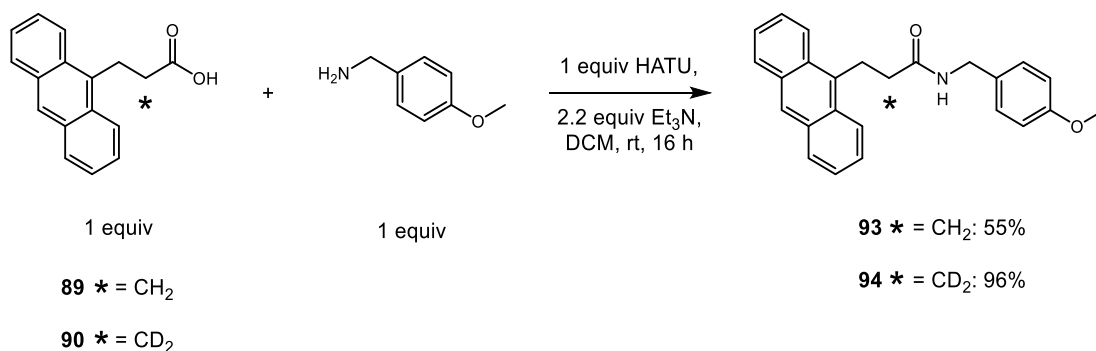
It was reasoned that based on the favourable characteristics outlined above, application of the analytical construct in the initial stages of a screening campaign would enable sensitive detection of the desired product in a relatively high throughput setting. Any positive results from this study could be progressed for further optimisation using more rigorously inert procedures if required.

Multigram quantities of the analytical construct were prepared from commercially available 9-anthraldehyde (**86**) according to literature procedures (Scheme 33).⁹⁵ Knoevenagel condensation of the aldehyde with Meldrum's acid afforded an intermediate alkylidene species (**87**) which was reduced to the corresponding alkane (**88**). Subsequent hydrolysis/decarboxylation with either water or deuterium oxide gave the acid (**89/90**) which could be esterified by treatment with acetyl chloride and methanol. This synthesis proved to be straightforward and most of the intermediates could be readily isolated by filtration. Therefore, high yields of the desired esters (**91/92**) were obtained without the need for extensive purification.



Scheme 33: Synthesis of analytical construct

In order to assist with HPLC method development, standard samples of the expected amide products (**93/94**) for the planned array were also prepared from the corresponding protonated or deuterated acid and *para*-methoxybenzylamine using a HATU-mediated coupling process (Scheme 34).



Scheme 34: Synthesis of amide standards

3.2 High Throughput Experimentation Using Known Carbene Systems

With a sufficient quantity of the required ester starting materials in hand, it was then possible to screen a palette of known carbene systems (Figure 16) to establish whether they were suitable catalysts for amide bond formation. A wide range of catalyst structures were

studied, with varying steric and electronic characteristics in order to determine if a preferential system existed. These included saturated and unsaturated systems based on either an imidazolium or triazolium scaffold.

Most of the commercially available NHCs obtained were supplied as the corresponding azolium salt, to improve stability and ease of handling. Reactions involving NHC salt precursors required the addition of exogenous base to perform *in situ* deprotonation to generate the active carbene catalyst. Formation of the carbene in the reaction vessel has been previously demonstrated in the literature to be a reliable method, providing similar results to reactions using the isolated carbene.⁶⁶ IMes (**54**) could be obtained as the free carbene due to its increased stability.⁷²

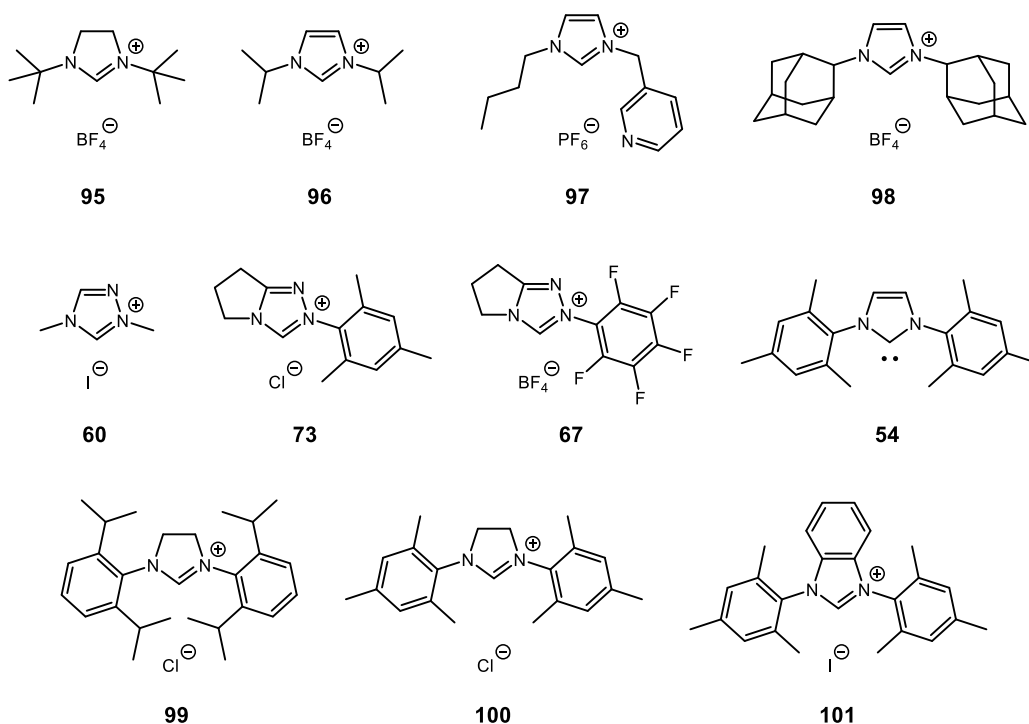


Figure 16: Commercially available carbenes⁹⁶

In addition to investigating a range of known carbene systems, a number of common peptide coupling additives were selected for testing to explore whether any synergistic combinations existed. Such additives have previously been shown to be advantageous in NHC-catalysed amidation reactions (Section 1.6.2).^{76,78,79} The additives chosen for evaluation, HOAt (**13**), HOBt (**12**), HFIP (**61**), pentafluorophenol (PFP, **102**) and *N*-hydroxysuccinimide (NHS, **103**) were selected based on their established ability to enhance amidation reactions.¹¹

Zr(*Ot*-Bu)₄ was also included in this investigation as group IV metal alkoxides had previously been shown to catalyse amidation of ester starting materials.⁴⁷

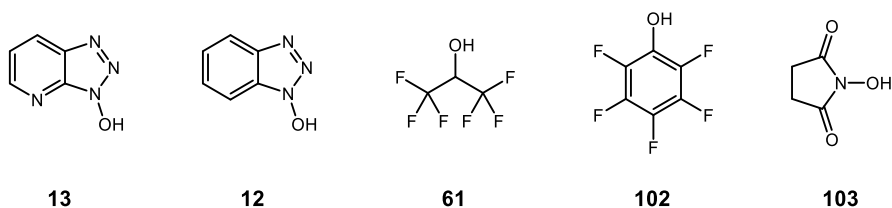
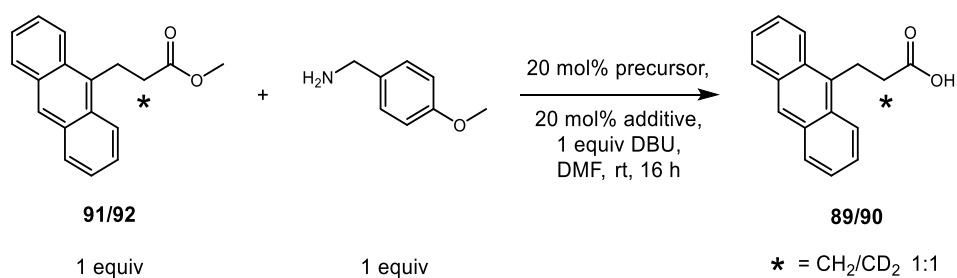


Figure 17: Selected additives

In order to screen known NHCs and additives, a model reaction was carried out using the analytical construct and *para*-methoxybenzylamine (Table 3). As the aim of this preliminary study was to gauge whether any NHC/additive combinations were promoting amide bond formation, relatively high catalyst and additive loadings were employed at the outset. It was reasoned that any positive results could then be subjected to further optimisation. In instances where the NHC was supplied as an azolium salt, DBU was also added to the reaction mixture to generate the free carbene *in situ*. Under these conditions, all selected carbenes and additives were tested, along with control reactions in the absence of carbene or additive in order to monitor any background reaction. This resulted in a total of 84 reactions which were screened in parallel and analysed using HPLC (Table 3).

Table 3: Results of preliminary precursor and additive screening



	Conversion to Carboxylic Acid 89/90 (%) ^a						
	HOAt	HOBt	HFIP	PFP	NHS	Zr(<i>Ot</i> -Bu) ₄	None
95	4	8	5	3	3	7	6
96	3	0	2	2	1	1	3
97	7	0	15	6	2	5	10
98	2	1	3	2	2	3	5
60	6	4	4	6	0	2	6
73	3	3	2	3	2	4	3
67	10	11	36	16	3	13	11
54	0	0	0	0	2	3	22
99	7	0	3	0	30	2	2
100	6	8	5	3	0	3	6
101	8	24	23	2	0	2	10
None	2	2	2	0	1	14	4

^aConversion determined by HPLC

Upon monitoring of these reactions, no conversion to amide product was observed by HPLC for any of the NHC/additive combinations tested. However, several reactions showed significant conversion (greater than 10%) to an unknown by-product. It was believed that hydrolysis of the ester starting material could be occurring *in situ*. Although HPLC retention times did not correspond with those of the standard carboxylic acid sample prepared in Scheme 33, it was presumed that this could be due to different protonation states of the

isolated product compared to the aliquoted reaction sample. Further analysis of these reaction mixtures by LCMS indicated that the mass of this peak did, indeed, correspond to that of the acid (**89/90**). Based on the results of this array, no obvious correlations existed between the use of a certain carbene or additive and the extent of hydrolysis observed. As the acid by-product was also identified in control reactions in which no carbene or additive was present, it was likely that base-mediated hydrolysis of the ester starting material was occurring as a result of adventitious water being present in the reaction mixture.

The results of this initial screening campaign showed no formation of amide product, suggesting that existing carbene systems were not competent as amidation catalysts. This is in agreement with Movassaghi's earlier work in which IMes was not capable of facilitating direct amidation of esters.⁷⁴ As described in the project aims (Section 2), it was believed that more elaborate systems would be required to promote this transformation, which would provide superior activation of the amine coupling partner.

3.3 Preparation and Screening of a Model Carbene

Prior to the design and evaluation of novel NHC systems, it was necessary to investigate known carbene catalysts to rule out the possibility of these being suitable amidation catalysts. Screening of a range of commercially available carbenes and additives in a preliminary assay showed no measurable conversion to amide product for any of the individual reactions studied. This indicated that a more appropriate catalyst was required for this transformation. Therefore, attention turned to the synthesis of a model NHC catalyst.

During the course of the initial screening study a 3-pyridyl substituted NHC (**97**) was investigated which, similarly to other commercially available systems, displayed no discernible activity in a trial amidation reaction. However, it was believed that exchanging the 3-pyridyl substituent for a 2-pyridyl group could improve interactions with the amine starting material through a potential hydrogen bond (**104**, Figure 18). As well as providing initial activation by lengthening of NH bonds in a similar manner to that observed for the carbene-alcohol complex identified by Movassaghi and activating the amine towards nucleophilic attack, a second hydrogen bonding interaction could occur between the amine and the pyridyl nitrogen. This type of system may then be able to facilitate a dual activation mode by directing the incoming amine towards nucleophilic attack on the carbonyl group

through a neighbouring group effect (**105**), similar to that observed for HOAt (**15**). Based on the above, it was hypothesised that this alternative catalyst could potentially offer an advantage over previously screened systems.

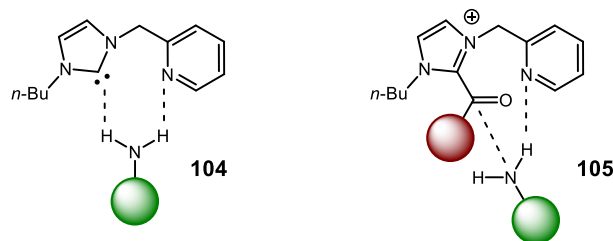
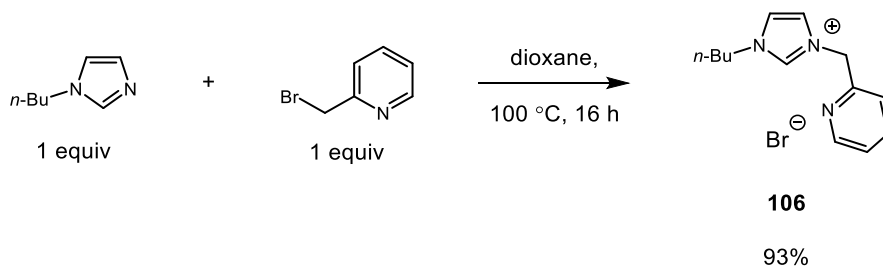


Figure 18: Proposed interactions of amine with 2-pyridyl substituted NHC

An added benefit of using this carbene precursor was the relative ease of preparation from commercially available starting materials. Butylimidazole and bromomethylpyridine were coupled by refluxing in dioxane to afford the imidazolium salt (**106**) in excellent yield (Scheme 35).



Scheme 35: Synthesis of 2-pyridyl carbene precursor⁹⁷

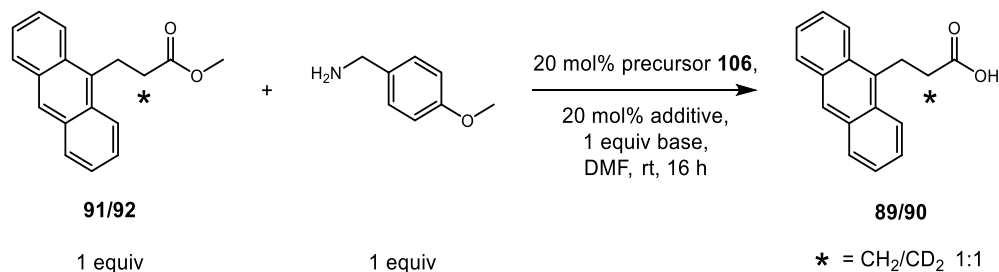
Following successful synthesis of this model precursor, it could be employed in a number of high throughput arrays in an attempt to identify reaction conditions for amide bond formation.

3.3.1 Screening of Bases and Additives

Having synthesised a model carbene precursor containing a 2-pyridyl substituent (**106**), this could then be used in additional studies to monitor its catalytic ability for this transformation. In conjunction with the additives that had been previously explored with commercially available catalysts, it was also decided to investigate alternative bases for performing *in situ* deprotonation of the imidazolium precursor. A range of bases (DBU, DIPEA, triethylamine (Et₃N) and sodium hydride (NaH)) were selected from consideration of existing literature on NHC systems, and all base/additive combinations were studied using the model precursor

in a trial amidation reaction (Table 4). As previously, the analytical construct was employed to facilitate sensitive detection of any amide product.

Table 4: Results of base and additive screening with model carbene precursor



	Conversion to Carboxylic Acid 89/90 (%) ^a						
	HOAt	HOBt	HFIP	PFP	NHS	Zr(<i>Ot</i> -Bu) ₄	None
DBU	46	44	25	28	27	38	89
DIPEA	0	0	1	0	0	3	14
Et₃N	3	4	4	5	4	9	6
NaH	33	54	17	24	21	21	34

^aConversion determined by HPLC

Results from this array (Table 4) showed little or no conversion of ester starting material when DIPEA or Et₃N were used but significant conversions in the presence of DBU or NaH. However, and in accord with the previous high throughput array, the conversions observed did not correspond to amide formation, and further analysis by LCMS indicated the presence of the corresponding acid (**89/90**). In this study, the extent of hydrolysis did not appear to be a function of the additive used. Indeed, the highest conversion to acid was detected when DBU was employed in the absence of any additive. Isolation of the product from this reaction mixture and full characterisation by NMR confirmed the structure of the acid (**89/90**).

As with previous investigations, it was believed that base-mediated hydrolysis was occurring as a result of the presence of adventitious water in the reaction mixture. However,

The results of this study showed that significant conversion to the carboxylic acid was only observed when using *t*-BuOK and NaOH (Table 5). Accordingly, control reactions were carried out for each of these bases in the absence of carbene catalyst. It was found that the acid was observed for both catalysed and control reactions, suggesting that the carbene was not mediating hydrolysis under these reaction conditions. The conversions observed in each case were lower than the equivalents of base present, supporting the theory that base-mediated hydrolysis was occurring. Since hydrolysis of the starting material appeared to be a recurring problem throughout these initial studies, it was necessary to reassess the reaction conditions used for screening of NHCs to determine whether a more stringent reaction setup was required.

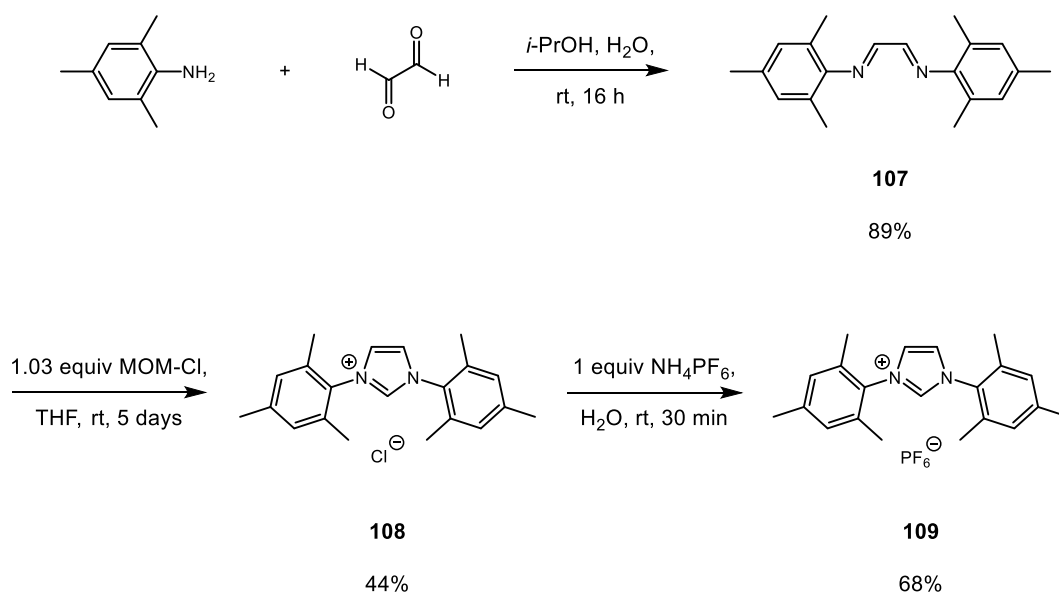
3.4 Investigation of Reaction Conditions Using IMes

Despite the execution of several high throughput arrays involving the screening of a large number of NHC precursors, additives, and bases, no amide product was observed for any of the systems examined. Therefore it was necessary to scrutinise the reaction conditions to determine whether this was solely as a result of catalyst selection or was attributable to the level of rigour required during the experimental procedure. Additionally, the continued observation of ester hydrolysis suggested that the presence of water in the reaction mixture was detrimental to the outcome of the reaction. These factors prompted a more comprehensive examination of the underlying experimental procedure. For the purpose of establishing suitable reaction conditions required for handling NHCs, IMes was chosen as a model system to study based on its ease of preparation and strong precedent in organocatalytic processes.⁶⁴ By examining a conventional NHC in our own hands, appropriate reaction conditions could be established by comparison with literature precedented results. In this way, future amidation arrays could be undertaken with a degree of confidence in the experimental setup and negative results could then be attributed to deficiencies in catalyst/additive design.

The corresponding IMes precursor could be readily synthesised from commercially available starting materials (Scheme 36). Condensation of 2,4,6-trimethylaniline and glyoxal gave the desired diimine (**107**) in high yield which was cyclised using chloromethyl methyl ether (MOM-Cl) to afford IMes chloride (**108**) in acceptable yield.⁷² As products precipitated from the reaction mixture, these could easily be isolated by filtration.

Results and Discussion - Investigation of Reaction Conditions Using IMes

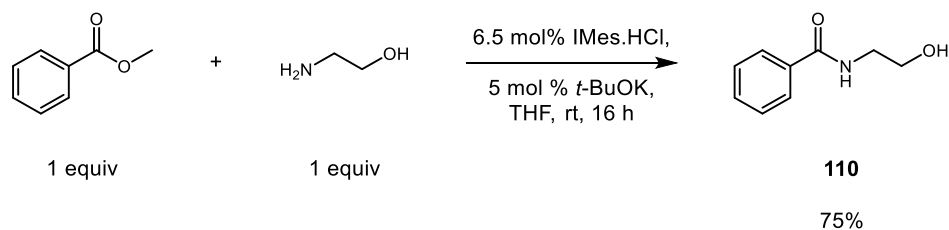
Additionally, this synthesis was readily amenable to scale, providing access to multigram quantities of the imidazolium salt precursor. A batch of material synthesised was retained as the chloride salt, whilst the remainder was converted to the corresponding hexafluorophosphate (PF₆) salt (**109**) in order to investigate the effect of substituting the counterion on the outcome of the reaction. As ester hydrolysis had been problematic in preliminary screening reactions, the use of a less hygroscopic counterion might reduce the amount of adventitious water present in the reaction mixture and therefore circumvent acid formation.



Scheme 36: Synthesis of IMes

Following successful isolation of both the chloride and hexafluorophosphate analogues of IMes, these could be used in subsequent studies to optimise reaction conditions. For this purpose, a known transformation was selected to study and benchmark the parameters required for product formation. As discussed in Section 1.4.3.1, Movassaghi has previously demonstrated NHC-mediated amidation of unactivated esters using amino alcohols by exploiting an initial transesterification process followed by rearrangement to the more stable amide.⁷⁴ A model reaction from this publication was chosen for optimisation studies in our own laboratory (Scheme 37).

Results and Discussion - Investigation of Reaction Conditions Using IMes

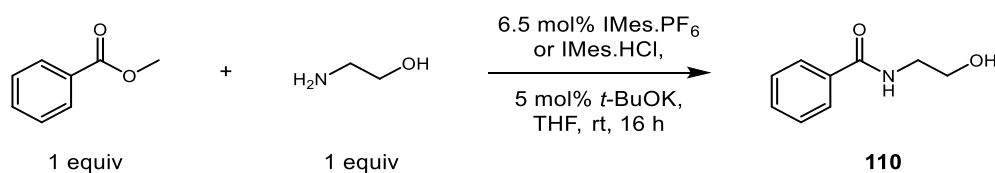


Scheme 37: Model reaction from previous publication⁷⁴

Whilst the majority of reactions in this publication are performed using the free carbene (**54**), the authors note that *in situ* formation of the catalyst by deprotonation of IMes chloride (**108**) with *t*-BuOK gave comparable results for selected examples.⁷⁴ Due to the practical advantages of using the imidazolium salt and to improve ease of handling, these conditions were adopted for the optimisation of reaction conditions. In order to confirm that the free carbene would be formed under these conditions, a solution of IMes chloride and *t*-BuOK in deuterated tetrahydrofuran (THF) was stirred for 30 minutes then analysed by proton NMR and compared to the original precursor sample. Analysis of these results showed the disappearance of the imidazolium proton signal, confirming that the salt was being completely deprotonated *in situ* to furnish the carbene system. Comparable results were obtained using the PF₆ salt and deuterated DMSO.

3.4.1 Investigation of Anhydrous Reaction Conditions

Upon confirmation that the active carbene was indeed being formed *in situ*, attention then focused on investigation of reaction conditions using this system. As stated above, a known reaction published by Movassaghi was chosen for repetition in our own hands to determine whether similar results could be recapitulated. Since hydrolysis of the ester starting materials had been frequently observed in initial studies, exclusion of water from the reaction mixture was a priority. To ascertain how rigorous the anhydrous conditions needed to be to achieve product formation, a range of conditions were attempted for the model reaction (Table 6). For all reactions, methyl benzoate and ethanolamine were distilled prior to use, and *t*-BuOK was purified by sublimation. All reaction vessels had been previously oven-dried.

Table 6: Optimisation of anhydrous reaction procedure

Entry	IMes Counterion	Reaction Vessel	Procedure	Conversion (%) ^a
1	PF ₆	Open vial	Open to air	0
2	Cl	Sealed vial	Purged with N ₂	0
3	PF ₆	Sealed vial	Purged with N ₂	0
4	Cl	Sealed vial	Maintained under positive pressure of N ₂	0
5	PF ₆	Sealed vial	Maintained under positive pressure of N ₂	0
6	PF ₆	Sealed vial	Maintained under positive pressure of N ₂ , 4 Å MS added	0
7	PF ₆	Round-bottomed flask	Maintained under positive pressure of N ₂	28
8	PF ₆ (tritirated)	Schlenk tube	Maintained under positive pressure of N ₂	52

^aConversion determined by HPLC with reference to an internal standard

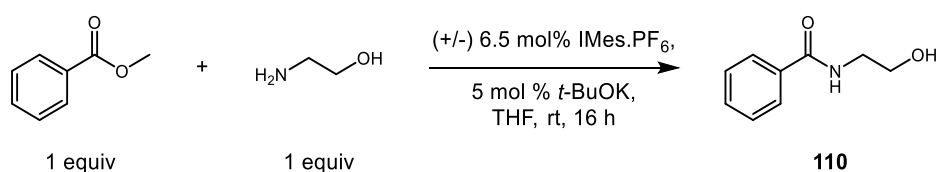
From analysis of the results of this investigation (Table 6), simply performing the reaction in an open vessel with anhydrous solvent and distilled starting material failed to show any conversion to the desired amide product (Entry 1). Similarly, sealed vials which had been evacuated and purged with nitrogen were not adequate for product formation using either the chloride or PF₆ salt form of the catalyst under a static nitrogen atmosphere (Entries 2 and 3). Purging with, then maintaining a positive pressure of nitrogen offered no added benefit (Entries 4 and 5). Next, molecular sieves were added to the reaction vessel in an attempt to capture any adventitious water in the system but again no product formation was observed (Entry 6).

Results and Discussion - Investigation of Reaction Conditions Using IMes

Based on these results, it became apparent that a more suitable reaction vessel was required to allow more inert conditions to be applied. Round bottomed flasks fitted with ground glass joints were employed to facilitate a more efficient evacuate and purge procedure (Entry 7) as it was reasoned that this procedure could be more effective at eliminating air and moisture from the system. Pleasingly, significant conversion to product **110** (28%) was observed upon monitoring of the reaction by HPLC.

Accordingly, it was concluded that performing the reaction using Schlenk techniques would be the ideal procedure for this reaction. Additionally, since extremely inert conditions appeared to be necessary, IMes.PF₆ (**109**) was selected for successive reactions as it was believed to be less hygroscopic than the corresponding chloride salt and would therefore help eliminate water from the system. However, the synthetic procedure for salt exchange required aqueous conditions (Scheme 36) and any residual traces of water from this process might be hindering the reaction. Therefore, a sample of IMesPF₆ was further purified by trituration with EtOAc/hexanes in an effort to remove any remaining water. Pleasingly, when the purified catalyst precursor was employed in this reaction under Schlenk conditions, acceptable conversion (52%) to amide product (**110**) was observed. In order to confirm that this conversion corresponded to formation of the desired product, the amide was isolated from the reaction mixture (Table 7, Entry 1) and fully characterised by NMR. An additional control experiment was carried out in the absence of IMes.PF₆ to check for the occurrence of any background reaction (Entry 2).

Table 7: Isolation of product using optimised reaction conditions



Entry	IMes.PF ₆ (mol%)	Conversion (%) ^a	Yield (%) ^b
1	6.5	52	54
2	0	53	54

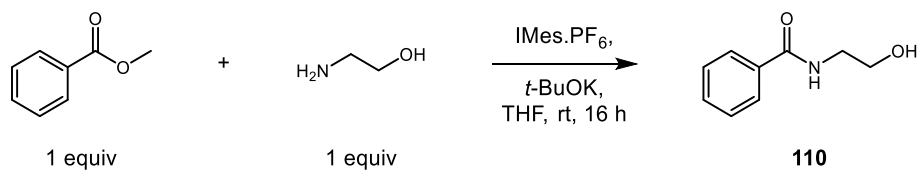
^aConversion determined by HPLC with reference to an internal standard; ^bIsolated yield

The desired amide product (**110**) was isolated in good yield, in agreement with the calculated conversion, using the optimised anhydrous reaction conditions (Entry 1). Notably, in the absence of catalyst precursor, when only a catalytic amount of base was present in the reaction mixture (Entry 2), results obtained for conversion and yield were comparable to those obtained for the NHC-catalysed reaction. This nascent observation suggested that the reaction may be proceeding *via* a base-catalysed mechanism rather than through the formation of an acylimidazolium intermediate as previously thought. Interestingly, the ability of *t*-BuOK to facilitate a significant background reaction was noted by Movassaghi in the original publication relating to this work. However, this was only indicated as a footnote in relation to selected substrates.⁷⁴ This result also implies that preferential activation of the alcohol by the carbene, as suggested by Movassaghi^{74,75} and Studer,^{71,76} is accurate, either through complex formation or direct deprotonation.

3.4.2 Further Investigation of Control Reactions

Following these initial observations where control reactions appeared to be as efficient as catalysed reactions, a subsequent study was executed to determine the consequence of varying catalyst and base equivalents. In order to probe the effect on the outcome of the reaction, 20, 50, and 100 mol% catalyst and base loadings were examined using the anhydrous conditions which had been developed previously (Table 8). Both NHC-catalysed and control reactions were carried out.

Table 8: Exploring equivalents of catalyst and base



Entry	IMes.PF ₆ (mol%)	<i>t</i> -BuOK (mol%)	Yield (%) ^a
1	6.5	5	54
2	0	5	54
3	20	20	65
4	0	20	57
5	50	50	56
6	0	50	51
7	100	100	30
8	0	100	100

^aIsolated yield

For the NHC-catalysed reaction (Entries 1, 3, 5, and 7), increasing the amount of carbene precursor and base did not result in an appreciable increase in yield from the original 54%. Indeed, when a stoichiometric amount of IMes.PF₆ was used, the isolated yield dropped to only 30% (Entry 7). At such a high NHC concentration, it is possible that complexation of IMes with ethanolamine may occur (Figure 19), reducing its availability to participate in the transformation. This type of complex has been previously alluded to by Movassaghi when investigating the interactions which occur between IMes and alcohols (Figure 13).⁷⁵ Additionally, this type of interaction is also consistent with related computational work by Studer (Section 1.4.3.1).⁷¹

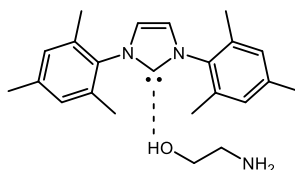
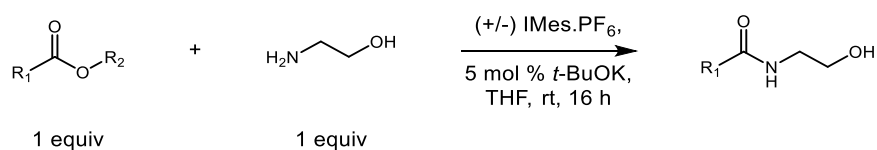


Figure 19: Formation of putative NHC-ethanolamine complex

For the base-mediated control reaction, increasing the equivalents of *t*-BuOK from 5 to 50 mol% did not significantly affect the isolated yield (Entries 2, 4, and 6). However, when a stoichiometric amount of base was added, the reaction proceeded to form the amide quantitatively (Entry 8). Based on relative pKa values (ethanolamine: 9.5 (H₂O))⁹⁸ and *t*-BuOK: 17 (extrapolated from H₂O)),⁹⁹ it is likely that complete deprotonation of the amino alcohol occurs prior to attack on the ester starting material. Therefore, it is unsurprising that a quantitative yield of amide (**110**) is observed when a full equivalent of base is employed. However, moderate yields to product are also observed when using catalytic amounts of *t*-BuOK, supporting the hypothesis that a base-catalysed mechanism may be operating in the absence of the carbene catalyst.

3.4.3 Exploring Alternative Ester Starting Materials

As optimisation of anhydrous reaction conditions had only employed methyl benzoate and ethanolamine as model substrates up until this point, we sought to investigate whether alternative ester starting materials were also susceptible to base-mediated amidation. Accordingly, a range of esters were subjected to both the carbene-catalysed and control reactions (Table 9) using ethanolamine as the coupling partner. Methyl phenylacetate underwent amidation in comparable yields for both the NHC and base-mediated processes (Entry 1). The use of aromatic esters containing an electron-withdrawing functionality at the *para*-position gave significantly higher yields for the reactions which were solely base-mediated (Entries 2 and 3). When a fluorine atom was incorporated at this position, the reaction proceeded to give the corresponding amide product (**112**) in quantitative yield (Entry 3). Methyl acetate was selected as an example of a simple aliphatic ester, again demonstrating superior reactivity in the base-catalysed process (Entry 4). Finally a benzyl ester was investigated to determine the effect of altering the leaving group (Entry 5). This substrate also exhibited improved activity for the control reaction.

Table 9: Initial exploration of ester scope

Entry	Ester	Product	Yield (%) ^a	
			+ IMes.PF ₆	- IMes.PF ₆
1		 58	28	27
2		 111	46	64
3		 112	13	100
4		 113	31	77
5		 113	33	60

^aIsolated yield

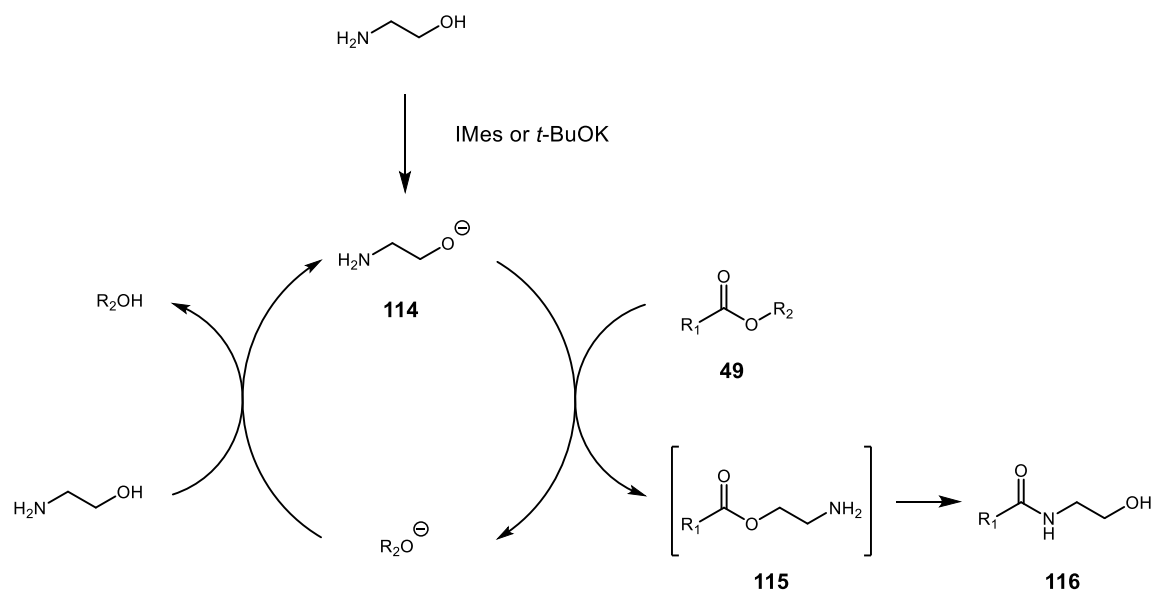
All substrates examined in this study demonstrated comparable or improved yield with the base-catalysed control reactions conducted in the absence of carbene precursor. This data validated the hypothesis that this reaction was proceeding by a base-catalysed mechanism.⁷⁴

3.4.4 Mechanistic Hypothesis

This initial study indicated that amide bond formation was possible in the absence of IMes for a range of ester starting materials, including aromatic and aliphatic substrates. Based on this, it is unlikely that the reaction proceeds *via* the formation of an acylimidazolium intermediate analogous to those proposed for transesterification reactions (Scheme 18).^{66,70}

In their earlier publication, Movassaghi and Schmidt postulate that IMes facilitates proton transfer between the amino alcohol nucleophile and the alcohol leaving group.

However, due to the results obtained when investigating this reaction in our own hands, where a catalytic amount of *t*-BuOK was competent at performing amidation using ethanolamine, it would appear that a mechanism involving preferential activation of the alcohol by the carbene is not occurring in this instance. Instead, it is proposed that deprotonation of ethanolamine initiates a base-catalysed cycle (Scheme 38). As NMR evidence supports the formation of the free carbene *in situ* under the reaction conditions employed (Section 3.4), it is believed that this basic species can deprotonate ethanolamine to give the corresponding anion (**114**). In relation to studies by Movassaghi investigating interactions between carbenes and alcohols, it is possible that an equilibrium exists between the fully deprotonated species and the NHC-ethanolamine complex suggested in Figure 13.⁷⁵ However, during this investigation, the authors obtained an X-ray crystal structure of IMes in complex with trifluoroethanol (TFE) which showed complete deprotonation to form the corresponding imidazolium ion. Based on relative pK_a values (ethanolamine: 9.5 (H₂O) and TFE: 12.5 (H₂O)), it is likely that ethanolamine will also undergo complete deprotonation upon reaction with the free carbene. In the absence of IMes, *t*-BuOK is capable of directly deprotonating the amino alcohol, supporting the existence of a base-catalysed rather than a nucleophilic mechanism.



Scheme 38: Proposed mechanism for base-catalysed amidation

Results and Discussion - Optimisation of Base-catalysed Amidation

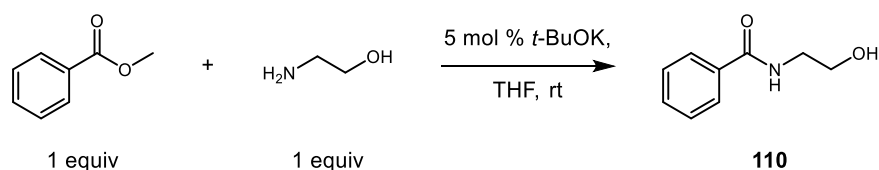
Following deprotonation, the ethanolamine anion can react with the ester starting material (**49**) to produce the transesterification intermediate (**115**), which rearranges to generate the more thermodynamically stable amide product (**116**). Upon nucleophilic attack of the ester, an equivalent of alkoxide is liberated, which can subsequently perform deprotonation of ethanolamine to complete the catalytic cycle, producing the corresponding alcohol as the sole by-product.

This postulated mechanism accounts for the comparable ability of both IMes and *t*-BuOK to effect this transformation. It also explains why, due to their increased acidity, alcohols are more reactive in this process. Indeed, when ethanolamine was substituted for propylamine in this reaction manifold no amide product was observed, indicating that the alcohol functionality is essential for reactivity, and highlighting the significance of the transesterification intermediate. More extensive mechanistic investigations relating to this proposed catalytic cycle will be detailed in subsequent sections.

3.5 Optimisation of Base-catalysed Amidation

Having identified a novel, base-catalysed amidation manifold, subsequent attention was directed to further development of this process.¹⁰⁰ It was believed that full optimisation of this reaction could enable a mild, efficient amidation process which could allow access to a wide range of amido alcohol products.

For the purposes of optimisation, methyl benzoate and ethanolamine were again selected as model substrates (Scheme 39). During the investigation of appropriate reaction procedures, unoptimised reaction conditions using *t*-BuOK and THF afforded the amide product (**110**) in moderate yield (54%). However, it was believed that the selection of a more appropriate base and solvent combination, followed by optimisation of reaction conditions, could increase conversion to product.



Scheme 39: Amidation of methyl benzoate

Results and Discussion - Optimisation of Base-catalysed Amidation

Prior to the assessment of alternative bases and solvents, the original unoptimised conditions were repeated in order to follow the progress of the reaction more closely. The coupling of methyl benzoate and ethanolamine was carried out in the presence of *t*-BuOK and conversion to amide product (**110**) was monitored over a 24 hour period. This data was used to generate a reaction profile which would act as a comparison to evaluate the efficacy of alternative systems (Figure 20).

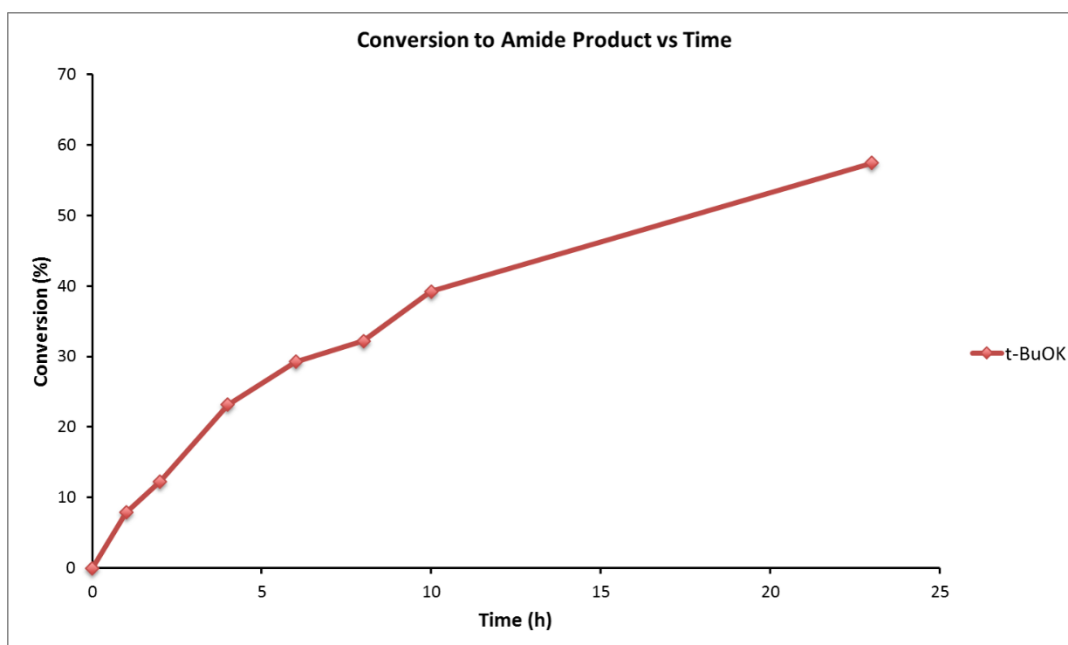


Figure 20: Reaction profile for *t*-BuOK catalysed reaction. Conversions were determined by HPLC with reference to an internal standard.

3.5.1 Base and Solvent Screening

The reaction profile generated for the *t*-BuOK-mediated reaction was then used as a point of reference on which to assess any modifications to reaction conditions. The initial phase of this optimisation campaign sought to determine if a more suitable base and solvent combination existed for this transformation. Accordingly, several bases were selected which would enable evaluation across a range of pKa values. The bases chosen for this study were: caesium carbonate (Cs_2CO_3), DBU, *t*-BuOK, 2-*tert*-butylimino-2-diethylamino-1,3-dimethylperhydro-1,3,2-diazaphosphorine (BEMP), and NaH (Table 10).

Table 10: Selected bases and corresponding pKa values⁹⁹

Base	pKa of Conjugate Acid
Cs ₂ CO ₃	10 (H ₂ O)
DBU	~12 (H ₂ O)
<i>t</i> -BuOK	17 (extrapolated from H ₂ O)
BEMP	28 (MeCN) ¹⁰¹
NaH	~36 (extrapolated from H ₂ O)

In order to select a range of diverse solvents to explore in conjunction with these bases, principal component analysis (PCA) was employed. Popularised by Carlson,¹⁰² PCA is a valuable statistical technique for examining discrete variables, simultaneously taking into account a variety of physical properties. Therefore, using this method, it was possible to directly compare different solvents and predict whether they were likely to behave in a similar manner.

Solvent choice was an important parameter to consider at this stage of optimisation as the molecular properties of a particular solvent may influence the outcome of the reaction. Although intrinsic molecular properties can't be measured directly, a multitude of data exists concerning measurable physical properties which are, in turn, related to chemical behaviour. Use of a multivariate statistical analysis method allows a number of measurable properties to be considered simultaneously and also accounts for any possible correlations between distinct physical properties.^{103,104}

According to a PCA method outlined by Carlson, data was compiled for 82 different solvents.¹⁰⁵ The eight physical properties or 'descriptors' under consideration were: melting point, boiling point, dielectric constant, dipole moment, refractive index, density, lipophilicity (as measured by logP), and an empirical polarity parameter (E_T) which is defined as the transition energy of the long wave absorption of a standard dye sample when dissolved in the solvent. Based on a plot of these properties, where the number of axes is equal to the number of descriptors, each solvent would be represented as a single point on an eight-dimensional graph. However, this multidimensional plot can be simplified by

combining the data into principal components. The first principal component, T1, represents the vector in which the plotted points show the largest variation. T2 describes the vector in which the next largest spread of data occurs, and so on. Descriptors which are correlated with each other are therefore represented by the same principal component. For the 82 solvents examined, T1 is mainly described by dielectric constant, dipole moment, and E_T – properties which correlate with polarity. T2 mainly takes into account refractive index which is an approximate indicator of polarisability. Density did not appear to participate in either principal component, and other properties such as melting point, boiling point, and log P contributed to both.¹⁰⁵ Together, these two principal components account for around 50% of the variation of physical properties.¹⁰⁴ Therefore, although the complexity of comparing a range of properties has been dramatically reduced, the granularity of the data has been reduced as a result.

However, by performing this type of statistical analysis, systematic variation across a range of properties can be described by only two parameters, making graphical analysis much simpler (Figure 21) as each solvent is represented by a single point on a two-dimensional plot. Solvents which have similar physical properties have similar principal component values and, hence, have similar coordinates on this plot. By examining the graph of 82 potential reaction solvents for the amidation reaction, and selecting points that were remote from each other, solvents could be selected which were as dissimilar as possible. Although statistically PCA can only be used as an approximate guide for comparing solvents, it remains a useful tool for designing experiments to have as large a variation of discrete factors as possible. Using PCA to aid solvent selection, dimethyl carbonate (DMC), acetonitrile (MeCN), *N*-methylpyrrolidone (NMP), toluene (PhMe), and THF were selected for screening in this study.

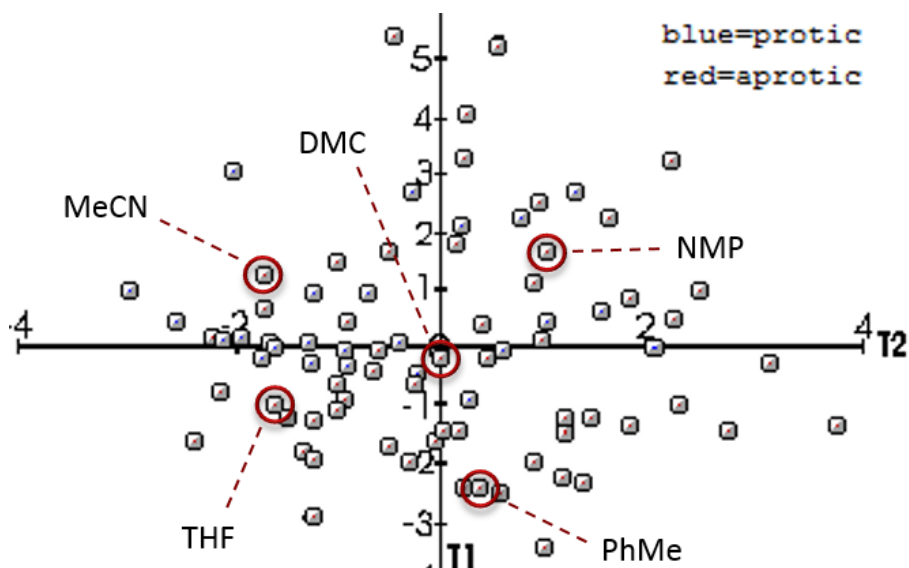
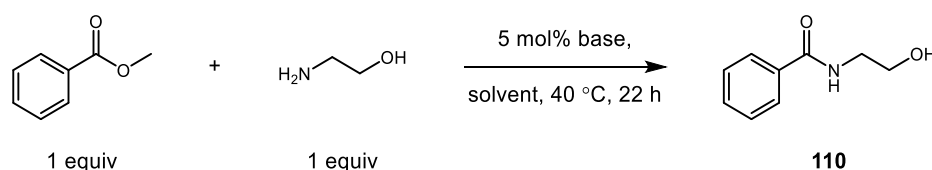


Figure 21: Graph of principal components. Points represent individual solvents

Having selected a range of bases and solvents for investigation, these were purified accordingly prior to use¹⁰⁶ in order to adhere to the anhydrous protocol developed previously (Section 3.4.1). All combinations of bases and solvents were screened in a trial reaction using methyl benzoate and ethanolamine at a slightly elevated temperature of 40 °C (Table 11). Conversions were monitored by HPLC over a 22 hour time period. Control reactions, performed in the absence of base for each solvent, showed less than 8% conversion after 22 hours.

Table 11: Results of base and solvent screening

	Conversion After 22 h (%) ^a				
	DMC	MeCN	NMP	PhMe	THF
Cs₂CO₃	3	53	62	19	17
DBU	4	10	5	6	10
<i>t</i>-BuOK	2	18	32	9	66
BEMP	2	63	7	7	7
NaH	3	32	9	28	18
None	2	5	3	2	7

^aConversion determined by HPLC with reference to an internal standard

Pleasingly, several results from this screening study (Table 11) indicated moderate conversion (greater than 50%) to product after 22 hours. Accordingly, reaction profiles were generated for any promising base and solvent combinations by plotting conversions at 4, 8, and 22 hour time points (Figure 22). Of the bases screened, BEMP (Figure 23), Cs₂CO₃, and *t*-BuOK all appeared to be suitable for catalysing the amidation reaction, displaying similar final conversions (53 – 66%) to amide product (**110**). However, the combination of BEMP and MeCN appeared to demonstrate increased reactivity, showing 61% conversion to product after only 8 hours. BEMP (**117**, Figure 23) belongs to a series of strong, neutral, non-nucleophilic phosphazene bases which were originally pioneered by Schwesinger for a range of applications in organic synthesis.¹⁰¹

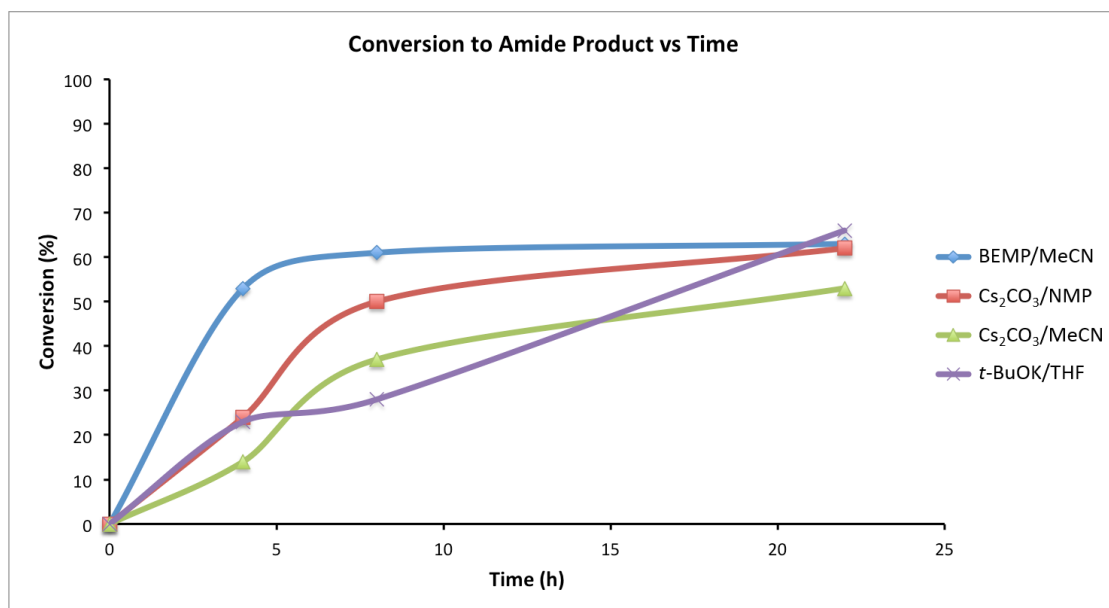
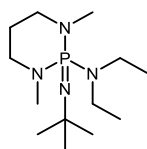


Figure 22: Selected reaction profiles from base and solvent screening.



117

Figure 23: BEMP¹⁰¹

Following base and solvent screening for a model amidation reaction, BEMP and MeCN appeared to be a superior combination for effecting this transformation. Compared to the original reaction conditions, which resulted in an isolated yield of 54%, conversion to amide product (**110**) had been increased to 63% by selection of a more appropriate base and solvent combination. It was believed that further optimisation of reaction conditions could lead to an additional increase in conversion. Accordingly, this system was progressed for advanced studies to explore the effect of altering reaction conditions.

3.5.2 Optimisation of Reaction Conditions Using Design of Experiments

As discussed in the previous sections, base and solvent screening identified BEMP and MeCN as a superior base and solvent combination for the amidation reaction. However, it was necessary to develop a set of optimised reaction conditions for use with this system in order to maximise conversion to amide product. As exploiting the statistical technique of

Results and Discussion - Optimisation of Base-catalysed Amidation

PCA to aid solvent selection had proven to be a success (Section 3.5.1), it was decided to employ a complementary statistical method to optimise reaction conditions.

Design of Experiments (DoE) is a powerful statistical technique for the optimisation of continuous factors such as temperature, pH, concentration, rate of addition, etc. By varying all factors under consideration simultaneously, relationships between variables, and their effect on the outcome of the reaction can be determined. In this way, maximum data can be obtained from a limited number of reactions, thus making economical use of time, cost, and resources. It was believed that this process could be used to our advantage to expedite the optimisation of reaction conditions for BEMP-catalysed amidation.

The most common approach to optimisation of continuous factors is by adjusting one parameter at a time whilst keeping all other variables constant. This process of linear screening may, indeed, lead to the optimisation of reaction conditions but does not account for any relationships between factors.¹⁰² As an example, for a hypothetical process shown in Figure 24a, a single factor such as pH may be varied sequentially, keeping all other factors constant. The best results from this set of experiments are used as the constant value to vary a second factor such as temperature, and so on. However, this may result in a ‘pseudo-convergent’ process, whereby a local maximum is reached as represented by a green dot (Figure 24a).¹⁰⁴ The ‘optimised’ set of conditions achieved in this case do not correspond to the maximum conversion that could have been realised for this process as the correlation between pH and temperature was not accounted for. Conversely, DoE offers a more systematic approach to optimisation which helps to overcome this issue. A design space is selected within which to study the effects of varying multiple parameters (Figure 24b). If the absolute optimum set of conditions is not obtained initially, data from each previous design can be used to influence future designs, ultimately leading in the direction of the maximum response.¹⁰⁴

Results and Discussion - Optimisation of Base-catalysed Amidation

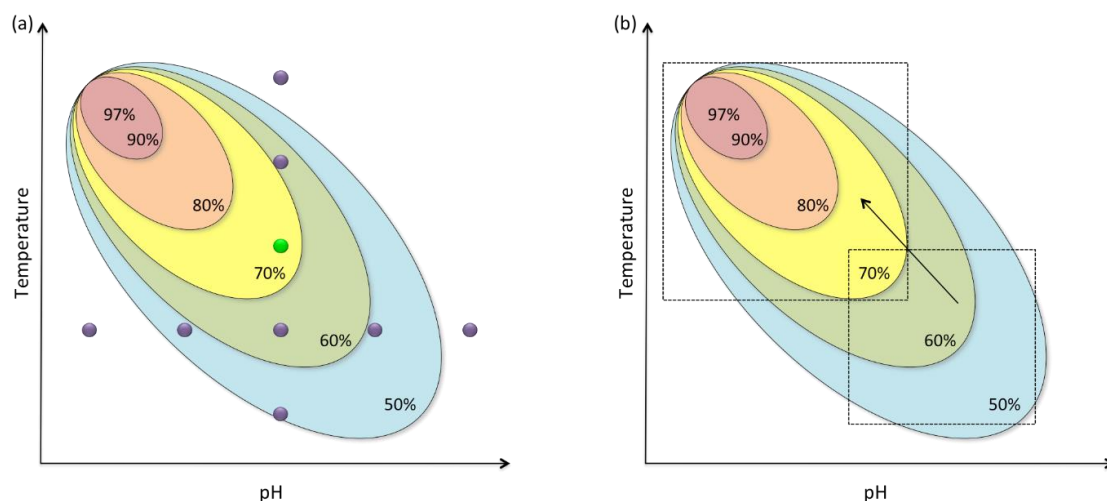


Figure 24: Experimental design vs linear screening. Green dot represents local maximum.

For the purpose of employing DoE as a tool for the optimisation of BEMP-catalysed amide bond formation, classical factorial designs were deemed suitable. These are categorised as two-level designs, indicating that the mildest and most forcing conditions (as defined by the user) are explored. For a full factorial design, the number of reactions required to examine all combinations of minimum and maximum values for each factor (k) equals 2^k . Therefore, for a two-level design exploring two factors (x and y , Figure 25a), four reactions (represented by red dots) are required to examine all permutations of minimum and maximum values. Control reactions (represented by orange dots) are also included at the centre point, which demonstrate repeatability of the reaction conditions and allow for the estimation of error in the system. Increasing the number of factors, a two-level, three-factor design (Figure 25b) requires eight reactions (plus centre points) to execute a full design.

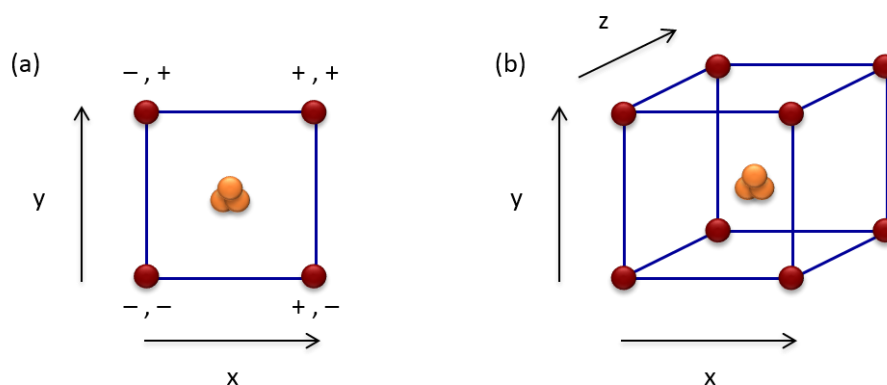


Figure 25: Two-level designs for (a) two factors and (b) three factors. x , y , and z denote different factors. Red dots represent reactions at minimum and maximum points; orange dots represent reactions at centre points.

Results and Discussion - Optimisation of Base-catalysed Amidation

For simple systems, the number of reactions required for a full factorial design is low so all possible reactions can be carried out readily. However, upon increasing the number of factors under consideration, the number of reactions increase exponentially as indicated in Table 12, and it becomes impractical to perform all of these experiments.¹⁰² Alternatively, half-fractional designs can be employed, allowing for only half of the total reactions to be carried out, while maximising the amount of data retrieved from each experiment.

Table 12: Number of reactions required for full and half-fractional factorial designs

Factors	Number of Reactions	
	Full	Half-Fractional
3	8	4
4	16	8
5	32	16
6	64	32
7	128	64
8	256	128

Half-fractional designs only incorporate half of the points at the maxima and minima, but these are selected in such a way as to cover as much of the design space as possible (Figure 26). Therefore, the points are orientated on the corners of a tetrahedron within the 3D design. This spans the maximum area possible with fewer points, allowing maximum data retrieval.¹⁰⁴

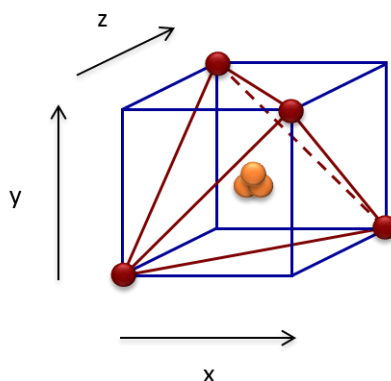


Figure 26: Half-fractional factorial design

Half-fractional designs are achieved by the statistical technique of aliasing – *i.e.* combining the effects of more than one factor.¹⁰² For example, for a two-level, three-factor, half-fractional design as depicted in Figure 26, each of the three main factors (x , y , and z) may have a significant effect on the response. Additionally, a combination of factors may affect the outcome, so two-factor interactions (xy and yz) and three-factor interactions (xyz) are also considered. More aliasing results in fewer reactions but as a caveat, makes it more difficult to interpret effects of individual factors. Classical designs are grouped in different resolutions according to the extent of aliasing involved (Table 13). Designs which have the lowest resolution classification have the largest degree of aliasing. For a resolution III design, single factor effects are combined with two-factor interactions. However, this can be misleading if the two-factor interaction has a significant effect on the response, which is common. As it is difficult to clearly identify which factors are affecting the response, this type of design is usually not accurate enough for a screening process. Resolution IV designs involve less aliasing, with single-factor effects being combined with three-factor interactions, which are generally considered to be negligible in comparison. Additionally, two-factor interactions may be combined with other two-factor interactions in this case. As this type of resolution allows for better interpretation of main effects, it is considered to be suitable for a screening design. Finally, resolution V designs feature the least amount of aliasing. All single- and two-factor effects can be discerned in this case.¹⁰²

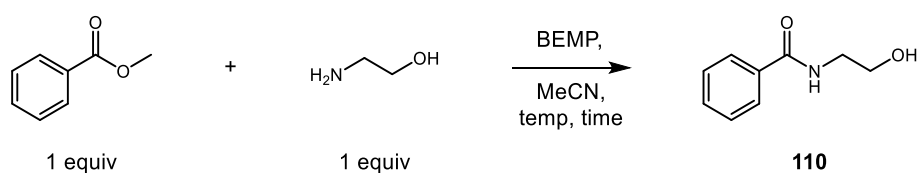
Table 13: Features of aliased designs

Resolution	Features
III	Single-factor effects are aliased with two-factor interactions (eg $x = yz$)
IV	Single-factor effects are aliased with three-factor interactions (eg $x = xyz$) Two-factor interactions may be aliased with other two-factor interactions ($xy = xz$)
V	All single-factor effects and two-factor interactions can be estimated Assumes three-factor interactions are negligible

As resolution IV designs are considered to offer a balance between the number of reactions required and the quality of data obtained, it was considered to be a good starting point for carrying out optimisation of reaction conditions.

Having selected a resolution IV design for the optimisation of BEMP-mediated amidation, it was decided to examine the effect of four factors on the conversion to amide product for the model reaction involving methyl benzoate and ethanolamine (Table 14). Minimum and maximum values were chosen which would enable examination of the mildest to most forcing conditions for this process. These values were selected according to the practicality of performing experiments, and with the intention of retaining mild reaction conditions.

Table 14: Ranges chosen for initial experimental design



Factor	Minimum Value	Maximum Value
Time (h)	8	22
Temperature (°C)	20	60
Concentration (M)	0.5	2
Catalyst Loading (mol%)	5	20

Results and Discussion - Optimisation of Base-catalysed Amidation

Using the input values outlined for each of the four factors selected, a two-level, half-fractional factorial design was created using Design Expert 8TM software.¹⁰⁷ This generated a set of eight reactions which varied all four factors in each experiment (Table 15). Two centre points were included to allow for estimation of error and to assess the repeatability of this reaction (Reactions 2 and 8).

Table 15: Results from half-fractional factorial design

Reaction	Time (h)	Temperature (°C)	Concentration (M)	Catalyst Loading (mol%)	Conversion (%)^a
1	22	20	2	5	60
2	15	40	1.25	12.5	98
3	8	20	0.5	5	32
4	22	20	0.5	20	92
5	22	60	2	20	97
6	8	60	2	5	55
7	22	60	0.5	5	67
8	15	40	1.25	12.5	100
9	8	20	2	20	100
10	8	60	0.5	20	96

^aConversion determined by HPLC with reference to an internal standard

The suggested reactions were carried out and conversion to product was determined at the end of each set reaction time. The results for each control reaction (Reactions 2 and 8) were in agreement within experimental error, demonstrating that the reaction conditions were reproducible. Pleasingly, conditions within the ranges selected appeared to be proficient in forming the product quantitatively (Reactions 8 and 9). Furthermore, for the majority of conditions examined during this study, good levels of conversion were observed.

Initial inspection of the experimental data suggested that a set of optimised conditions could be achieved using this design. However, further investigation of experimental results using

Results and Discussion - Optimisation of Base-catalysed Amidation

Design Expert 8TM software was necessary to accurately identify which factor or combination of factors was having the most significant effect on the response. Accordingly, the conversions shown in Table 15 were processed by the software and analysed using a series of graphical representations. Firstly, a half-normal plot was generated (Figure 27) which assisted in the identification of significant effects. Each factor or combination of factors is represented by a point on this graph and a best-fit line is applied to the data. Points furthest from this line have a larger standard deviation compared to other points on the line, therefore the corresponding factor or combination of factors is likely to be having the greatest effect on the response.¹⁰² From consideration of the half-normal plot for this set of results (Figure 27), it was determined that catalyst loading (D) had the largest standard deviation compared to other factors and was therefore likely to be having the most significant effect on conversion to product (**110**) in the BEMP-catalysed amidation reaction.

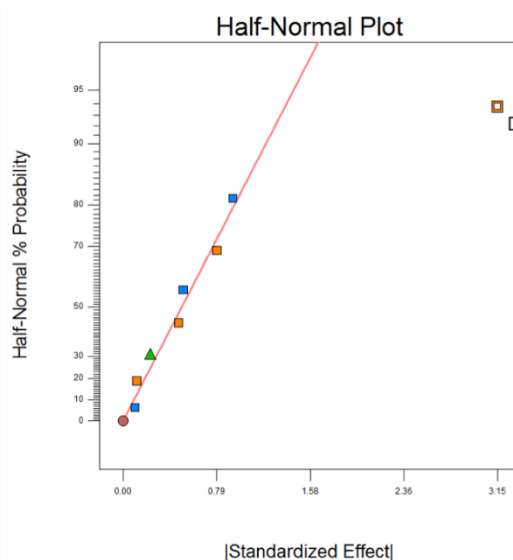


Figure 27: Half-normal plot for completed design where D is catalyst loading

As another indication of significance, a Pareto chart was plotted for the experimental data (Figure 28). This type of analysis estimates significance based on t-value limits. Factors with t-values above a lower limit (represented in black in Figure 28) are deemed 'possibly significant' to the overall response. Factors with t-values above the Bonferroni limit (a statistical correction for multiple comparisons, represented in red in Figure 28) are almost certainly significant. In agreement with the half-normal plot, catalyst loading (D) falls above this limit, indicating it is substantially influencing the outcome of the reaction.

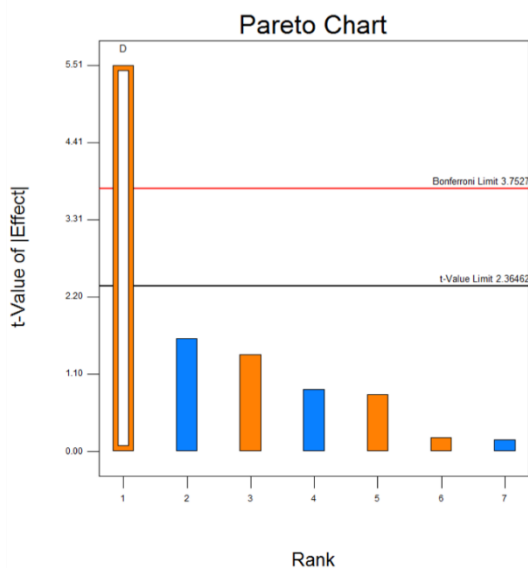


Figure 28: Pareto chart for completed design where D is catalyst loading

From these representations of the data (Figures 27 and 28), it was apparent that catalyst loading was influencing conversion to amide product in this reaction. However, with statistical analyses of this type, it is possible for large effects to obscure smaller ones. In order to investigate whether any other factors or combinations of factors were having an effect on the outcome of the reaction, a 3D graph of the experimental results was also considered (Figure 29), which plotted catalyst loading against concentration. In accordance with the previous analysis, this plot indicated that increasing catalyst loading dramatically increased conversion. However, it was noted that increasing concentration also had a positive effect on conversion but to a lesser extent. Furthermore, it appeared that the highest conversion to product within the ranges defined was obtained when both concentration and catalyst loading were maximised, indicating that these factors were having a combined effect on the response. This finding highlighted the benefit of using DoE for optimisation of this reaction as a two-factor interaction of this type would not have been evident using linear screening methods (Figure 24).

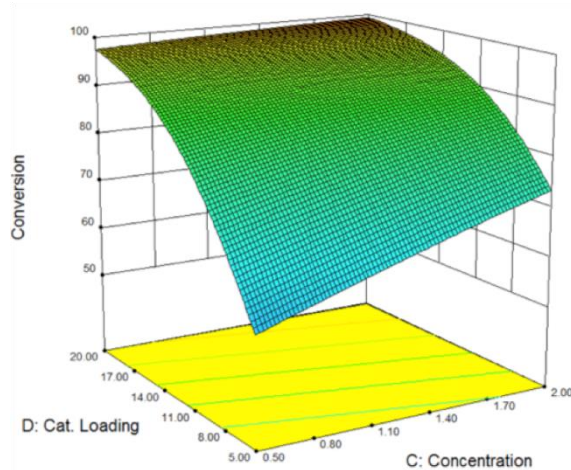


Figure 29: 3D plot of experimental results comparing catalyst loading and concentration

With this two-factor interaction in mind, attention was focused on identifying a set of reaction conditions which would maximise conversion to product whilst making economical use of the base catalyst. Based on analysis of DoE results, time and temperature did not appear to be exerting a significant effect on the outcome of the reaction. Consequently, with the intention of maintaining mild reaction conditions, temperature was set to the lowest value within the ranges defined. Similarly, a 15 hour reaction time was selected as it was deemed to be the most practical. High concentrations were shown to favour product formation (Figure 29), therefore a 2 M reaction concentration was retained. Finally, as the intention was to develop an atom-economical amidation method, it was important to keep the catalyst loading as low as possible. Therefore, using the conditions described, two further reactions were performed using 10 and 20 mol% BEMP in order to determine the consequence of lowering catalyst loading (Table 16). Pleasingly, only a small difference in conversion was observed between these two reactions, with 90% conversion being obtained using only 10 mol% of the base catalyst. Isolated yields were in good agreement with HPLC-derived conversions, indicating that amide products could be readily isolated from the reaction mixture in high purity.

Table 16: Results from additional experiments

Reaction	Time (h)	Temperature (°C)	Concentration (M)	Catalyst Loading (mol%)	Conversion (%)^a	Yield (%)^b
11	15	20	2	10	90	87
12	15	20	2	20	94	92

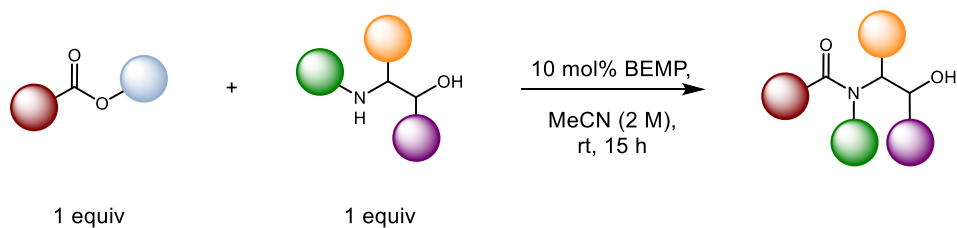
^aConversion determined by HPLC with reference to an internal standard; ^bIsolated yield

Employing DoE to expedite the optimisation of reaction conditions proved to be extremely effective for this process. Having previously identified BEMP and MeCN as a superior combination for base-catalysed amidation, it was possible to fully optimise this process in a rapid fashion whilst performing a minimal number of experiments. Using DoE software, it was possible to identify significant effects on the response and gain a clearer understanding of which factors were important for generating high conversion to amide product. Ultimately, optimised reaction conditions (Table 16, Reaction 11) demonstrated an increase in conversion from 63% to 90% compared to the maximum results obtained during base and solvent screening. This represents an appreciable improvement in the efficiency of this process.

3.5.3 Examination of Substrate Scope for BEMP-catalysed Amidation

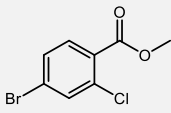
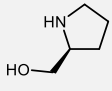
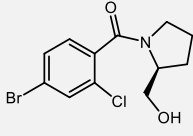
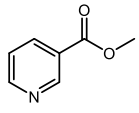
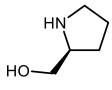
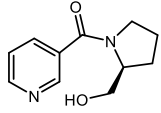
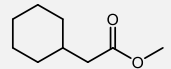
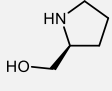
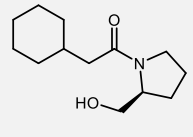
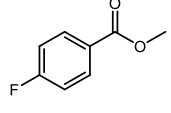
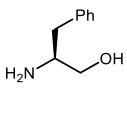
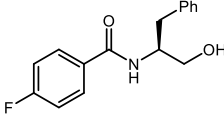
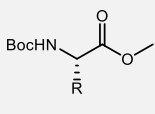
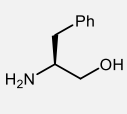
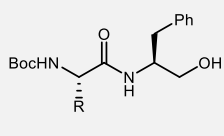
Following the development of optimised reaction conditions for BEMP-mediated amidation of methyl benzoate using ethanolamine, it was necessary to determine whether these conditions would also be applicable to amide bond formation when employing alternative starting materials. To this end, a range of substrates were investigated for their suitability in this reaction (Table 17).

Results and Discussion - Optimisation of Base-catalysed Amidation

 Table 17: Substrate scope for BEMP-catalysed amidation¹⁰⁰


Entry	Ester	Amino Alcohol	Product	Yield (%) ^a
1	 R = H		 R = H (110)	87
2	R = 4-CF ₃		R = 4-CF ₃ (111)	95
3	R = 4-MeO		R = 4-MeO (118)	82
4	R = 2-Me		R = 2-Me (119)	60 (94) ^b
5	 R = Ph		 R = Ph (58)	99
6	R = Cy		R = Cy (120)	100
7	 X = O, R = Me		 X = O (121)	94
8	X = S, R = Et		X = S (122)	99
9	 R ₁ = Me, R ₂ = Me		 R ₁ = Me (113)	97
10	R ₁ = <i>i</i> -Pr, R ₂ = Me		R ₁ = <i>i</i> -Pr (123)	99
11	R ₁ = <i>t</i> -Bu, R ₂ = Me		R ₁ = <i>t</i> -Bu (124)	61 (91) ^b
12	R ₁ = Me, R ₂ = <i>i</i> -Pr		R ₁ = Me (113)	100
13	R ₁ = Me, R ₂ = <i>t</i> -Bu		R ₁ = Me (113)	9 (70) ^b
14	 R = H		 125	89

Results and Discussion - Optimisation of Base-catalysed Amidation

Entry	Ester	Amino Alcohol	Product	Yield (%) ^a
15				93 (92) ^c
16				86
17				40 (75) ^b
18				58 (69) ^b
19				75
20	R = CH ₂ Ph		R = CH ₂ Ph (131)	80 ^d

^aIsolated yield; ^bReaction performed at 40 °C; ^cPrepared on 2.5 g scale; ^dd.r. = 86:14, determined by chiral HPLC

Variation of the ester starting material indicated that both electron-withdrawing (Entry 2) and electron-donating (Entry 3) aromatic substituents were tolerated. A methyl group in the *ortho*-position (Entry 4) caused the yield to decrease to 60%, due to steric hindrance at the carbonyl group. However, it was possible to overcome this issue by increasing the temperature to 40 °C, resulting in an improved isolated yield of 94%.

Aliphatic (Entries 5, 6, and 9 – 13) and heterocyclic (Entries 7 and 8) esters were also suitable for amide formation and gave isolated products in excellent yield. Variation of the leaving group (Entries 8, 12, and 13) indicated that ethyl, *iso*-propyl, and *tert*-butyl

Results and Discussion - Optimisation of Base-catalysed Amidation

functionalities were suitable although the latter displayed lower yields (Entry 13) due to increased steric hindrance at the carbonyl group. However, when the temperature was increased to 40 °C, a concomitant improvement in yield was observed.

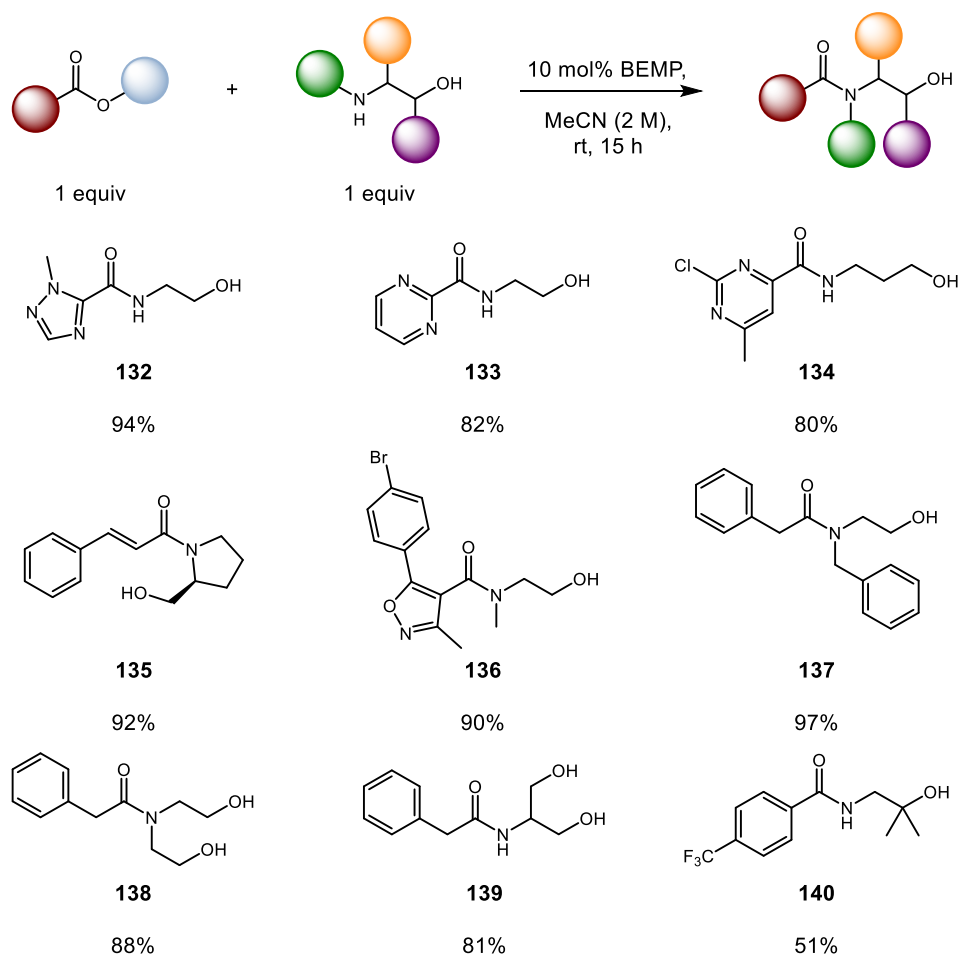
Subsequently, alternative amino alcohol substrates were assessed for use in this reaction. Increasing the chain length to propanolamine (Entry 14) proceeded to form amide **125** in excellent yield. A cyclic secondary amino alcohol was also examined as an alternative starting material (Entries 15 – 17). (*S*)-Prolinol was reacted with aromatic (Entry 15), heterocyclic (Entry 16), and aliphatic (Entry 17) esters to furnish the corresponding products in good yield. Furthermore, amide **126** could be prepared in excellent yield on a larger scale, producing almost 3 grams of material for use as an intermediate in an in-house medicinal chemistry programme (*vide infra*). Previous syntheses of this particular compound using stoichiometric reagents such as HATU, COMU and propylphosphonic acid solution (T3P) were either low yielding or had significant problems associated with the removal of the urea by-product in the case of uronium reagents. Therefore, this methodology allowed facile access to this compound in high yield, purity, and on an acceptable scale.

Phenylalaninol could be employed as the amino alcohol partner, albeit displaying slightly lower yields when coupled with an aromatic ester (Entry 18). Two examples of amino acid-derived substrates were also prepared using the phenylalaninol starting material (Entries 19 and 20). However, determination of the diastereomeric ratio (d.r.) for compound **131**, which was derived from Boc-phenylalanine methyl ester, showed slight erosion of the chiral integrity at the α -position (d.r. = 86:14), indicating a potential limitation of using this methodology with chiral esters. The development of alternative catalytic amidation methods helped address this issue and will be discussed in subsequent sections.

Following the initial elucidation of substrate scope as displayed in Table 17, it was demonstrated that a broad range of esters and amino alcohols were tolerated using the optimised conditions for BEMP-mediated amidation. Coupled products were isolated in excellent yield for the majority of substrates. Subsequent work by other members of our laboratory sought to perform a more comprehensive investigation of substrate scope in order to fully establish the utility of this process.^{108,109} To date, an extensive range of amide products have been prepared (53 examples, 40 – 100%), emphasising the wide applicability of this mild, organocatalytic amide bond forming method, and pertinent examples are

Results and Discussion - Optimisation of Base-catalysed Amidation

highlighted in Scheme 40. A variety of alternative heterocyclic ester starting materials were explored, with triazole- (**132**), pyrimidine- (**133** and **134**), and isoxazole-derived (**136**) amides being obtained in excellent yield. Further examination of the amino alcohol scope demonstrated that both cyclic (**135**) and acyclic (**136 – 138**) secondary amido alcohols could successfully be prepared using this methodology. Both primary and secondary diols were also tolerated to form compounds **138** and **139**. Finally, a tertiary alcohol-containing compound was coupled with an electron-deficient ester forming amide **140**, albeit in slightly reduced yield. No reaction with a tertiary alcohol was observed in the case of electron-neutral esters, suggesting that the presence of an electron-withdrawing group in the *para*-position was essential to activate the carbonyl towards nucleophilic attack by the alcohol functionality in this instance. The reduced yield for this substrate was attributed to reduced ability of a sterically bulky tertiary alcohol to undergo transesterification. Subsequent rearrangement of the ester intermediate to the corresponding amide should be relatively fast, promoted by the gem-dimethyl group as a result of the Thorpe-Ingold effect.¹¹⁰



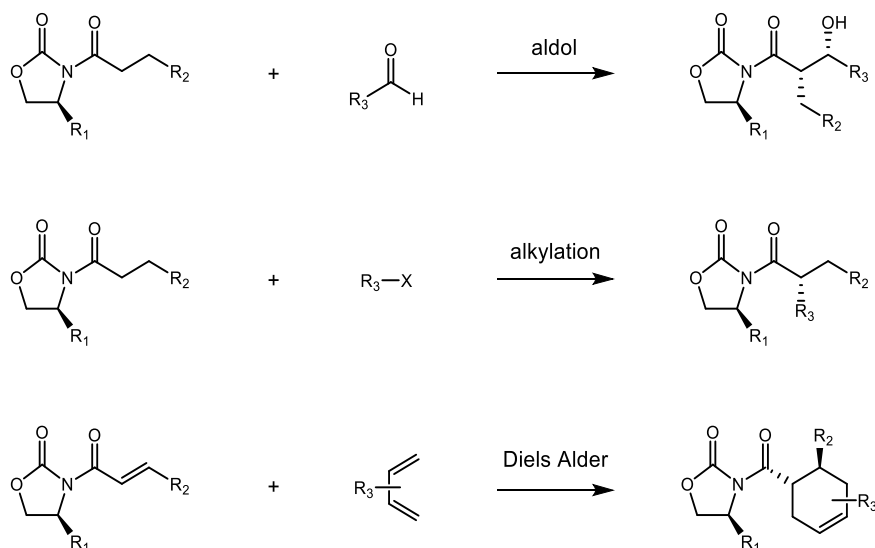
Scheme 40: Selected examples from extensive examination of substrate scope^{108,109}

Results from this investigation showed that in each case, isolated yields in the presence of alternative phosphazene bases (Entries 2 and 3) were comparable to that previously obtained with BEMP (Entry 1). This suggests that these bases could be suitable as cost-effective alternatives to BEMP. Indeed, subsequent literature reports have indicated how other cost-effective reagents (e.g. sodium carbonate) are effective in this reaction, albeit with more elevated temperatures being required.¹¹¹

3.5.3.2 Synthesis of Oxazolidinone Derivatives

Following the extensive evaluation of substrate scope for this process, it was evident that BEMP-mediated amidation was applicable to a wide range of ester and amino alcohol starting materials. Subsequently, attention turned to determining whether this methodology could also be utilised in other areas of organic synthesis. It was reasoned that substitution of the ester coupling partner for dimethylcarbonate could facilitate access to oxazolidinone-derived products. Pioneered by Evans, oxazolidinone motifs are commonly encountered as chiral auxiliaries in second generation asymmetric syntheses.¹¹² These structures are readily accessed from amino acids and can facilitate diastereoselective reactions, generating products with high enantiomeric excess (ee) upon removal of the auxiliary. The oxazolidinone group is usually attached to a prochiral substrate using the appropriate acid chloride in the presence of base, allowing diastereoselective reactions to occur at the α -carbon or a conjugated alkene. Asymmetric aldol,¹¹³ alkylation,¹¹⁴ and Diels Alder transformations¹¹⁵ can be executed in this manner (Scheme 41). The auxiliary can then be removed by derivatisation to a variety of products with generally high ee.

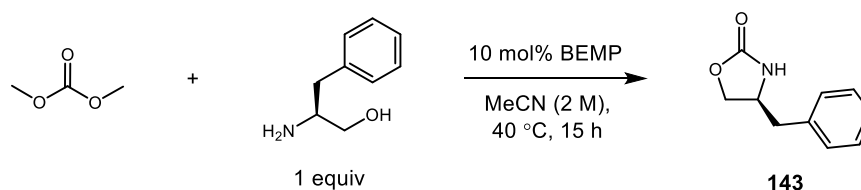
Results and Discussion - Optimisation of Base-catalysed Amidation



Scheme 41: Asymmetric syntheses using oxazolidinones as chiral auxiliaries

As intimated previously, oxazolidinone structures are commonly derived from amino acids. Typical syntheses of these compounds involve reduction to the corresponding amino alcohol, followed by cyclisation using diethyl carbonate. However, the cyclisation reaction commonly requires elevated temperatures (135 °C). It was believed that employing the BEMP-catalysed amidation method could enable the transformation to occur at milder temperatures and could potentially offer a more favourable route to this type of compound.

Accordingly investigation into the synthesis of oxazolidinones was carried out in conjunction with another member of our laboratory.¹⁰⁹ Using the conditions which had been employed previously for substrate scope, at a slightly elevated temperature (40 °C), a brief investigation of stoichiometry was carried out in a trial reaction with dimethyl carbonate (DMC) and phenylalaninol (Table 19). Results from this study indicated that three equivalents of DMC were optimal, displaying high conversion to the desired oxazolidinone product (**143**). Additionally, conversion to product was found to be greater when the reaction was performed in MeCN, rather than using neat DMC. Using an excess of DMC with respect to the amino alcohol was not considered to be detrimental as this reagent is relatively inexpensive and can be readily removed under vacuum prior to purification of products.

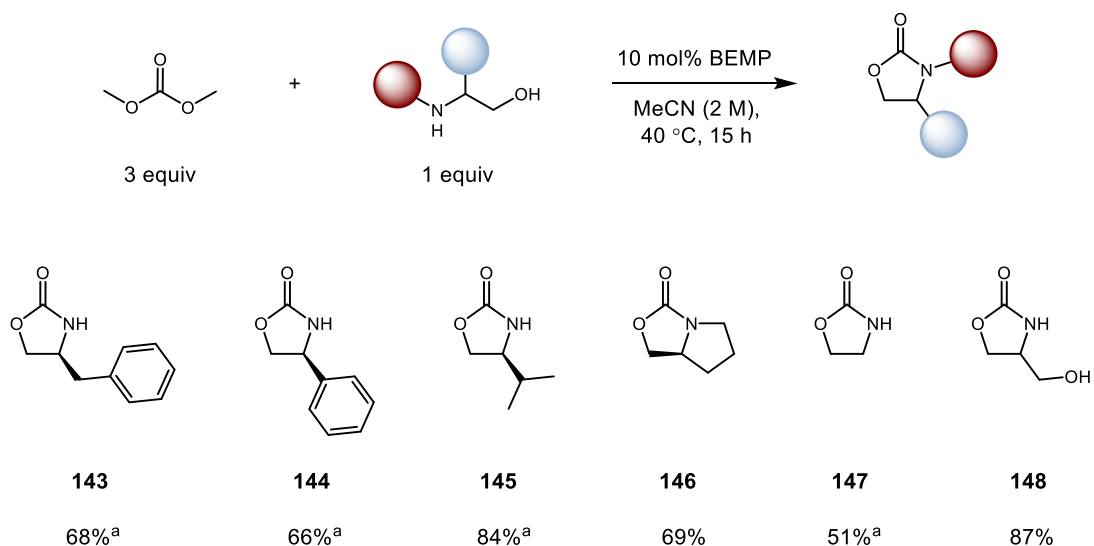
Table 19: Investigation of DMC stoichiometry¹⁰⁸

Entry	Dimethyl carbonate (equiv)	Conversion (%) ^a
1	1	68
2	3	72
3	5	69
4	6 (neat)	61

^aConversion determined by HPLC with reference to an internal standard

Therefore, using the optimised reaction conditions developed and as communicated in Section 3.5.2 as a starting point, slight modification to the stoichiometry of starting material was sufficient to adapt this process for use with a different class of compound. Following this short screening process, a number of oxazolidinone derivatives were prepared in comparable yield to progenitor processes (Scheme 42). Phenylalanine, phenylglycine, and valine-derived amino alcohols all proceeded to give the corresponding oxazolidinone systems (**143** – **145**) in good yield. These types of compounds in particular are commonly encountered as second generation chiral auxiliaries for the reactions described above. As an additional proteinogenic example, proline could be successfully converted to its oxazolidinone equivalent (**146**). An ethanolamine-derived substrate (**147**) displayed only moderate yields but this was attributed with purification issues. It is believed that further optimisation of this procedure would result in increased yields. Finally, it was shown that diols were also tolerated in this reaction (**148**). In general, this synthesis represents an improved method for the formation of oxazolidinones, furnishing products under considerably milder conditions.

Results and Discussion - Optimisation of Base-catalysed Amidation



Scheme 42: Application of methodology to the synthesis of oxazolidinone derivatives. ^aCompound prepared by another member of our laboratory^{108,109}

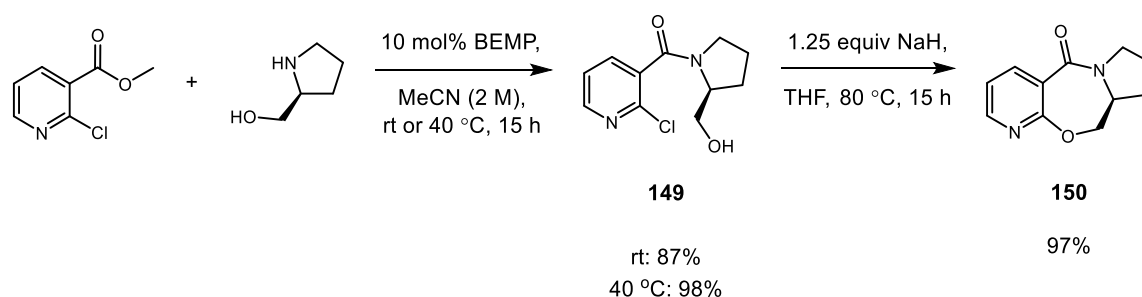
3.5.3.3 Synthesis of Medicinally-relevant Compounds

In addition to the application of the BEMP-catalysed amidation process to the preparation of oxazolidinone derivatives, we next sought to exemplify the methodology in the synthesis of some biologically active compounds. As discussed in Section 1.1, amide bond formation is the most prevalent reaction performed in a pharmaceutical setting, and marketed drug molecules commonly contain this functionality.^{1,3} Therefore, it was important to demonstrate that the developed methodology could be applied to the synthesis of medicinally-relevant compounds. Drug-like compounds which contained an amido alcohol functionality could potentially be prepared using the novel base-catalysed amidation method as the key reaction step. This could enable a mild, catalytic alternative to the synthesis of this type of compound. As mentioned in Section 3.5.3, application of the BEMP-catalysed amidation method to the synthesis of a key intermediate (**126**) in our own medicinal chemistry programme had facilitated access to a gram scale amount of material which exhibited improved yield and purity compared to previous syntheses of this compound. Therefore, we were keen to determine whether this would also be the case with other drug-like compounds.

Accordingly, Org 26576 (**150**),¹¹⁶ a positive allosteric modulator of the α -amino-3-hydroxy-5-methyl-4-isoxazole propionic acid (AMPA) receptor was selected as the first target compound. Due to their association with cognitive function, AMPA receptors have been

Results and Discussion - Optimisation of Base-catalysed Amidation

implicated in the treatment of a range of neurological diseases.¹¹⁷ Based on this, Org 26576 has undergone Phase 2 clinical trials for Attention Deficit/Hyperactivity Disorder (ADHD) and depression. A previously reported synthesis of this compound used stoichiometric quantities of DCC and HOBT in the presence of *N*-methylmorpholine to couple nicotinic acid and (*S*)-prolinol, forming the desired intermediate (**149**) in 87% yield.¹¹⁸ However, by adapting this synthesis and using the optimised BEMP-catalysed protocol to perform amidation of the corresponding nicotinate ester, this key intermediate could be synthesised in comparable yield to the progenitor process (Scheme 43) using only a catalytic amount of base. Furthermore, increasing the temperature slightly to 40 °C proceeded to form this product in almost quantitative yield. Treatment of the amide with NaH enabled the requisite nucleophilic aromatic substitution reaction to furnish the desired cyclised product. Therefore, exploitation of base-catalysed amidation in this instance allowed access to the desired drug molecule in excellent yield over two steps, representing a much more efficient synthesis of this useful compound.

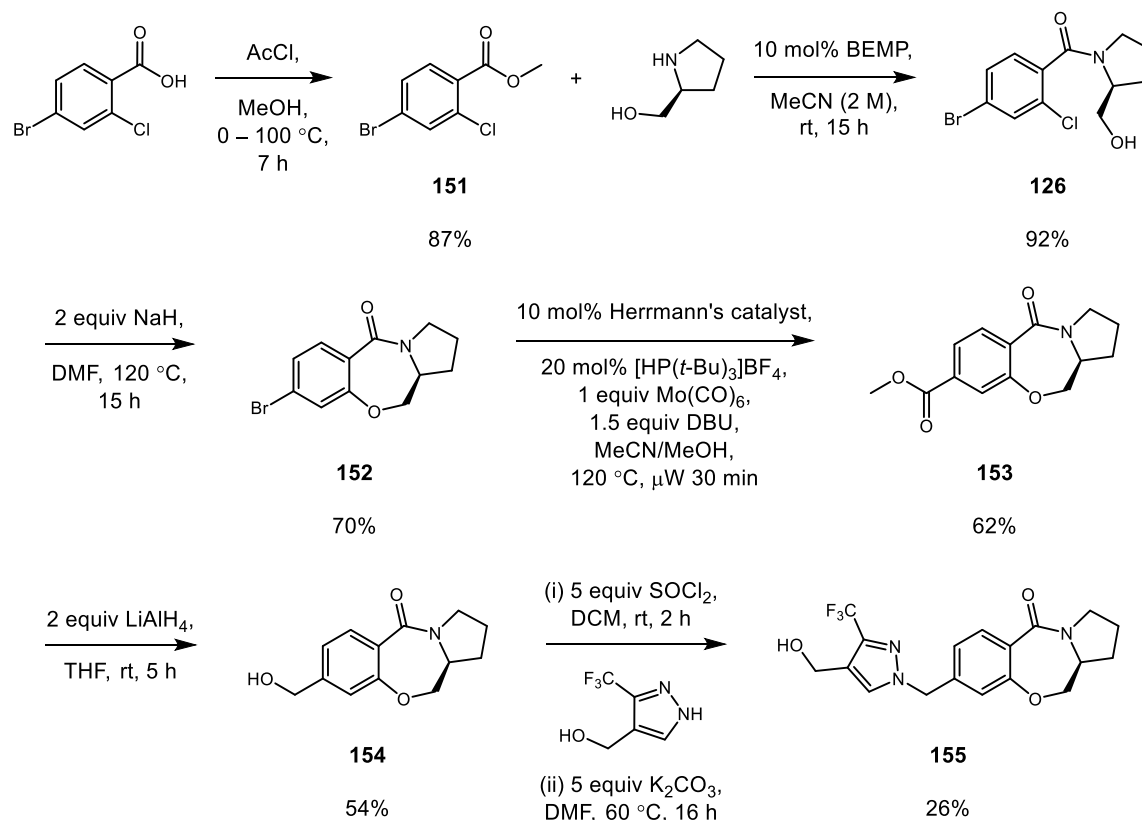


Scheme 43: Synthesis of Org 26576

In addition to the preparation of a known AMPA receptor modulator, this methodology was also exploited in the synthesis of novel compounds targeting the AMPA receptor (Scheme 44). As mentioned in Section 3.6, amide **126** could be prepared in excellent yield on a gram scale, allowing facile access to this compound for use in an in-house medicinal chemistry programme. As part of this effort, a novel AMPA receptor modulator (**155**) was designed *via* a hybridisation approach, combining important functionalities from different literature chemotypes. Employing the optimised BEMP-catalysed amidation process enabled access to a key intermediate (**126**) in the synthesis of this target compound, in higher yield and purity than could previously be achieved using a range of traditional stoichiometric coupling reagents. Subsequent S_NAr cyclisation furnished the corresponding tricyclic intermediate (**152**). A palladium-catalysed carbonylation reaction followed by reduction produced the

Results and Discussion - Optimisation of Base-catalysed Amidation

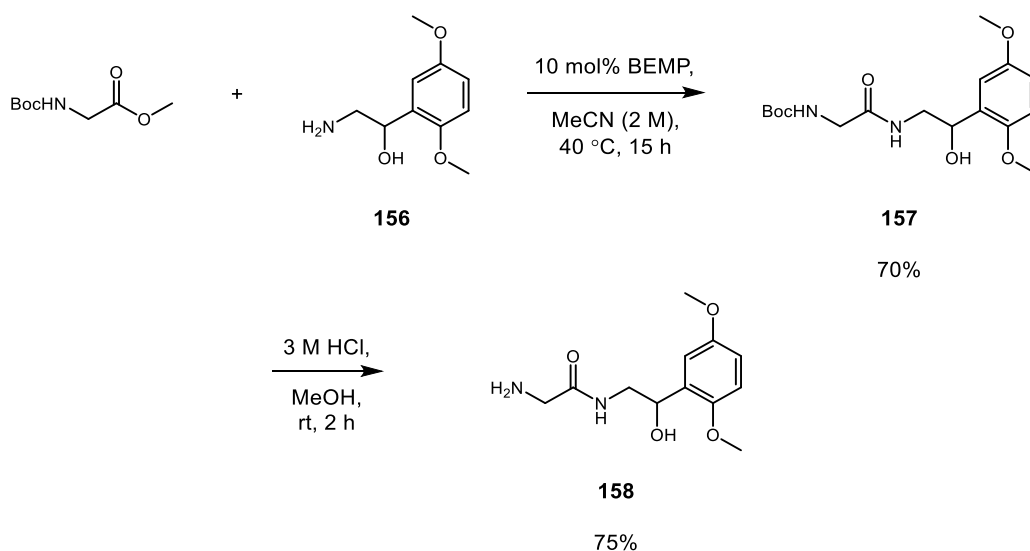
desired alcohol precursor (**154**), which could be subjected to chlorination and substitution to form the requisite pyrazole-derived product (**155**). Pleasingly, biological results for this novel compound indicated greater potency and efficacy compared to progenitor compounds,¹¹⁹ underlining the value of the current methodology in target molecule synthesis in a medicinal chemistry setting.



Scheme 44: Synthesis of a novel AMPA receptor modulator¹¹⁹

Finally, a third molecule was targeted through exploitation of this methodology (Scheme 45). Midodrine (**158**) is an α_1 -receptor agonist used clinically for the treatment of orthostatic hypotension.¹²⁰ Boc glycine methyl ester could be coupled with the commercially available amino alcohol (**156**) to form the protected product in 70% yield. As noted in the case of compound **140**, sterically hindered alcohols are more challenging substrates for this process, so slightly elevated temperatures were employed from the outset for reacting a secondary alcohol. Subsequent deprotection of the Boc group delivered the final product in 75% isolated yield. These syntheses (Schemes 43 – 45) proceeded to form the desired product through exploitation of BEMP-mediated amidation as a key reaction step, highlighting the utility of this method in a medicinal chemistry setting.

Results and Discussion - Optimisation of Base-catalysed Amidation

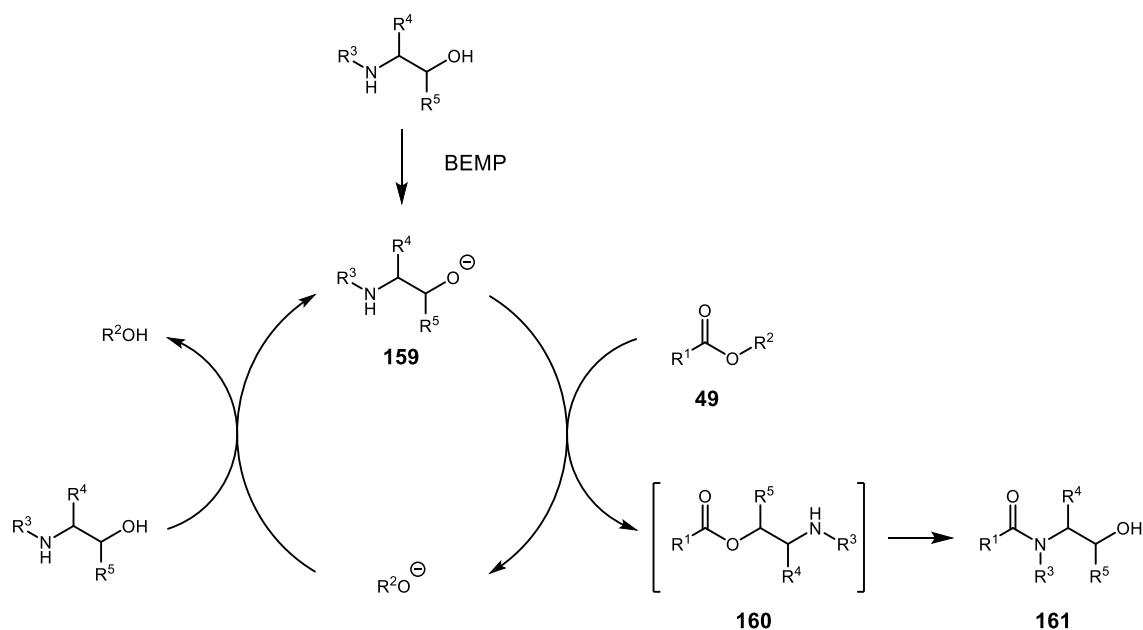


Scheme 45: Synthesis of Midodrine

3.5.4 Investigation of Mechanism for BEMP-mediated Amidation

It had been established that BEMP-mediated amidation was applicable to an extensive range of substrates and could also be extended to the synthesis of oxazolidinone derivatives and medically-relevant compounds. The next stage of this study was to further investigate the underlying mechanism of this process (Scheme 46). As stated in Section 3.4.4, the proposed mechanism for this reaction involves attack of the ester starting material (**49**) by an amino alcohol anion (**159**) to form the corresponding transesterification intermediate (**160**), which undergoes rearrangement to the more thermodynamically stable amide product (**161**). As the inclusion of an alcohol functionality is crucial for the reaction to proceed, progression through an ester intermediate is valid. However, it was not possible to isolate this type of intermediate from the reaction mixture for any of the substrates examined, even when sterically hindered amino alcohols were employed, as in the case of the tertiary alcohol-derived compound (**140**). Similarly, the presence of such an intermediate was not observed when following the course of the reaction by HPLC. Additionally, for the progenitor NHC-mediated process elucidated by Movassaghi and Schmidt,⁷⁴ React-IR analysis of reaction progression showed only a transient peak corresponding to the proposed transesterification intermediate. This evidence would suggest that if the proposed mechanism is operating, transesterification is the rate-determining step of this transformation and, upon formation of the transient ester species, rapid rearrangement to the amide product occurs. Therefore, as part of this investigation, it was important to confirm the existence of this putative ester intermediate, and whether the subsequent rearrangement process was intra- or

intermolecular in nature. These investigations were carried out in conjunction with another member of our laboratory.^{108,109}

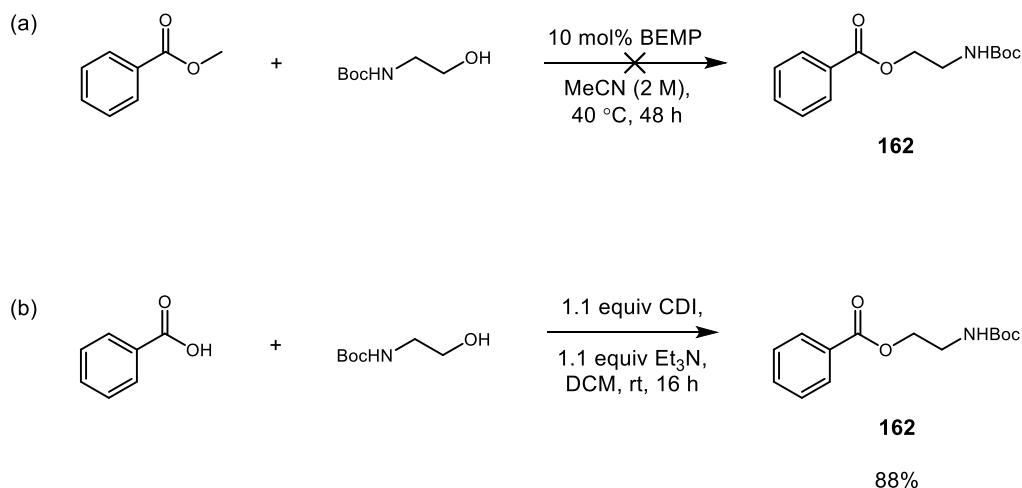


Scheme 46: Proposed mechanism for BEMP-catalysed amidation

3.5.4.1 Rearrangement of Ester

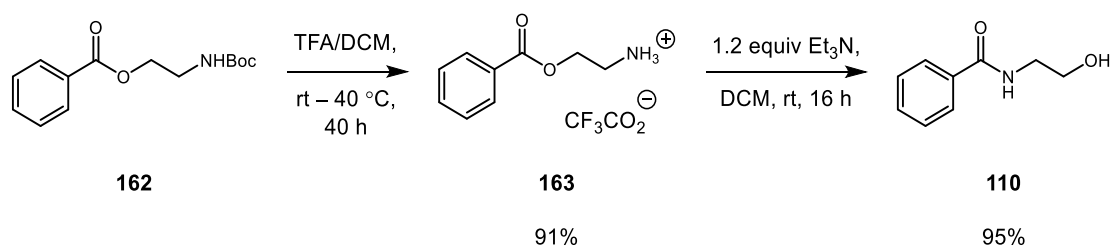
In order to directly examine the ester to amide rearrangement reaction, a model ester substrate (**162**) was synthesised independently (Scheme 47). Boc-protected ethanolamine was employed for this purpose in order to preclude spontaneous rearrangement to the amide upon formation of the ester species. Initial attempts to isolate the ester *via* BEMP-mediated amidation of methyl benzoate were unsuccessful, even under more forcing conditions (40 °C, 48 h). Presumably the esterification reaction is reversible if rearrangement to the more stable amide cannot take place, and so the equilibrium lies predominantly on the side of the starting materials. Consequently, the desired ester was prepared using 1,1'-carbonyldiimidazole (CDI)-mediated esterification of benzoic acid.

Results and Discussion - Optimisation of Base-catalysed Amidation



Scheme 47: Preparation of an ester intermediate^{108,109}

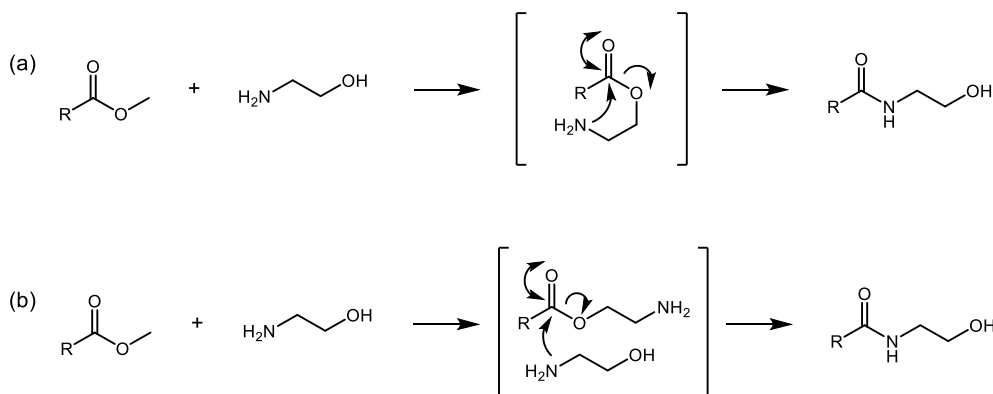
Following isolation of this Boc-protected compound, it could be used in subsequent studies to determine whether an ester of this type was capable of rearranging to the corresponding amide. Removal of the Boc protecting group using trifluoroacetic acid (TFA) allowed the deprotected amine to be obtained as the corresponding salt (**163**), preventing premature rearrangement to the amide by forming a positively charged, non-nucleophilic amine species. Subsequent treatment of the amine salt with Et₃N resulted in almost quantitative conversion to the desired amide (**110**). Isolation of this product in excellent yield and analysis by infrared (IR) spectroscopy showed a shift of the carbonyl absorbance from 1725 to 1625 cm⁻¹, confirming the rearrangement of ester to amide. This study validated the hypothesis that an intermediate ester of this type was capable of undergoing the proposed rearrangement reaction.



Scheme 48: Rearrangement of ester intermediate^{108,109}

In the absence of exogenous amino alcohol, smooth conversion of intermediate ester **163** to amide **110** was observed, indicating that this process was intramolecular in nature. However, under the base-mediated amidation conditions in the presence of excess amino alcohol, it is

possible that both intra- and intermolecular rearrangement mechanisms could operate (Scheme 49).



Scheme 49: Proposed mechanisms for rearrangement reaction *via* (a) intramolecular and (b) intermolecular pathways

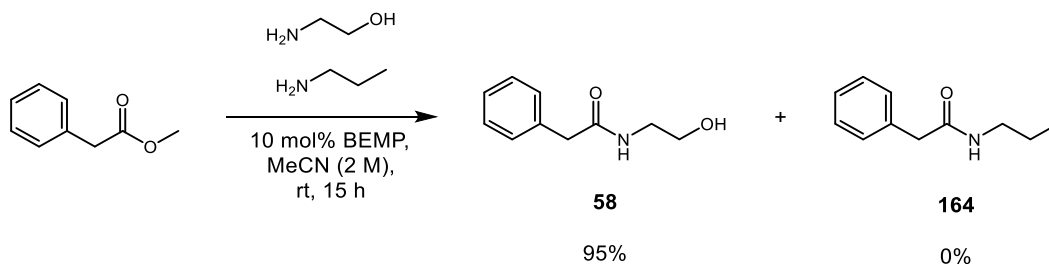
The intramolecular rearrangement process (Scheme 49a), which proceeds *via* a five-membered transition state in the case of ethanolamine, is entropically more favourable.¹²¹ However, in order to explore this further and determine whether intramolecular rearrangement was occurring under the base-catalysed reaction manifold, a number of probe substrates were designed.

3.5.4.2 Competition Reactions

Results from a preliminary study where almost quantitative conversion of an isolated ester substrate (**163**) to the corresponding amide was observed (**110**, Scheme 48), confirmed that intramolecular rearrangement of this type of substrate was possible. However, it was uncertain whether this was the sole rearrangement mechanism operating under standard conditions, as an intermolecular process could also be conceived. Therefore, a reaction was designed to examine whether competing intermolecular rearrangement could occur. Previous work by Movassaghi demonstrated that for the progenitor NHC-catalysed amidation reaction, a competition reaction employing both ethanolamine and benzylamine gave the amido alcohol-derived product exclusively (Scheme 20).⁷⁴ However, it was deemed prudent to perform a similar competition reaction in our own hands to determine whether this was also the case under the novel base-catalysed amidation reaction conditions. Therefore, methyl phenylacetate was reacted with an equivalent of both ethanolamine and propylamine (Scheme 50). If an intermolecular rearrangement process of the type shown in Scheme 49b were to occur, a mixture of products should be formed as a result of

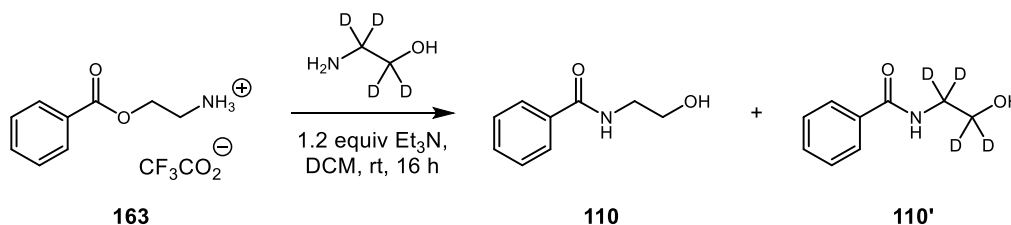
Results and Discussion - Optimisation of Base-catalysed Amidation

propylamine reacting with the intermediate ethanolamine-derived ester. However, no conversion to the aliphatic amine-derived product (**164**) was observed by HPLC or LCMS analysis during the course of the reaction and the amido alcohol (**58**) was isolated exclusively in 95% yield. This result supports the view that an intramolecular rearrangement mechanism is more favourable for this process.



Scheme 50: Competing reaction with ethanolamine and propylamine^{108,109}

Future work to conclusively exclude the possibility of an intermolecular rearrangement process occurring in the case of amino alcohols could involve the use of a labelled starting material. A cyclisation reaction using the isolated ester intermediate (**163**) in the presence of deuterium-labelled ethanolamine could be carried out (Scheme 51). If no labelled material is observed in the product, the possibility of a simultaneous intermolecular reaction can be ruled out.



Scheme 51: Proposed reaction using deuterium-labelled ethanolamine

3.5.4.3 Further Investigation of Rearrangement

Based on evidence from a competition reaction employing both an amino alcohol and an aliphatic amine where only the amido alcohol product was observed, it was likely that an intramolecular rearrangement mechanism was operating. For the ethanolamine trial substrate used, the proposed rearrangement step would take place *via* a favourable five-membered transition state (Scheme 49a). Therefore, in order to observe whether intermolecular rearrangement would occur for alternative amino alcohols, an additional set

Results and Discussion - Optimisation of Base-catalysed Amidation

of substrates were examined which were more sterically constrained than those employed for previous mechanistic studies (Figure 30). Again this work was carried out by another member of our laboratory.^{108,109} Each amino alcohol was examined in a trial reaction with methyl phenylacetate using the standard BEMP-catalysed amidation conditions (Table 16, Reaction 11). Firstly, 4-hydroxypiperidine was used, which was conformationally locked and thus incapable of forming the cyclic transition state required to undergo intramolecular rearrangement. No conversion to the corresponding amide (**165**) was observed, suggesting that an intermolecular mechanism does not occur when the intramolecular rearrangement process is precluded. Similarly, no product (**166**) was isolated using 4-aminomethylbenzylalcohol due to the inability of this substrate to perform the desired intramolecular rearrangement. No ester by-products were observed using either substrate, which could be due to the reversible nature of this reaction when the thermodynamic driving force of amide bond formation is not operating. This is in accordance with previous unsuccessful attempts to isolate a representative ester intermediate (Scheme 47).

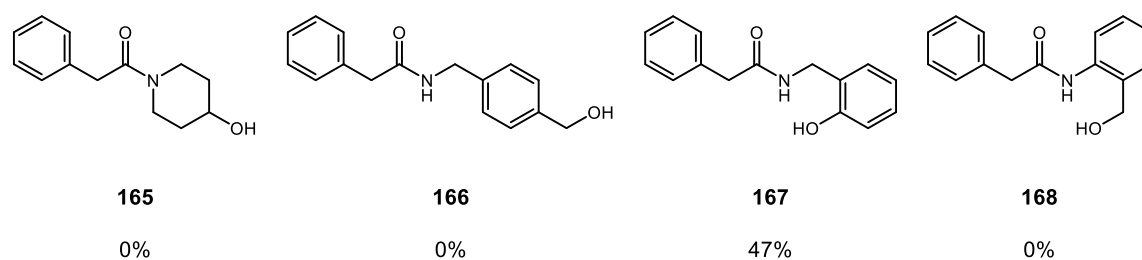


Figure 30: Probe molecules to investigate intermolecular rearrangement¹⁰⁸

In order to further probe the limitations of this methodology, two additional substrates (**167** and **168**) were examined, employing isomeric starting materials which would be capable of undergoing intramolecular rearrangement. Whilst 2-(aminomethyl)phenol could be coupled in moderate yield, a reaction using the analogous starting material, 2-aminobenzylalcohol, was unsuccessful. This suggests that whilst phenols are capable of performing the initial transesterification reaction, anilines are not competent substrates, presumably due to reduced nucleophilicity in the rearrangement process. As the substrates examined in this instance were isomeric, it is likely that electronic rather than steric effects are responsible for the lack of reactivity for anilines.

During investigation of the substrates outlined in Figure 30, no amide products were observed when sterically constrained amino alcohols were employed, suggesting that a

competing intermolecular rearrangement mechanism was not operating. Additionally, it appeared that aniline-containing substrates were unable to participate in the rearrangement process due to reduced nucleophilicity. However, the outcomes of these reactions could also be related to their pKa values and, consequently, ability to undergo the initial transesterification event. As phenol is more acidic (pKa: ~10 (H₂O)) than an aliphatic alcohol (pKa: ~15 (H₂O)), it may be more readily deprotonated by BEMP and, hence, more reactive in the transesterification reaction. Conversely, as no ester by-product was observed in the attempted synthesis of amides **165**, **166**, and **168**, it is possible that the benzyl or aliphatic alcohol functionalities were less readily deprotonated and were therefore unable to undergo esterification.

3.5.4.4 Altering Chain Length

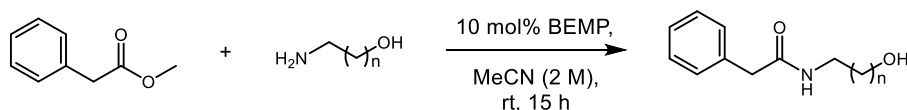
Rearrangement of an isolated ester intermediate and complementary studies examining reactions which had been designed to investigate the underlying mechanism of ester to amide rearrangement supported the proposal that an intramolecular reaction was taking place. However, pKa of the alcohol functionality could also be a factor in the reduced reactivity of these substrates, precluding the initial transesterification reaction required for subsequent amide bond formation. In order to provide additional evidence in support of an intramolecular rearrangement mechanism, a final study was carried out to observe the effect of altering the amino acid chain length sequentially from ethanolamine to pentanolamine. It was hypothesised that homologation of the carbon linker of the amino alcohol should have a detrimental effect on the yield of the reaction due to the increased ring strain associated with larger ring systems (Table 20). Based solely on the ring strain energies shown in Table 20, propanolamine should be the most reactive starting material in this process due to the formation of a six-membered cyclic transition state. However, it was also anticipated that increasing the chain length could result in a decrease in yield due to the increased flexibility of the system which would disfavour the intramolecular rearrangement process.

Table 20: Ring strain energies associated with cycloalkane ring sizes¹²²

Ring Size	Strain Energy (kcal/mol)
5	6.2
6	0.1
7	6.2
8	9.7

In order to test this hypothesis, a range of amido alcohols were prepared by another member of our laboratory from methyl phenylacetate (Table 21).^{108,109} The amino alcohol chain length was incrementally increased from ethanolamine to pentanolamine, thus increasing the proposed cyclic transition state from a five-membered to an eight-membered ring. Previously, the ethanolamine-derived substrate (**58**) had been obtained in almost quantitative yield from this process (Table 17, Entry 5). In comparison, a slight reduction in yield was observed when replacing ethanolamine with propanolamine (Table 21, Entry 2). As stated above, propanolamine should offer the greatest reactivity in this reaction manifold based exclusively on ring strain energy, therefore it appeared that the increased flexibility was having a detrimental effect on conversion. A more pronounced effect was observed in the case of butanolamine with the isolated product (**170**) only being obtained in 40% yield at elevated temperatures. Finally, pentanolamine showed no conversion to the corresponding amide product (**171**) even at elevated temperatures. This result was unsurprising as this amino alcohol had a higher degree of flexibility and would also incur more ring strain through the formation of an eight-membered cyclic transition state.

Table 21: Effect of altering chain length



Entry	Chain Length (n)	Product	Yield (%) ^a
1	1	 58	99
2 ¹⁰⁸	2	 169	80
3 ¹⁰⁸	3	 170	20 (40) ^b
4 ¹⁰⁸	4	 171	0 ^b

^aIsolated yield; ^bReaction performed at 40 °C

In addition to entropic considerations and penalties associated with the formation of unfavourable ring systems, it was possible that the pKa of the amino alcohol derivative could be affecting the outcome of the reaction, as was inferred for the substrates examined in Figure 30. An increase in pKa could lead to reduced reactivity in the initial transesterification reaction, decreasing the yield for the overall process. Ethanolamine has a measured pKa value of 9.5 (H₂O),⁹⁸ which is considerably lower than that of an aliphatic alcohol (pKa ~ 15 (H₂O)). Therefore, based on a similar argument to that outlined above for the phenol-derived substrate (**167**), ethanolamine is likely to be more readily deprotonated and, hence, more reactive in the transesterification reaction. The increased acidity of the alcohol moiety in the case of ethanolamine could be attributed to the electron-withdrawing nature of the nitrogen atom in the amino alcohol chain. Alternatively, a stabilising hydrogen-bonding interaction could exist between the deprotonated alcohol and an amine proton through the formation of a cyclic species (Figure 31), which would also account for increased acidity of the alcohol. Upon increasing the chain length of the amino alcohol, it

would be expected that pKa values would increase due to the extra inductively electron-donating alkyl groups preventing the effect of the electron-withdrawing nitrogen atom on the alcohol functionality. Additionally, if a stabilised cyclic species was being formed, increasing the chain length of the amino alcohol would consequently increase the size of the ring system formed, incurring a greater degree of strain. Therefore, greater stabilisation effects may be observed for ethanolamine and propanolamine due to the formation of favourable ring sizes.

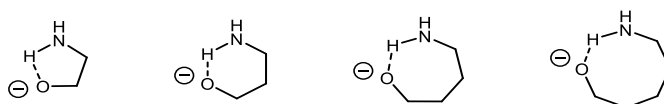


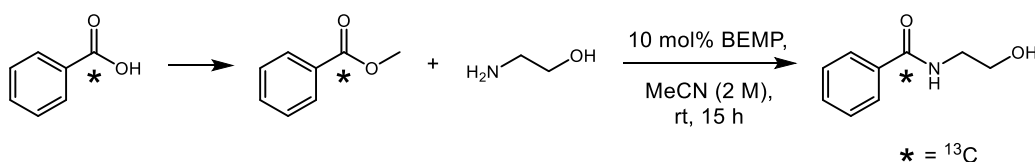
Figure 31: Proposed stabilisation of deprotonated amino alcohols

However, upon consideration of calculated pKa values¹²³ for propanolamine (9.9), butanolamine (10.3), and pentanolamine (10.5), these did not vary significantly. As all pKa values were well below those of both BEMP and methoxide, complete deprotonation should occur and the initial transesterification process should be feasible for all of these substrates. Therefore, differences in reactivity observed upon increasing the chain length of the amino alcohol were unlikely to be attributable to changes in pKa. It is likely that the reduction in yield observed upon increasing the chain length of the amino alcohol (Table 21) occurred as a result of increased flexibility of the system hindering the rearrangement process.

Reinforcing results from preceding efforts, this homologation study further validated the proposed intramolecular rearrangement mechanism. If an intermolecular process was operating, increasing the chain length of the amino alcohol should not significantly affect the yield of the reaction.

In summary, to date, a range of mechanistic studies have been carried out in order to validate the proposed mechanism for BEMP-catalysed amidation (Scheme 46). Isolation of a model ester substrate and conversion to the corresponding amide indicated that rearrangement was viable for the type of substrates under consideration. More extensive investigation of the underlying mechanism of rearrangement through the execution of competition reactions (Scheme 50) suggests that an intramolecular process is in operation. Furthermore, since the reaction does not progress in the presence of an aliphatic amine, the alcohol moiety is critical for providing reactivity in this reaction manifold, and so the progression through an ester

intermediate is probable. Additional reactions examining the effect of increasing chain length (Table 21) and using conformationally-locked amino alcohol starting materials (Figure 30) are also consistent with the proposal of an intramolecular process. Based on results from all of the studies described, it is highly likely that the mechanism originally presented for this base-mediated amidation reaction is reasonable. However, as the initial transesterification is believed to be the rate-determining step in this process, and subsequent rearrangement to the more stable amide is extremely rapid, detection of the ester intermediate was not possible using HPLC techniques. Future NMR studies, for example employing ^{13}C -labelled methyl benzoate (Scheme 52) could enable enhanced monitoring of reaction progression over a shorter time scale and may offer further conclusive evidence of ester formation.



Scheme 52: Proposed NMR experiment using ^{13}C -labelled methyl benzoate

3.5.5 Limitations of BEMP-catalysed Amidation

Following extensive substrate scope investigation and subsequent mechanistic studies, it was apparent that the BEMP-catalysed amidation method was widely applicable to a range of ester and amino alcohol starting materials. A diverse set of amido alcohol products were isolated in generally excellent yields using mild reaction conditions which, as indicated previously, offer several advantages over the use of traditional stoichiometric coupling reagents. In addition, the methodology could be extended to the preparation of oxazolidinone derivatives and medicinally-relevant compounds.

However, throughout these studies, a small number of problematic substrates were encountered which represent limitations to this methodology. These challenging substrates are summarised in Figure 32. As discussed previously, during the preparation of an amino-acid derived substrate (**131**), the use of an α -chiral ester starting material resulted in slight erosion of stereochemistry under the base-catalysed reaction conditions. The measured diastereomeric ratio for this compound was 86:14, suggesting that this method is not optimal for use with this type of substrate. However, subsequent development of a more sustainable

amidation process showed that alternative bases did not racemise the stereochemistry at this position and are more appropriate for use with α -chiral ester substrates. Development and optimisation of this process is discussed in subsequent sections. Another challenging substrate encountered during the elucidation of substrate scope contained a tertiary alcohol functionality (**140**). This particular amino alcohol could only be coupled with an electron-withdrawing aromatic ester at elevated temperature (40 °C). The reduced yield observed in this case is attributed to reduced reactivity of the alcohol moiety in the initial transesterification process due to increased steric bulk. The presence of an electron-withdrawing group at the *para*-position of the aromatic ring is believed to increase the electrophilicity of the carbonyl group, allowing the reaction to occur.

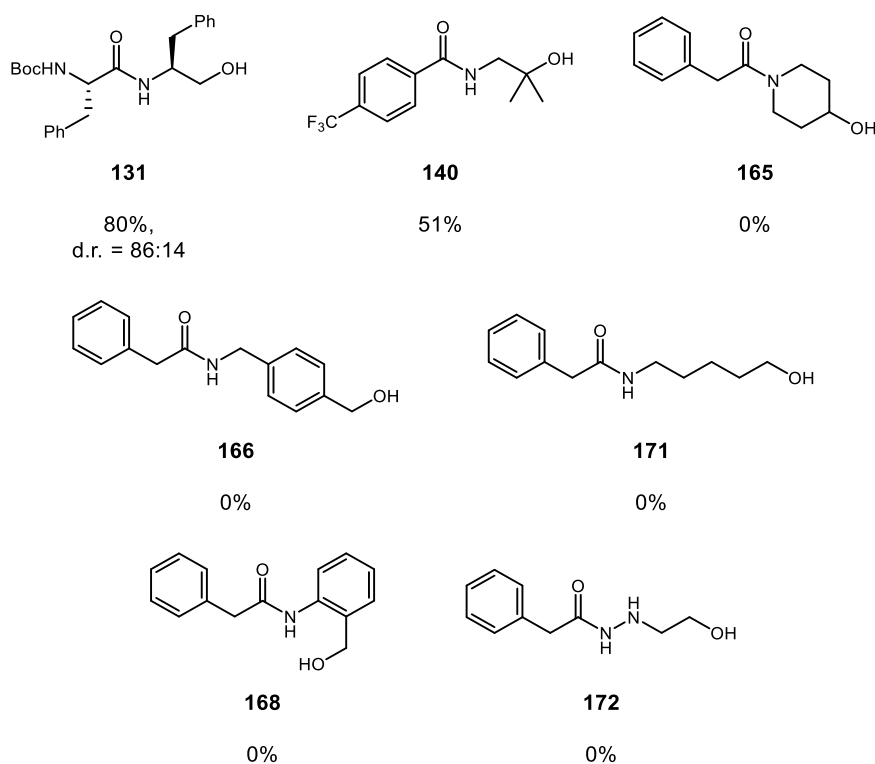


Figure 32: Problematic substrates

Throughout subsequent mechanistic investigations, a number of probe molecules were examined in order to validate the proposed mechanism for this reaction (Figure 30). Although confirming our hypothesis, these again represent substrates for which this methodology is not applicable. Under this reaction manifold, amide bond formation is achieved through exploitation of an initial transesterification reaction followed by intramolecular rearrangement to the corresponding amide. Therefore, compounds such as **165** and **166**, which are incapable of forming the requisite cyclic transition state to allow the

rearrangement process to proceed cannot be synthesised by BEMP-catalysed amidation. Similarly, due to increased flexibility, long chain amino alcohols were unreactive in this process (**171**).

Aniline-containing amino alcohols (**168**) represent another substrate class which is not amenable to BEMP-catalysed amidation due to reduced nucleophilicity of the amine. Conversely, phenol derivatives could be successfully coupled due to their proficiency in the initial transesterification reaction. Finally, hydrazinoethanol was also unreactive towards BEMP-catalysed amidation. It was expected that this amino alcohol starting material should demonstrate improved reactivity in this reaction as it benefits from increased nucleophilicity due to the α -effect. However, despite this, no hydrazide product (**172**) was isolated in this instance, and only starting materials were isolated.

3.6 Development of a Sustainable Base-catalysed Amidation Process

As discussed in previous sections, BEMP-catalysed amidation represents a mild, efficient method for amide bond formation, which can be applied to a broad range of substrates, including biologically active compounds. In contrast to the use of stoichiometric coupling reagents, the use of catalytic base results in an overall improvement in the atom economy of this transformation. However, it was believed that there was scope to further address the sustainability of this process.

In recent years, there has been an increasing focus on reducing the environmental impact of synthetic chemistry activities. Indeed, organisations such as the American Chemical Society (ACS) and Environmental Protection Agency (EPA) actively promote research into the design of more sustainable chemical and engineering processes, with the aim of preventing pollution and improving health and safety. Accordingly, major pharmaceutical companies such as GSK^{10,124,125} and Pfizer¹²⁶ have adopted ‘green chemistry’ practices in order to address the potential long-term effects associated with drug discovery.

An early guide to improving the sustainability of chemical processes outlined twelve principles of green chemistry.¹²⁷ A number of these guidelines are applicable to amide bond formation such as: prevention of waste, improving atom economy, and using catalysts rather than stoichiometric reagents. These aspects were somewhat addressed though the

development of the BEMP-catalysed method, which used catalytic quantities of base to enable amidation of esters with amino alcohols. This avoided the need to use a stoichiometric coupling reagent to form an activated ester intermediate and, consequently, prevented by-product formation. As a result, the overall atom economy of the amidation reaction was significantly improved. However, from consideration of green chemistry principles, there were still certain aspects of this methodology which could be addressed from a sustainability perspective.

Two areas of improvement which were identified were choice of base and solvent. Whilst effective, and used in catalytic quantities, BEMP was relatively expensive (Table 18), limiting its applicability for large scale reactions. Selection of a more cost-effective, environmentally-benign base for use as a catalyst could concomitantly provide a more sustainable process and improve scalability. Secondly, solvent choice was considered as this parameter represents up to 56% of total waste in an industrial setting¹²⁴ and is therefore an important factor. The original process was not particularly intensive in its use of solvent as a reaction concentration of 2 M was found to be optimal within the ranges defined for DoE optimisation. However, a more sustainable alternative to acetonitrile would be advantageous for this process, especially with a view to scaling up the reaction. Acetonitrile is considered to have some significant issues from a sustainability perspective,¹²⁴ therefore exploration of alternatives seemed appropriate. From consideration of all of the above, a range of more innocuous bases and solvents were considered for use in the amidation reaction.¹²⁸

3.6.1 Base and Solvent Screening

As with previous optimisation, preliminary screening involved the selection of an appropriate base and solvent combination. Choice of bases for this study was aided by consideration of their associated risk factors;⁹⁶ bases were selected for screening which would minimise risk and environmental impact.

A recent guide published by GSK ranks a range of common acids and bases, based on an overall greenness score,¹²⁵ which improves ease of selection according to the sustainability of individual systems. Similarly to a previous reagent selection guide published by the same authors,¹⁰ several factors were taken into account when calculating the greenness score, including environmental impact, safety, and ease of handling. Using this rubric, higher

scores are taken to represent more attractive reagents from a sustainability perspective. According to this base selection guide, BEMP has a score of 6.0, whereas bases such as Et₃N, potassium phosphate (K₃PO₄), and K₂CO₃ have scores of 6.9, 7.3, and 8.8, respectively, indicating they could offer a more sustainable alternative.

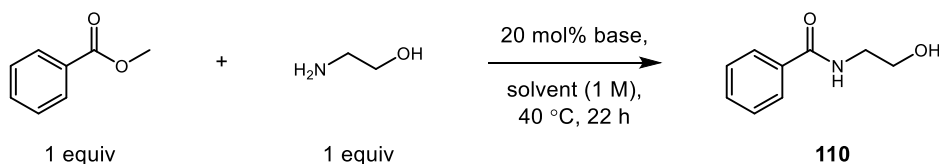
With the intention of developing a greener amidation method, a range of bases with appropriate sustainability credentials were selected for screening in a trial reaction. As Et₃N, K₃PO₄ and K₂CO₃ all appeared to be innocuous replacements for BEMP, these bases were chosen for examination under this reaction manifold. Additionally the carbonate mineral hydrotalcite, and the clay-based reagent montmorillonite were included in this study, as the use of such catalysts would result in lower environmental impact. Additionally, both hydrotalcite¹²⁹ and montmorillonite¹³⁰ had previously been utilised in transesterification reactions, so could theoretically catalyse the first step of the amidation process. These bases were all readily available at low cost from commercial sources,⁹⁶ and as most of them would act as heterogeneous catalysts, removal by filtration from the reaction mixture would result in less environmental waste. Based on the above, it was believed that the five bases selected would offer improved sustainability and scalability in a base-catalysed amidation reaction.

Next, attention was directed towards selecting a range of alternative solvents to explore in conjunction with these bases. As stated above, analysis of materials used in the preparation of APIs has indicated that solvents account for a significant fraction of the total mass used.¹²⁴ Therefore the use of environmentally-benign solvents is an important consideration when developing novel methodologies. Consequently, a number of solvent selection guides have been published which suggest suitable replacements for solvents which are considered to be unsafe or have a negative impact on the environment.^{124,126} Through consideration of solvent guides of this type, a range of solvents were selected for screening which had been reported to be sustainable substitutes for common organic solvents. Accordingly, cyclopentyl methyl ether (CPME),^{131,132} 2-methyltetrahydrofuran (2-MeTHF),¹³¹ *iso*-propanol (*i*-PrOH), and *tert*-butyl methyl ether (TBME)¹³³ were selected for study in order to develop a sustainable base-catalysed amidation reaction.

Having identified a range of bases and solvents which could be suitable replacements for BEMP and MeCN, all possible combinations were screened in a trial reaction involving methyl benzoate and ethanolamine (Table 22). As before, conversions were measured by

HPLC over a 22 hour time period. Control reactions for each solvent in the absence of base showed less than 4% conversion to product.

Table 22: Results of base and solvent screening



	Conversion After 22 h (%) ^a			
	CPME	2-MeTHF	<i>i</i> -PrOH	TBME
Et₃N	4	3	2	4
K₂CO₃	17	12	10	13
K₃PO₄	36	16	35	23
Hydrotalcite	9	6	2	13
Montmorillonite	5	3	2	5
None	2	3	1	2

^aConversion determined by HPLC with reference to an internal standard

Based on results from this initial screen (Table 22), K₃PO₄ appeared to be the most competent base for catalysing the amidation reaction, showing significant conversion to the product in several of the replacement solvents examined. Accordingly, reaction profiles were generated for reactions involving K₃PO₄, showing conversions to amide (**110**) at 4, 8, and 22 hour time points. From analysis of this plot (Figure 33), it was evident that CPME and *i*-PrOH were the most effective solvents for use with this base, showing increased conversions to product. However, *i*-PrOH appeared to demonstrate slightly higher conversion at the 8 hour time point and, upon consideration of the ready availability and low cost, this was selected as the most appropriate solvent for use in this process. Therefore, the combination of K₃PO₄ in *i*-PrOH was progressed for further development of reaction conditions.

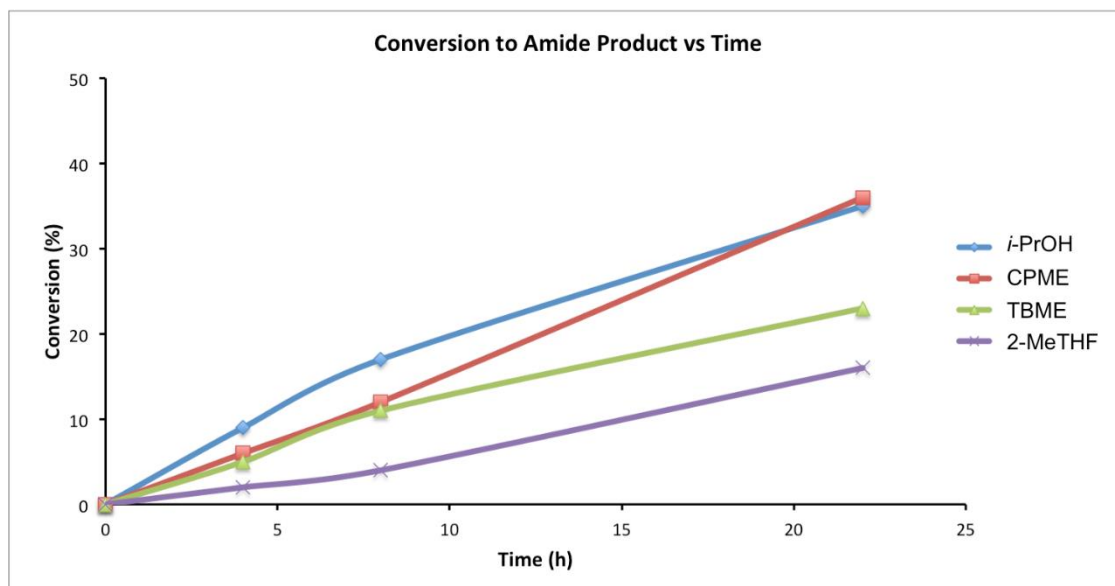
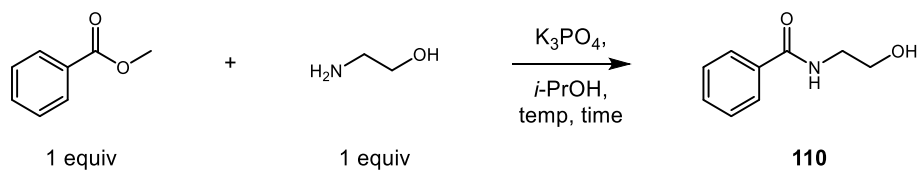


Figure 33: Reaction profiles for K₃PO₄-mediated reactions

3.6.2 Optimisation of Reaction Conditions Using Design of Experiments

Due to the success of experimental design in the previous optimisation campaign, it was again employed for the optimisation of reaction conditions for K₃PO₄-catalysed amidation in *i*-PrOH. As before, a two-level, half-fractional factorial design was selected as a starting point for screening of four factors for the model reaction employing methyl benzoate and ethanolamine. Time, temperature, concentration, and catalyst loading were selected as the most important factors for investigation, therefore appropriate minimum and maximum values were selected for each of these parameters (Table 23) based on practicality and the intent to develop a set of mild reaction conditions for this process. After consideration of the impact of catalyst loading on the outcome of the BEMP-mediated process, it was decided to employ slightly higher catalyst loadings (10 – 30 mol%) from the outset in this instance. Due to the considerably lower cost of K₃PO₄ compared to BEMP, and its relatively environmentally-benign nature, a slightly higher catalyst loading was considered acceptable in this context.

Table 23: Ranges chosen for initial experimental design



Factor	Minimum Value	Maximum Value
Time (h)	8	22
Temperature (°C)	20	60
Concentration (M)	0.5	2
Catalyst Loading (mol%)	10	30

Utilising Design Expert 8TM software,¹⁰⁷ the parameters outlined in Table 23 were used to create a two-level, half-fractional factorial design. This generated a set of eight reactions which would vary all combinations of factors (Table 24), alongside two control reactions at the centre point (Reactions 4 and 8) to allow estimation of error and demonstrate repeatability. This gave a series of ten reactions which would hopefully provide an understanding of which factor or combination of factors were responsible for affecting the conversion to amide product (**110**).

Table 24: Results from half-fractional factorial design

Reaction	Time (h)	Temperature (°C)	Concentration (M)	Catalyst Loading (mol%)	Conversion (%) ^a	Yield (%) ^b
1	8	60	0.5	30	31	–
2	22	60	0.5	10	17	–
3	8	20	2	30	8	–
4	15	40	1.25	20	19	–
5	22	20	0.5	30	14	–
6	8	60	2	10	37	–
7	22	60	2	30	82	80
8	15	40	1.25	20	20	–
9	8	20	0.5	10	3	–
10	22	20	2	10	5	–

^aConversion determined by HPLC with reference to an internal standard; ^bIsolated yield

The proposed reaction conditions were evaluated, and conversions were determined by HPLC at the end of each set reaction time. The results for the centre points (Reactions 4 and 8) were in agreement within experimental error, indicating that the process was repeatable. From initial consideration of the data shown in Table 24, it appeared likely that the most forcing conditions examined in this design (Reaction 7) were required to generate high conversion to product. Pleasingly, an isolated yield of 80% was obtained using this set of conditions, representing a significant increase compared to the highest conversion obtained during base and solvent screening (35%), and again demonstrating the utility of using a DoE-based approach to expediently optimise this process.

Further analysis of the results from this screening design was carried out by generating a series of visual representations of the experimental data. Consultation of the corresponding half-normal plot (Figure 35) indicated that catalyst loading (D) and temperature (B) displayed the largest standard deviation and these two factors were therefore most likely to

be having the greatest effect on the response. The other variables examined for this reaction did not appear to be having a significant effect influence on conversion to the amide product (110).

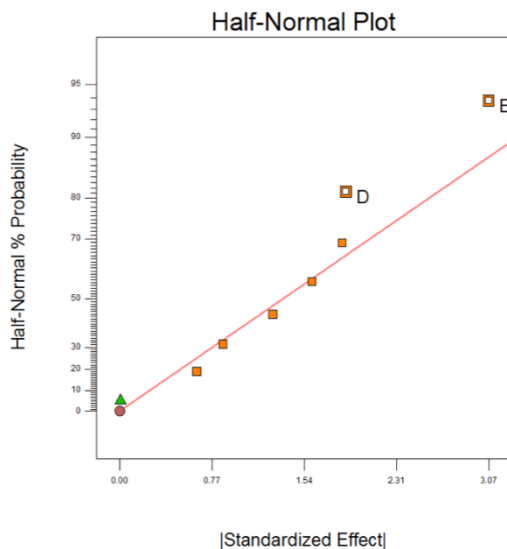


Figure 34: Half-normal plot for completed design where D is catalyst loading and B is temperature

Following consideration of this half-normal chart, where catalyst loading and temperature appeared to be significant, a 3D plot was generated to allow comparison of both of these factors (Figure 36). From this graph, it could be determined that while increasing either catalyst loading or temperature had a positive impact on the outcome of the reaction, the highest conversions were obtained for this process when both of these variables were maximised. This indicated that a two-factor interaction was occurring and a combination of high temperature and catalyst loading were important to achieve high conversion to product.

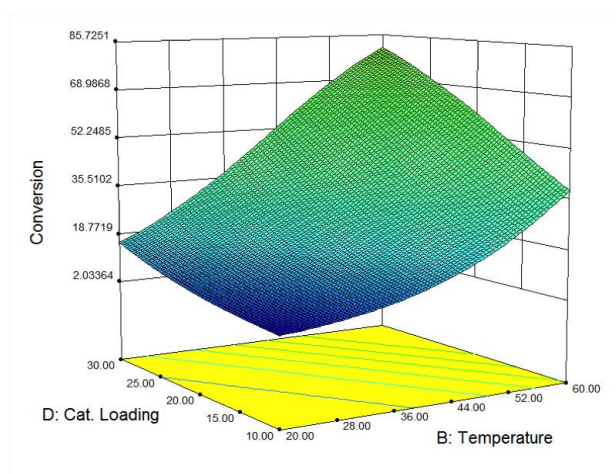


Figure 35: 3D plot of experimental results comparing catalyst loading and temperature

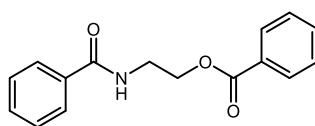
Having determined that higher temperatures were advantageous for product formation, we next decided to observe the effect of performing this reaction at reflux. Catalyst loading also appeared to be an important parameter but, with a view to developing a sustainable amidation process, it was essential to make economical use of the base catalyst. It was reasoned that if a drop in conversion was observed upon lowering catalyst loading, a concomitant increase in temperature might offset this effect. As time and concentration did not appear to be significant within the ranges defined, a reaction time of 15 h was selected as this was deemed to be the most practical. Additionally, high concentrations could be employed, which allowed for the use of less solvent. Based on the above, two further experiments were carried out at 80 °C using 10 or 20 mol% catalyst loadings, respectively (Table 25).

Table 25: Results from additional experiments

Reaction	Time (h)	Temperature (°C)	Concentration (M)	Catalyst Loading (mol%)	Conversion (%) ^a
11	15	80	2	10	41
12	15	80	2	20	71

^aConversion determined by HPLC with reference to an internal standard

However, upon evaluating this next set of reaction conditions, a decrease in conversion to the desired product (**110**) was observed at elevated temperatures, suggesting that reducing catalyst loading was not countered by a simultaneous increase in temperature. Furthermore, formation of a bis-acylated by-product (**173**, Figure 36) was observed at higher temperatures, indicating that these were not suitable for carrying out this reaction. Therefore, it was decided that conditions generated in the initial design (Table 24, Reaction 7) were optimal for achieving high conversion to product while minimising by-product formation. Accordingly, these conditions were selected to examine substrate scope for this reaction.



173

Figure 36: Bis-acylated by-product

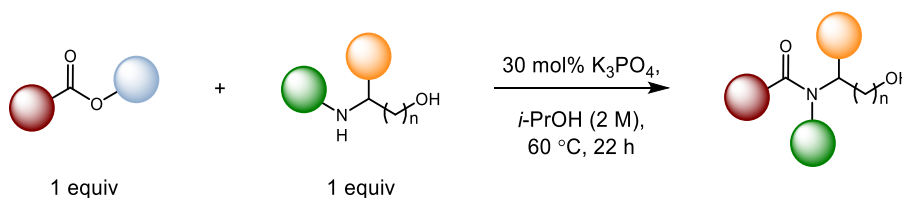
3.6.3 Examination of Substrate Scope for K₃PO₄-catalysed Amidation

Having developed a set of optimised reaction conditions for the sustainable amidation process, it was necessary to explore the utility of this reaction. In order to directly compare the efficiency of K₃PO₄-catalysed amidation with the progenitor BEMP process, a range of identical substrates were prepared (Table 26). Additionally, as the aim of this optimisation campaign was to develop a sustainable method for amide bond formation, the reaction mass efficiency was calculated for each product to assess the greenness of this process compared to traditional amidation reactions. Reported by Curzons,¹³⁴ reaction mass efficiency (RME) is a useful metric for evaluating the green credentials of a synthetic reaction. According to Equation 1, RME compares the total mass output of a reaction to the combined mass input, and so was believed to be a useful way to assess the efficiency of the novel K₃PO₄-mediated amidation process.

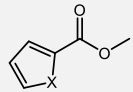
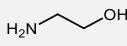
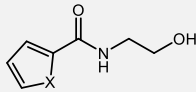
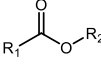
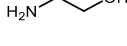
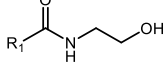
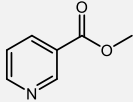
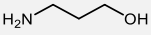
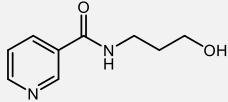
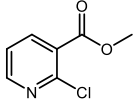
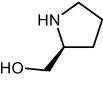
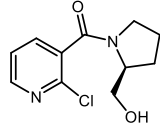
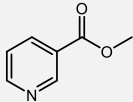
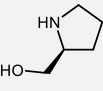
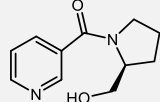
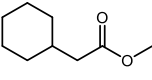
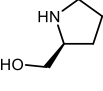
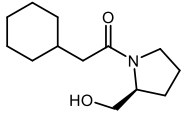
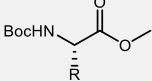
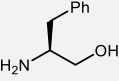
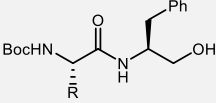
$$\text{Reaction mass efficiency (\%)} = \frac{\text{mass of isolated product}}{\text{total mass of reactants}} \times 100$$

Equation 1: Calculation of reaction mass efficiency

Table 26: Substrate scope for K₃PO₄-catalysed amidation¹²⁸



Entry	Ester	Amino Alcohol	Product	Yield (%) ^a	RME (%)
1	 R = H		 R = H (110)	80	67
2	R = 4-CF ₃		R = 4-CF ₃ (111)	98	86
3	R = 3-MeO		R = 3-MeO (174)	73	63
4	R = 2-Me		R = 2-Me (119)	75	64
5	 R = Cy		 R = Cy (120)	100	85
6	R = Ph		R = Ph (58)	99 (85) ^b	84 (72) ^b

Entry	Ester	Amino Alcohol	Product	Yield (%) ^a	RME (%)
7 8	 X = O, R = Me X = S, R = Et		 X = O (121) X = S (122)	100 (92) ^b 100 (81) ^c	83 (76) ^b 79 (64) ^c
9 10	 R ₁ = Me, R ₂ = Me R ₁ = <i>i</i> -Pr, R ₂ = Me		 R ₁ = Me (113) R ₁ = <i>i</i> -Pr (123)	98 100	75 79
11			 (125)	88	75
12			 (149)	61	54
13			 (127)	84	73
14			 (128)	67	59
15 16	 R = H R = CH ₂ Ph		 R = H (130) R = CH ₂ Ph (131)	66 42 ^d	60 39

^aIsolated yield; ^bReaction performed on 10 mmol scale; ^cReaction performed in round-bottomed flask with no prior purification of base/solvent; ^dd.r. = 98:2 as determined by chiral HPLC

In general, based on the results shown in Table 26, substrates employed in the BEMP-mediated process are also amenable to the K_3PO_4 -catalysed amidation reaction. A range of aromatic (Entries 1 – 4), aliphatic (Entries 5 – 6 and 9 – 10), and heterocyclic (Entries 7 – 8) esters were tolerated in the reaction with ethanolamine, providing products in comparable yield to the progenitor method. Homologation of the amino alcohol chain was successful, furnishing a propanolamine-derived amide (**125**) in excellent yield (Entry 11). Alternative amino alcohol substrates could also be coupled with a range of ester partners to form products in good to excellent yields (Entries 12 – 15). When Boc-phenylalanine methyl ester was coupled with phenylalaninol (Entry 16), a lower yield of amide **130** (42%) was observed than that obtained with the BEMP methodology. However, the integrity of the chiral centre was conserved throughout the reaction with a diastereomeric ratio of 98:2 as measured by chiral HPLC, representing an improvement over the BEMP-catalysed process where the d.r. was 86:14.

As K_3PO_4 had been partly selected based on its amenability to scale up, two substrates (**58** and **121**) were prepared on a 10 mmol scale in order to assess the scalability of this amidation method (Entries 5 and 7). Pleasingly, gram scale quantities of both products were obtained in high yield, indicating that the optimised process could be adapted for use on a larger scale in a discovery chemistry setting. Additionally, a trial reaction was carried out using the thiophene substrate (leading to product **122**) in which no prior purification of base or solvent had been carried out, and without using Schlenk conditions (Entry 8). This resulted in a drop in yield of almost 20% but indicated the utility of this process in a setting where anhydrous conditions are not as readily achievable.

Finally, in addition to overall yields, RMEs were calculated for each product as an attempt to quantify the efficiency of the K_3PO_4 -catalysed amidation process. The average reported RME for amide bond formation using a variety of reagents is 62%.¹³⁴ By examination of the data shown in Table 26, with the exception of Entries 12, 14, 15, and 16, all RMEs calculated are in excess of this value. Indeed, the average RME calculated for this process is 70%, which represents a clear improvement in the efficiency and sustainability of the K_3PO_4 -catalysed process compared to conventional amidation methods involving the use of a coupling reagent.

The sustainable base-catalysed amidation method was shown to be applicable to a range of substrates, demonstrating similar yields to those obtained using BEMP. However, as discussed, this process makes use of a more innocuous base and solvent combination, resulting in an overall improvement in terms of sustainability. Calculation of RMEs for products isolated during substrate scope investigation indicated that this process also represented a substantial improvement in efficiency compared to stoichiometric approaches. Furthermore, as the base employed is relatively inexpensive, the K_3PO_4 amidation reaction is much more amenable to large scale processes.

Using a combination of base and solvent screening and a DoE-based approach to optimise reaction conditions had again resulted in the development of an extremely effective amidation process. K_3PO_4 -mediated amidation and the complementary BEMP-catalysed process have been demonstrated to be efficient and widely applicable to the synthesis of an extensive range of amido alcohol derivatives. However, a limitation of both methods was the requirement for an alcohol functional group present in the starting material to facilitate the initial transesterification reaction. Whilst amido alcohol motifs are not uncommon, and have been exemplified in the current study in the form of several medicinally- and synthetically-relevant compounds, it was recognised that the direct formation of amides from esters could represent a more attractive transformation. Therefore, based on this, attention turned to the development of an amidation method which could utilise amines instead of amino alcohols.

3.7 Development of a Direct Amidation Method

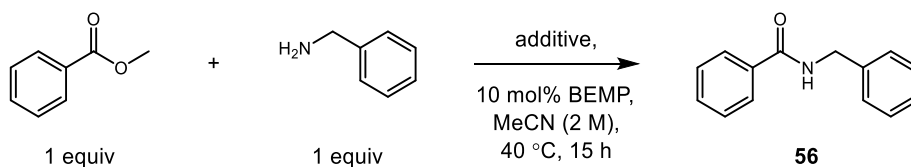
As the previous sections have shown, two novel base-catalysed amidation methods had been fully optimised and applied to a diverse range of amino alcohol substrates.^{100,108,128} However, it was realised that further development of the base-catalysed amidation methodology to allow direct use of amines in this process would be beneficial in terms of potentially expanding substrate scope. Based on an understanding of the underlying mechanism, which had been developed through the execution of several experimental investigations of the BEMP-catalysed reaction, it was evident that an alcohol functionality was vital for reactivity. It appeared that an initial esterification event was ultimately responsible for promoting amidation. However, it was proposed that inclusion of an external alcohol additive might facilitate *in situ* formation of an active ester intermediate, allowing reaction

with an amine coupling partner. From consideration of this, it was believed that an exogenous alcohol could therefore allow base-catalysed amidation to be adapted to the synthesis of products which did not contain an alcohol motif.

3.7.1 Additive Screening

Accordingly, the first stage of optimisation of a direct amidation method was to identify a suitable additive for use in this process.¹³⁵ It was decided to examine a range of common peptide coupling additives¹¹ to determine whether they would be competent systems to use in a trial reaction employing methyl benzoate and benzylamine (Table 27). A similar range of additives were employed to those previously investigated with carbene systems (Figure 17), with the addition of ethyl-1-hydroxy-1*H*-1,2,3-triazole-4-carboxylate (HOCT, **175**),¹³⁶ and trifluoroethanol (CF₃CH₂OH, **176**). As a starting point, conditions used for the BEMP-catalysed process were employed for initial screening reactions. It was reasoned that any additive systems which enabled conversion to product (**56**) could be progressed for further optimisation of reaction conditions. As the purpose of this study was to identify whether any additive was capable of effecting this transformation, both catalytic (10 mol%) and stoichiometric (1 equiv) quantities were examined in the first instance.

Table 27: Results of additive screening



Additive	Conversion to Amide 56 (%) ^a	
	10 mol% additive	1 equiv additive
HOAt (13)	0	0
HOBt (12)	0	0
HOAt (175)	3	0
Oxyma (16)	0	0
NHS (103)	0	1
HFIP (61)	1	0
CF₃CH₂OH (176)	0	6
None	0	0

^aConversion determined by HPLC with reference to an internal standard

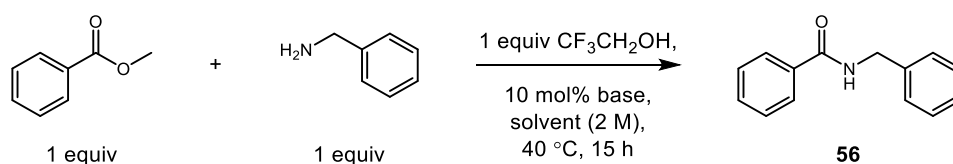
Unfortunately, when a catalytic amount of additive was employed, none of the systems examined demonstrated any significant conversion to amide product (**56**). Similarly, using an equivalent of each additive was unsuccessful in most cases. From this initial study,

trifluoroethanol was the only additive studied which demonstrated any appreciable conversion to product (6%), and only when used in stoichiometric amounts. However, it was decided to progress this system for further studies to observe the effect of altering the base and solvent system. Additionally, since a DoE-based approach had previously been effective at maximising conversion to product, it was believed that this technique could also be exploited in this instance to improve the overall outcome of the direct amidation reaction.

3.7.2 Base and Solvent Screening

In the next phase of the study, base and solvent screening was undertaken in order to determine whether a more suitable combination could result in increased conversion to product. A similar range of bases and solvents to those investigated previously for the BEMP-catalysed amidation reaction were examined for this reaction manifold (Table 28). Since K_3PO_4 had demonstrated superior reactivity for the sustainable amidation approach, this base was included to determine whether it would have a positive effect on conversion. Additionally, since DMC had not demonstrated compatibility in the progenitor BEMP-mediated reaction, it was substituted for DMF in this screening process. Finally, an equivalent of trifluoroethanol was used throughout as the intention of this study was to determine whether product formation was enhanced by choice of base/solvent. Control reactions, which were carried out in the absence of base and/or trifluoroethanol, showed no significant conversion to product.

Table 28: Results of base and solvent screening



	Conversion to Amide 56 (%) ^a				
	DMF	MeCN	NMP	PhMe	THF
DBU	4	3	3	8	9
K₃PO₄	8	5	6	13	14
<i>t</i>-BuOK	5	5	6	13	13
BEMP	7	6	6	5	7
NaH	8	4	7	14	19
No base	0	0	0	0	1
No base, no CF₃CH₂OH	0	0	0	0	1

^aConversion determined by HPLC with reference to an internal standard

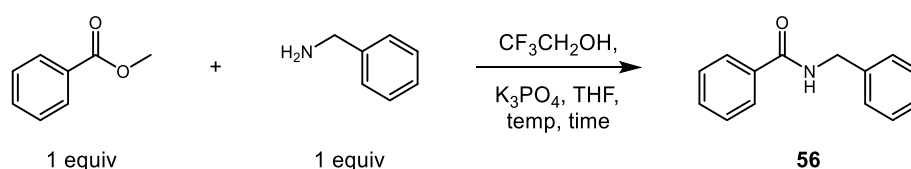
Pleasingly, results from this investigation (Table 28) demonstrated that conversion to product could be increased by the selection of an alternative base and solvent combination. K₃PO₄, *t*-BuOK, and NaH appeared to be superior bases for this reaction, affording up to 19% conversion to product in both toluene and THF. However, when NaH was used, some hydrolysis of the ester starting material was also observed so it was deemed less suitable for this particular transformation. Based on the ease of handling and purification of K₃PO₄, which could be oven-dried prior to use, and according to the green credentials outlined previously (Section 3.8.1), this system was selected for further optimisation. As the highest conversion using K₃PO₄ was observed in THF, this was considered to be the most appropriate solvent for this process.

3.7.3 Optimisation of Reaction Conditions Using Design of Experiments

Base and solvent screening had identified K₃PO₄ and THF as a more suitable combination for use in conjunction with trifluoroethanol in the direct amidation process. However, conversions were at best low, affording only 14% of product **56**. Nevertheless, there was

scope to improve this result through optimisation of reaction conditions. DoE had been previously used to good effect to maximise conversion in the amino alcohol-based processes. It was believed that this technique could again be employed to our advantage for optimisation of the trifluoroethanol-mediated direct amidation reaction. In this next study, five factors were selected for examination: time, temperature, concentration, and equivalents of trifluoroethanol and base (Table 29). As amide bond formation in this reaction manifold would occur *via* an intermolecular process, it was rationalised that higher temperatures might be required, therefore minimum and maximum values of 40 and 80 °C were selected for this parameter. Additionally, since an equivalent of trifluoroethanol had been required to provide sufficient conversions in the initial additive screen, higher catalyst and base loadings were examined from the outset for the experimental design.

Table 29: Ranges chosen for initial experimental design



Factor	Minimum Value	Maximum Value
Time (h)	8	22
Temperature (°C)	40	80
Concentration (M)	0.5	2
CF ₃ CH ₂ OH (equiv)	0.2	1
K ₃ PO ₄ (equiv)	0.2	1

As a two-level, half-fractional design had previously been adequate for optimising reaction conditions, it was decided to use this design for examination of the five factors outlined. This generated a set of 20 reactions (Table 30), which included four centre point control reactions (Reactions 1, 8, 12, and 14).

Table 30: Results from half-fractional factorial design

Reaction	Time (h)	Temp. (°C)	Concentration (M)	CF ₃ CH ₂ OH (equiv)	K ₃ PO ₄ (equiv)	Conversion (%) ^a
1	15	60	1.25	0.6	0.6	42
2	8	80	0.5	1	1	38
3	8	80	2	0.2	1	54
4	8	40	0.5	0.2	1	2
5	22	80	2	0.2	0.2	53
6	22	80	0.5	0.2	1	58
7	22	80	0.5	1	0.2	55
8	15	60	1.25	0.6	0.6	44
9	8	40	0.5	1	0.2	3
10	22	40	0.5	1	1	13
11	22	40	2	1	0.2	32
12	15	60	1.25	0.6	0.6	45
13	8	40	2	1	1	20
14	15	60	1.25	0.6	0.6	43
15	22	40	0.5	0.2	0.2	2
16	22	40	2	0.2	1	31
17	8	80	0.5	0.2	0.2	6
18	22	80	2	1	1	67
19	8	40	2	0.2	0.2	5
20	8	80	2	1	0.2	61

^aConversion determined by HPLC with reference to an internal standard

As a preliminary triage of this data, the four control reactions were in agreement within experimental error, indicating that the process demonstrated satisfactory repeatability. Results from this study (Table 30) indicated that higher conversions could be obtained (up

to 67% using the most forcing conditions within the ranges defined, Reaction 18), representing a significant improvement over the original conversion of 6% for the trifluoroethanol-mediated process. However, it was unclear from initial consideration of the data shown which factor or combination of factors were important for achieving high conversions. Therefore, the experimental data was analysed using a number of approaches in order to gain a better understanding of which variables were significant. The half-normal plot (Figure 37) for this series of experimental data indicated that temperature (A) demonstrated the highest standard deviation, and therefore was most likely to be significantly affecting the response. None of the other factors examined appeared to be having a substantial effect.

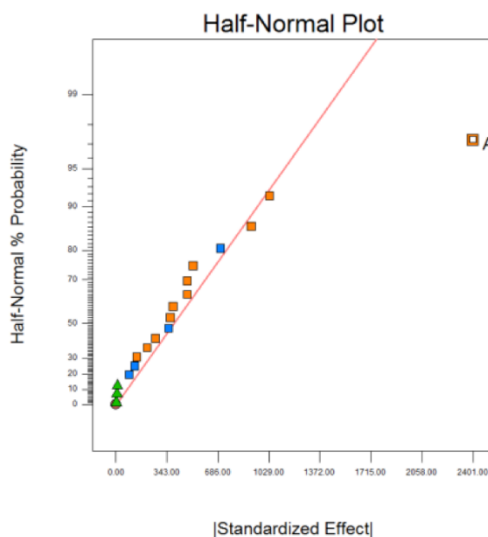


Figure 37: Half-normal plot for half-fractional factorial design where A is temperature

Initial examination of the corresponding 3D response surfaces were in agreement with the conclusions drawn from analysis of the half-normal plot. Comparison of temperature with other factors such as concentration (Figure 38a) showed a dramatic effect upon increasing temperature but negligible effects for other variables. Similarly, upon consideration of additive and base equivalents, a relatively flat profile was observed (Figure 38b), suggesting that the stoichiometry of trifluoroethanol or K_3PO_4 were insignificant under this reaction manifold.

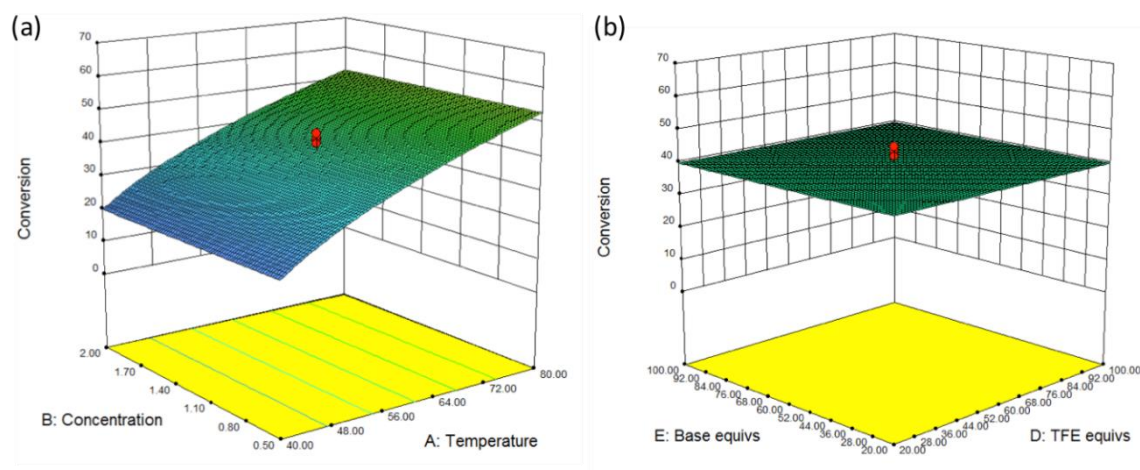


Figure 38: 3D plots of experimental data comparing (a) concentration and temperature and (b) trifluoroethanol and base equivalents

The results from this analysis, which indicated that the amount of base and additive present was inconsequential to the outcome of the reaction, did not agree with initial additive screening (Table 27) which suggested an equivalent of trifluoroethanol was necessary for product formation. Therefore, several further experiments were carried out to investigate the effects of modifying base and additive loading. Based on the response surface shown in Figure 38b, lower equivalents of base and additive (e.g. 0.1 equiv) should be sufficient to achieve moderate conversion to product when an elevated temperature of 80 °C is employed. However, experimental results were not consistent with this hypothesis (Table 31, Reaction 21) and only a 12% conversion was observed using these conditions. Concurrently, control reactions in the absence of trifluoroethanol and/or K_3PO_4 were carried out at the higher temperature to monitor the occurrence of any background reaction. No significant conversion was detected in any of these cases (Reactions 22 – 24).

Table 31: Further experiments to observe effects of lowering additive and base equivalents

Reaction	Time (h)	Temp. (°C)	Concentration (M)	CF ₃ CH ₂ OH (equiv)	K ₃ PO ₄ (equiv)	Conversion (%) ^a
21	22	80	2	0.1	0.1	12
22	22	80	2	0	0	1
23	22	80	2	0	1	1
24	22	80	2	1	0	2

^aConversion determined by HPLC with reference to an internal standard

Based on all of the above, it was concluded that the initial half-fractional design was not adequate to accurately model the direct amidation process as experimental results were not in agreement with the corresponding 3D plots. Whilst half-fractional designs proved to be more than adequate for previous optimisation studies, it was believed that they were not appropriate in this instance to generate a suitable response surface. Consequently, a central composite design (CCD) was selected for further investigation of this system. As illustrated in Figure 39, a CCD involves investigating combinations of minimum and maximum values (factorial points, represented by red dots) as before, alongside centre points (represented by orange dots) which determine repeatability and allow calculation of error. However, extra points are added to the design by extending out from the centre points in order to probe more extreme values for each factor under consideration. By inclusion of these axial points (represented by green dots), this type of design is believed to offer superior modelling of any curvature in the response surface.¹⁰² It was therefore reasoned that a CCD could therefore provide a more accurate representation of the experimental data obtained from the direct amidation reaction.

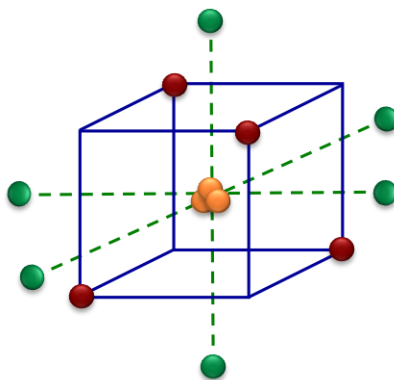


Figure 39: Central composite design

Consequently, a CCD was generated using Design Expert 8TM software. The input values originally selected for the five factors shown in Table 29, were again employed for this design. In this way the data obtained from previous experiments (Table 30), representing factorial and centre points of the design could still be utilised, and ten additional reactions to examine axial points of the CCD could be carried out to complete the design. The conditions and results for these experiments are shown in Table 32.

Table 32: Results from central composite design

Reaction	Time (h)	Temp. (°C)	Concentration (M)	CF ₃ CH ₂ OH (equiv)	K ₃ PO ₄ (equiv)	Conversion (%) ^a
25	15	60	0.13	0.6	0.6	3
26	25	60	1.25	0.6	0.6	38
27	15	60	1.25	0.6	1.2	41
28	15	60	1.25	0.6	0.002	4
29	15	60	1.25	1.2	0.6	44
30	15	90	1.25	0.6	0.6	88
31	15	60	1.25	0.002	0.6	1
32	15	30	1.25	0.6	0.6	7
33	15	60	2.37	0.6	0.6	63
34	4.5	60	1.25	0.6	0.6	9

^aConversion determined by HPLC with reference to an internal standard

From consideration of this data, high temperatures appeared to be critical for achieving good conversion to product (Reaction 30), which is in itself not surprising. Consultation of the corresponding half-normal plot showed a similar result to that shown in Figure 37, indicating that temperature was the most significant factor under consideration. However, previous experiments had indicated that the effects of other variables had not been well modelled, and it was important to determine whether the execution of a CCD would provide a more accurate representation of the data. Therefore, several response surfaces were considered (Figure 40).

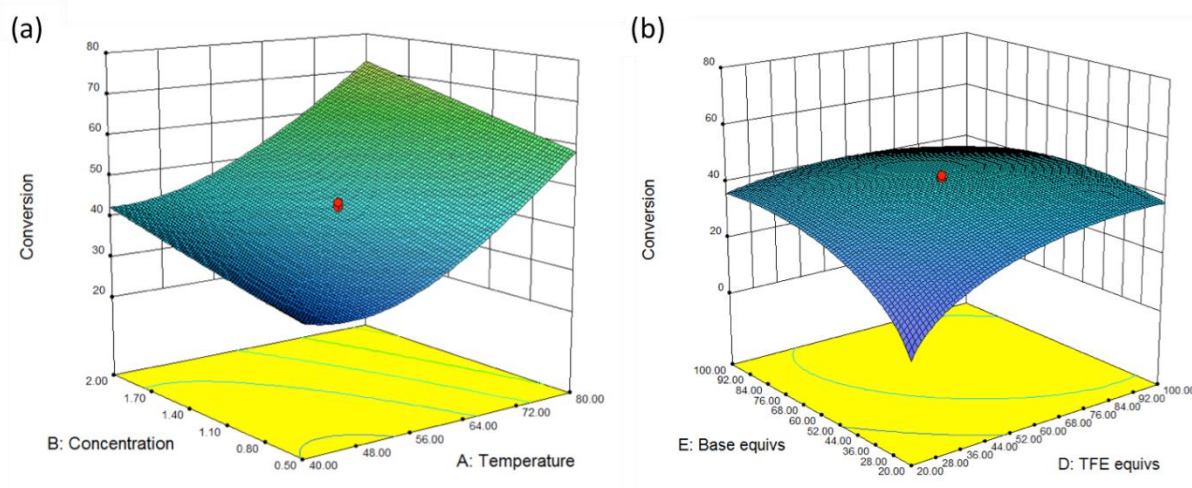


Figure 40: 3D plots of experimental data from CCD comparing (a) concentration and temperature and (b) trifluoroethanol and base equivalents modelled at 60 °C

Generation of analogous 3D plots to those which had been obtained previously (Figure 38) did indeed indicate that the CCD had been more appropriate for modelling the curvature of the response factor for this process. As shown in Figure 40a, temperature still appeared to have the most dramatic effect on the outcome of the reaction, however a slight increase in conversion was observed upon increasing the concentration. Furthermore, a plot of K_3PO_4 and trifluoroethanol equivalents indicated that an optimum balance existed between these two variables, with conversion dramatically dropping when low loadings were employed (Figure 40b). This is in accordance with the experimental result which demonstrated a low yield of product when 10 mol% of additive and base were used (Table 31, Reaction 21). Further investigation of the 3D plot suggested that when the data was modelled at a higher temperature (i.e. 90 °C), this effect was not as pronounced (Figure 41). Based on this, it was hypothesised that by performing the reaction at an elevated temperature, and employing higher quantities of base it might be possible to offset the resulting drop in conversion which would occur when using lower equivalents of additive. As the aim was to develop a catalytic amidation method, it was important to determine whether lower loadings of trifluoroethanol could be tolerated. Therefore, in the final stage of this optimisation campaign, it was decided to investigate whether the balance between base and additive equivalents could be exploited to our advantage.

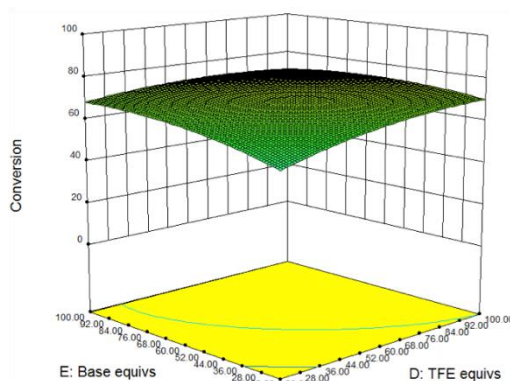


Figure 41: Response surface showing interaction between base/trifluoroethanol stoichiometry, modelled at 90 °C

Clearly, the execution of a CCD had provided a more detailed representation of the effects of altering base and additive equivalents than was previously obtained from a half-fractional factorial design. Based on these results, it was believed that in order to enable a catalytic amidation process, increasing the amount of base used could counter the resulting drop in conversion which would result from employing lower equivalents of additive. Therefore, an additional experiment was performed to confirm this hypothesis (Table 33). Pleasingly, the desired product (**56**) was isolated in 86% yield from this reaction, indicating that by employing an equivalent of base, a catalytic amount (20 mol%) of additive could be used to facilitate amidation. As K_3PO_4 was relatively inexpensive and benign, the use of a full equivalent was not considered to be detrimental to this process.

Table 33: Results from additional experiment at 90 °C

Reaction	Time (h)	Temperature (°C)	Concentration (M)	$\text{CF}_3\text{CH}_2\text{OH}$ (equiv)	K_3PO_4 (equiv)	Yield (%) ^a
35	22	90	2	0.2	1	86

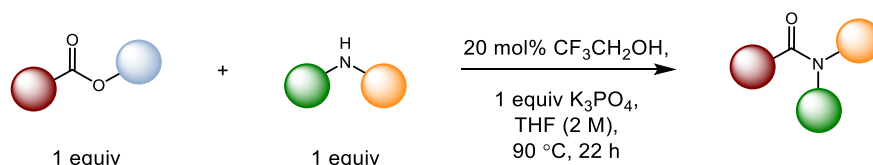
^aIsolated yield

In this study, a combination of additive, base, and solvent screening, followed by exploitation of DoE techniques had been extremely effective for the development of a direct catalytic amidation process. A dramatic increase in conversion had been realised, based on an initial hit of only 6%. Having established a set of optimised reaction conditions for a model amide product, it was then necessary to determine whether this method was also applicable for the synthesis of other substrates.

3.7.4 Examination of Substrate Scope for Trifluoroethanol-catalysed Amidation

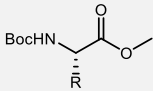
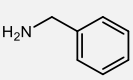
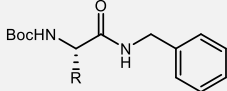
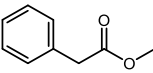
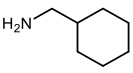
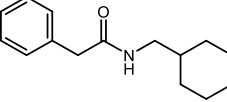
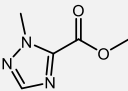
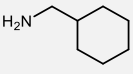
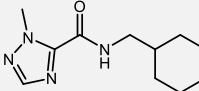
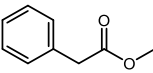
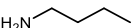
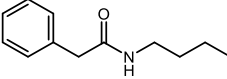
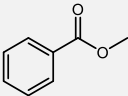
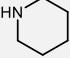
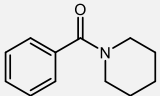
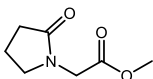
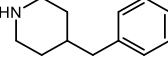
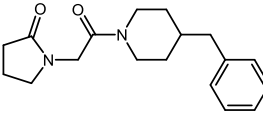
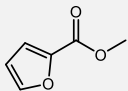
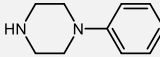
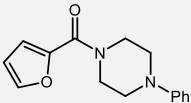
Accordingly, the optimised conditions shown in Table 33 were used to explore alternative ester and amine starting materials for use in this reaction (Table 34).

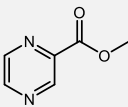
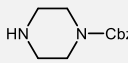
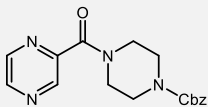
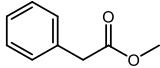
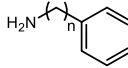
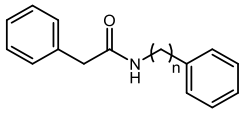
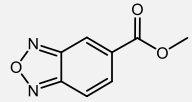
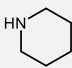
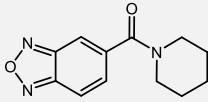
Table 34: Substrate scope for trifluoroethanol-catalysed amidation¹³⁵



Entry	Ester	Amine	Product	Yield (%) ^a
1	 R = H		 R = H (56)	86
2	R = 4-CF ₃		R = 4-CF ₃ (177)	95
3	R = 4-CN		R = 4-CN (178)	60
4	R = 4-Br		R = 4-Br (179)	87
5	R = 4-MeO		R = 4-MeO (180)	41
6	 R = Ph		 R = Ph (181)	90
7	R = Cy		R = Cy (182)	80
8	R = 2-Py		R = 2-Py (183)	86
9	 R = 2-Py		 (184)	76
10	 X = N, Y = CH, Z = CH		 X = N, Y = CH, Z = CH (185)	67
11	X = CH, Y = N, Z = N		X = CH, Y = N, Z = N (186)	66
12	X = N, Y = CH, Z = N		X = N, Y = CH, Z = N (187)	64

Results and Discussion - Development of a Direct Amidation Method

Entry	Ester	Amine	Product	Yield (%) ^a
13 14	 R = H R = CH ₂ Ph		 R = H (188) R = CH ₂ Ph (189)	76 42 ^b
15			 (190)	64
16			 (191)	80
17			 (192)	38
18			 (193)	77
19			 (194)	63
20			 (195)	64

Entry	Ester	Amine	Product	Yield (%) ^a
21			 (196)	36
22 23		 n = 2 n = 3	 n = 2 (197) n = 3 (198)	67 70
24			 (199)	60

^aIsolated yield; ^bee = 8% as determined by chiral HPLC

Exploration of substrate scope (Table 34) indicated that a range of aromatic esters could be tolerated in this reaction (Entries 1 – 5), including those with electron-withdrawing (Entries 2 and 3) and electron-donating substituents (Entry 5). However, the use of more electron-rich aryl esters resulted in a slight decrease in yield. Aliphatic ester partners could also be employed, furnishing the desired amide products in excellent yields (Entries 6 – 8). Esters containing phenyl (Entry 6), cyclohexyl (Entry 7), and pyridyl (Entry 8) functionalities were successfully coupled with benzylamine. As a further extension of ester substrate scope, heterocyclic systems were also competent in this process. Thiophene- (Entry 9), pyridine- (Entry 10), pyrimidine- (Entry 11), and pyrazine-derived (Entry 12) amides could all be obtained in high yield.

Investigation of amino acid-derived building blocks indicated that Boc-glycine (Entry 13) and Boc-phenylalanine (Entry 14) methyl esters could be employed as starting materials. However, significant erosion of the stereochemistry at the α -chiral centre was observed in the case of the latter, resulting in an ee of 8% for compound **189**. This substrate class represents a limitation of using this particular set of conditions. Efforts to address this issue by selection of a more appropriate additive will be discussed in subsequent sections.

Results and Discussion - Development of a Direct Amidation Method

Next, attention was directed to the examination of alternative amine coupling partners. Aliphatic primary amines such as cyclohexanemethylamine (Entries 15 and 16) and butylamine (Entry 17) were successfully employed to form amides with heterocyclic (Entry 16) and aliphatic esters (Entries 15 and 17). Several examples of secondary amides could also be exemplified using this amidation method (Entries 18 – 23). Piperidine (Entry 18) and substituted derivatives of piperidine (Entry 19) and piperazine systems (Entries 20 and 21) were isolated in good to excellent yields. Extending the amine chain length was also tolerated, facilitating access to homologated products **197** and **198**.

As was the case for the BEMP-mediated amidation method, we were keen to establish whether trifluoroethanol-catalysed amidation could be applied in a medicinal chemistry setting. Therefore, Farampator (**199**)¹³⁷ was selected as an appropriate target molecule to determine whether the developed methodology could be applied to the synthesis of a biologically active compound (Entry 24). Farampator is another example of a positive allosteric modulator of the AMPA receptor, which due to their association with cognitive function have been implicated in the treatment of a range of CNS disorders.¹¹⁷ This compound could be successfully prepared in a single step by coupling the requisite ester with piperidine using trifluoroethanol-catalysed amidation conditions, further demonstrating the utility of this method.

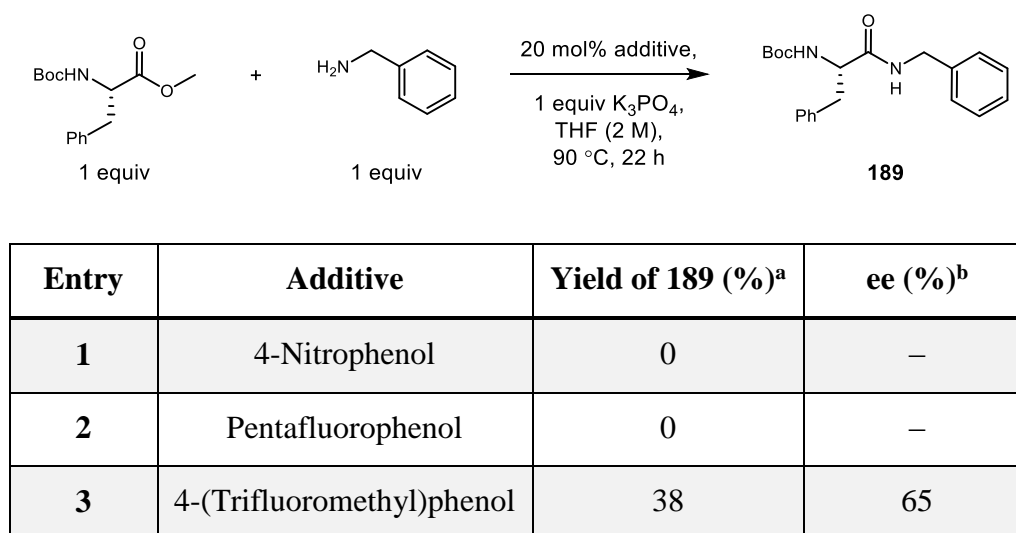
Following examination of the utility of this amidation approach, it was apparent that this process was widely applicable to a range of ester and amine substrates. A range of amide products could be prepared in good to excellent yield using this methodology, representing a considerable improvement over initial conversions that were obtained in the optimisation phase of this study. The use of a catalytic amount of trifluoroethanol, in the presence of a relatively innocuous base enabled the synthesis of amide products directly from esters and amines, avoiding the major drawbacks associated with the use of stoichiometric coupling reagents as indicated in previous sections. Furthermore, it was demonstrated that this method could be of utility in a medicinal chemistry setting, and was applicable to the synthesis of the Ampakine, Farampator (**199**).

However, during the course of this investigation, a small number of compounds proved to be problematic and could not be synthesised using the optimised direct amidation conditions. These challenging substrates represent slight limitations to this methodology. As highlighted

Results and Discussion - Development of a Direct Amidation Method

above, esters containing an α -chiral centre suffered from significant erosion of the stereochemistry at this position and so these conditions were therefore unsuitable for the preparation of amino acid-derived compounds. A subsequent study was carried out to determine whether alternative additives could be used under the optimised conditions to prepare the Boc-phenylalanine-derived amide **189** without causing the same degree of racemisation (Table 35). Several phenol additives were selected based on their previous use with substrates of this type.¹³⁸ Both 4-nitrophenol and pentafluorophenol (Entries 1 and 2) were unsuccessful in this context, showing no conversion to the desired product. Conversely, 4-(trifluoromethyl)phenol (Entry 3) was able to promote amide bond formation, producing the desired compound in 38% isolated yield, which is in agreement with that previously obtained using trifluoroethanol (Table 34, Entry 14). However, determination of ee by chiral HPLC showed that the phenol additive did not cause the same degree of erosion to the stereochemistry (ee = 65%). Although this represented a significant improvement over the trifluoroethanol-catalysed conditions in this instance, it is believed that full optimisation of this process for use with this particular substrate class could result in further improvement to ee.

Table 35: Investigation of alternative additives for use with an amino acid-derived ester substrate



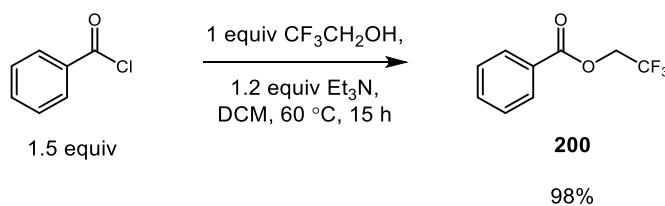
^aIsolated yield; ^bee determined by chiral HPLC

Several amine coupling partners also proved to be problematic during the examination of substrate scope. For example, bulky amines were not tolerated due to steric hindrance at the nucleophilic centre. Anilines were similarly unreactive, as was observed in the case of the BEMP-catalysed reaction, due to the reduced nucleophilicity of this functionality. Finally,

a range of secondary acyclic aliphatic amines were investigated, but were all unsuccessful in this reaction.

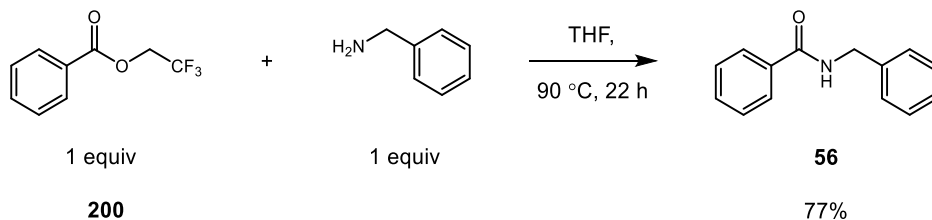
3.7.5 Mechanistic Investigations

Having examined the substrate scope of this method, and demonstrated that trifluoroethanol-catalysed amidation was suitable for the synthesis of a range of amide derivatives, it was necessary to further investigate the underlying mechanism. It was believed that amidation was being facilitated by the *in situ* formation of an activated trifluoroethyl ester intermediate. Studer had previously shown that an ester of this type was an active acylating species in studies with IMes (Table 2),⁷¹ but it was necessary to investigate whether this was also the case under the reaction conditions employed for direct amidation. Therefore, a model trifluoroethyl ester (**200**) was independently synthesised from the corresponding acid chloride according to a literature procedure (Scheme 53).⁷¹



Scheme 53: Synthesis of trifluoroethyl ester

Following isolation of this intermediate, it could be used in subsequent studies to observe whether amide bond formation would occur upon treatment with an amine. Accordingly, trifluoroethyl benzoate (**200**) was reacted with benzylamine (Scheme 54) and conversion to amide product (**56**) was monitored over a 22 hour time period.



Scheme 54: Conversion of trifluoroethyl ester intermediate to amide

Results from this study showed consumption of the trifluoroethyl ester with concomitant formation of the benzylamine-derived amide product **56** (Figure 42). This indicated that this ester was reactive under these conditions, and was likely to be the active acylating species

Results and Discussion - Development of a Direct Amidation Method

in this instance. The desired product was isolated in 77% yield from this reaction, which is in broad agreement with the previous yield obtained for this substrate (Table 34, Entry 1). Further investigation of the synthesis of amide **56** from methyl benzoate under the optimised reaction conditions showed trace amounts of the ester intermediate (~6%, measured by HPLC) throughout the progression of the reaction, confirming the formation of this species *in situ*.

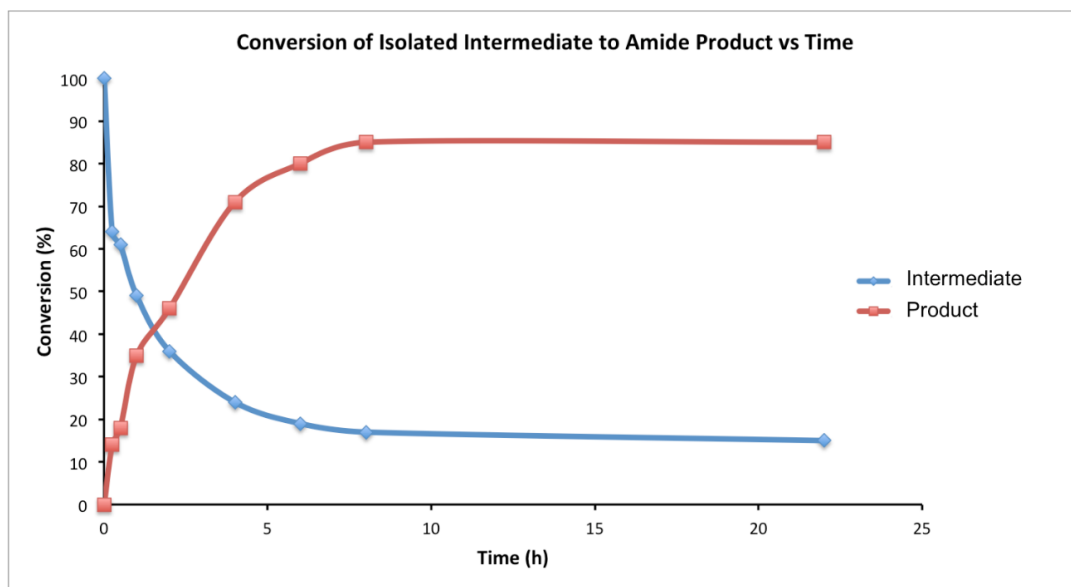


Figure 42: Conversion of isolated intermediate 200 to amide product 56, determined by HPLC with reference to an internal standard

In summary, adapting the progenitor base-catalysed amidation methodology by exploiting an external additive had allowed direct amide synthesis without the need for incorporation of an alcohol motif in the starting material. Initial additive screening indicated that trifluoroethanol was capable of effecting this transformation, albeit in low yield. However, by selecting a more appropriate base and solvent combination, and fully optimising the reaction conditions, yields of product could be dramatically improved (to 86% for a model substrate). This successful optimisation campaign highlighted the value of employing statistical methods, such as DoE, for reaction optimisation in this setting. Furthermore, the process could be applied to the synthesis of a range of amide derivatives, indicating that the reaction conditions developed had wide utility.

Since control reactions in the absence of trifluoroethanol had failed to generate any of the desired amide product under the optimised conditions, it was evident that this species was

critical for reactivity under this reaction manifold. Therefore, an activated trifluoroethyl ester intermediate (**200**) was proposed, analogous to the transesterification intermediate formed in BEMP- and K_3PO_4 -mediated processes. Independent synthesis of the trifluoroethyl ester and reaction with an amine demonstrated that this species was capable of amide bond formation, and was likely to be acting as the active acylating agent. Further scrutiny of the catalytic process showed trace amounts of this ester *in situ*, indicating that it could be formed from the corresponding methyl ester.

Although high temperatures were required to facilitate the intermolecular reaction of amines with the ester intermediate, this catalytic approach to amide bond formation offers a number of advantages over traditional methods. Low loadings of trifluoroethanol (20 mol%) were tolerated by increasing the amount of base used. However, as K_3PO_4 was inexpensive, environmentally benign, and easily removed from the reaction mixture by filtration of aqueous work up, the use of a full equivalent was not considered to be problematic. No stoichiometric by-products were formed using this approach, so this method represents a considerable improvement to the overall atom economy of the amidation reaction.

Therefore, from the initial observation that base-catalysed amidation of unactivated esters using amino alcohols could take place in the absence of a carbene catalyst, three novel amidation methods have been fully optimised and applied to the synthesis of a range of diverse substrates. Both amido alcohols and amides have been exemplified in these processes. However, a small number of drawbacks were inherent in the direct amidation process such as the need to employ elevated temperatures. Therefore, attention was redirected to the original aim of this project, which was to design a novel NHC capable of facilitating direct amidation from simple ester starting materials. It was believed that the development of a superior catalyst system could enable activation of the amine coupling partner, allowing amide bond formation to occur under milder reaction conditions. Additionally, based on the success of optimising the trifluoroethanol-catalysed process from an initial hit of only 6%, we were confident that any catalysts demonstrating activity could be fully optimised using a similar strategy.

3.8 Design and Synthesis of Bespoke Carbene Systems

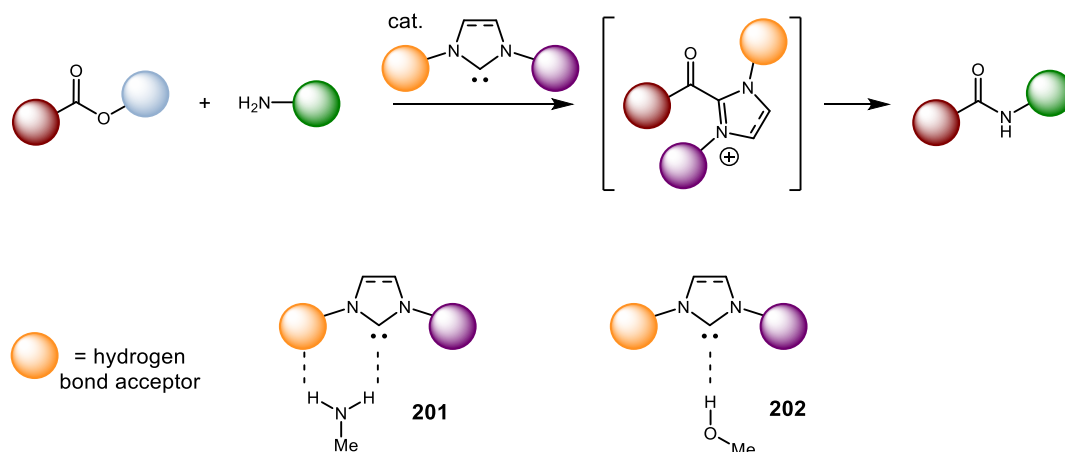
Previous examination of commercially available NHCs and additives in a model reaction employing an analytical construct had been unsuccessful at generating any of the corresponding amide product (Section 3.2), indicating that known carbene systems were not appropriate for use in this process. Similarly, a model 2-pyridyl substituted NHC (**106**) failed to demonstrate conversion to product during extensive evaluation of additive and base combinations (Sections 3.3.1 and 3.3.2). Throughout these initial high throughput arrays, hydrolysis of the ester starting material was commonly observed, necessitating a more stringent examination of the underlying experimental procedure. Therefore, a conventional NHC, IMes, was selected as a model system with which to study appropriate reaction conditions. As stated previously, comparison of results with a literature precedented reaction⁷⁴ showed that extremely rigorous anhydrous conditions were essential for handling of these species. All reagents, catalysts, and solvents required appropriate purification prior to use, as discussed in Section 3.4. Reactions were performed under an inert atmosphere, and Schlenk techniques were necessary to eliminate air and moisture from the system. NMR studies confirmed the generation of the free carbene *in situ* by deprotonation of the corresponding azolium precursor, so this method was employed to avoid isolation of the free carbene. Based on this prior experience of handling NHC systems, these anhydrous conditions were adopted for all subsequent screening reactions employing NHC systems. Consequently, with confidence in the experimental procedure, negative results could be attributed to inherent issues of reactivity relating to the catalysts themselves.

As the study of known NHCs had excluded these from the investigation, attention could be directed to the design of novel systems which were specifically designed to facilitate direct amidation of simple ester starting materials. As discussed in Section 1.4.4, previous work by Movassaghi had highlighted the existence of a favourable interaction between IMes and methanol. An X-ray structure obtained of an NHC-MeOH complex (Figure 13) indicated the presence of a hydrogen bonding interaction between the alcohol proton and the carbene centre.^{74,75} Computational studies on this system by Studer *et al.* showed lengthening of the OH bond by about 0.03 Å compared to the free alcohol, indicating an activation event was occurring.⁷³ No similar activation mode was observed for benzylamine with the NHC system studied, but it is conceivable that a superior catalyst could be designed which was appropriate for use with amines.

Work within our laboratory has indicated that bases are capable of effecting amidation of esters using amino alcohols and, subsequently, amines in the presence of an alcohol additive, by performing initial deprotonation of the alcohol, avoiding the need to use an NHC for this process. However, based on the experimental and computational data discussed above, it was believed that a second generation NHC catalyst could be designed which would activate amines preferentially, allowing direct reaction with ester starting materials. This could enable a novel amidation method which could form amides directly without the need to exploit intermediate ester formation, through enhancement of the nucleophilicity of the amine partner.

In order to expedite the evaluation of novel NHCs and prioritise catalysts for synthesis, *in silico* data was generated by the author for all proposed systems, using the Gaussian 09 program.¹³⁹ Calculations were performed using an M06 functional and 6-311G(d,p) basis set as this combination was believed to be most suitable for geometry optimisation of the systems under investigation. *In silico* screening enabled comparison of a high number of potential catalyst systems, and acted as an initial assessment of their suitability for facilitating amine activation. It was rationalised that NHCs which showed positive results during computation screening could be progressed for synthesis and investigation in an amidation reaction to observe whether experimental results agreed with theoretical calculations.

As previous work had suggested that hydrogen bonding to the carbene was a prerequisite for alcohol activation, this parameter was considered in the first instance for novel catalysts under consideration. Therefore, optimised geometries were calculated for each NHC system studied in complex with methylamine (**201**), which was used as a model amine substrate (Scheme 55). As previous computational studies of NHC systems, carried out by Studer *et al.* had examined NHC-alcohol complexes, optimised geometries of were also generated for the methanol complex of each novel NHC examined (**202**) to act as a comparison. Based on the optimised geometry, hydrogen bond distances could be measured and the extent of NH bond elongation could be calculated with respect to the non-complexed amine. Results of these calculations could also be used to determine the theoretical enthalpy change (Equation 2) which occurred upon complexation of the amine or alcohol with the carbene. This would give an indication of which systems were more favourable and, hence, more conducive to catalysing this process.



Scheme 55: Proposed modelling experiments

$$\Delta H = [E_{complex}] - [E_{carbene} + E_{amine/alcohol}]$$

Equation 2: Calculation of enthalpy change upon complexation with carbene

Based on all of the above, the first level of theoretical investigation involved calculation of hydrogen bonding distances, NH or OH bond elongations, and enthalpy change. This facilitated an initial triage of all new catalysts proposed for synthesis. In this way, several series of novel carbene systems were designed and evaluated.

3.8.1 Catalysts Designed to Facilitate a Dual Catalysis Mode

As discussed previously (Section 2), it was believed that incorporation of a hydrogen bond acceptor substituent as part of the NHC structure could facilitate access to a dual activation pathway. Initial activation could occur through hydrogen bonding with the amine and subsequent nucleophilic attack onto the carbonyl group of the proposed acylazolium intermediate could be assisted by a neighbouring group effect (Scheme 32), similar to that observed with HOAt. Based on this, the method of ‘dual catalysis’ could potentially offer an advantage over previously examined systems. After intensive investigations of compounds of this type, a number of carbenes were prioritised based on initial calculations of hydrogen bond length and NH elongation. These systems are summarised in Figure 43.

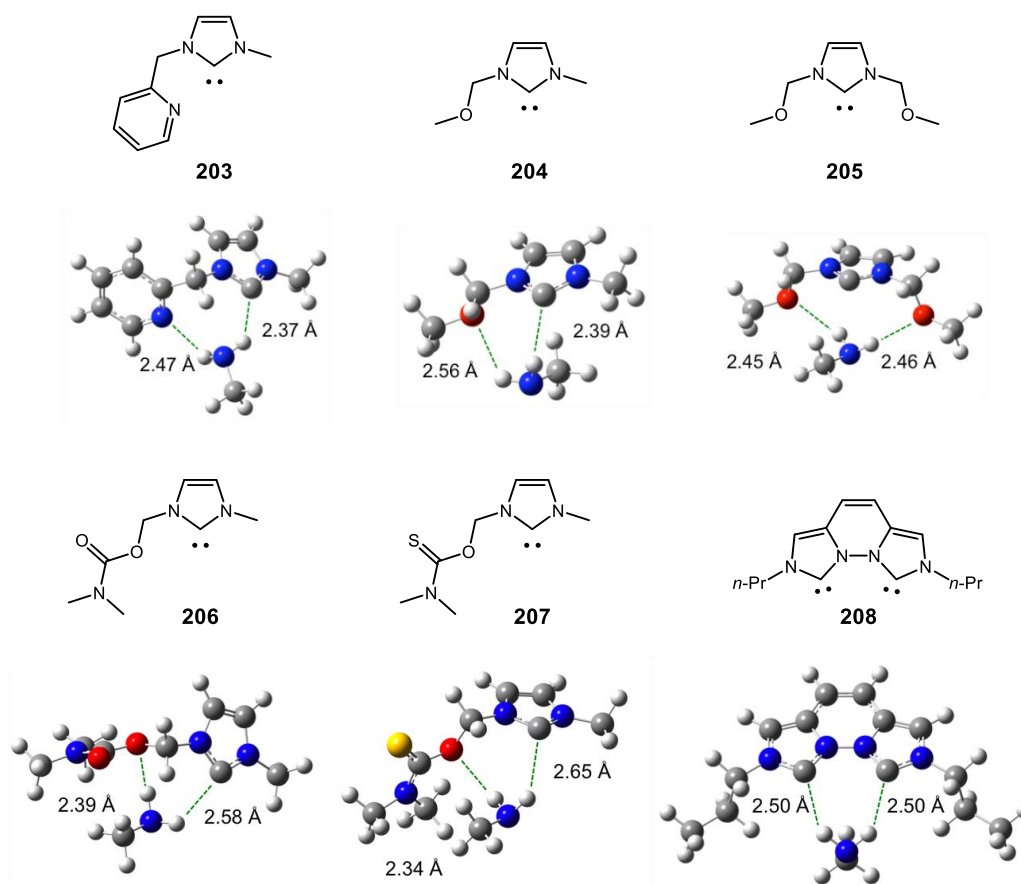


Figure 43: Prioritised compounds for 'dual catalysis' series showing hydrogen bonding distances for carbene-amine complexes. Geometry optimisations performed in Gaussian 09 using M06/6-311G(d,p).

Consideration of the data obtained from geometry optimisation of these particular systems indicated that, for most of the systems examined, weak hydrogen bonds existed between an amine proton and the carbene centre. However, these weak interactions could be compensated for by the presence of a second hydrogen bond between the other amine proton and the hydrogen bond acceptor substituent. This effect, which is not possible with NHC-alcohol complexes, could potentially offer a preferential activation mode for amines. Several functionalities were investigated for their ability to form a hydrogen bonding interaction with the incoming amine with pyridyl, ether, carbamate, and thiocarbamate side chains showing favourable results in this initial phase of computational studies (Figure 43). As the 2-pyridyl substituted carbene precursor (**106**) examined previously (Sections 3.3.1 and 3.3.2) did not appear to be suitable for amide bond formation, a less bulky methyl side chain was incorporated in this system to reduce steric hindrance of the amine. Additionally, a substrate containing two ether substituents (**205**) was examined computationally, and showed hydrogen bonding of the amine protons to both side chains rather than to the carbene

centre. As it was unknown whether this would be detrimental to the catalyst reactivity, it was decided to progress this particular catalyst for further theoretical studies. A biscarbene system (**208**) was also included in this investigation as it was believed that this type of catalyst could also result in the formation of two hydrogen bonds with the amine partner. This effect was, indeed, observed during modelling experiments.

Having assessed that weak hydrogen bonding interactions could be observed between the carbene and the incoming amine for a number of systems examined, the extent of NH bond elongation and enthalpy change upon complex formation were evaluated as the second stage of prioritisation of novel systems. Data for the amine complexes shown in Figure 43 were compared with that obtained for the corresponding NHC-methanol complexes (Table 36).

Table 36: Modelling results for prioritised carbene systems in 'dual catalysis' series

Carbene	Amine Complex		Alcohol Complex		
	NH Elongation (Å)	ΔH Complex Formation (kcal/mol)	OH Elongation (Å)	Carbene-OH Hydrogen Bond Length	ΔH Complex Formation (kcal/mol)
203	0.007	-8.3	0.03	1.95	-17.0
204	0.006	-6.2	0.02	1.98	-15.0
205	–	-7.0	0.02	2.00	-15.0
206	0.005	-6.6	0.02	2.01	-13.0
207	0.004	-6.9	0.02	1.96	-13.5
208	0.006 (x 2)	-7.4	0.02	2.02	-13.1

From the results shown in Table 36 it was apparent that slight elongation of the NH bond was observed upon complexation with the carbene compared to the free amine. Interestingly, in the case of the biscarbene (**208**) studied, elongation of both NH bonds was observed, indicating that this system could provide superior activation of the incoming amine. The extent of NH bond lengthening for these systems was found to differ by around 3 – 5 fold compared to the analogous alcohol complexes. However, it is expected that the increased acidity of alcohols would more than likely account for the differences observed.

Additionally, the extent of bond elongation in the case of the alcohol complexes observed correlated with results reported by Studer,⁷³ indicating that the computational methods employed were suitable for investigation of these systems.

Based on calculated enthalpy changes, it was reasoned that formation of an NHC-amine complex would be favourable. Again, more favourable results were obtained with the carbene-alcohol complexes but this is likely to be due to the more polarisable nature of the OH bond. When the NHC was substituted with two ether side chains, no elongation of the NH bond length was observed as the amine was not able to interact with the carbene. However, the corresponding enthalpy change (-7.0 kcal/mol) indicates that the formation of an NHC-amine complex would be favourable.

These initial modelling experiments highlighted a number of systems which may provide suitable reactivity in a catalytic amidation reaction by facilitating amine activation. In order to further refine this series and select compounds for synthesis, partial charge and molecular orbital calculations were undertaken in an attempt to assess the likely reactivity of the systems shown in Figure 43. Perhaps unsurprisingly, partial charge calculations indicated that the carbene was the most negatively charged centre for each compound studied (Figure 44). The biscarbene (**208**) showed equal negative charges for both carbene centres.

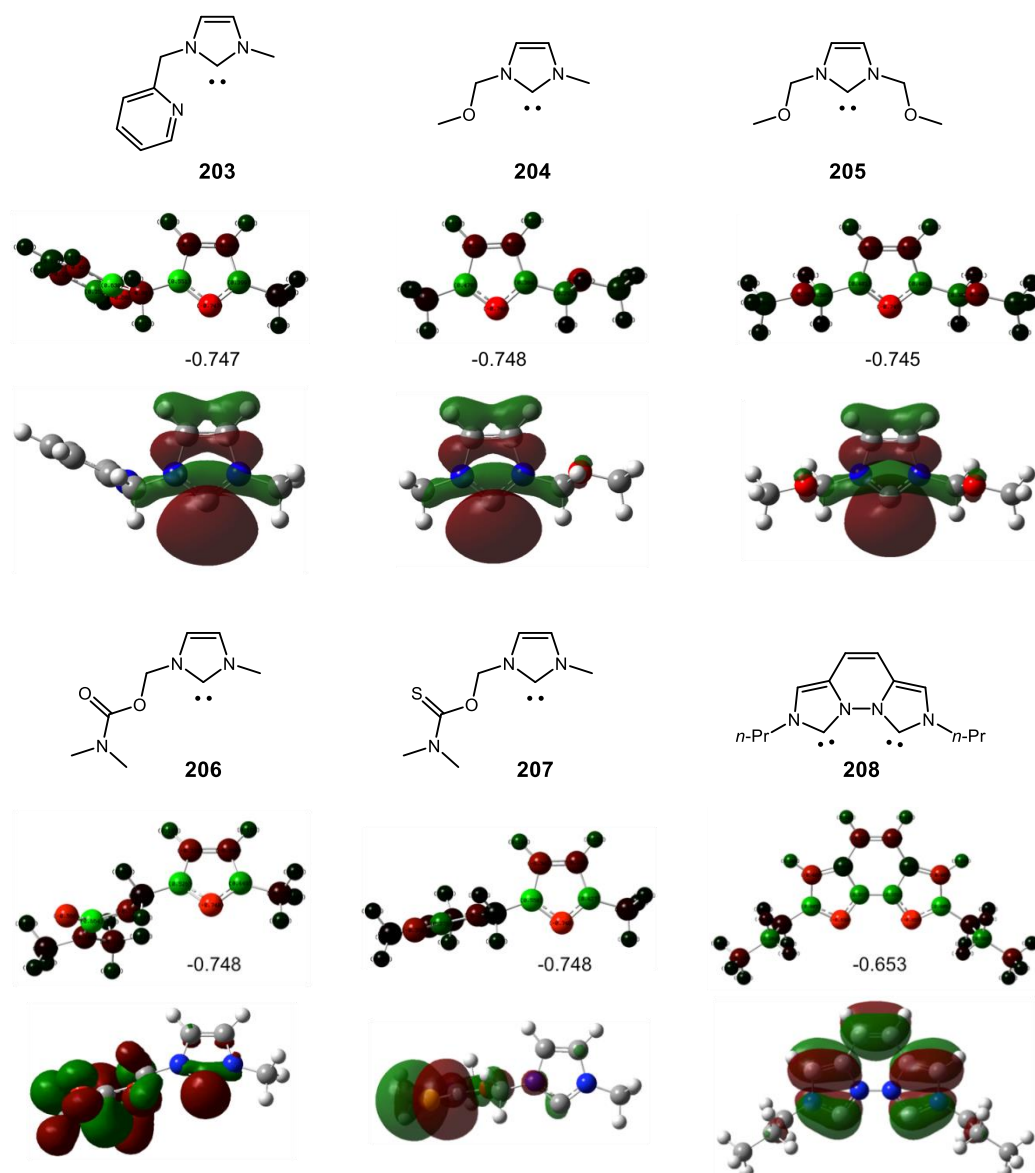


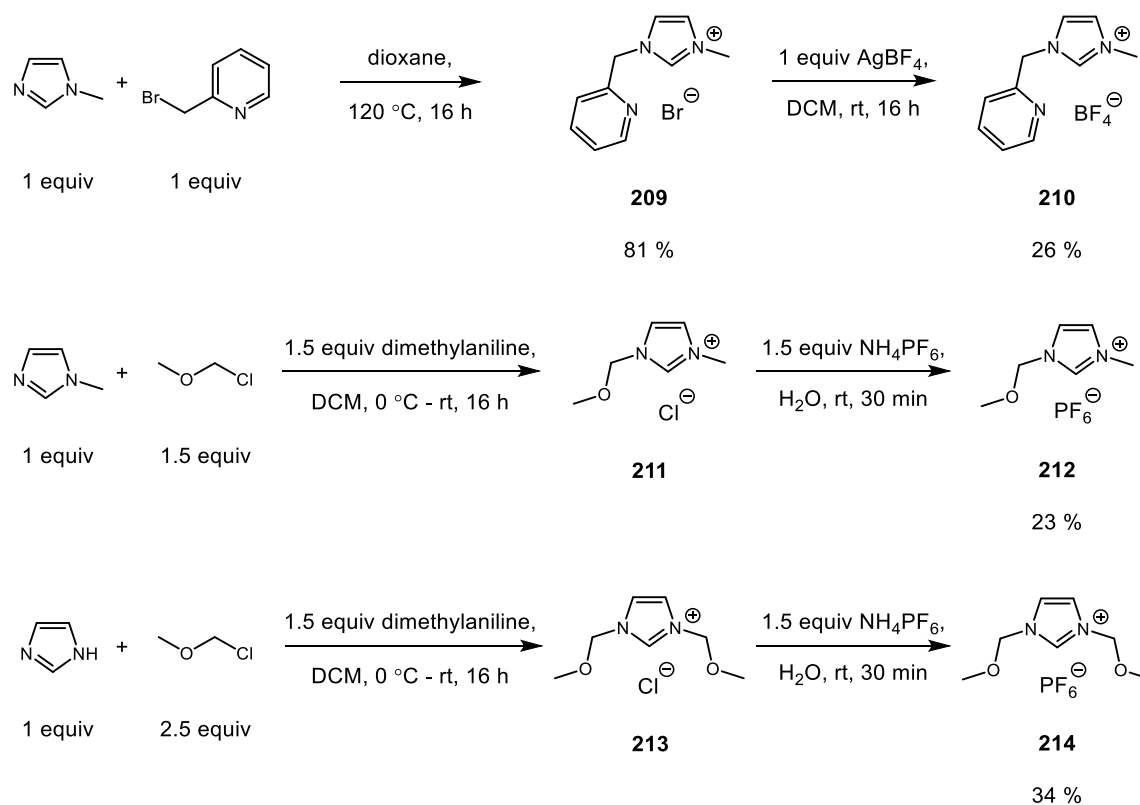
Figure 44: Partial charge and molecular orbital calculations for 'dual catalysis' series. Values indicate most negative charge (represented in red on molecules). Population analysis and HOMO/LUMO calculations performed in Gaussian 09 using M06/6-311G(d,p).

Molecular orbital calculations showed that for highest occupied molecular orbital (HOMO), the electron density resided mainly on the carbene for the pyridyl (**203**) and ether (**204** and **205**) substituted carbenes, indicating this was the most reactive part of these systems. The biscarbene (**208**) was slightly more delocalised but still indicated that the majority of electron density was present on the carbene centre. However for the carbamate (**206**) and thiocarbamate (**207**) substituted carbenes, the majority of electron density was located on the side chain, potentially suggesting that these systems were less likely to be as reactive as others in this series.

Based on results from molecular orbital calculations, it was decided that the carbamate (**206**) and thiocarbamate (**207**) substituted species should not be progressed to synthesis. However, since all other systems in this series showed potential across a range of calculations, all four remaining analogues were prioritised for synthesis.

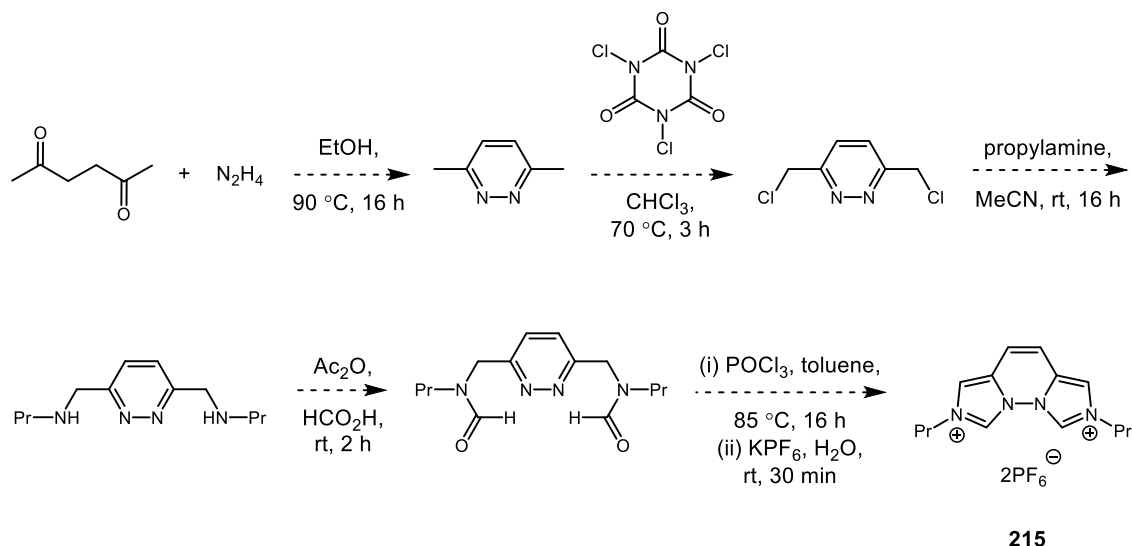
The NHC precursors for catalysts **203** to **205** were synthesised by introducing the required side chain group to either imidazole or methyl imidazole (Scheme 56). Compound **209** was prepared by refluxing methyl imidazole and bromomethyl pyridine in dioxane to give the corresponding bromide salt (**209**) in high yield.⁹⁷ As previous studies with IMes (Table 6) had suggested that halide salts were less suitable for use in the amidation reaction, presumably due to their increased hygroscopicity, all novel catalyst precursors synthesised were converted to their corresponding tetrafluoroborate (BF₄) or hexafluorophosphate (PF₆) salts in an attempt to exclude moisture from the system. As an additional advantage, purification of the BF₄ or PF₆ salts by trituration afforded these products as solids, which improved the ease of handling of these systems. Compounds **211** and **213** were formed by reacting MOM-Cl with imidazole or methyl imidazole, as required.¹⁴⁰ This reaction was not successful in the presence of DIPEA, and dimethylaniline was found to be a more appropriate base according to literature precedent.¹⁴⁰ The order of addition was also found to be important for a successful outcome in this reaction; MOM-Cl and dimethylaniline were combined before the addition of either imidazole or methyl imidazole. As an excess (1.5 equivalents) of base was used for these reactions, some residual dimethylaniline was present alongside the imidazolium chloride product. Therefore, purification by strong cation exchange (SCX-2) was performed in order to remove excess base prior to salt exchange to the corresponding PF₆ salt.

Results and Discussion - Design and Synthesis of Bespoke Carbene Systems



Scheme 56: Synthesis of catalyst precursors from ‘dual catalysis’ series

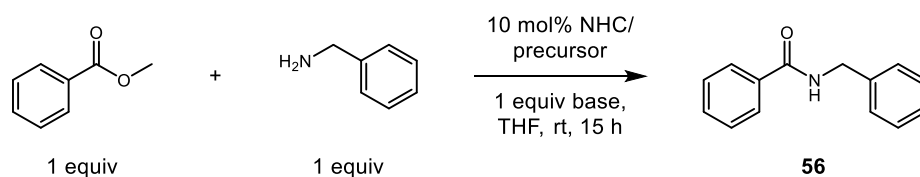
The proposed synthesis for the biscarbene precursor, shown in Scheme 57,¹⁴¹ is based on a 3,6-dimethylpyridazine core which can be formed *via* a condensation reaction between 2,5-hexanedione and hydrazine.¹⁴² The required chlorine groups can then be inserted by employing trichloroisocyanuric acid, an electrophilic chlorinating reagent. Substitution with propylamine should generate the corresponding diamine which can undergo formylation and cyclisation to form the requisite biscarbene precursor **215**. As discussed above, salt exchange to the desired PF₆ salt will be carried out in order to comply with optimised anhydrous conditions developed previously.

Scheme 57: Proposed synthesis of biscarbene precursor^{141,142}

Following successful isolation of three of the four prioritised precursors in this series, these could be progressed for experimental evaluation in a model amidation reaction. Initial arrays with known carbene systems had failed to demonstrate any conversion to amide product, which could be attributed to low catalytic activity in this reaction. However, as fully optimised anhydrous conditions had not been employed for previous screening reactions with NHCs, it was possible that negative results could have resulted from the use of incompatible experimental procedures. Therefore, it was decided to examine a targeted selection of commercially available NHCs under more rigorously inert conditions for their ability to catalyse a model amidation reaction between methyl benzoate and benzylamine. Although, it was reasoned that carbenes which had been specifically designed for this purpose would show superior reactivity in this reaction manifold, it was necessary to completely rule out the possibility of known systems being suitable catalysts for amide bond formation.

Based on the above, as a starting point for examination of these systems, it was decided to examine NHC precursors in combination with a range of bases (Table 37). Although a catalytic amount of base would be sufficient to perform *in situ* deprotonation and form the active free carbene, a full equivalent of base was used in this initial study. It was rationalised that even low conversions to product could be subsequently optimised employing a DoE-based strategy.

Table 37: Screening of novel NHC precursors in conjunction with known systems



	Conversion (%) ^a				
	Et ₃ N	<i>t</i> -BuOK	NaH	BEMP	None
IMes (54)	1	5	1	0	0
IMes.PF₆ (109)	0	4	2	0	0
67	0	0	0	2	0
210	0	4	0	0	0
212	0	2	0	0	0
214	0	0	0	0	0
None	0	2	0	0	0

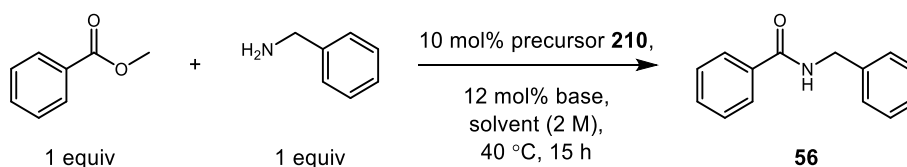
^aConversion determined by HPLC with reference to an internal standard

Results from this preliminary array showed low conversion to product in a number of cases. It appeared that the pyridyl-substituted carbene (**210**) demonstrated a slightly higher conversion than other modelled systems when used in combination with *t*-BuOK, indicating that this system could potentially be superior. Additionally, of the known carbenes screened, IMes appeared to be slightly more active, generating measurable conversion to amide product in both the free carbene (**54**) and PF₆ salt forms (**109**). Owing to previous success in optimising the trifluoroethanol-catalysed process from an initial conversion of only 6%, it was decided to advance both of these systems for further investigation to determine whether the outcome of the reaction could be affected by the selection of more appropriate reaction conditions.

Based on this, a second array was planned to investigate the activity of the pyridyl carbene system (**210**) alongside a range of alternative bases and solvents (Table 38). In order to make economical use of the base, only a sufficient amount was added to the reaction mixture to perform *in situ* deprotonation of the imidazolium precursor. Results from this study showed

little or no conversion for most of the systems examined. However, significant conversion to amide product was observed when using *t*-BuOK in DMF, NMP, or PhMe. In order to confirm that this increased conversion was as a result of the selection of a superior catalyst and base combination, it was also necessary to perform the appropriate control reactions in the absence of carbene precursor.

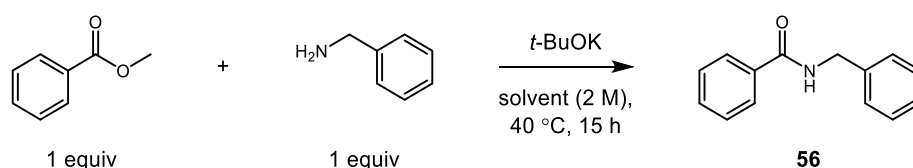
Table 38: Base and solvent screening with pyridyl NHC precursor



	Conversion (%) ^a				
	DMF	MeCN	NMP	PhMe	THF
DBU	1	1	1	0	2
K₃PO₄	0	1	1	0	1
<i>t</i>-BuOK	10	2	10	11	2
NaH	0	1	1	0	0
BEMP	1	1	0	0	0

^aConversion determined by HPLC with reference to an internal standard

Accordingly, in order to determine whether the positive results obtained during the screening of alternative bases and solvents was a function of the carbene catalyst employed, and not solely due to a base-mediated background reaction, a number of control reactions were executed (Table 39). Both catalytic and stoichiometric amounts of base were studied in all of the solvents previously examined, without the presence of the pyridyl carbene precursor.

Table 39: *t*-BuOK control reactions in the absence of NHC precursor

	Conversion (%) ^a	
	12 mol% <i>t</i> -BuOK	1 equiv <i>t</i> -BuOK
DMF	0	62
MeCN	13	29
NMP	0	55
PhMe	53	78
THF	34	69

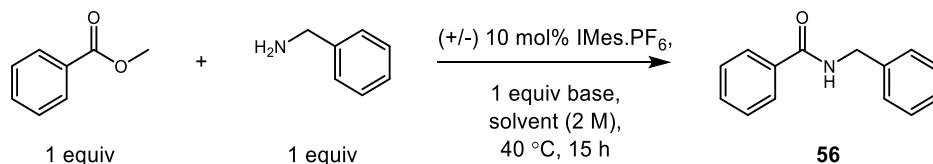
^aConversion determined by HPLC with reference to an internal standard

Unfortunately, results from these control reactions (Table 39) showed significant conversion to product in the absence of a carbene catalyst when both catalytic and stoichiometric amounts of *t*-BuOK were examined. Isolation of product from these reactions and subsequent NMR analysis confirmed the structure of the amide product (**56**). This suggested that *t*-BuOK alone was responsible for mediating the effects seen previously (Table 38). Examination of the literature indicated that *t*-BuOK-mediated amidation of esters with amines was a known transformation,^{143,144} proposed to occur *via* a radical mechanism.¹⁴⁴ Since no promising results were observed when using alternative bases with this catalyst, it was decided not to progress pyridyl precursor **210** for any further studies.

Instead, attention turned to investigation of IMes, which had also demonstrated slightly increased conversion to product during initial screening of catalysts and bases (Table 37). As the imidazolium precursor offered more facile ease of handling, IMes.PF₆ was selected as the most appropriate system with which to carry out further studies. As with the previous precursor examined, an initial array was performed to examine the use of alternative bases and solvents with this catalyst. As *t*-BuOK had been shown to be capable of effecting a significant background reaction, it was excluded from future experiments. For each of the

remaining bases, control reactions were performed in the absence of IMes.PF₆ to ensure this effect did not occur with other systems (Table 40).

Table 40: Base and solvent screening with IMes.PF₆



	Conversion (%) ^a				
	DMF	MeCN	NMP	PhMe	THF
IMes.PF₆ + DBU	1	3	1	3	5
DBU	1	1	1	1	1
IMes.PF₆ + K₃PO₄	0	0	0	0	1
K₃PO₄	0	0	0	0	0
IMes.PF₆ + NaH	1	1	1	0	0
NaH	1	1	1	3	0
IMes.PF₆ + BEMP	2	2	7	7	0
BEMP	1	0	0	0	0

^aConversion determined by HPLC with reference to an internal standard

Results from this study indicated that no significant conversion was observed for control reactions in the alternative solvents investigated. However, low conversion to product was detected for carbene-catalysed reactions in the presence of BEMP in both NMP and PhMe. As the latter was deemed to be a more suitable solvent for use in the amidation reaction, the combination of BEMP in toluene was progressed for further investigation to determine whether the initial conversion of 7% could be increased through optimisation of reaction conditions.

Accordingly, the technique of DoE was again employed in an attempt to optimise reaction conditions for the IMes-catalysed amidation reaction in the presence of BEMP and PhMe.

Table 42: Results from half-fractional factorial design

Reaction	Time (h)	Temperature (°C)	Concentration (M)	Catalyst Loading (mol%)	Conversion (%) ^a
1	8	100	0.5	0.5	0
2	8	100	1	0.1	0
3	22	40	1	0.1	0
4	22	40	0.5	0.5	0
5	22	100	0.5	0.1	5
6	8	40	0.5	0.1	0
7	15	70	0.75	0.3	0
8	8	40	1	0.5	0
9	22	100	1	0.5	5
10	15	70	0.75	0.3	0

^aConversion determined by HPLC with reference to an internal standard

However, upon performing the experiments outlined in Table 42, no improvement was observed over the original 7% conversion, even under the most forcing conditions examined for this process (Reaction 9). Based on the results described, initial arrays examining a series of novel carbene catalysts in a model amidation reaction were unsuccessful at generating satisfactory conversion to the desired product (**56**). Although a pyridyl-substituted system (**210**) demonstrated slightly increased conversion over other catalysts examined, attempts to enhance this further were not productive.

Similarly, investigation of a known NHC system, IMes.PF₆, failed to demonstrate desired levels of conversion, and it was decided that this system was not appropriate for performing amide bond formation. This concurred with preliminary results utilising an analytical construct described previously (Section 3.2).

According to modelling studies, it is anticipated that other catalysts in the ‘dual catalysis’ series might offer an advantage over the systems examined. For example, a biscarbene

structure (**208**) appeared to perform well across a range of calculations. Additionally, as an increase in bond length was believed to be an indicator of activation by the carbene, this catalyst shows considerable promise as both amine NH bonds were elongated when complexed with the biscarbene. Therefore, future studies examining this NHC in the context of amide bond formation should be performed to determine whether it is superior for this purpose.

3.8.2 Pyrrolidine-derived Catalysts

Having theoretically and experimentally assessed catalysts capable of forming two hydrogen bonds with an amine, a second series was investigated which established only one hydrogen bonding interaction (Figure 45). It was hypothesised that the introduction of a second nitrogen atom adjacent to those on the *N*-heterocyclic ring could potentially increase electron density at the carbene centre due to the α -effect. As a result, this could strengthen the hydrogen bonding interaction between the carbene and the amine. A number of systems of this type were subjected to a similar range of calculations as those discussed previously. Based on promising results from a pyrrolidine-derived compound (**215**), further analogues in this series were explored to determine whether the addition of backbone methyl groups or the introduction of saturation could also increase electron density at the carbene centre.

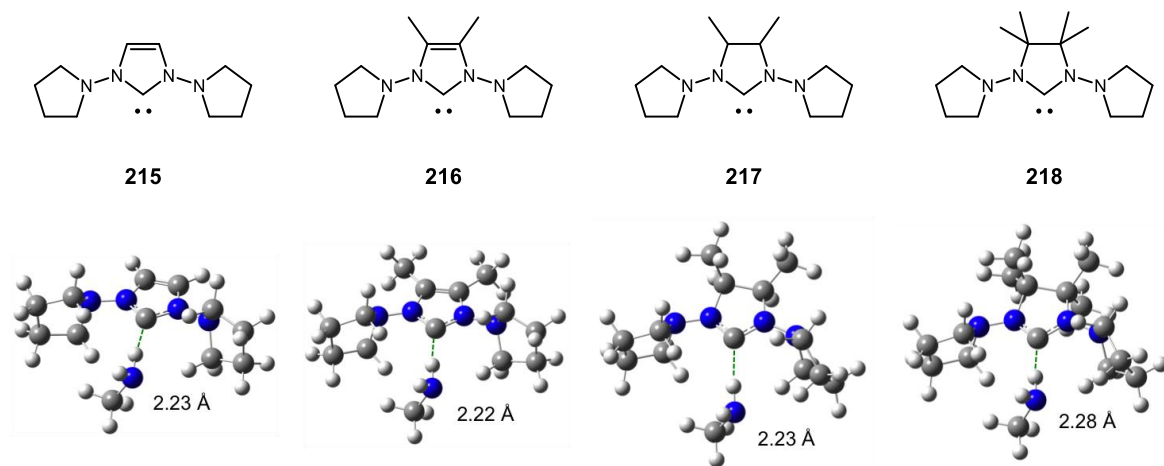


Figure 45: Prioritised pyrrolidine-derived compounds showing hydrogen bonding distances for carbene-amine complexes. Geometry optimisations performed in Gaussian 09 using M06/6-311G(d,p).

Results from the initial geometry optimisation of each of the pyrrolidine-derived compounds suggested an improvement in calculated hydrogen bond length compared to previous systems where a bifurcated interaction was targeted. This implied that the presence of a

single hydrogen bond resulted in a stronger interaction with the amine. Accordingly, the extent of elongation of the NH bond and the corresponding enthalpy change upon complex formation were assessed for these systems. Data for the amine complexes shown in Figure 45 was again compared with that of the corresponding NHC-methanol complexes (Table 43).

Table 43: Modelling results for prioritised pyrrolidine-derived carbene systems

Carbene	Amine Complex		Alcohol Complex		
	NH Elongation (Å)	ΔH Complex Formation (kcal/mol)	OH Elongation (Å)	Carbene-OH Hydrogen Bond Length	ΔH Complex Formation (kcal/mol)
215	0.009	-8.1	0.02	1.94	-13.5
216	0.01	-8.1	0.03	1.93	-14.9
217	0.01	-8.2	0.02	1.95	-13.1
218	0.009	-8.1	0.03	1.94	-13.1

Results from this set of calculations indicated a commensurate increase in NH bond length due to the stronger hydrogen bonding interaction observed for pyrrolidine-derived NHCs. In comparison to the ‘dual catalysis’ series, the extent of bond elongation only differs by around 2 – 3 fold with respect to the analogous alcohol complexes. This suggests that these systems might provide increased activation compared to the previous series. Similarly, calculated enthalpy changes for the formation of an NHC-amine complex suggest that the interaction of the amine with pyrrolidine-derived systems is likely to be favourable. Based on these calculations, comparable results were obtained for each of the catalysts investigated. Therefore, partial charge and molecular orbital calculations were carried out in an attempt to further discriminate between individual systems (Figure 46).

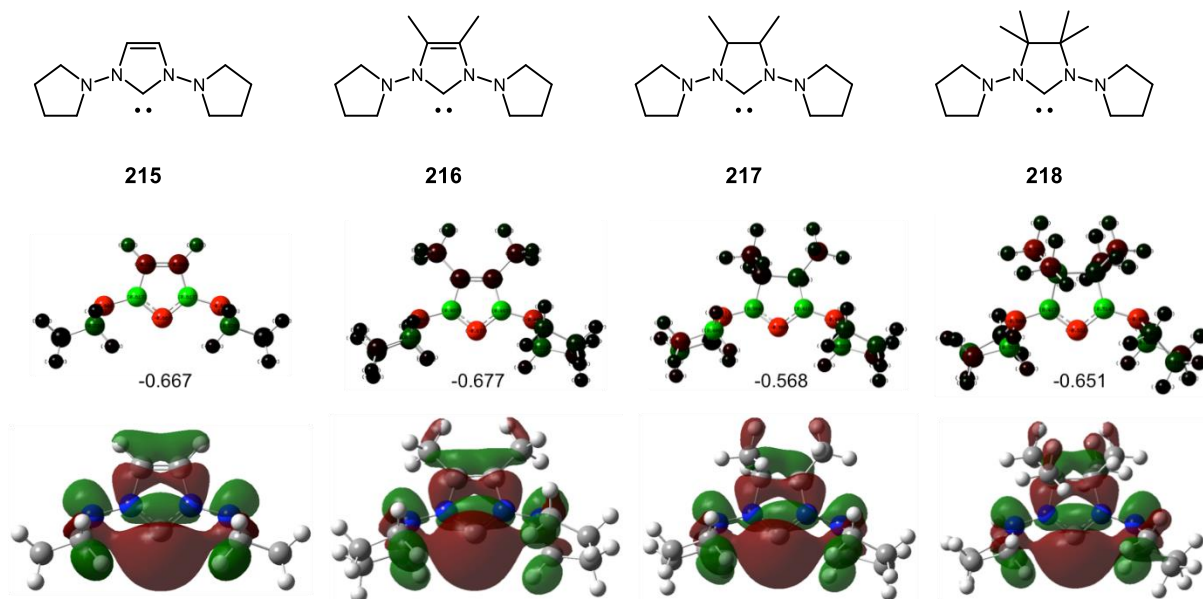


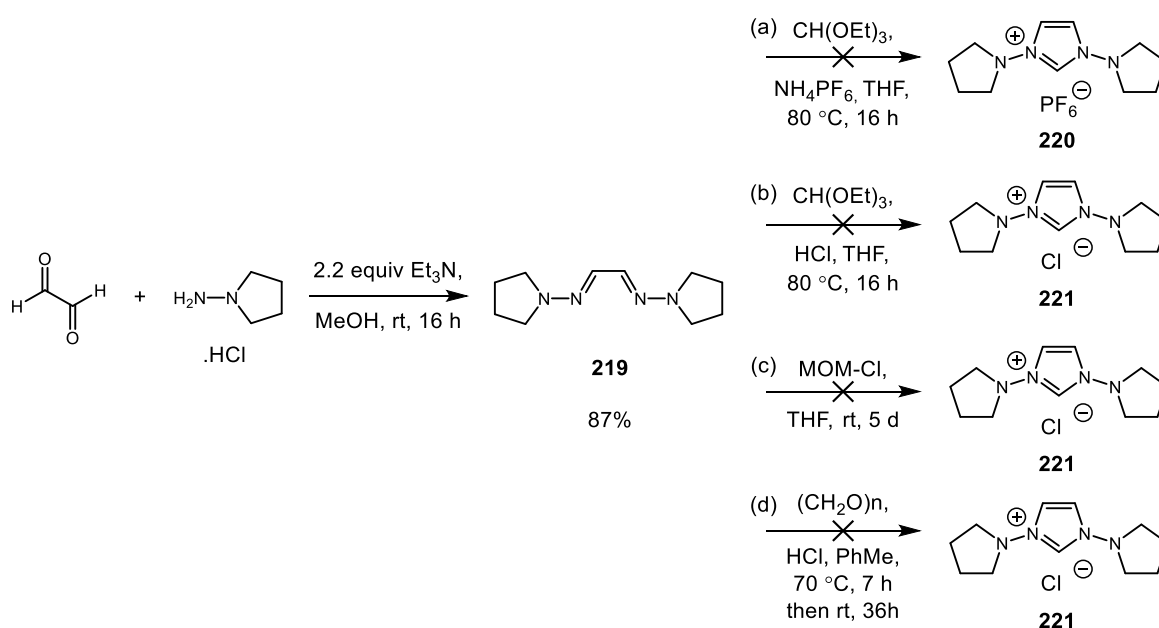
Figure 46: Partial charge and molecular orbital calculations for pyrrolidine-derived systems. Values indicate most negative charge (represented in red on molecules). Population analysis and HOMO/LUMO calculations performed in Gaussian 09 using M06/6-311G(d,p).

Partial charge calculations indicated that introducing methyl groups or incorporating a saturated backbone did not result in marked difference in negative charge on the carbene centre compared to the progenitor system (**215**). Molecular orbital calculations suggest that the majority of electron density resides on the carbene centre for each system, as anticipated in the original design hypothesis.

At this level of theory, the series of pyrrolidine analogues performed similarly across a range of calculations. Therefore, prioritisation of a certain catalyst for synthesis and screening was difficult based on consideration of the theoretical data generated. As a result, it was decided that the progenitor unsubstituted system (**215**) would be progressed for use in a trial amidation reaction due to the ready availability of starting materials. Experimental observation of this catalyst would establish if a single, stronger hydrogen bond was more optimal for amide bond formation than previous systems in the ‘dual catalysis’ series which displayed two hydrogen bonding interactions.

The initial step in the synthesis of the prioritised precursor involved condensation of glyoxal with 1-aminopyrrolidine to form the required diimine intermediate (**219**, Scheme 58). Examination of literature procedures for cyclisation to the imidazolium species indicated a number of possible methods for effecting this transformation.⁶⁵ These involved using

triethylorthoformate, MOM-Cl, or formaldehyde to install the C1 carbon centre. These procedures could result in the direct formation of the preferred PF₆ salt (**220**, Scheme 58a) or could generate the corresponding halide salt (**221**, Scheme 58b-d) which could then be subjected to a salt exchange procedure. However, despite repeated experimentation, all the cyclisation methods attempted were unsuccessful for the diimine system and no desired product was observed for any of these reactions. Based on the theoretical calculations, a saturated backbone demonstrated similar results in a range of modelling experiments. Therefore, reduction of the diimine to the corresponding diamine and subsequent use in the cyclisation reactions could potentially allow access to this type of system.



Scheme 58: Synthesis of pyrrolidine precursor

Following successful isolation of a pyrrolidine-derived precursor, it could then be subjected to experimental screening in a trial amidation reaction. It is hypothesised that the formation of a stronger hydrogen bonding interaction with the incoming amine could offer superior reactivity over previously tested novel systems.

In this phase of the programme, the execution of computational studies allowed for the design and assessment of novel catalyst structures in a high throughput manner. A portfolio of modelling results were developed which could aid prioritisation of NHC catalysts for screening in a model amide bond forming reaction. Initial results from testing of these systems indicated only low conversion to product, and further attempts to optimise this process were unsuccessful with systems investigated in the ‘dual catalysis’ series. However,

it is possible that a biscarbene carbene system (**208**) could potentially offer an advantage over the systems tested, by providing two hydrogen bonding interactions with the amine, each of which is capable of effecting NH elongation, indicating activation of the amine towards nucleophilic attack. Isolation of the corresponding precursor (**215**) and observation in an experimental setting will allow assessment of the reactivity of this catalyst.

A second generation of pyrrolidine-derived carbenes showed promising results across a number of calculations, indicating that these systems might enable the formation of a stronger interaction with the amine coupling partner and, hence, provide superior activation. Successful synthesis of a catalyst of this type would allow for experimental investigation in order to evaluate its ability to catalyse an amidation reaction.

4 Conclusions

The initial aim of this research programme was to design a new generation of NHC catalysts which would be capable of facilitating direct amidation of unactivated esters by enhancing the nucleophilicity of the amine coupling partner. It was believed that this organocatalytic approach to amide bond formation could offer several advantages over traditional methods which commonly utilise stoichiometric coupling reagents.

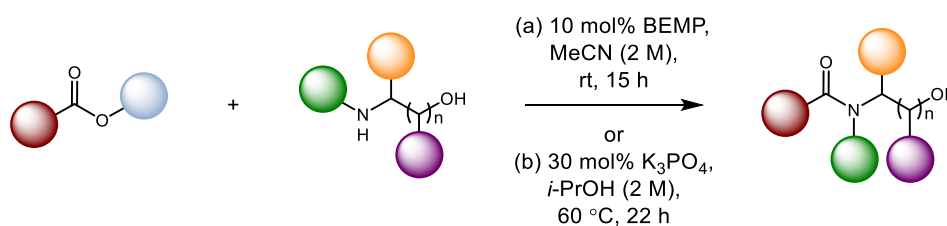
Prior to the design and evaluation of novel systems, an extensive range of known catalyst precursors, additives, and bases were evaluated in a series of high throughput arrays. Throughout these studies, no conversion to the desired amide product was observed and hydrolysis of the ester starting material was found to be a recurring issue. This prompted a comprehensive investigation of the underlying experimental procedure required for handling NHC systems.

Therefore, a known transformation was selected for examination in our own laboratories in order to establish appropriate reaction conditions for product formation. NHC-catalysed amidation of unactivated esters using amino alcohols was studied using IMes as a conventional carbene catalyst. As it was reasoned that hydrolysis was occurring as a result of moisture in the reaction mixture, it was believed that a more rigorously anhydrous protocol was required. A thorough investigation of experimental conditions using this model reaction indicated that a strict anhydrous protocol was necessary for the handling of air- and moisture-sensitive carbenes. Interestingly, when performing this study, control reactions in the absence of carbene catalyst, when only a catalytic amount of *t*-BuOK was present in the reaction mixture, demonstrated comparable results to the NHC-catalysed process. This led to the proposal of an alternative base-catalysed mechanism for this reaction.

Having identified a novel, base-catalysed amidation manifold, full optimisation of this process was undertaken. Following base and solvent screening, which revealed BEMP and MeCN to be the optimal combination, the powerful statistical technique of Design of Experiments was employed to optimise additional parameters such as reaction time, temperature concentration, and catalyst loading. Having established optimal conditions (Scheme 59a) which maximised conversion to product for a model reaction, the utility of this method was determined by exploring substrate scope. A wide range of esters and amino

Conclusions

alcohols were competent substrates in this reaction, generally giving good to excellent yields of amido alcohol products (53 examples, 40 – 100%). The optimised amidation method could also be extended to the synthesis of oxazolidinone derivatives and medically-relevant compounds. Two known biologically active molecules, Org 26576 and midodrine, were prepared *via* this method, demonstrating its utility in a medicinal chemistry setting. Furthermore, BEMP-catalysed amidation could also be exploited for the synthesis of a key intermediate in the preparation of a novel AMPA receptor modulator as part of an in-house medicinal chemistry programme.



Scheme 59: Novel methods for base-catalysed amidation of esters using amino alcohols

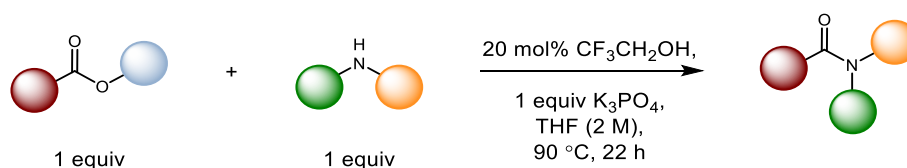
As part of this study, and in conjunction with another member of our laboratory, a range of mechanistic investigations were carried out in order to validate the proposed mechanism for this reaction. Results from these studies confirmed that the reaction was likely to proceed *via* an initial transesterification event, followed by intramolecular rearrangement to the more stable amide product.

Subsequently, development and optimisation of a more sustainable base-catalysed amidation process was carried out in order to address the green credentials of this reaction. Initial screening identified K₃PO₄ and *i*-PrOH as a suitable, more environmentally friendly base and solvent combination. The technique of DoE was again employed to fully optimise reaction conditions (Scheme 59b). A number of substrates were examined and found to be applicable with this reaction, demonstrating good yields and associated reaction mass efficiencies, a key metric in determining the sustainability of a reaction. Therefore, based on the initial identification of a potential base-catalysed manifold, two novel amide bond forming processes were developed for the synthesis of a diverse range of amido alcohol-containing products.

Although these methods were efficient and widely applicable, a limitation was the requirement for an alcohol functional group in the starting material to facilitate the initial

Conclusions

transesterification reaction. Therefore, a more direct amidation method was developed, using an alcohol additive to form the ester intermediate *in situ*. Evaluation of a range of additives showed trifluoroethanol to be the only system to demonstrate significant conversion (6%) to a model amide substrate, and only when used in stoichiometric amounts. However, by employing the strategy of base and solvent screening followed by DoE-based optimisation of reaction conditions, conversion to product was maximised. Optimised conditions enabled trifluoroethanol to be used in catalytic amounts, and a range of amide products were successfully isolated using this method (Scheme 60).



Scheme 60: Novel trifluoroethanol-catalysed amidation of esters

Following the optimisation of several novel amidation methods, attention returned to the design of a new generation of NHC catalysts which would facilitate direct amidation of simple ester starting materials. Computational methods were used to aid the evaluation of all proposed NHCs and prioritise certain catalysts for synthesis. Carbenes capable of forming additional interactions with the incoming amine *via* hydrogen bonding to the substituents, and those derived from pyrrolidine systems displayed promising results across a range of modelling experiments. Of these, several were prioritised for synthesis. Initial investigation of novel precursors in a model amidation reactions did not demonstrate any conversion to the desired product. However, a raft of *in silico* data was generated which could aid prioritisation of alternative novel catalysts. Other systems which performed well in a range of calculations, such as a biscarbene (**208**) and a pyrrolidine-derived system (**215**) could potentially offer superior reactivity in a catalytic amidation reaction.

5 Future Work

Investigation of anhydrous reaction conditions required for handling of NHCs led to the identification of a novel base-catalysed amidation manifold. As a result of this nascent observation, three novel amidation methods were successfully developed.

Returning to the original hypothesis, it was believed that direct amidation could also be enabled through the rational design of a new generation of NHC catalysts which would tune the nucleophilicity of the amine coupling partner. As discussed, the formation of a hydrogen bond between an amine proton and the carbene centre was believed to be an indicator of amine activation. Additionally, it was believed that the resulting elongation of the NH bond upon complexation to the carbene could also point to an increase in reactivity of the amine towards nucleophilic attack.

Therefore, molecular modelling techniques were employed to evaluate proposed systems and determine whether NH bond elongation was observed when the amine was hydrogen bonded to the carbene centre. Based on the results from a range of calculations, two diverse classes of NHC catalysts were prioritised for synthesis. Experimental screening of NHCs with a substituent capable of forming an additional hydrogen bonding interaction with the amine were not found to be active in a model interaction, indicating that these catalysts were not suitable for this purpose. However, if NH bond elongation is a harbinger for activation of the amine, two remaining systems which were prioritised based on promising theoretical results may offer increased activity (Figure 47). A biscarbene catalyst (**208**) demonstrated elongation of both NH bonds upon complexation with an amine, which could provide superior activation. Furthermore a pyrrolidine system (**215**), which only formed a single hydrogen bonding interaction, demonstrated increased elongation of the NH bond. This could again be an indication that this system could improve the nucleophilicity of the amine. Therefore, synthesis of the corresponding catalyst precursors and experimental investigation would determine whether these bespoke carbenes were suitable catalysts for performing direct amidation of unactivated esters.

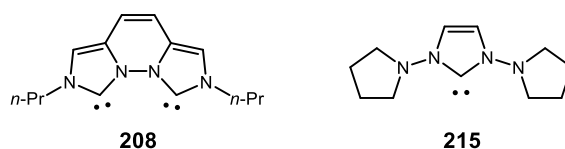
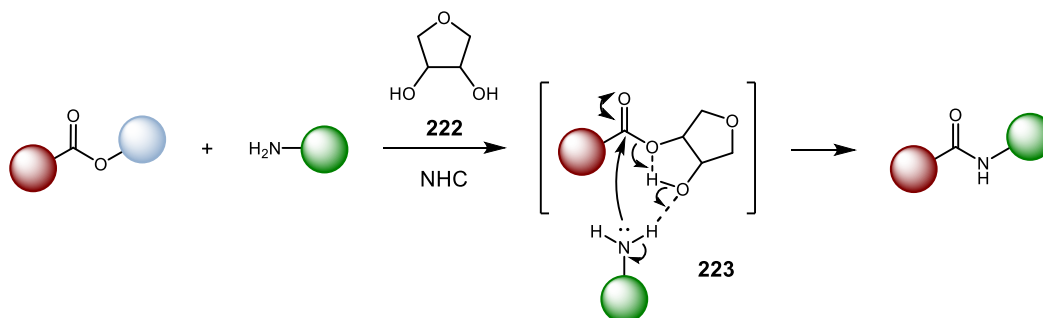


Figure 47: Remaining prioritised precursors

In addition to the design and evaluation of bespoke carbene systems, another proposed investigation in the area of NHC-mediated amidation takes inspiration from ribosomal peptide bond formation (Scheme 61).¹⁴⁵ Analysis of crystal structures of ribosomal subunits, and mutagenesis studies have indicated that amidation in this context is facilitated by a ‘proton shuffle’ mechanism. Therefore, formation of an analogous ester intermediate (**223**) could facilitate amide bond formation in a similar manner, directing nucleophilic attack of the amine onto the carbonyl group through the formation of a hydrogen bonding interaction.



Scheme 61: Proposed NHC-mediated amidation mimicking ribosomal peptide bond formation mechanism

As NHC-catalysed transesterification is well established, it is believed that this transformation could be exploited to synthesise the intermediate ester species (**223**) using anhydroerythritol (**222**) or related sugars. NHC-catalysed transesterification has been shown to operate under relatively mild conditions, therefore could allow amidation to occur at lower temperatures than those previously employed for the trifluoroethanol-mediated amidation process (Section 3.9.3). Additionally, low catalyst loadings are tolerated, so the use of a full equivalent of base could potentially be avoided. Therefore, optimisation of this process could allow access to a novel, efficient NHC-mediated amidation manifold which has thus far proven to be elusive when using simple unactivated esters as substrates.

6 Experimental

6.1 General Techniques

All reagents and solvents were obtained from commercial suppliers and were used without further purification unless otherwise stated. Purification was carried out according to standard laboratory methods.¹⁰⁶ Where purification was carried out by distillation, desiccants are indicated in brackets if used.

6.1.1 Purification of Solvents

- i) Anhydrous PhMe and THF were obtained from a PureSolv SPS-400-5 solvent purification system.¹⁴⁶
- ii) CPME, DMC (CaH₂), MeCN (CaH₂), 2-MeTHF (CaH₂), *i*-PrOH (KOH), and TBME were purified by fractional distillation.
- iii) DMF (MgSO₄) and NMP (CaH₂) were purified by vacuum distillation.
- iv) Purified solvents were transferred to and stored in a septum-sealed oven-dried flask over activated 4 Å molecular sieves and purged with and stored under nitrogen.

6.1.2 Purification of Reagents and Catalysts

- i) Et₃N (CaH₂) and trifluoroethanol (Na₂SO₄) were purified by fractional distillation.
- ii) BEMP (CaH₂), benzylamine (KOH), DBU, ethanolamine (KOH), iodobenzene (CaH₂), and methyl benzoate (K₂CO₃) were purified by vacuum distillation.
- iii) *t*-BuOK was purified by sublimation, Cs₂CO₃ was purified by recrystallization from ethanol, and NaH was purified by washing with petroleum ether 40-60.
- iv) K₂CO₃, K₃PO₄, montmorillonite and hydrotalcite were oven-dried prior to use.

6.1.3 Experimental Details

- i) Moisture-sensitive reactions were carried out under Schlenk conditions using oven-dried glassware, which was evacuated and purged with N₂ before use.
- ii) Purging refers to a vacuum/nitrogen-refilling procedure.
- iii) Room temperature was generally *ca.* 20 °C.

Experimental - General Techniques

- iv) Reactions were carried out at elevated temperatures using a temperature-regulated hotplate/stirrer.
- v) Phase separation was carried out using IST Isolute Phase Separator Cartridges.

6.1.4 Purification of Products

- i) Thin layer chromatography was carried out using Merck silica plates coated with fluorescent indicator UV254. These were analysed under 254 nm UV light or developed using potassium permanganate solution or phosphomolybdic acid.
- ii) Flash column chromatography was carried out using IST Isolute Flash Silica SPE cartridges.
- iii) Strong cation exchange chromatography was carried out using Silicycle SiliaPrep™ Propylsulfonic Acid (SCX-2) cartridges.
- iv) Reversed phase HPLC was carried out on a Gilson 151 Preparative HPLC, using a gradient method and eluting with 5 – 80% MeCN/water.

6.1.5 Analysis of Products

- i) Fourier Transformed Infra-Red (FTIR) spectra were obtained on a Shimadzu IRAffinity-1 machine.
- ii) ^1H and ^{13}C NMR spectra were obtained on a Bruker DRX 500 spectrometer at 500 and 126 MHz, respectively; or on a Bruker AV3 400 spectrometer at 400 and 101 MHz, respectively. Chemical shifts are reported in ppm and coupling constants are reported in Hz with CDCl_3 referenced at 7.27 (^1H) and 77.23 ppm (^{13}C), DMSO referenced at 2.50 (^1H) and 39.51 ppm (^{13}C) and MeOD referenced at 3.31 (^1H) and 49.15 ppm (^{13}C).
- iii) High-resolution mass spectra were obtained on a Thermofisher LTQ Orbitrap XL instrument at the EPSRC National Mass Spectrometry Service Centre, Swansea.
- iv) LCMS data was obtained on an Agilent 1200 series LCMS with a 6130 single quadrupole.
- v) Analytical reversed phase HPLC data was obtained on an Agilent 1200 series HPLC using a Machery-Nagel Nucleodur C18 column, which was maintained at a constant temperature of 40 °C.

- vi) Chiral HPLC data was obtained on an Agilent 1260 Infinity HPLC using a Chiralpak IA column at room temperature.

6.1.6 Reversed Phase HPLC Methods

- i) Analytical reversed phase analysis was performed using a gradient method, eluting with 5 – 80% MeCN/water over 5 minutes at a flow rate of 2 mL/min. Two different HPLC methods were developed, which were adapted slightly to enable adequate separation of analyte peaks. Retention times are shown for relevant compounds analysed by each method.

Table 44: HPLC method 1 for determining conversion to 3-(anthracen-9-yl)-N-(4-methoxybenzyl)propanamide (93/94) to N-(2-hydroxyethyl)benzamide (110), showing relevant retention times

Time (min)	Concentration of MeCN (%)	Compound	Retention Time (min)
0.0	5	Methyl 3-(anthracen-9-yl)propanoate (91/92)	2.6
0.8	60	3-(Anthracen-9-yl)-N-(4-methoxybenzyl)propanamide (93/94)	2.1
1.8	60	3-(Anthracen-9-yl)propanoic acid (89/90)	1.8
3.7	80	Methyl benzoate	1.8
3.9	80	N-(2-hydroxyethyl)benzamide (110)	1.2
4.3	5	Iodobenzene (internal standard)	2.6
5.0	5		

Table 45: HPLC method 2 for determining conversion to *N*-benzylbenzamide **56**, showing relevant retention times

Time (min)	Concentration of MeCN (%)	Compound	Retention Time (min)
0.0	5	Methyl benzoate	2.0
1.0	55	2,2,2-Trifluoroethyl benzoate (200)	2.5
3.9	60	<i>N</i> -Benzylbenzamide (56)	1.9
4.1	80	Iodobenzene (internal standard)	2.9
4.3	5		
5.0	5		

- ii) For reactions employing the analytical construct, conversions were calculated directly from the ratio of peak areas.
- iii) For reactions using an internal standard, prior HPLC calibration was carried out using samples containing varying molarities of product and iodobenzene, allowing calculation of the response factor by substituting values into the following equation:

$$\text{Response Factor} = \frac{\left(\frac{\text{Area}}{\text{Molarity}}\right)_{\text{Product}}}{\left(\frac{\text{Area}}{\text{Molarity}}\right)_{\text{Standard}}}$$

- iv) Screening reactions were carried out using a known molarity of iodobenzene internal standard as indicated in the relevant general experimental procedures.
- v) Samples for HPLC analysis were prepared by diluting a 10 μL aliquot from the reaction mixture to 1 mL with MeCN.
- vi) Unknown molarities of product were calculated by rearranging the above equation, using the average value for the response factor as determined during calibration.
- vii) Conversion to product was calculated as a percentage of the theoretical molarity for the reaction.

6.1.7 Normal Phase HPLC Method

- i) Chiral HPLC analysis was performed using an isocratic method, eluting with 10% *i*-PrOH/hexanes over 40 minutes at a flow rate of 1 mL/min.

Table 46: HPLC method 3 for determining diastereomeric ratio or enantiomeric excess, showing relevant retention times

Compound	Retention Time of Major Stereoisomer (min)	Retention Time of Minor Stereoisomer (min)
tert-Butyl ((<i>S</i>)-1-(((<i>S</i>)-1-hydroxy-3-phenylpropan-2-yl)amino)-1-oxo-3-phenylpropan-2-yl)carbamate (131)	13.1	19.2
(<i>S</i>)-tert-Butyl (1-(benzylamino)-1-oxo-3-phenylpropan-2-yl)carbamate (189)	7.6	11.5

6.2 General Experimental Procedures

6.2.1 Screening Reactions with Known Carbene Systems

General Experimental Procedure A for Precursor and Additive Screening

To a vial containing a 1:1 mixture of methyl 3-(anthracen-9-yl)propanoate and methyl 3-(anthracen-9-yl)-(2-*d*₂)-propanoate (**91/92**, 13 mg, 0.05 mmol, 1 equiv), 4-methoxybenzylamine (6.5 μ L, 0.05 mmol, 1 equiv), carbene precursor (0.01 mmol, 0.2 equiv), additive (0.01 mmol, 0.2 equiv), and DMF (0.8 mL) was added DBU (7.5 μ L, 0.05 mmol, 1 equiv). The reaction mixture was stirred at room temperature for 16 h. Conversion to product **93/94** was determined by HPLC (Method 1). Further analysis by LCMS indicated hydrolysis of ester starting material.

6.2.2 Screening Reactions with Model Carbene System

General Experimental Procedure B for Base and Additive Screening

To a vial containing a 1:1 mixture of methyl 3-(anthracen-9-yl)propanoate and methyl 3-(anthracen-9-yl)-(2-*d*₂)-propanoate (**91/92**, 13 mg, 0.05 mmol, 1 equiv), 4-methoxybenzylamine (6.5 μ L, 0.05 mmol, 1 equiv), 1-butyl-3-(pyridin-2-ylmethyl)-1*H*-imidazol-3-ium bromide (**106**, 3 mg, 0.01 mmol, 0.2 equiv), additive (0.01 mmol, 0.2 equiv), and DMF (0.8 mL) was added base (0.05 mmol, 1 equiv). The reaction mixture was stirred at room temperature for 16 h. Conversion to product **93/94** was determined by HPLC (Method 1). Further analysis by LCMS indicated hydrolysis of ester starting material.

General Experimental Procedure C for Alternative Base Screening

To a vial containing a 1:1 mixture of methyl 3-(anthracen-9-yl)propanoate and methyl 3-(anthracen-9-yl)-(2-*d*₂)-propanoate (**91/92**, 26 mg, 0.1 mmol, 1 equiv), 4-methoxybenzylamine (13 μ L, 0.1 mmol, 1 equiv), 1-butyl-3-(pyridin-2-ylmethyl)-1*H*-imidazol-3-ium bromide (**106**, 6 mg, 0.02 mmol, 0.2 equiv), and DMF (0.8 mL) was added base (0.02 mmol, 0.2 equiv). The reaction mixture was stirred at room temperature for 16 h. Conversion to product **93/94** was determined by HPLC (Method 1). Control reactions were conducted in the absence of 1-butyl-3-(pyridin-2-ylmethyl)-1*H*-imidazol-3-ium bromide (**106**) for reactions showing significant conversion.

6.2.3 Investigation of Reaction Conditions Using IMes

General Experimental Procedure D for Optimisation of Anhydrous Reaction Procedure

To an oven-dried vessel containing 1,3-dimesityl-1*H*-imidazol-3-ium chloride (**108**, 16 mg, 0.046 mmol, 0.065 equiv) or 1,3-dimesityl-1*H*-imidazol-3-ium hexafluorophosphate (**109**, 21 mg, 0.046 mmol, 0.065 equiv), potassium *tert*-butoxide (4 mg, 0.036 mmol, 0.05 equiv), and THF (0.8 mL) was added methyl benzoate, (89 μ L, 0.71 mmol, 1 equiv), and ethanolamine (43 μ L, 0.71 mmol, 1 equiv). The reaction mixture was stirred at room temperature for 16 h. Conversion to product **110** was determined by HPLC (Method 1) with reference to iodobenzene (0.7 M), which was used as an internal standard.

General Experimental Procedure E for Investigation of Control Reaction in the Absence of Carbene Precursor

To an oven-dried Schlenk tube containing 1,3-dimesityl-1*H*-imidazol-3-ium hexafluorophosphate (**109**, 21 mg, 0.046 mmol, 0.065 equiv), potassium *tert*-butoxide (4 mg, 0.036 mmol, 0.05 equiv), and THF (0.8 mL) was added methyl benzoate (89 μ L, 0.71 mmol, 1 equiv) and ethanolamine (43 μ L, 0.71 mmol, 1 equiv). The reaction mixture was stirred at room temperature for 16 h. Conversion to product **110** was determined by HPLC (Method 1) with reference to iodobenzene (0.7 M), which was used as an internal standard. A control reaction was performed in the absence of 1,3-dimesityl-1*H*-imidazol-3-ium hexafluorophosphate (**109**).

General Experimental Procedure F for Exploring Equivalent of Catalyst Precursor and Base

To an oven-dried Schlenk tube containing 1,3-dimesityl-1*H*-imidazol-3-ium hexafluorophosphate (**109**, 0 – 0.71 mmol, 0 – 1 equiv), potassium *tert*-butoxide (0.035 mmol – 0.71 mmol, 0.05 – 1 equiv), and THF (1.4 mL) was added methyl benzoate (89 μ L, 0.71 mmol, 1 equiv) and ethanolamine (43 μ L, 0.71 mmol, 1 equiv). The reaction mixture was stirred at room temperature for 16 h then concentrated to a residue that was purified by flash column chromatography (methanol/DCM).

General Experimental Procedure G for Expanding Ester Substrate Scope

To an oven-dried Schlenk tube containing 1,3-dimesityl-1*H*-imidazol-3-ium hexafluorophosphate (**109**, 42 mg, 0.092 mmol, 0.065 equiv), potassium *tert*-butoxide (8 mg, 0.071 mmol, 0.05 equiv) and THF (1.4 mL) was added ester (1.42 mmol, 1 equiv) and ethanolamine (86 μ L, 1.42 mmol, 1 equiv). The reaction mixture was stirred at room temperature for 16 h then concentrated to a residue that was purified by flash column chromatography (methanol/DCM). Control reactions were performed in the absence of 1,3-dimesityl-1*H*-imidazol-3-ium hexafluorophosphate (**109**).

6.2.4 Optimisation of Base-catalysed Amidation

General Experimental Procedure H for Base and Solvent Screening

To an oven-dried Schlenk tube containing base (0.07 mmol, 0.05 equiv) and solvent (1.4 mL) was added methyl benzoate (178 μ L, 1.42 mmol, 1 equiv) and ethanolamine (86 μ L, 1.42 mmol, 1 equiv). The reaction mixture was stirred at 40 °C for 22 h. The reaction mixture was sampled at 4, 8 and 22 hour time points and the conversion to product **110** was determined by HPLC (Method 1) with reference to iodobenzene (0.7 M), which was used as an internal standard.

General Experimental Procedure I for Optimisation of BEMP-catalysed Amidation Using Design of Experiments

To an oven-dried Schlenk tube containing BEMP (**117**, 0.07 mmol – 0.28 mmol, 0.05 – 0.2 equiv) and MeCN (0.5 – 2 M) was added methyl benzoate (178 μ L, 1.42 mmol, 1 equiv) and ethanolamine (86 μ L, 1.42 mmol, 1 equiv). The reaction mixture was stirred at the required temperature (20 – 60 °C) for 8 – 22 hours. The reaction mixture was sampled at the end of the required reaction time and conversion to product **110** was determined by HPLC (Method 1) with reference to iodobenzene (0.7 M), which was used as an internal standard.

General Experimental Procedure J for Synthesis of Amido Alcohols *via* BEMP-catalysed Amidation

To an oven-dried Schlenk tube containing BEMP (**117**, 41 μ L, 0.14 mmol, 0.1 equiv) and MeCN (700 μ L) was added ester (1.42 mmol, 1 equiv) and amino alcohol (1.42 mmol, 1 equiv). The reaction mixture was stirred at room temperature for 15 h then concentrated to a residue that was purified by flash column chromatography (methanol/DCM). For substrates that required elevated temperatures, reactions were performed at 40 °C.

General Experimental Procedure K for Investigation of Alternative Phosphazene Bases

To an oven-dried Schlenk tube containing phosphazene base (0.14 mmol, 0.1 equiv) and MeCN (700 μ L) was added methyl 2-phenyl acetate (200 μ L, 1.42 mmol, 1 equiv) and ethanolamine (86 μ L, 1.42 mmol, 1 equiv). The reaction mixture was stirred at room

temperature for 15 h then concentrated to a residue that was purified by flash column chromatography (methanol/DCM).

General Experimental Procedure L for Synthesis of Oxazolidinones via BEMP-catalysed Amidation

To an oven-dried Schlenk tube containing BEMP (**117**, 41 μL , 0.14 mmol, 0.1 equiv) and MeCN (700 μL) was added dimethyl carbonate (359 μL , 4.26 mmol, 3 equiv) and amino alcohol (1.42 mmol, 1 equiv). The reaction mixture was stirred at 40 °C for 15 h then concentrated to a residue that was purified by flash column chromatography (methanol/DCM).

6.2.5 Optimisation of Sustainable Base-catalysed Amidation

General Experimental Procedure M for Base and Solvent Screening

To an oven-dried Schlenk tube containing base (0.28 mmol, 0.2 equiv) and solvent (1.4 mL) was added methyl benzoate (178 μL , 1.42 mmol, 1 equiv) and ethanolamine (86 μL , 1.42 mmol, 1 equiv). The reaction mixture was stirred at 40 °C for 22 h. The reaction mixture was sampled at 4, 8 and 22 hour time points and the conversion to product **110** was determined by HPLC (Method 1) with reference to iodobenzene (0.7 M), which was used as an internal standard.

General Experimental Procedure N for Optimisation of K_3PO_4 -catalysed Amidation Using Design of Experiments

To an oven-dried Schlenk tube containing K_3PO_4 (0.1 – 0.3 equiv) and *i*-PrOH (0.5 – 2 M) was added methyl benzoate (178 μL , 1.42 mmol, 1 equiv) and ethanolamine (86 μL , 1.42 mmol, 1 equiv). The reaction mixture was stirred at the required temperature (20 – 60 °C) for 8 – 22 hours. The reaction mixture was sampled at the end of the required reaction time and the conversion to product **110** was determined by HPLC (Method 1) with reference to iodobenzene (0.7 M), which was used as an internal standard.

General Experimental Procedure O for Synthesis of Amido Alcohols via K_3PO_4 -catalysed Amidation

To an oven-dried Schlenk tube containing K_3PO_4 (90 mg, 0.43 mmol, 0.3 equiv) and *i*-PrOH (700 μ L) was added ester (1.42 mmol, 1 equiv) and amino alcohol (1.42 mmol, 1 equiv). The reaction mixture was stirred at 60 °C for 22 h then concentrated to a residue that was purified by flash column chromatography (methanol/DCM).

6.2.6 Optimisation of a Direct Catalytic Amidation Method

General Experimental Procedure P for Additive Screening

To an oven-dried sealed Schlenk tube containing additive (0.14/1.42 mmol, 0.1/1 equiv), BEMP (**117**, 41 μ L, 0.14 mmol, 0.1 equiv), and MeCN (700 μ L) was added methyl benzoate (178 μ L, 1.42 mmol, 1 equiv) and benzylamine (155 μ L, 1.42 mmol, 1 equiv). The reaction mixture was stirred at 40 °C for 15 h. Conversion to product **56** was determined by HPLC (Method 2) with reference to iodobenzene (1.4 M), which was used as an internal standard.

General Experimental Procedure Q for Base and Solvent Screening

To an oven-dried Schlenk tube containing trifluoroethanol (**176**, 102 μ L, 1.42 mmol, 1 equiv), base (0.14 mmol, 0.1 equiv), and solvent (700 μ L) was added methyl benzoate (178 μ L, 1.42 mmol, 1 equiv) and benzylamine (155 μ L, 1.42 mmol, 1 equiv). The reaction mixture was stirred at 40 °C for 15 h. Conversion to product **56** was determined by HPLC (Method 2) with reference to iodobenzene (1.4 M), which was used as an internal standard.

General Experimental Procedure R for Optimisation of Trifluoroethanol-catalysed Amidation Using Design of Experiments

To an oven-dried Schlenk tube containing trifluoroethanol (**176**, 0.28 – 1.42 mmol, 0.2 – 1 equiv), K_3PO_4 (0.28 – 1.42 mmol, 0.2 – 1 equiv), and THF (0.5 – 2 M) was added methyl benzoate (178 μ L, 1.42 mmol, 1 equiv) and benzylamine (155 μ L, 1.42 mmol, 1 equiv). The reaction mixture was stirred at the required temperature (40 – 80 °C) for 8 – 22 hours. The reaction mixture was sampled at the end of the required reaction time and the conversion to product **56** was determined by HPLC (Method 2) with reference to iodobenzene (1.4 M), which was used as an internal standard.

General Experimental Procedure S for Synthesis of Amides *via* Trifluoroethanol-catalysed Amidation

To an oven-dried sealed Schlenk tube containing trifluoroethanol (**176**, 20 μL , 0.28 mmol, 0.2 equiv), K_3PO_4 (301 mg, 1.42 mmol, 1 equiv), and THF (700 μL) was added ester (1.42 mmol, 1 equiv) and amine (1.42 mmol, 1 equiv). The reaction mixture was stirred at 90 $^\circ\text{C}$ for 22 h then diluted with EtOAc (10 mL), washed with water (3 x 10 mL), passed through a hydrophobic frit, and concentrated to a residue that was purified by flash column chromatography (methanol/DCM or EtOAc/pet. ether).

General Experimental Procedure T for Investigation of Alternative Additives

To an oven-dried sealed Schlenk tube containing additive (0.28 mmol, 0.2 equiv), K_3PO_4 (301 mg, 1.42 mmol, 1 equiv), and THF (700 μL) was added Boc-phenylalanine methyl ester (397 mg, 1.42 mmol, 1 equiv) and benzylamine (155 μL , 1.42 mmol, 1 equiv). The reaction mixture was stirred at 90 $^\circ\text{C}$ for 22 h then diluted with EtOAc (10 mL), washed with water (3 x 10 mL), passed through a hydrophobic frit, and concentrated to a residue that was purified by flash column chromatography (1% methanol/DCM).

6.2.7 Screening Reactions with Novel Carbene Systems

General Experimental Procedure U for Precursor and Base Screening

To an oven-dried Schlenk tube containing carbene precursor (0.0125 mmol, 0.1 equiv), base (0.125 mmol, 1 equiv), and THF (1 mL) was added methyl benzoate (16 μL , 0.125 mmol, 1 equiv) and benzylamine (14 μL , 0.125 mmol, 1 equiv). The reaction mixture was stirred at rt for 15 h. Conversion to product **56** was determined by HPLC (Method 2) with reference to iodobenzene (1.4 M), which was used as an internal standard.

General Experimental Procedure V for Base and Solvent Screening with Pyridyl Carbene Precursor

To an oven-dried Schlenk tube containing carbene precursor (**210**, 36 mg, 0.14 mmol, 0.1 equiv), base (0.17 mmol, 0.12 equiv), and solvent (700 μL) was added methyl benzoate (178 μL , 1.42 mmol, 1 equiv) and benzylamine (155 μL , 1.42 mmol, 1 equiv). The reaction mixture was stirred at 40 $^\circ\text{C}$ for 15 h. Conversion to product **56** was determined by HPLC (Method 2) with reference to iodobenzene (1.4 M), which was used as an internal standard.

General Experimental Procedure W for Investigation of Control Reactions in the Absence of Carbene Precursor

To an oven-dried Schlenk tube containing base (0.17/1.42 mmol, 0.12/1 equiv), and solvent (700 μL) was added methyl benzoate (178 μL , 1.42 mmol, 1 equiv) and benzylamine (155 μL , 1.42 mmol, 1 equiv). The reaction mixture was stirred at 40 $^{\circ}\text{C}$ for 15 h. Conversion to product **56** was determined by HPLC (Method 2) with reference to iodobenzene (1.4 M), which was used as an internal standard.

General Experimental Procedure X for Base and Solvent Screening with IMes.PF₆

To an oven-dried Schlenk tube containing IMes.PF₆ (**109**, 63 mg, 0.14 mmol, 0.1 equiv), base (1.42 mmol, 1 equiv), and solvent (700 μL) was added methyl benzoate (178 μL , 1.42 mmol, 1 equiv) and benzylamine (155 μL , 1.42 mmol, 1 equiv). The reaction mixture was stirred at 40 $^{\circ}\text{C}$ for 15 h. Conversion to product **56** was determined by HPLC (Method 2) with reference to iodobenzene (1.4 M), which was used as an internal standard. Control reactions were conducted in the absence of IMes.PF₆ (**109**) for all base and solvent combinations.

General Experimental Procedure Y for Optimisation of IMes.PF₆-catalysed Amidation Using Design of Experiments

To an oven-dried Schlenk tube containing IMes.PF₆ (**109**, 0.035 – 0.14 mmol, 0.05 – 0.2 equiv), BEMP (**117**, 202 μL , 0.7 mmol, 1 equiv), and PhMe (0.7 – 1.4 mL, 0.5 – 1 M) was added methyl benzoate (88 μL , 0.7 mmol, 1 equiv) and benzylamine (76 μL , 0.7 mmol, 1 equiv). The reaction mixture was stirred at the required temperature (40 – 100 $^{\circ}\text{C}$) for 8 – 22 hours. The reaction mixture was sampled at the end of the required reaction time and the conversion to product **56** was determined by HPLC (Method 2) with reference to iodobenzene (1.4 M), which was used as an internal standard.

6.3 Results from Screening Reactions

6.3.1 Screening Reactions with Known Carbene Systems

Precursor and Additive Screening with Known Carbene Systems

Reactions were performed according to General Experimental Procedure A (Table 3, Page 48).

Table 47: Results of preliminary precursor and additive screening

Carbene (Amount)	Conversion to Carboxylic Acid 89/90 (%)						
	HOAt (16 μ L)	HOBt (1.5 mg)	HFIP (1.7 μ L)	PFP (1.8 mg)	NHS (1.2 mg)	Zr(O <i>t</i> -Bu) ₄ (3.9 μ L)	None
95 (2.7 mg)	4	8	5	3	3	7	6
96 (2.4 mg)	3	0	2	2	1	1	3
97 (3.6 mg)	7	0	15	6	2	5	10
98 (4.2 mg)	2	1	3	2	2	3	5
60 (2.3 mg)	6	4	4	6	0	2	6
73 (2.6 mg)	3	3	2	3	2	4	3
67 (3.6 mg)	10	11	36	16	3	13	11
54 (3.0 mg)	0	0	0	0	2	3	22
99 (4.3 mg)	7	0	3	0	30	2	2
100 (3.4 mg)	6	8	5	3	0	3	6
101 (3.8 mg)	8	24	23	2	0	2	10
None	2	2	2	0	1	14	4

6.3.2 Screening Reactions with Model Carbene System

Base and Additive Screening with Model Carbene Precursor

Reactions were performed according to General Experimental Procedure B (Table 4, Page 51).

Table 48: Results of base and additive screening with model carbene precursor

Base (Amount)	Conversion to Carboxylic Acid 89/90 (%)						
	HOAt (16 μ L)	HOBt (1.5 mg)	HFIP (1.7 μ L)	PFP (1.8 mg)	NHS (1.2 mg)	Zr(<i>Ot</i> -Bu) ₄ (3.9 μ L)	None
DBU (7.5 μ L)	46	44	25	28	27	38	89
DIPEA (8.7 μ L)	0	0	1	0	0	3	14
Et ₃ N (6.9 μ L)	3	4	4	5	4	9	6
NaH (1.2 mg)	33	54	17	24	21	21	34

Alternative Base Screening with Model Carbene Precursor

Reactions were performed according to General Experimental Procedure C (Table 5, Page 52).

Table 49: Results of alternative catalytic base screening with model carbene precursor

Base (Amount)	Conversion to Carboxylic Acid 89/90 (%)	
	+ Carbene Precursor 106 (6 mg)	– Carbene Precursor 106
<i>t</i> -BuOK (2.2 mg)	18	8
K ₂ CO ₃ (2.8 mg)	0	N.D.
DMAP (2.4 mg)	3	N.D.
Pyridine (1.6 μ L)	3	N.D.
NaOH (0.8 mg)	15	13
(NH ₄) ₂ CO ₃ (1.9 mg)	3	N.D.

6.3.3 Investigation of Reaction Conditions Using IMes

Optimisation of Anhydrous Reaction Procedure

Reactions were performed according to General Experimental Procedure D (Table 6, Page 56).

Table 50: Optimisation of anhydrous reaction conditions

Entry	Catalyst (Amount)	Reaction Vessel	Procedure	Conversion (%)
1	IMes.PF ₆ (21 mg)	Open vial	Open to air	0
2	IMes.Cl (16 mg)	Sealed vial	Purged with N ₂	0
3	IMes.PF ₆ (21 mg)	Sealed vial	Purged with N ₂	0
4	IMes.Cl (16 mg)	Sealed vial	Maintained under positive pressure of N ₂	0
5	IMes.PF ₆ (21 mg)	Sealed vial	Maintained under positive pressure of N ₂	0
6	IMes.PF ₆ (21 mg)	Sealed vial	Maintained under positive pressure of N ₂ , 4Å MS added	0
7	IMes.PF ₆ (21 mg)	Round-bottomed flask	Maintained under positive pressure of N ₂	28
8	IMes.PF ₆ (trituated) (21 mg)	Schlenk tube	Maintained under positive pressure of N ₂	52

Investigation of Control Reaction in the Absence of Carbene Precursor

Reactions were performed according to General Experimental Procedure E (Table 7, Page 57).

Table 51: Investigation of Control Reaction

Entry	IMes.PF ₆ (mol%)	Conversion (%)
1	6.5 (21 mg)	52
2	0	53

6.3.4 Optimisation of Base-catalysed Amidation

Generation of Reaction Profile for *t*-BuOK-catalysed Reaction

To an oven-dried Schlenk tube containing potassium *tert*-butoxide (8 mg, 0.071 mmol, 0.05 equiv) and THF (1.4 mL) was added methyl benzoate (178 μ L, 1.42 mmol, 1 equiv) and ethanolamine (86 μ L, 1.42 mmol, 1 equiv). The reaction mixture was stirred at room temperature for 24 h. The reaction mixture was sampled at several time points and the conversion to product **110** was determined by HPLC (Method 1) with reference to iodobenzene (0.7 M), which was used as an internal standard (Figure 20, Page 64).

Table 52: Profiling of *t*-BuOK-catalysed reaction

Time (h)	Conversion (%)
0	0
1	8
2	12
4	23
6	29
8	32
10	39
24	57

Base and Solvent Screening

Reactions were performed according to General Experimental Procedure H (Table 11, Page 68).

Table 53: Results of base and solvent screening

Base (Amount)	Conversion (%)														
	DMC			MeCN			NMP			PhMe			THF		
	Time (h)			Time (h)			Time (h)			Time (h)			Time (h)		
	4	8	22	4	8	22	4	8	22	4	8	22	4	8	22
Cs₂CO₃ (23 mg)	2	3	3	14	37	53	24	50	62	13	16	19	3	5	17
DBU (11 μL)	1	3	4	4	6	10	1	5	5	2	6	6	3	4	10
<i>t</i>-BuOK (8 mg)	1	1	2	13	14	18	15	26	32	8	9	9	23	28	66
BEMP (21 μL)	3	3	2	53	61	63	3	3	7	5	6	7	3	4	7
NaH (1.7 mg)	3	3	3	31	30	32	6	9	9	8	14	28	12	15	18
None	2	2	2	4	3	5	1	4	3	4	3	2	3	6	7

Optimisation of BEMP-catalysed Amidation Using Design of Experiments

Reactions were performed according to General Experimental Procedure I (Table 15/16, Page 75/79).

Table 54: Results from half-fractional factorial design

Reaction	Time (h)	Temp (°C)	Conc (M)	MeCN (mL)	Cat. Loading (mol%)	BEMP (µL)	Conversion (%)
1	22	20	2	0.7	5	21	60
2	15	40	1.25	1.1	12.5	51	98
3	8	20	0.5	2.8	5	21	32
4	22	20	0.5	2.8	20	82	92
5	22	60	2	0.7	20	82	97
6	8	60	2	0.7	5	21	55
7	22	60	0.5	2.8	5	21	67
8	15	40	1.25	1.1	12.5	51	100
9	8	20	2	0.7	20	82	100
10	8	60	0.5	2.8	20	82	96
11	15	20	2	0.7	10	41	90
12	15	20	2	0.7	20	82	94

The data from Reactions 1 – 10 was processed using Design Expert™ software v8.0.¹⁰⁷ Modelling of the data using the SQRT transform enabled generation of a response surface and a half-normal plot. From this, it could be inferred that that most important parameters were catalyst loading and concentration.

Using the optimisation module, conditions were sought in order to maximize conversion to the amide product (**110**). This analysis revealed the conditions shown in Reactions 11 and 12 in the table above as possible solutions. Repeating the screen using General Experimental

Experimental - Results from Screening Reactions

Procedure I with the quantities of reagents indicated above gave 90 and 94% conversion, respectively.

6.3.5 Optimisation of Sustainable Base-catalysed Amidation

Base and Solvent Screening

Reactions were performed according to General Experimental Procedure M (Table 22, Page 106).

Table 55: Results of base and solvent screening

Base (Amount)	Conversion (%)											
	CPME			2-MeTHF			<i>i</i> -PrOH			TBME		
	Time (h)			Time (h)			Time (h)			Time (h)		
	4	8	22	4	8	22	4	8	22	4	8	22
Et₃N (39 μ L)	3	2	4	1	1	3	1	0	2	2	2	4
K₂CO₃ (39 mg)	5	8	17	2	3	12	3	4	10	3	5	13
K₃PO₄ (60 mg)	6	12	36	2	4	16	9	17	35	5	11	23
Hydrotalcite (169 mg)	4	5	9	2	3	6	2	1	2	2	5	13
Montmorillonite (39 mg)	1	2	5	1	1	3	2	1	2	1	2	5
None	1	1	2	2	2	3	1	1	1	1	1	2

Optimisation of K₃PO₄-catalysed Amidation Using Design of Experiments

Reactions were performed according to General Experimental Procedure N (Table 24/25, Page 109/111).

Table 56: Results from half-fractional factorial design

Reaction	Time (h)	Temp (°C)	Conc (M)	<i>i</i> -PrOH (mL)	Cat. Loading (mol%)	K ₃ PO ₄ (mg)	Conversion (%)
1	8	60	0.5	2.8	30	90	31
2	22	60	0.5	2.8	10	30	17
3	8	20	2	0.7	30	90	8
4	15	40	1.25	1.1	20	60	19
5	22	20	0.5	2.8	30	90	14
6	8	60	2	0.7	10	30	37
7	22	60	2	0.7	30	90	82
8	15	40	1.25	1.1	20	60	20
9	8	20	0.5	2.8	10	30	3
10	22	20	2	0.7	10	30	5
11	15	80	2	0.7	10	30	41
12	15	80	2	0.7	20	60	71

The data from Reactions 1 – 10 was processed using Design Expert™ software v8.0.¹⁰⁷ Modelling of the data using the SQRT transform enabled generation of a response surface and a half-normal plot. From this, it could be inferred that the most important parameters were temperature and catalyst loading.

Using the optimisation module, conditions were sought in order to maximize conversion to the amide product (**110**). This analysis revealed the conditions shown in Entries 11 and 12 in the table above as possible solutions. Repeating the screen using General Experimental Procedure N with the quantities of reagents indicated above gave 41 and 71% conversion, respectively.

6.3.6 Optimisation of a Direct Catalytic Amidation Method

Additive Screening

Reactions were performed according to General Experimental Procedure P (Table 27, Page 117).

Table 57: Results of additive screening

Additive (Amount)	Conversion (%)	
	10 mol% additive	1 equiv additive
HOAt (33/331 μ L, 0.6 M in DMF)	0	0
HOBt (19/191 mg)	0	0
HOAt (22/223 mg)	3	0
Oxya (20/201 mg)	0	0
NHS (16/163 mg)	0	1
HFIP (15/150 μ L)	1	0
CF₃CH₂OH (10/102 μ L)	0	6
None	0	0

Base and Solvent Screening

Reactions were performed according to General Experimental Procedure Q (Table 28, Page 119).

Table 58: Results of base and solvent screening

Base (Amount)	Conversion (%)				
	DMF	MeCN	NMP	PhMe	THF
DBU (21 μL)	4	3	3	8	9
K₃PO₄ (30 mg)	8	5	6	13	14
<i>t</i>-BuOK (16 mg)	5	5	6	13	13
BEMP (41 μL)	7	6	6	5	7
NaH (3 mg)	8	4	7	14	19
No base	0	0	0	0	1
No base, no CF₃CH₂OH	0	0	0	0	1

Optimisation of Trifluoroethanol-catalysed Amidation Using Design of Experiments – Half-fractional Factorial Design

Reactions were performed according to General Experimental Procedure R (Table 30/31, Page 121/123).

Table 59: Results from half-fractional factorial design

Reaction	Time (h)	Temp (°C)	Conc (M)	THF (mL)	TFE (equiv)	TFE (µL)	K₃PO₄ (equiv)	K₃PO₄ (mg)	Conv (%)
1	15	60	1.25	1.1	0.6	61	0.6	181	42
2	8	80	0.5	2.8	1	102	1	301	38
3	8	80	2	0.7	0.2	20	1	301	54
4	8	40	0.5	2.8	0.2	20	1	301	2
5	22	80	2	0.7	0.2	20	0.2	60	53
6	22	80	0.5	2.8	0.2	20	1	301	58
7	22	80	0.5	2.8	1	102	0.2	60	55
8	15	60	1.25	1.1	0.6	61	0.6	181	44
9	8	40	0.5	2.8	1	102	0.2	60	3
10	22	40	0.5	2.8	1	102	1	301	13
11	22	40	2	0.7	1	102	0.2	60	32
12	15	60	1.25	1.1	0.6	61	0.6	181	45
13	8	40	2	0.7	1	102	1	301	20
14	15	60	1.25	1.1	0.6	61	0.6	181	43
15	22	40	0.5	2.8	0.2	20	0.2	60	2
16	22	40	2	0.7	0.2	20	1	301	31
17	8	80	0.5	2.8	0.2	20	0.2	60	6
18	22	80	2	0.7	1	102	1	301	67
19	8	40	2	0.7	0.2	20	0.2	60	5

Experimental - Results from Screening Reactions

20	8	80	2	0.7	1	102	0.2	60	61
21	22	80	2	0.7	0.1	10	0.1	30	12
22	22	80	2	0.7	0	0	0	0	1
23	22	80	2	0.7	0	0	1	301	1
24	22	80	2	0.7	1	102	0	0	2

The data from Reactions 1 – 20 was processed using Design Expert™ software v8.0.¹⁰⁷ Modelling of the data using the SQRT transform enabled generation of a response surface and a half-normal plot. From this, it could be inferred that the most important parameter was temperature, and the amount of additive and base present did not appear to affect the outcome of the reaction.

Using the optimisation module, conditions were sought in order to maximize conversion to the amide product (**56**) whilst minimising use of additive and base. This analysis revealed the conditions shown in Reaction 21 in the table above as a possible solution. However, repeating the screen using General Experimental Procedure R with the quantities of reagents indicated above gave only 12% conversion. Control reactions in the absence of trifluoroethanol and/or K_3PO_4 were also carried out at the higher temperature with no significant conversion being detected in any of these cases (Reactions 22 – 24). This suggested that a half-fractional design was not adequate to model the experimental data and, consequently, a central composite design was employed in order to give a more accurate representation of the data.

Optimisation of Trifluoroethanol-catalysed Amidation Using Design of Experiments – Central Composite Design

Reactions were performed according to General Experimental Procedure R (Table 32/33, Page 125/127). Values for each of the variables of interest outwith the ranges specified in the general experimental procedure represent axial points of the central composite design.

Table 60: Results from Central Composite Design

Reaction	Time (h)	Temp (°C)	Conc (M)	THF (mL)	TFE (equiv)	TFE (μL)	K ₃ PO ₄ (equiv)	K ₃ PO ₄ (mg)	Conv (%)
25	15	60	0.13	10.8	0.6	61	0.6	181	3
26	25	60	1.25	1.1	0.6	61	0.6	181	38
27	15	60	1.25	1.1	0.6	61	1.2	362	41
28	15	60	1.25	1.1	0.6	61	0.002	0.6	4
29	15	60	1.25	1.1	1.2	123	0.6	181	44
30	15	90	1.25	1.1	0.6	61	0.6	181	88
31	15	60	1.25	1.1	0.002	0.2	0.6	181	1
32	15	30	1.25	1.1	0.6	61	0.6	181	7
33	15	60	2.37	0.6	0.6	61	0.6	181	63
34	4.5	60	1.25	1.1	0.6	61	0.6	181	9
35	22	90	2	0.7	0.2	20	1	301	86

The data from Reactions 25 – 34 was processed with the data from the half-fractional design (Table 59, Reactions 1 – 20) using Design Expert™ software v8.0.¹⁰⁷ Analysis of the data using a quadratic model enabled generation of a response surface and a half-normal plot. From this, it could be inferred that the most important parameter was temperature, and an optimum balance existed for additive and base equivalents.

Using the optimisation module, conditions were sought in order to maximize conversion to the amide product (**56**) whilst minimising trifluoroethanol equivalents. This analysis revealed the conditions shown in Reaction 35 in the table above as a possible solution. Repeating the screen using General Experimental Procedure R with the quantities of reagents indicated above gave 86% conversion.

HPLC Study Examining Conversion of Isolated Intermediate to Product

To an oven-dried sealed Schlenk tube containing 2,2,2-trifluoroethyl benzoate (**200**, 290 mg, 1.42 mmol, 1 equiv) and THF (700 μ L) was added benzylamine (155 μ L, 1.42 mmol, 1 equiv). The reaction mixture was stirred at 90 °C for 22 hours. The reaction mixture was sampled at several time points and the conversion to product **56** was determined by HPLC (Method 2) with reference to iodobenzene (1.4 M), which was used as an internal standard (Figure 42, Page 134).

Table 61: Profiling of *t*-BuOK-catalysed reaction

Time (h)	Conversion of Intermediate 200 (%)	Conversion to Product 56 (%)
0	100	0
0.25	64	14
0.5	61	18
1	49	35
2	36	46
4	24	71
6	19	80
8	17	85
22	15	85

6.3.7 Screening Reactions with Novel Carbene Systems**Precursor and Base Screening**

Reactions were performed according to General Experimental Procedure U (Table 37, Page 146).

Table 62: Screening of novel NHC precursors in conjunction with known systems

Precursor (Amount)	Conversion (%)				
	Et ₃ N (17 μ L)	<i>t</i> -BuOK (14 mg)	NaH (3 mg)	BEMP (36 μ L)	None
IMes, 54 (3.8 mg)	1	5	1	0	0
IMes.PF ₆ , 109 (5.6 mg)	0	4	2	0	0
67 (4.5 mg)	0	0	0	2	0
210 (3.3 mg)	0	4	0	0	0
212 (3.4 mg)	0	2	0	0	0
214 (3.8 mg)	0	0	0	0	0
None	0	2	0	0	0

Base and Solvent Screening with Pyridyl Carbene Precursor

Reactions were performed according to General Experimental Procedure V (Table 38, Page 147).

Table 63: Base and solvent screening with pyridyl NHC precursor

Base (Amount)	Conversion (%)				
	DMF	MeCN	NMP	PhMe	THF
DBU (25 μ L)	1	1	1	0	2
K ₃ PO ₄ (36 mg)	0	1	1	0	1
<i>t</i> -BuOK (19 mg)	10	2	10	11	2
NaH (4 mg)	0	1	1	0	0
BEMP (49 μ L)	1	1	0	0	0

Investigation of Control Reactions in the Absence of Carbene Precursor

Reactions were performed according to General Experimental Procedure W (Table 39, Page 148).

Table 64: *t*-BuOK control reactions in the absence of NHC precursor

Solvent	Conversion (%)	
	12 mol% <i>t</i> -BuOK (19 mg)	1 equiv <i>t</i> -BuOK (159 mg)
DMF	0	62
MeCN	13	29
NMP	0	55
PhMe	53	78
THF	34	69

Base and Solvent Screening with IMes.PF₆

Reactions were performed according to General Experimental Procedure X (Table 40, Page 149).

Table 65: Base and solvent screening with IMes.PF₆

Precursor/Base (Amount)	Conversion (%)				
	DMF	MeCN	NMP	PhMe	THF
IMes.PF ₆ + DBU (212 μL)	1	3	1	3	5
DBU (212 μL)	1	1	1	1	1
IMes.PF ₆ + K ₃ PO ₄ (301 mg)	0	0	0	0	1
K ₃ PO ₄ (301 mg)	0	0	0	0	0
IMes.PF ₆ + NaH (34 mg)	1	1	1	0	0
NaH (34 mg)	1	1	1	3	0
IMes.PF ₆ + BEMP (411 μL)	2	2	7	7	0
BEMP (411 μL)	1	0	0	0	0

Optimisation of IMes.PF₆-catalysed Amidation Using Design of Experiments

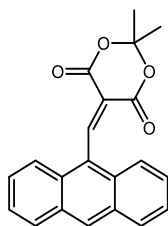
Reactions were performed according to General Experimental Procedure Y (Table 42, Page 151).

Table 66: Results from half-fractional factorial design

Reaction	Time (h)	Temp (°C)	Conc (M)	PhMe (mL)	Cat. Loading (equiv)	IMes.PF₆ (mg)	Conv (%)
1	8	100	0.5	1.4	0.5	158	0
2	8	100	1	0.7	0.1	32	0
3	22	40	1	0.7	0.1	32	0
4	22	40	0.5	1.4	0.5	158	0
5	22	100	0.5	1.4	0.1	32	5
6	8	40	0.5	1.4	0.1	32	0
7	15	70	0.75	1.1	0.3	95	0
8	8	40	1	0.7	0.5	158	0
9	22	100	1	0.7	0.5	158	5
10	15	70	0.75	0.9	0.3	95	0

6.4 Characterisation Data for Isolated Products

Compound 87. 5-(anthracen-9-ylmethylene)-2,2-dimethyl-1,3-dioxane-4,6-dione



To a round-bottomed flask containing 9-anthraldehyde (13.0 g, 63.0 mmol, 1 equiv) and Meldrum's acid (9.1 g, 63.0 mmol, 1 equiv) was added pyridine (20 mL). The reaction mixture was stirred at room temperature for 16 h then concentrated under vacuum. A solution of 20% ethyl acetate/hexanes was added and the resulting precipitate was collected by filtration, washed with 20% ethyl acetate/hexanes, then dried under vacuum to afford the title compound as a yellow solid (20.2 g, 96%).

ν_{\max} (neat): 3029, 2997, 2946, 1763, 1732, 1630 cm^{-1}

^1H NMR (400 MHz, CDCl_3): δ 9.49 (d, 1H, CH, $J = 0.8$ Hz), 8.57 (s, 1H, ArH), 8.09 – 8.04 (m, 2H, 2 x ArH), 7.88 – 7.82 (m, 2H, 2 x ArH), 7.56 – 7.49 (m, 4H, 4 x ArH), 1.91 (s, 6H, 2 x CH_3)

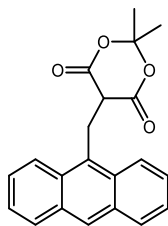
^{13}C NMR (101 MHz, CDCl_3): δ 157.7, 131.0, 130.3, 129.3, 129.0, 127.4, 127.1, 127.0, 125.6, 124.5, 104.2, 28.2, 1C missing (overlapping peak)

HRMS ($\text{C}_{21}\text{H}_{17}\text{O}_4$) [$\text{M}+\text{H}^+$] requires 333.1121, found [$\text{M}+\text{H}^+$] 333.1125

m.p. 193 – 195 $^\circ\text{C}$

Consistent with previously reported data⁹⁵

Compound 88. 5-(anthracen-9-ylmethyl)-2,2-dimethyl-1,3-dioxane-4,6-dione



To a round-bottomed flask containing 5-(anthracen-9-ylmethylene)-2,2-dimethyl-1,3-dioxane-4,6-dione (**87**, 20.2 g, 60.8 mmol, 1 equiv) and MeOH (30 mL) at 0 °C was added NaBH₄ (4.6 g, 121.6 mmol, 2 equiv). The reaction mixture was stirred at room temperature for 16 h. HCl (2 M) was added dropwise and the resulting precipitate was collected by filtration and washed with ice-cold water, then dried under vacuum to afford the title compound as an orange solid (18.3 g, 90%).

ν_{max} (neat): 3055, 2997, 2878, 1775, 1737, 1387, 1303 cm⁻¹

¹H NMR (400 MHz, CDCl₃): δ 8.51 – 8.42 (m, 3H, 3 x ArH), 8.04 (d, 2H, 2 x ArH, J = 8.5 Hz), 7.62 – 7.55 (m, 2H, 2 x ArH), 7.54 – 7.46 (m, 2H, 2 x ArH), 4.52 (d, 2H, CH₂, J = 5.2 Hz), 3.98 (t, 1H, CH, J = 5.2 Hz), 1.78 (s, 3H, CH₃), 1.66 (s, 3H, CH₃)

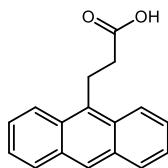
¹³C NMR (101 MHz, CDCl₃): δ 165.7, 131.9, 130.3, 129.7, 128.3, 127.9, 126.6, 125.3, 124.6, 104.2, 49.5, 29.1, 24.1

HRMS (C₂₁H₁₉O₄) [M+H⁺] requires 335.1278, found [M+H⁺] 335.1283

m.p. 164 – 165 °C

Consistent with previously reported data⁹⁵

Compound 89. 3-(anthracen-9-yl)propanoic acid



To a round-bottomed flask containing 5-(anthracen-9-ylmethyl)-2,2-dimethyl-1,3-dioxane-4,6-dione (**88**, 9.0 g, 26.9 mmol, 1 equiv) and pyridine (40 mL) was added H₂O (11 mL). The reaction mixture was heated at 120 °C for 16 h then concentrated under vacuum. The reaction mixture was diluted with HCl (1 M) and extracted with EtOAc. The organics were combined, washed with brine, passed through a hydrophobic frit, and concentrated under vacuum to afford the title compound as an orange solid (6.7 g, 100%).

ν_{max} (neat): 3056, 2916, 2872, 1694, 1682, 1408, 1213 cm⁻¹

¹H NMR (400 MHz, CDCl₃): δ 8.41 (s, 1H, ArH), 8.29 (d, 2H, 2 x ArH, $J = 8.8$ Hz), 8.04 (d, 2H, 2 x ArH, $J = 8.5$ Hz), 7.61 – 7.46 (m, 4H, 4 x ArH), 4.05 – 3.98 (m, 2H, CH₂), 2.91 – 2.83 (m, 2H, CH₂), 1H missing (exchangeable)

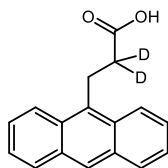
¹³C NMR (101 MHz, MeOD): δ 176.6, 133.7, 133.1, 130.7, 130.3, 127.3, 126.9, 125.9, 124.9, 36.2, 24.2

HRMS (C₁₇H₁₅O₂) [M+H⁺] requires 251.1067, found [M+H⁺] 251.1064

m.p. 191 – 192 °C

Consistent with previously reported data⁹⁵

Compound 90. 3-(anthracen-9-yl)-(2-*d*₂)-propanoic acid



To a round-bottomed flask containing 5-(anthracen-9-ylmethyl)-2,2-dimethyl-1,3-dioxane-4,6-dione (**88**, 9.0 g, 26.9 mmol, 1 equiv) and pyridine (40 mL) was added D₂O (11 mL). The reaction mixture was heated at 120 °C for 16 h then concentrated under vacuum. The reaction mixture was diluted with HCl (1 M) and extracted with EtOAc. The organics were combined, washed with brine, passed through a hydrophobic frit, and concentrated under vacuum to afford the title compound as an orange solid (6.7 g, 99%).

ν_{\max} (neat): 3051, 2956, 2916, 2868, 1694, 1682, 1404, 1219 cm⁻¹

¹H NMR (400 MHz, CDCl₃): δ 8.41 (s, 1H, ArH), 8.29 (d, 2H, 2 x ArH, $J = 9.5$ Hz), 8.05 (d, 2H, 2 x ArH, $J = 9.0$ Hz), 7.60 – 7.47 (m, 4H, 4 x ArH), 4.01 (s, 2H, CH₂), 1H missing (exchangeable)

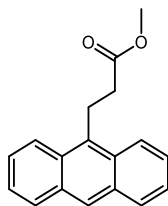
¹³C NMR (101 MHz, CDCl₃): δ 178.1, 131.9, 131.6, 129.5, 129.4, 126.5, 126.1, 125.0, 123.8, 22.9, 1C missing (α carbon)

HRMS (C₁₇H₁₃D₂O₂) [M+H⁺] requires 253.1193, found [M+H⁺] 253.1193

m.p. 187– 188 °C

Consistent with previously reported data⁹⁵

Compound 91. methyl 3-(anthracen-9-yl)propanoate



To a round-bottomed flask containing MeOH (25 mL) at 0 °C was added acetyl chloride (1.2 mL, 16.8 mmol, 2 equiv) and the reaction mixture was stirred at 0 °C for 10 min. A solution of 3-(anthracen-9-yl)propanoic acid (**89**, 2.1 g, 8.4 mmol, 1 equiv) in MeOH (25 mL) was added dropwise and the reaction mixture was heated at 100 °C for 16 h. The reaction mixture was neutralised with sat. NaHCO₃ then concentrated under vacuum. The residue was dissolved in DCM, washed with water, passed through a hydrophobic frit, and concentrated to a residue that was purified by flash column chromatography (20% EtOAc/pet. ether) to afford the title compound as a yellow solid (2.0 g, 92%).

ν_{\max} (neat): 3049, 2988, 2947, 2843, 1728, 1620, 1437, 1196 cm⁻¹

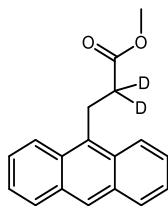
¹H NMR (400 MHz, CDCl₃): δ 8.49 (s, 1H, ArH), 8.29 (d, 2H, 2 x ArH, $J = 9.2$ Hz), 8.07 (d, 2H, 2 x ArH, $J = 8.4$ Hz), 7.59 – 7.48 (m, 4H, 4 x ArH), 3.92 – 3.85 (m, 2H, CH₂), 3.60 (s, 3H, CH₃), 2.74 – 2.67 (m, 2H, CH₂)

¹³C NMR (101 MHz, CDCl₃): δ 173.7, 132.2, 131.8, 129.7, 129.5, 126.6, 126.1, 125.1, 124.1, 52.0, 35.3, 23.5

HRMS (C₁₈H₁₇O₂) [M+H⁺] requires 265.1223, found [M+H⁺] 265.1224

m.p. 71 – 72 °C

Compound 92. methyl 3-(anthracen-9-yl)-(2-*d*₂)-propanoate



To a round-bottomed flask containing MeOH (25 mL) at 0 °C was added acetyl chloride (1.4 mL, 19.8 mmol, 2 equiv) and the reaction mixture was stirred at 0 °C for 10 min. A solution of 3-(anthracen-9-yl)-(2-*d*₂)-propanoic acid (**90**, 2.5 g, 9.9 mmol, 1 equiv) in MeOH (25 mL) was added dropwise and the reaction mixture was heated at 100 °C for 16 h. The reaction mixture was neutralised with sat. NaHCO₃ then concentrated under vacuum. The residue was dissolved in DCM, washed with water, passed through a hydrophobic frit, and concentrated to a residue that was purified by flash column chromatography (20% EtOAc/pet. ether) to afford the title compound as a yellow solid (2.5 g, 95%).

ν_{\max} (neat): 3051, 2988, 2947, 1728, 1620, 1494, 1256 cm⁻¹

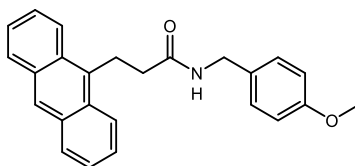
¹H NMR (400 MHz, CDCl₃): δ 8.39 (s, 1H, ArH), 8.28 (d, 2H, 2 x ArH, *J* = 8.0 Hz), 8.03 (d, 2H, 2 x ArH, *J* = 8.5 Hz), 7.57 – 7.45 (m, 4H, 4 x ArH), 3.97 (s, 2H, CH₂), 3.75 (s, 3H, CH₃)

¹³C NMR (101 MHz, CDCl₃): δ 173.7, 132.5, 131.8, 129.5, 128.9, 126.6, 126.5, 125.6, 124.1, 52.0, 23.4, 1C missing (α carbon)

HRMS (C₁₈H₁₅D₂O₂) [M+H⁺] requires 267.1349, found [M+H⁺] 267.1349

m.p. 69 – 70 °C

Compound 93. 3-(anthracen-9-yl)-N-(4-methoxybenzyl)propanamide



To a round-bottomed flask containing 3-(anthracen-9-yl)propanoic acid (**89**, 200 mg, 0.8 mmol, 1 equiv), 4-methoxybenzylamine (105 μ L, 0.8 mmol, 1 equiv), HATU (247 mg, 0.8 mmol, 1 equiv) and DCM (10 mL) was added Et₃N (244 μ L, 1.8 mmol, 2.2 equiv). The reaction mixture was stirred at room temperature for 16 h. The reaction mixture was quenched with sat. NaHCO₃, extracted with DCM, washed with HCl (2 M), passed through a hydrophobic frit, and concentrated to a residue that was purified by flash column chromatography (10% MeOH/DCM) to afford the title compound as a pale yellow solid (163 mg, 55%).

ν_{\max} (neat): 3294, 3060, 2886, 1628, 1537, 1512, 1246 cm⁻¹

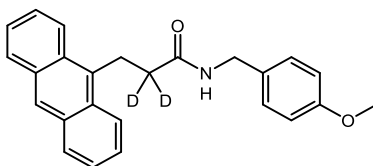
¹H NMR (400 MHz, CDCl₃): δ 8.38 (s, 1H, ArH), 8.31 (d, 2H, 2 x ArH, $J = 8.8$ Hz), 8.03 (d, 2H, 2 x ArH, $J = 8.4$ Hz), 7.60 – 7.41 (m, 4H, 4 x ArH), 6.96 (d, 2H, 2 x ArH, $J = 8.4$ Hz), 6.78 (d, 2H, 2 x ArH, $J = 8.4$ Hz), 4.28 (d, 2H, CH₂, $J = 5.6$ Hz), 4.04 (t, 2H, CH₂, $J = 8.0$ Hz), 3.78 (s, 3H, CH₃), 2.68 (t, 2H, CH₂, $J = 7.8$ Hz), 1H missing (exchangeable)

¹³C NMR (126 MHz, DMSO): δ 171.2, 136.2, 134.6, 131.4, 131.1, 129.0, 128.5, 125.8, 125.7, 125.0, 124.3, 113.6, 55.0, 43.7, 39.0, 38.2, 1C missing (overlapping peaks)

HRMS (C₂₅H₂₄NO₂) [M+H⁺] requires 370.1802, found [M+H⁺] 370.1803

m.p. 178 – 180 °C

Compound 94. 3-(anthracen-9-yl)-(2-*d*₂)-*N*-(4-methoxybenzyl)propanamide



To a round-bottomed flask containing 3-(anthracen-9-yl)-(2-*d*₂)-propanoic acid (**90**, 200 mg, 0.8 mmol, 1 equiv), 4-methoxybenzylamine (105 μ L, 0.8 mmol, 1 equiv), HATU (247 mg, 0.8 mmol, 1 equiv) and DCM (10 mL) was added Et₃N (244 μ L, 1.8 mmol, 2.2 equiv). The reaction mixture was stirred at room temperature for 16 h. The reaction mixture was quenched with sat. NaHCO₃, extracted with DCM, washed with HCl (2 M), passed through a hydrophobic frit, and concentrated under vacuum. The residue was redissolved in DCM, hexane was added dropwise and the resulting precipitate was collected by filtration and dried under vacuum to afford the title compound as a pale yellow solid (284 mg, 96%).

ν_{max} (neat): 3291, 3064, 2872, 1624, 1535, 1510, 1217 cm^{-1}

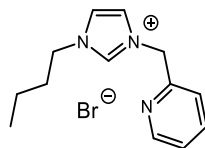
¹H NMR (400 MHz, DMSO): δ 8.50 (s, 1H, ArH), 8.36 (d, 2H, 2 x ArH, $J = 9.2$ Hz), 8.09 (d, 2H, 2 x ArH, $J = 9.2$ Hz), 7.60 – 7.49 (m, 4H, 4 x ArH), 7.07 (d, 2H, 2 x ArH, $J = 8.8$ Hz), 6.81 (d, 2H, 2 x ArH, $J = 8.8$ Hz), 4.20 (d, 2H, CH₂, $J = 6.0$ Hz), 3.85 (s, 2H, CH₂), 3.71 (s, 3H, CH₃), 1H missing (exchangeable)

¹³C NMR (126 MHz, DMSO): δ 171.2, 136.4, 133.7, 131.3, 131.1, 129.0, 128.6, 125.8, 125.7, 125.1, 124.3, 113.6, 55.0, 45.7, 41.6, 2C missing (overlapping peaks and α carbon)

HRMS (C₂₅H₂₂D₂NO₂) [M+H⁺] requires 372.1929, found [M+H⁺] 372.1929

m.p. 168 – 170 °C

Compound 106. 1-butyl-3-(pyridin-2-ylmethyl)-1*H*-imidazol-3-ium bromide



Bromomethylpyridine hydrobromide (1.0 g, 4.0 mmol, 1 equiv) was neutralised with sat. Na_2CO_3 , extracted with Et_2O , then dried over MgSO_4 , filtered and added to a solution of butylimidazole (526 μL , 4.0 mmol, 1 equiv) in 1,4-dioxane (25 mL). Et_2O was removed under vacuum and the reaction mixture was heated at 100 °C for 16 h then concentrated under vacuum to afford the title compound as a brown oil (1.10 g, 93%).

ν_{max} (neat): 3321, 3109, 3020, 1568, 1423 cm^{-1}

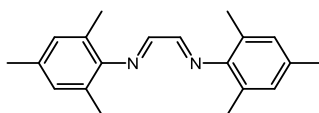
^1H NMR (500 MHz, CDCl_3): δ 10.56 (s, 1H, ArH), 8.52 – 8.51 (m, 1H, ArH), 7.82 (d, 1H, ArH, $J = 8.0$ Hz), 7.72 (td, 1H, ArH, $J = 8.0, 1.6$ Hz), 7.66 (app. t, 1H, ArH, $J = 1.8$ Hz), 7.37 (app. t, 1H, ArH, $J = 1.8$ Hz), 7.28 – 7.25 (m, 1H, ArH), 5.79 (s, 2H, CH_2), 4.28 (t, 2H, CH_2 , $J = 7.5$ Hz), 1.93 – 1.87 (m, 2H, CH_2), 1.37 (sextet, 2H, CH_2 , $J = 7.5$ Hz), 0.94 (t, 3H, CH_3 , $J = 7.3$ Hz)

^{13}C NMR (126 MHz, DMSO): δ 153.5, 149.6, 137.6, 136.9, 123.9, 123.3, 122.5, 121.1, 53.1, 48.7, 31.3, 18.8, 13.3

HRMS ($\text{C}_{13}\text{H}_{18}\text{N}_3$) [M^+] requires 216.1495, found [M^+] 216.1494

Consistent with previously reported data⁹⁷

Compound 107. (*N,N'E,N,N'E*)-*N,N'*-(ethane-1,2-diylidene)bis(2,4,6-trimethylaniline)



To a round-bottomed flask containing 2,4,6-trimethylaniline (11.5 mL, 82 mmol, 2 equiv) and *i*-PrOH (45 mL) was added a mixture of glyoxal solution (40 wt.% in water, 5.9 mL, 41 mmol, 1 equiv), *i*-PrOH (15 mL) and deionised water (8 mL). The reaction mixture was stirred at room temperature for 16 h. Deionised water (10 mL) was added and the resulting precipitate was collected by filtration and dried under vacuum to afford the title compound as a yellow solid (10.73 g, 89%).

ν_{\max} (neat): 2968, 2916, 2853, 1614, 1593, 1476, 1373, 1202 cm^{-1}

^1H NMR (500 MHz, DMSO): δ 8.10 (s, 2H, 2 x CH), 6.91 (s, 4H, 4 x ArH), 2.23 (s, 6H, 2 x CH₃), 2.08 (s, 12H, 4 x CH₃)

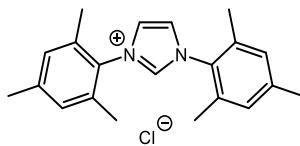
^{13}C NMR (126 MHz, DMSO): δ 163.4, 151.2, 133.4, 128.7, 125.8, 20.3, 17.8

HRMS (C₂₀H₂₅N₂) [M+H⁺] requires 293.2012, found [M+H⁺] 293.2012

m.p. 160 – 161 °C

Consistent with previously reported data⁷²

Compound 108. 1,3-dimesityl-1*H*-imidazol-3-ium chloride



To a round-bottomed flask containing chloromethyl methyl ether (2.26 mL, 29.8 mmol, 1.03 equiv) and THF (6 mL) was added a solution of (*N,N'E,N,N'E*)-*N,N'*-(ethane-1,2-diylidene)bis(2,4,6-trimethylaniline) (**107**, 8.46 g, 28.9 mmol, 1 equiv) in THF (80 mL). The reaction mixture was stirred at room temperature for 5 days. The resulting precipitate was collected by filtration and dried under vacuum to afford the title compound as an off-white solid (4.29 g, 44%).

ν_{\max} (neat): 3302, 3157, 3028, 2791, 1626, 1609, 1537, 1481, 1447, 1232 cm^{-1}

^1H NMR (400 MHz, DMSO): δ 9.66 (t, 1H, ArH, $J = 1.4$ Hz), 8.27 (d, 2H, 2 x ArH, $J = 1.2$ Hz), 7.20 (s, 4H, 4 x ArH), 2.35 (s, 6H, 2 x CH_3), 2.12 (s, 12H, 4 x CH_3)

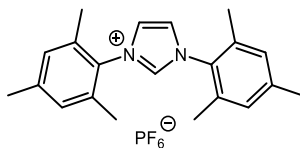
^{13}C NMR (126 MHz, DMSO): δ 140.6, 138.5, 134.3, 131.0, 129.3, 124.8, 20.6, 16.9

HRMS ($\text{C}_{21}\text{H}_{25}\text{N}_2$) [M^+] requires 305.2004, found [M^+] 305.2008

m.p. > 300 $^\circ\text{C}$

Consistent with previously reported data⁷²

Compound 109. 1,3-dimesityl-1*H*-imidazol-3-ium hexafluorophosphate



To a round-bottomed flask containing a saturated solution of 1,3-dimesityl-1*H*-imidazol-3-ium chloride (**108**, 4.0 g, 11.7 mmol, 1 equiv) in water was added a saturated solution of ammonium hexafluorophosphate (1.9 g, 11.7 mmol, 1 equiv) in water. The reaction mixture was stirred at room temperature for 30 minutes. The resulting precipitate was collected by filtration and triturated with EtOAc/hexanes to afford the title compound as a white solid (3.56 g, 68%).

ν_{\max} (neat): 3146, 2942, 1682, 1566, 1533, 1481, 1454, 1224 cm^{-1}

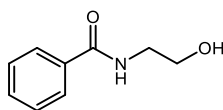
^1H NMR (400 MHz, DMSO): δ 9.63 (t, 1H, ArH, $J = 1.4$ Hz), 8.27 (d, 2H, 2 x ArH, $J = 1.6$ Hz), 7.20 (s, 4H, 4 x ArH), 2.35 (s, 6H, 2 x CH_3), 2.12 (s, 12H, 4 x CH_3)

^{13}C NMR (101 MHz, DMSO): δ 140.6, 138.4, 134.3, 130.9, 129.3, 124.8, 20.6, 16.8

HRMS ($\text{C}_{21}\text{H}_{25}\text{N}_2$) [M^+] requires 305.2012, found [M^+] 305.2012

m.p. > 300 $^\circ\text{C}$

Compound 110. *N*-(2-hydroxyethyl)benzamide



Synthesised according to General Experimental Procedure E (Table 7, Entry 1, Page 57) using methyl benzoate (89 μ L, 0.71 mmol, 1 equiv), ethanolamine (43 μ L, 0.71 mmol, 1 equiv), 1,3-dimesityl-1*H*-imidazol-3-ium hexafluorophosphate (**109**, 21 mg, 0.046 mmol, 0.065 equiv), potassium *tert*-butoxide (4 mg, 0.036 mmol, 0.05 equiv), and purified by flash column chromatography (5% methanol/DCM) to afford the title compound as a white solid (127 mg, 54%).

Synthesised according to General Experimental Procedure E (Table 7, Entry 2, Page 57) using methyl benzoate (89 μ L, 0.71 mmol, 1 equiv), ethanolamine (43 μ L, 0.71 mmol, 1 equiv), potassium *tert*-butoxide (4 mg, 0.036 mmol, 0.05 equiv), and purified by flash column chromatography (5% methanol/DCM) to afford the title compound as a white solid (127 mg, 54%).

Synthesised according to General Experimental Procedure F (Table 8, Entry 3, Page 59) using methyl benzoate (89 μ L, 0.71 mmol, 1 equiv), ethanolamine (43 μ L, 0.71 mmol, 1 equiv), 1,3-dimesityl-1*H*-imidazol-3-ium hexafluorophosphate (**109**, 64 mg, 0.14 mmol, 0.2 equiv), potassium *tert*-butoxide (16 mg, 0.14 mmol, 0.2 equiv), and purified by flash column chromatography (5% methanol/DCM) to afford the title compound as a white solid (152 mg, 65%).

Synthesised according to General Experimental Procedure F (Table 8, Entry 4, Page 59) using methyl benzoate (89 μ L, 0.71 mmol, 1 equiv), ethanolamine (43 μ L, 0.71 mmol, 1 equiv), potassium *tert*-butoxide (16 mg, 0.14 mmol, 0.2 equiv), and purified by flash column chromatography (5% methanol/DCM) to afford the title compound as a white solid (134 mg, 57%).

Experimental - Characterisation Data for Isolated Products

Synthesised according to General Experimental Procedure F (Table 8, Entry 5, Page 59) using methyl benzoate (89 μL , 0.71 mmol, 1 equiv), ethanolamine (43 μL , 0.71 mmol, 1 equiv), 1,3-dimesityl-1*H*-imidazol-3-ium hexafluorophosphate (**109**, 160 mg, 0.36 mmol, 0.5 equiv), potassium *tert*-butoxide (40 mg, 0.36 mmol, 0.5 equiv), and purified by flash column chromatography (5% methanol/DCM) to afford the title compound as a white solid (66 mg, 56%).

Synthesised according to General Experimental Procedure F (Table 8, Entry 6, Page 59) using methyl benzoate (89 μL , 0.71 mmol, 1 equiv), ethanolamine (43 μL , 0.71 mmol, 1 equiv), potassium *tert*-butoxide (40 mg, 0.36 mmol, 0.5 equiv), and purified by flash column chromatography (5% methanol/DCM) to afford the title compound as a white solid (60 mg, 51%).

Synthesised according to General Experimental Procedure F (Table 8, Entry 7, Page 59) using methyl benzoate (89 μL , 0.71 mmol, 1 equiv), ethanolamine (43 μL , 0.71 mmol, 1 equiv), 1,3-dimesityl-1*H*-imidazol-3-ium hexafluorophosphate (**109**, 320 mg, 0.71 mmol, 1 equiv), potassium *tert*-butoxide (80 mg, 0.71 mmol, 1 equiv), and purified by flash column chromatography (5% methanol/DCM) to afford the title compound as a white solid (35 mg, 30%).

Synthesised according to General Experimental Procedure F (Table 8, Entry 8, Page 59) using methyl benzoate (89 μL , 0.71 mmol, 1 equiv), ethanolamine (43 μL , 0.71 mmol, 1 equiv), potassium *tert*-butoxide (80 mg, 0.71 mmol, 1 equiv), and purified by flash column chromatography (5% methanol/DCM) to afford the title compound as a white solid (117 mg, 100%).

Synthesised according to General Experimental Procedure I (Table 16, Reaction 11, Page 79) using methyl benzoate (178 μL , 1.42 mmol, 1 equiv) and ethanolamine (86 μL , 1.42 mmol, 1 equiv), and BEMP (**117**, 41 μL , 0.14 mmol, 0.1 equiv), and purified by flash column chromatography (5% methanol/DCM) to afford the title compound as a white solid (204 mg, 87%).

Experimental - Characterisation Data for Isolated Products

Synthesised according to General Experimental Procedure J (Table 16, Reaction 12, Page 79) using methyl benzoate (178 μL , 1.42 mmol, 1 equiv), ethanolamine (86 μL , 1.42 mmol, 1 equiv), and BEMP (**117**, 82 μL , 0.28 mmol, 0.2 equiv), and purified by flash column chromatography (5% methanol/DCM) to afford the title compound as a white solid (216 mg, 92%).

Synthesised according to General Experimental Procedure O (Table 26, Entry 1, Page 112) using methyl benzoate (178 μL , 1.42 mmol, 1 equiv), ethanolamine (86 μL , 1.42 mmol, 1 equiv) and K_3PO_4 (90 mg, 0.43 mmol, 0.3 equiv), and purified by flash column chromatography (5% methanol/CPME) to afford the title compound as a white solid (188 mg, 80%).

ν_{max} (neat): 3296, 2937, 2876, 1634, 1537 cm^{-1}

^1H NMR (500 MHz, CDCl_3): δ 7.80 – 7.78 (m, 2H, 2 x ArH), 7.51 (tt, 1H, ArH, $J = 7.3, 1.6$ Hz), 7.45 – 7.41 (m, 2H, 2 x ArH), 6.75 (br. s, 1H, NH), 3.83 (t, 2H, CH_2 , $J = 5.0$ Hz), 3.63 (q, 2H, CH_2 , $J = 5.2$ Hz), 1H missing (exchangeable)

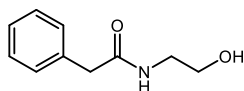
^{13}C NMR (126 MHz, CDCl_3): δ 168.9, 134.3, 131.9, 128.8, 127.2, 62.6, 43.1

HRMS ($\text{C}_9\text{H}_{12}\text{NO}_2$) $[\text{M}+\text{H}^+]$ requires 166.0863, found $[\text{M}+\text{H}^+]$ 166.0860

m.p. 59 – 60 $^\circ\text{C}$

Consistent with previously reported data⁷⁴

Compound 58. N-(2-hydroxyethyl)-2-phenylacetamide



Synthesised according to General Experimental Procedure G (Table 9, Entry 1, Page 61) using methyl 2-phenyl acetate (202 μ L, 1.42 mmol, 1 equiv), ethanolamine (86 μ L, 1.42 mmol, 1 equiv), 1,3-dimesityl-1*H*-imidazol-3-ium hexafluorophosphate (**109**, 42 mg, 0.092 mmol, 0.065 equiv), and potassium *tert*-butoxide (8 mg, 0.071 mmol, 0.05 equiv), and purified by flash column chromatography (6% methanol/DCM) to afford the title compound as a white solid (71 mg, 28%).

Synthesised according to General Experimental Procedure G (Table 9, Entry 1, Page 61) using methyl 2-phenyl acetate (202 μ L, 1.42 mmol, 1 equiv), ethanolamine (86 μ L, 1.42 mmol, 1 equiv), and potassium *tert*-butoxide (8 mg, 0.071 mmol, 0.05 equiv), and purified by flash column chromatography (6% methanol/DCM) to afford the title compound as a white solid (68 mg, 27%).

Synthesised according to General Experimental Procedure J at rt (Table 17, Entry 5, Page 80) using methyl 2-phenyl acetate (202 μ L, 1.42 mmol, 1 equiv) and ethanolamine (86 μ L, 1.42 mmol, 1 equiv), and purified by flash column chromatography (6% methanol/DCM) to afford the title compound as a white solid (253 mg, 99%).

Synthesised according to General Experimental Procedure K (Table 18, Entry 2, Page 84) using methyl 2-phenyl acetate (202 μ L, 1.42 mmol, 1 equiv), ethanolamine (86 μ L, 1.42 mmol, 1 equiv), and P₁-*t*-Bu (**141**, 36 μ L, 0.14 mmol, 0.1 equiv), and purified by flash column chromatography (6% methanol/DCM) to afford the title compound as a white solid (237 mg, 93%).

Synthesised according to General Experimental Procedure K (Table 18, Entry 3, Page 84) using methyl 2-phenyl acetate (202 μ L, 1.42 mmol, 1 equiv), ethanolamine (86 μ L, 1.42 mmol, 1 equiv), and BTPP (**142**, 43 μ L, 0.14 mmol, 0.1 equiv), and purified by flash column chromatography (6% methanol/DCM) to afford the title compound as a white solid (209 mg, 82%).

Experimental - Characterisation Data for Isolated Products

Synthesised according to General Experimental Procedure O (Table 26, Entry 6, Page 112) using methyl 2-phenyl acetate (202 μL , 1.42 mmol, 1 equiv) and ethanolamine (86 μL , 1.42 mmol, 1 equiv), and purified by flash column chromatography (6% methanol/DCM) to afford the title compound as a white solid (252 mg, 99%).

Synthesised according to General Experimental Procedure O (Table 26, Entry 6, Page 112) using methyl 2-phenyl acetate (1.4 mL, 10 mmol, 1 equiv), ethanolamine (604 μL , 10 mmol, 1 equiv), K_3PO_4 (637 mg, 3 mmol, 0.3 equiv) and *i*-PrOH (5 mL), and purified by flash column chromatography (6% methanol/DCM) to afford the title compound as a white solid (1.52 g, 85%).

ν_{max} (neat): 3426, 3064, 2918, 1624, 1566 cm^{-1}

^1H NMR (500 MHz, CDCl_3): δ 7.37 (tt, 2H, 2 x ArH, $J = 7.3, 1.4$ Hz), 7.32 – 7.27 (m, 3H, 3 x ArH), 5.92 (br. s, 1H, NH), 3.67 (t, 2H, CH_2 , $J = 5.0$ Hz), 3.60 (s, 2H, CH_2), 3.38 (q, 2H, CH_2 , $J = 5.2$ Hz), 2.49 (br. s, 1H, OH)

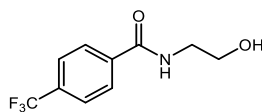
^{13}C NMR (126 MHz, CDCl_3): δ 172.6, 134.9, 129.4, 129.0, 127.4, 61.8, 43.6, 42.6

HRMS ($\text{C}_{10}\text{H}_{14}\text{NO}_2$) [$\text{M}+\text{H}^+$] requires 180.1019, found [$\text{M}+\text{H}^+$] 180.1017

m.p. 62 – 63 $^\circ\text{C}$

Consistent with previously reported data⁷⁴

Compound 111. *N*-(2-hydroxyethyl)-4-(trifluoromethyl)benzamide



Synthesised according to General Experimental Procedure G (Table 9, Entry 2, Page 61) using methyl 4-trifluoromethyl benzoate (229 μL , 1.42 mmol, 1 equiv), ethanolamine (86 μL , 1.42 mmol, 1 equiv), 1,3-dimesityl-1*H*-imidazol-3-ium hexafluorophosphate (**109**, 42 mg, 0.092 mmol, 0.065 equiv), and potassium *tert*-butoxide (8 mg, 0.071 mmol, 0.05 equiv), and purified by flash column chromatography (5% methanol/DCM) to afford the title compound as a white solid (152 mg, 46%).

Synthesised according to General Experimental Procedure G (Table 9, Entry 2, Page 61) using methyl 4-trifluoromethyl benzoate (229 μL , 1.42 mmol, 1 equiv), ethanolamine (86 μL , 1.42 mmol, 1 equiv), and potassium *tert*-butoxide (8 mg, 0.071 mmol, 0.05 equiv), and purified by flash column chromatography (5% methanol/DCM) to afford the title compound as a white solid (212 mg, 64%).

Synthesised according to General Experimental Procedure J at rt (Table 17, Entry 2, Page 80) using methyl 4-trifluoromethyl benzoate (229 μL , 1.42 mmol, 1 equiv) and ethanolamine (86 μL , 1.42 mmol, 1 equiv), and purified by flash column chromatography (5% methanol/DCM) to afford the title compound as a white solid (313 mg, 95%).

Synthesised according to General Experimental Procedure O (Table 26, Entry 2, Page 112) using methyl 4-trifluoromethyl benzoate (229 μL , 1.42 mmol, 1 equiv) and ethanolamine (86 μL , 1.42 mmol, 1 equiv), and purified by flash column chromatography (5% methanol/DCM) to afford the title compound as a white solid (324 mg, 98%).

ν_{max} (neat): 3292, 2972, 2891, 1639, 1551, 1321 cm^{-1}

^1H NMR (500 MHz, CDCl_3): δ 7.91 (d, 2H, 2 x ArH, $J = 8.0$ Hz), 7.72 (d, 2H, 2 x ArH, $J = 8.5$ Hz), 6.64 (br. s, 1H, NH), 3.88 (t, 2H, CH_2 , $J = 5.0$ Hz), 3.68 (q, 2H, CH_2 , $J = 5.2$ Hz), 1.77 (br. s, 1H, OH)

Experimental - Characterisation Data for Isolated Products

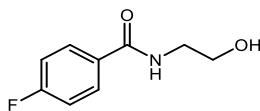
^{13}C NMR (126 MHz, DMSO): δ 165.1, 138.3, 131.0 (q, $^2J_{\text{CF}} = 31.7$ Hz), 128.1, 125.2 (q, $^3J_{\text{CF}} = 4.0$ Hz), 122.9 (q, $^1J_{\text{CF}} = 272.6$ Hz), 59.6, 42.3

HRMS ($\text{C}_{10}\text{H}_{11}\text{F}_3\text{NO}_2$) $[\text{M}+\text{H}^+]$ requires 234.0736, found $[\text{M}+\text{H}^+]$ 234.0736

m.p. 125 – 126 °C

Consistent with previously reported data⁷⁴

Compound 112. 4-fluoro-*N*-(2-hydroxyethyl)benzamide



Synthesised according to General Experimental Procedure G (Table 9, Entry 3, Page 61) using methyl 4-fluorobenzoate (184 μL , 1.42 mmol, 1 equiv), ethanolamine (86 μL , 1.42 mmol, 1 equiv), 1,3-dimesityl-1*H*-imidazol-3-ium hexafluorophosphate (**109**, 42 mg, 0.092 mmol, 0.065 equiv), and potassium *tert*-butoxide (8 mg, 0.071 mmol, 0.05 equiv), and purified by flash column chromatography (2% methanol/DCM) to afford the title compound as a white solid (34 mg, 13%).

Synthesised according to General Experimental Procedure G (Table 9, Entry 3, Page 61) using methyl 4-fluorobenzoate (184 μL , 1.42 mmol, 1 equiv), ethanolamine (86 μL , 1.42 mmol, 1 equiv), potassium *tert*-butoxide (8 mg, 0.071 mmol, 0.05 equiv) and purified by flash column chromatography (2% methanol/DCM) to afford the title compound as a white solid (260 mg, 100%).

ν_{max} (neat): 3319, 3125, 3030, 1639, 1423 cm^{-1}

^1H NMR (500 MHz, CDCl_3): δ 7.81 – 7.76 (m, 2H, ArH), 7.09 – 7.05 (m, 2H, ArH), 3.80 (t, 2H, CH_2 , $J = 5.0$ Hz), 3.59 (q, 2H, CH_2 , $J = 5.0$ Hz), 2H missing (exchangeable)

^{13}C NMR (126 MHz, CDCl_3): δ 165.3, 163.8, (d, $^1J_{\text{CF}} = 248.2$ Hz), 131.0, (d, $^4J_{\text{CF}} = 1.9$ Hz), 129.8 (d, $^3J_{\text{CF}} = 8.8$ Hz), 115.1 (d, $^2J_{\text{CF}} = 21.6$ Hz), 59.7, 42.2

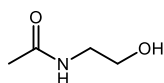
Experimental - Characterisation Data for Isolated Products

HRMS (C₉H₁₁FNO₂) [M+H⁺] requires 184.0766, found [M+H⁺] 184.0767

m.p. 112 – 114 °C

Consistent with previously reported data⁷⁴

Compound 113. *N*-(2-hydroxyethyl)acetamide



Synthesised according to General Experimental Procedure G (Table 9, Entry 4, Page 61) using methyl acetate (113 μL, 1.42 mmol, 1 equiv), ethanolamine (86 μL, 1.42 mmol, 1 equiv), 1,3-dimesityl-1*H*-imidazol-3-ium hexafluorophosphate (**109**, 42 mg, 0.092 mmol, 0.065 equiv), and potassium *tert*-butoxide (8 mg, 0.071 mmol, 0.05 equiv), and purified by flash column chromatography (10% methanol/DCM) to afford the title compound as a colourless oil (45 mg, 31%).

Synthesised according to General Experimental Procedure G (Table 9, Entry 4, Page 61) using methyl acetate (113 μL, 1.42 mmol, 1 equiv), ethanolamine (86 μL, 1.42 mmol, 1 equiv), and potassium *tert*-butoxide (8 mg, 0.071 mmol, 0.05 equiv), and purified by flash column chromatography (10% methanol/DCM) to afford the title compound as a colourless oil (79 mg, 77%).

Synthesised according to General Experimental Procedure G (Table 9, Entry 5, Page 61) using benzyl acetate (202 μL, 1.42 mmol, 1 equiv), ethanolamine (86 μL, 1.42 mmol, 1 equiv), 1,3-dimesityl-1*H*-imidazol-3-ium hexafluorophosphate (**109**, 42 mg, 0.092 mmol, 0.065 equiv), and potassium *tert*-butoxide (8 mg, 0.071 mmol, 0.05 equiv), and purified by flash column chromatography (10% methanol/DCM) to afford the title compound as a colourless oil (34 mg, 33%).

Experimental - Characterisation Data for Isolated Products

Synthesised according to General Experimental Procedure G (Table 9, Entry 5, Page 61) using benzyl acetate (202 μL , 1.42 mmol, 1 equiv), ethanolamine (86 μL , 1.42 mmol, 1 equiv), and potassium *tert*-butoxide (8 mg, 0.071 mmol, 0.05 equiv) and purified by flash column chromatography (10% methanol/DCM) to afford the title compound as a colourless oil (62 mg, 60%).

Synthesised according to General Experimental Procedure J at rt (Table 17, Entry 9, Page 80) using methyl acetate (113 μL , 1.42 mmol, 1 equiv) and ethanolamine (86 μL , 1.42 mmol, 1 equiv), and purified by flash column chromatography (10% methanol/DCM) to afford the title compound as a colourless oil (142 mg, 97%).

Synthesised according to General Experimental Procedure J at rt (Table 17, Entry 12, Page 80) using isopropyl acetate (167 μL , 1.42 mmol, 1 equiv) and ethanolamine (86 μL , 1.42 mmol, 1 equiv), and purified by flash column chromatography (10% methanol/DCM) to afford the title compound as a colourless oil (146 mg, 100%).

Synthesised according to General Experimental Procedure J at rt (Table 17, Entry 13, Page 80) using *tert*-butyl acetate (191 μL , 1.42 mmol, 1 equiv) and ethanolamine (86 μL , 1.42 mmol, 1 equiv), and purified by flash column chromatography (10% methanol/DCM) to afford the title compound as a colourless oil (13 mg, 9%).

Synthesised according to General Experimental Procedure J at 40 °C (Table 17, Entry 13, Page 80) using *tert*-butyl acetate (191 μL , 1.42 mmol, 1 equiv) and ethanolamine (86 μL , 1.42 mmol, 1 equiv), and purified by flash column chromatography (10% methanol/DCM) to afford the title compound as a colourless oil (103 mg, 70%).

Synthesised according to General Experimental Procedure O (Table 26, Entry 9, Page 112) using methyl acetate (113 μL , 1.42 mmol, 1 equiv) and ethanolamine (86 μL , 1.42 mmol, 1 equiv), and purified by flash column chromatography (10% methanol/DCM) to afford the title compound as a colourless oil (143 mg, 98%).

ν_{max} (neat): 3292, 2930, 2894 1628, 1548 cm^{-1}

Experimental - Characterisation Data for Isolated Products

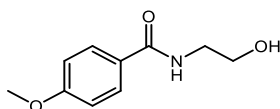
^1H NMR (500 MHz, CDCl_3): δ 6.68 (br. s, 1H, NH), 3.67 (t, 2H, CH_2 , $J = 5.3$ Hz), 3.61 (br.s, 1H, OH), 3.36 (q, 2H, CH_2 , $J = 5.3$ Hz), 1.99 (s, 3H, CH_3)

^{13}C NMR (126 MHz, CDCl_3): δ 171.8, 61.3, 42.4, 23.0

HRMS ($\text{C}_4\text{H}_{10}\text{NO}_2$) [$\text{M}+\text{H}^+$] requires 104.0706, found [$\text{M}+\text{H}^+$] 104.0703

Consistent with previously reported data⁷⁴

Compound 118. *N*-(2-hydroxyethyl)-4-methoxybenzamide



Synthesised according to General Experimental Procedure J at rt (Table 17, Entry 3, Page 80) using methyl 4-methoxy benzoate (236 mg, 1.42 mmol, 1 equiv) and ethanolamine (86 μL , 1.42 mmol, 1 equiv), and purified by flash column chromatography (5% methanol/DCM) to afford the title compound as a white solid (227 mg, 82%).

ν_{max} (neat): 3306, 2928, 2866, 1622, 1548, 1504 cm^{-1}

^1H NMR (500 MHz, CDCl_3): δ 7.76 (d, 2H, 2 x ArH, $J = 8.5$ Hz), 6.93 (d, 2H, 2 x ArH, $J = 8.5$ Hz), 6.63 (br. s, 1H, NH), 3.86 – 3.83 (m, 5H, $\text{CH}_3 + \text{CH}_2$), 3.63 - 3.61 (m, 2H, CH_2), 2.22 (br. s, 1H, OH)

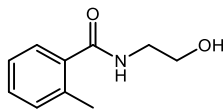
^{13}C NMR (126 MHz, DMSO): δ 165.8, 161.4, 129.0, 126.8, 113.4, 59.9, 55.3, 42.1

HRMS ($\text{C}_{10}\text{H}_{14}\text{NO}_3$) [$\text{M}+\text{H}^+$] requires 196.0968, found [$\text{M}+\text{H}^+$] 196.0970

m.p. 106 – 107 $^{\circ}\text{C}$

Consistent with previously reported data⁷⁴

Compound 119. *N*-(2-hydroxyethyl)-2-methylbenzamide



Synthesised according to General Experimental Procedure J at rt (Table 17, Entry 4, Page 80) using methyl 2-methyl benzoate (199 μ L, 1.42 mmol, 1 equiv) and ethanolamine (86 μ L, 1.42 mmol, 1 equiv), and purified by flash column chromatography (6% methanol/DCM) to afford the title compound as a white solid (152 mg, 60%).

Synthesised according to General Experimental Procedure J at 40 $^{\circ}$ C (Table 17, Entry 4, Page 80) using methyl 2-methyl benzoate (199 μ L, 1.42 mmol, 1 equiv) and ethanolamine (86 μ L, 1.42 mmol, 1 equiv), and purified by flash column chromatography (6% methanol/DCM) to afford the title compound as a white solid (239 mg, 94%).

Synthesised according to General Experimental Procedure O (Table 26, Entry 4, Page 112) using methyl 2-methyl benzoate (199 μ L, 1.42 mmol, 1 equiv) and ethanolamine (86 μ L, 1.42 mmol, 1 equiv), and purified by flash column chromatography (6% methanol/DCM) to afford the title compound as a white solid (191 mg, 75%).

ν_{\max} (neat): 3271, 2930, 2872, 1641, 1537 cm^{-1}

^1H NMR (500 MHz, CDCl_3): δ 7.37 (dd, 1H, ArH, $J = 7.6$ Hz, 1.1 Hz), 7.31 (td, 1H, ArH, $J = 7.5$ Hz, 1.0 Hz), 7.20 (dd, 2H, 2 x ArH, $J = 7.5$, 1.5 Hz), 6.29 (br. s, 1H, NH), 3.83 (t, 2H, CH_2 , $J = 5.0$ Hz), 3.60 (q, 2H, CH_2 , $J = 5.2$ Hz), 2.46 (s, 3H, CH_3), 2.24 (br. s, 1H, OH)

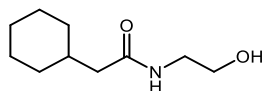
^{13}C NMR (126 MHz, CDCl_3): δ 171.5, 136.3, 131.2, 130.2, 127.0, 125.9, 62.5, 42.8, 20.0, 1C missing (overlapping peaks)

HRMS ($\text{C}_{10}\text{H}_{14}\text{NO}_2$) [$\text{M}+\text{H}^+$] requires 180.1019, found [$\text{M}+\text{H}^+$] 180.1017

m.p. 61 – 62 $^{\circ}$ C

Consistent with previously reported data¹⁴⁷

Compound 120. 2-Cyclohexyl-N-(2-hydroxyethyl)acetamide



Synthesised according to General Experimental Procedure J at rt (Table 17, Entry 6, Page 80) using methyl cyclohexylacetate (233 μ L, 1.42 mmol, 1 equiv) and ethanolamine (86 μ L, 1.42 mmol, 1 equiv), and purified by flash column chromatography (6% methanol/DCM) to afford the title compound as a white solid (263 mg, 100%).

Synthesised according to General Experimental Procedure O (Table 26, Entry 5, Page 112) using methyl cyclohexylacetate (233 μ L, 1.42 mmol, 1 equiv) and ethanolamine (86 μ L, 1.42 mmol, 1 equiv), and purified by flash column chromatography (6% methanol/DCM) to afford the title compound as a white solid (263 mg, 100%).

ν_{max} (neat): 3287, 2916, 2845, 1638, 1553 cm^{-1}

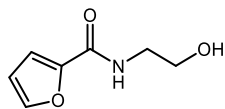
^1H NMR (500 MHz, CDCl_3): δ 6.09 (br. s, 1H, NH), 3.72 (t, 2H, CH_2 , $J = 5.0$ Hz), 3.42 (q, 2H, CH_2 , $J = 5.2$ Hz), 2.86 (br. s, 1H, OH), 2.08 (d, 2H, CH_2 , $J = 7.0$ Hz), 1.84 – 1.61 (m, 6H, 6 x CH), 1.32 – 1.24 (m, 2H, 2 x CH), 1.18 – 1.09 (m, 1H, CH), 0.99 – 0.91 (m, 2H, 2 x CH)

^{13}C NMR (126 MHz, CDCl_3): δ 174.1, 62.8, 44.9, 42.7, 35.6, 33.3, 26.4, 26.3

m.p. 87 – 88 $^{\circ}\text{C}$

HRMS ($\text{C}_{10}\text{H}_{20}\text{NO}_2$) [$\text{M}+\text{H}^+$] requires 186.1489, found [$\text{M}+\text{H}^+$] 186.1486

Compound 121. N-(2-hydroxyethyl)furan-2-carboxamide



Synthesised according to General Experimental Procedure J at rt (Table 17, Entry 7, Page 80) using methyl 2-furoate (152 μ L, 1.42 mmol, 1 equiv) and ethanolamine (86 μ L, 1.42 mmol, 1 equiv), and purified by flash column chromatography (5% methanol/DCM) to afford the title compound as a yellow oil (206 mg, 94%).

Synthesised according to General Experimental Procedure O (Table 26, Entry 7, Page 112) using methyl 2-furoate (152 μ L, 1.42 mmol, 1 equiv) and ethanolamine (86 μ L, 1.42 mmol, 1 equiv), and purified by flash column chromatography (5% methanol/DCM) to afford the title compound as a yellow oil (220 mg, 100%).

Synthesised according to General Experimental Procedure O (Table 26, Entry 7, Page 112) using methyl 2-furoate (1.1mL, 10 mmol, 1 equiv), ethanolamine (604 μ L, 10 mmol, 1 equiv), K_3PO_4 (637 mg, 3 mmol, 0.3 equiv) and *i*-PrOH (5 mL), and by flash column chromatography (5% methanol/DCM) to afford the title compound as a yellow oil (1.43 g, 92%).

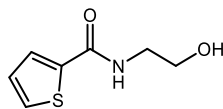
ν_{max} (neat): 3302, 2938, 2870, 1634, 1593, 1530 cm^{-1}

1H NMR (500 MHz, $CDCl_3$) δ 7.44 (dd, 1H, ArH, $J = 1.5, 0.5$ Hz), 7.12 (dd, 1H, ArH, $J = 3.6, 0.6$ Hz), 6.87 (br. s, 1H, NH), 6.50 (dd, 1H, ArH, $J = 3.5, 2.0$ Hz), 3.81 (t, 2H, CH_2 , $J = 5.0$ Hz), 3.60 (q, 2H, CH_2 , $J = 5.3$ Hz), 2.65 (br. s, 1H, OH)

^{13}C NMR (126 MHz, $CDCl_3$): δ 159.6, 147.9, 144.3, 114.7, 112.4, 62.2, 42.2

HRMS ($C_7H_{10}NO_3$) $[M+H^+]$ requires 156.0655, found $[M+H^+]$ 156.0651

Compound 122. *N*-(2-hydroxyethyl)thiophene-2-carboxamide



Synthesised according to General Experimental Procedure J at rt (Table 17, Entry 8, Page 80) using ethyl 2-thiophenecarboxylate (191 μ L, 1.42 mmol, 1 equiv) and ethanolamine (86 μ L, 1.42 mmol, 1 equiv), and purified by flash column chromatography (5% methanol/DCM) to afford the title compound as a white solid (240 mg, 99%).

Synthesised according to General Experimental Procedure O (Table 26, Entry 8, Page 112) using ethyl 2-thiophenecarboxylate (191 μ L, 1.42 mmol, 1 equiv) and ethanolamine (86 μ L, 1.42 mmol, 1 equiv), and purified by flash column chromatography (5% methanol/DCM) to afford the title compound as a white solid (243 mg, 100%).

Synthesised according to General Experimental Procedure O (Table 26, Entry 8, Page 112) in a round-bottomed flask using reagents and solvent with no prior purification, and purified by flash column chromatography (5% methanol/DCM) to afford the title compound as a white solid (194 mg, 81%).

ν_{max} (neat): 3287, 2922, 2862, 1614, 1553 cm^{-1}

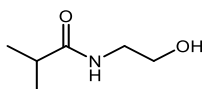
^1H NMR (500 MHz, DMSO): δ 8.45 (t, 1H, NH, $J = 5.8$ Hz), 7.74 (dd, 2H, 2 x ArH, $J = 15.0, 4.3$ Hz), 7.13 (dd, 1H, ArH, $J = 4.8, 3.8$ Hz), 4.73 (t, 1H, OH, $J = 5.5$ Hz), 3.50 (q, 2H, CH_2 , $J = 6.0$ Hz), 3.29 (q, 2H, CH_2 , $J = 6.0$ Hz)

^{13}C NMR (126 MHz, DMSO): δ 161.2, 140.2, 130.5, 127.9, 127.8, 59.7, 42.0

HRMS ($\text{C}_7\text{H}_{10}\text{NO}_2\text{S}$) [$\text{M}+\text{H}^+$] requires 172.0427, found [$\text{M}+\text{H}^+$] 172.0426

m.p. 95 – 96 $^{\circ}\text{C}$

Compound 123. *N*-(2-hydroxyethyl)isobutyramide



Synthesised according to General Experimental Procedure J at rt (Table 17, Entry 10, Page 80) using methyl isobutyrate (163 μL , 1.42 mmol, 1 equiv) and ethanolamine (86 μL , 1.42 mmol, 1 equiv), and purified by flash column chromatography (4% methanol/DCM) to afford the title compound as a white solid (184 mg, 99%).

Synthesised according to General Experimental Procedure O (Table 26, Entry 10, Page 112) using methyl isobutyrate (163 μL , 1.42 mmol, 1 equiv) and ethanolamine (86 μL , 1.42 mmol, 1 equiv), and purified by flash column chromatography (4% methanol/DCM) to afford the title compound as a white solid (186 mg, 100%).

ν_{max} (neat): 3302, 2965, 2930, 2874, 1641, 1545 cm^{-1}

^1H NMR (500 MHz, CDCl_3): δ 6.17 (br. s, 1H, NH), 3.72 (t, 2H, CH_2 , $J = 5.0$ Hz), 3.41 (q, 2H, CH_2 , $J = 5.2$ Hz), 2.77 (br. s, 1H, OH), 2.40 (spt, 1H, CH, $J = 6.9$ Hz), 1.17 (d, 6H, 2 x CH_3 , $J = 7.0$ Hz)

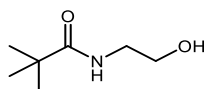
^{13}C NMR (126 MHz, CDCl_3): δ 178.7, 62.4, 42.5, 35.7, 19.7

HRMS ($\text{C}_6\text{H}_{14}\text{NO}_2$) [$\text{M}+\text{H}^+$] requires 132.1019, found [$\text{M}+\text{H}^+$] 132.1016

m.p. 63 – 64 $^\circ\text{C}$

Consistent with previously reported data¹⁴⁸

Compound 124. *N*-(2-hydroxyethyl)pivalamide



Synthesised according to General Experimental Procedure J at rt (Table 17, Entry 11, Page 80) using methyl trimethylacetate (189 μ L, 1.42 mmol, 1 equiv) and ethanolamine (86 μ L, 1.42 mmol, 1 equiv), and purified by flash column chromatography (4% methanol/DCM) to afford the title compound as a yellow oil (126 mg, 61%).

Synthesised according to General Experimental Procedure J at 40 $^{\circ}$ C (Table 17, Entry 11, Page 80) using methyl trimethylacetate (189 μ L, 1.42 mmol, 1 equiv) and ethanolamine (86 μ L, 1.42 mmol, 1 equiv), and purified by flash column chromatography (4% methanol/DCM) to afford the title compound as a yellow oil (188 mg, 91%).

ν_{max} (neat): 3323, 2961, 2872, 1634, 1530 cm^{-1}

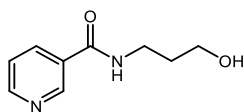
^1H NMR (500 MHz, CDCl_3): δ 6.20 (br. s, 1H, NH), 3.72 (t, 2H, CH_2 , $J = 5.0$ Hz), 3.42 (q, 2H, CH_2 , $J = 5.0$ Hz), 2.66 (br. s, 1H, OH), 1.22 (s, 9H, 3 x CH_3)

^{13}C NMR (126 MHz, CDCl_3): δ 180.2, 62.7, 42.8, 38.9, 27.7

HRMS ($\text{C}_7\text{H}_{16}\text{NO}_2$) [$\text{M}+\text{H}^+$] requires 146.1176, found [$\text{M}+\text{H}^+$] 146.1175

^1H and ^{13}C NMR consistent with previously reported data¹⁴⁹

Compound 125. N-(3-hydroxypropyl)nicotinamide



Synthesised according to General Experimental Procedure J at rt (Table 17, Entry 14, Page 80) using methyl nicotinate (195 mg, 1.42 mmol, 1 equiv) and 3-amino-1-propanol (109 μ L, 1.42 mmol, 1 equiv), and purified by flash column chromatography (5% methanol/DCM) to afford the title compound as a colourless oil (227 mg, 89%).

Synthesised according to General Experimental Procedure O (Table 26, Entry 11, Page 112) using methyl nicotinate (195 mg, 1.42 mmol, 1 equiv) and 3-amino-1-propanol (109 μ L, 1.42 mmol, 1 equiv), and purified by flash column chromatography (5% methanol/DCM) to afford the title compound as a colourless oil (225 mg, 88%).

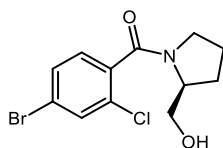
ν_{\max} (neat): 3273, 3065, 2939, 2874, 1638, 1543 cm^{-1}

^1H NMR (500 MHz, CDCl_3): δ 8.99 (s, 1H, ArH), 8.68 (d, 1H, ArH, $J = 4.0$ Hz), 8.16 (d, 1H, ArH, $J = 8.0$ Hz), 7.50 (br. s, 1H, NH), 7.39 (dd, 1H, ArH, $J = 8.0, 5.0$ Hz), 3.78 (t, 2H, CH_2 , $J = 5.5$ Hz), 3.64 (q, 2H, CH_2 , $J = 5.8$ Hz), 2.93 (br. s, 1H, OH), 1.84 (quintet, 2H, CH_2 , $J = 5.8$ Hz)

^{13}C NMR (126 MHz, CDCl_3): δ 166.3, 152.1, 147.9, 135.7, 130.5, 123.9, 60.7, 38.3, 31.7

HRMS ($\text{C}_9\text{H}_{13}\text{N}_2\text{O}_2$) [$\text{M}+\text{H}^+$] requires 181.0972, found [$\text{M}+\text{H}^+$] 181.0972

Compound 126. (S)-(4-bromo-2-chlorophenyl)(2-(hydroxymethyl)pyrrolidin-1-yl)methanone



Synthesised according to General Experimental Procedure J at rt (Table 17, Entry 15, Page 80) using methyl 4-bromo-2-chlorobenzoate (354 mg, 1.42 mmol, 1 equiv) and (S)-(+)-2-(hydroxymethyl)pyrrolidine (140 μ L, 1.42 mmol, 1 equiv), and purified by flash column chromatography (4% methanol/DCM) to afford the title compound as a colourless oil (421 mg, 93%).

Synthesised according to General Experimental Procedure J at rt (Table 17, Entry 15, Page 80) using methyl 4-bromo-2-chlorobenzoate (2.5 g, 10 mmol, 1 equiv), (S)-(+)-2-(hydroxymethyl)pyrrolidine (987 μ L, 10 mmol, 1 equiv), BEMP (290 μ L, 1 mmol, 0.1 equiv) and MeCN (5 mL) and purified by flash column chromatography (4% methanol/DCM) to afford the title compound as a colourless oil (2.92 g, 92%).

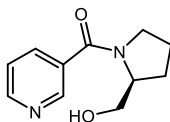
ν_{max} (neat): 3389, 2949, 2876, 1612, 1581, 1425 cm^{-1}

^1H NMR (500 MHz, CDCl_3): δ 7.60 (d, 1H, ArH, $J = 1.5$ Hz), 7.48 (dd, 1H, ArH, $J = 8.3, 1.8$ Hz), 7.21 (d, 1H, ArH, $J = 8.0$ Hz), 4.48 (br. s, 1H, OH), 4.36 (qd, 1H, CH, $J = 7.3, 3.6$ Hz), 3.85 – 3.73 (m, 2H, 2 x CH), 3.27 – 3.26 (m, 2H, CH_2), 2.22 – 2.15 (m, 1H, CH), 2.02 (spt, 1H, CH, $J = 5.8$ Hz), 1.91 (m, 1H, CH), 1.86 – 1.82 (m, 1H, CH)

^{13}C NMR (126 MHz, CDCl_3): δ 168.2, 135.9, 132.6, 130.8, 128.7, 123.6, 66.7, 61.7, 49.5, 28.7, 24.6, 1C missing (overlapping peaks)

HRMS ($\text{C}_{12}\text{H}_{14}^{79}\text{BrClINO}_2$) $[\text{M}+\text{H}^+]$ requires 317.9891, found $[\text{M}+\text{H}^+]$ 317.9896

Compound 127. (S)-(2-(hydroxymethyl)pyrrolidin-1-yl)(pyridin-3-yl)methanone



Synthesised according to General Experimental Procedure J at rt (Table 17, Entry 16, Page 80) using methyl nicotinate (195 mg, 1.42 mmol, 1 equiv) and (S)-(+)-2-(hydroxymethyl)pyrrolidine (140 μ L, 1.42 mmol, 1 equiv), and purified by flash column chromatography (6% methanol/DCM) to afford the title compound as a yellow oil (251 mg, 86%).

Synthesised according to General Experimental Procedure O (Table 26, Entry 13, Page 112) using methyl nicotinate (195 mg, 1.42 mmol, 1 equiv) and (S)-(+)-2-(hydroxymethyl)pyrrolidine (140 μ L, 1.42 mmol, 1 equiv), and purified by flash column chromatography (6% methanol/DCM) to afford the title compound as a yellow oil (246 mg, 84%).

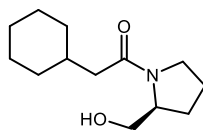
ν_{\max} (neat): 3379, 2968, 2876, 1607, 1433 cm^{-1}

^1H NMR (500 MHz, CDCl_3): δ 8.77 (s, 1H, ArH), 8.67 (d, 1H, ArH, $J = 4.0$ Hz), 7.85 (dt, 1H, ArH, $J = 4.8, 2.3$ Hz), 7.37 (dd, 1H, ArH, $J = 8.0, 5.0$ Hz), 4.40 (qd, 1H, CH, $J = 7.3, 2.8$ Hz), 3.83 (dd, 1H, CH, $J = 11.8, 2.8$ Hz), 3.75 (dd, 1H, CH, $J = 11.5, 7.0$ Hz), 3.53 – 3.50 (m, 2H, CH_2), 2.20 – 2.15 (m, 1H, CH), 1.95 – 1.91 (m, 1H, CH), 1.81 – 1.72 (m, 2H, 2 x CH), 1H missing (exchangeable)

^{13}C NMR (126 MHz, CDCl_3): δ 169.7, 151.3, 148.2, 135.2, 132.8, 123.6, 66.9, 61.9, 51.3, 28.6, 25.2

HRMS ($\text{C}_{11}\text{H}_{15}\text{N}_2\text{O}_2$) $[\text{M}+\text{H}^+]$ requires 207.1128, found $[\text{M}+\text{H}^+]$ 207.1126

Compound 128. (*S*)-2-cyclohexyl-1-(2-(hydroxymethyl)pyrrolidin-1-yl)ethanone



Synthesised according to General Experimental Procedure J at rt (Table 17, Entry 17, Page 80) using methyl cyclohexylacetate (233 μL , 1.42 mmol, 1 equiv) and (*S*)-(+)-2-(hydroxymethyl)pyrrolidine (140 μL , 1.42 mmol, 1 equiv), and purified by flash column chromatography (6% methanol/DCM) to afford the title compound as a colourless oil (127 mg, 40%).

Synthesised according to General Experimental Procedure J at 40 $^{\circ}\text{C}$ (Table 17, Entry 17, Page 80) using methyl cyclohexylacetate (233 μL , 1.42 mmol, 1 equiv) and (*S*)-(+)-2-(hydroxymethyl)pyrrolidine (140 μL , 1.42 mmol, 1 equiv), and purified by flash column chromatography (6% methanol/DCM) to afford the title compound as a colourless oil (239 mg, 75%).

Synthesised according to General Experimental Procedure O (Table 26, Entry 14, Page 112) using methyl cyclohexylacetate (233 μL , 1.42 mmol, 1 equiv) and (*S*)-(+)-2-(hydroxymethyl)pyrrolidine (140 μL , 1.42 mmol, 1 equiv), and purified by flash column chromatography (6% methanol/DCM) to afford the title compound as a colourless oil (214 mg, 67%).

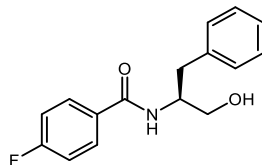
ν_{max} (neat): 3375, 2918, 2849, 1612, 1444 cm^{-1}

^1H NMR (500 MHz, CDCl_3): δ 4.25 – 4.23 (m, 1H, CH), 3.66 (dd, 1H, CH, $J = 11.0, 2.5$ Hz), 3.59 – 3.53 (m, 2H, 2 x CH), 3.49 – 3.44 (m, 1H, CH), 2.19 (d, 2H, CH_2 , $J = 7.0$ Hz), 2.06 – 2.02 (m, 1H, CH), 1.95 – 1.65 (m, 8H, 8 x CH), 1.59 – 1.56 (m, 1H, CH), 1.31 – 1.26 (m, 3H, 3 x CH), 1.16 – 1.13 (m, 1H, CH), 0.99 – 0.94 (m, 2H, 2 x CH)

^{13}C NMR (126 MHz, CDCl_3): δ 174.3, 67.9, 61.3, 48.6, 42.8, 35.0, 33.6, 28.5, 26.4, 26.3, 24.6

HRMS (C₁₃H₂₄NO₂) [M+H⁺] requires 226.1802, found [M+H⁺] 226.1804

Compound 129. (S)-4-fluoro-N-(1-hydroxy-3-phenylpropan-2-yl)benzamide



Synthesised according to General Experimental Procedure J at rt (Table 17, Entry 18, Page 80) using methyl 4-fluorobenzoate (184 μ L, 1.42 mmol, 1 equiv) and (S)-(-)-2-amino-3-phenyl-1-propanol (215 mg, 1.42 mmol, 1 equiv), and purified by flash column chromatography (4% methanol/DCM) to afford the title compound as an off-white solid (226 mg, 58%).

Synthesised according to General Experimental Procedure J at 40 °C (Table 17, Entry 18, Page 80) using methyl 4-fluorobenzoate (184 μ L, 1.42 mmol, 1 equiv) and (S)-(-)-2-amino-3-phenyl-1-propanol (215 mg, 1.42 mmol, 1 equiv), and purified by flash column chromatography (4% methanol/DCM) to afford the title compound as an off-white solid (269 mg, 69%).

ν_{\max} (neat): 3366, 3308, 1641, 1605, 1537, 1333 cm⁻¹

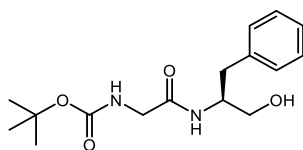
¹H NMR (500 MHz, DMSO): δ 8.18 (d, 1H, ArH, J = 8.0 Hz), 7.87 – 7.84 (m, 2H, 2 x ArH), 7.28 – 7.24 (m, 6H, 5 x Ar + NH), 7.17 – 7.13 (m, 1H, ArH), 4.82 (t, 1H, OH, J = 5.8 Hz), 4.18 – 4.11 (m, 1H, CH), 3.49 (app. quintet, 1H, CH, J = 5.4 Hz), 3.42 (app. quintet, 1H, CH, J = 5.6 Hz), 2.94 (dd, 1H, CH, J = 13.5, 5.0 Hz), 2.78 (dd, 1H, CH, J = 13.5, 9.3 Hz)

¹³C NMR (126 MHz, DMSO): δ 164.9, 163.7 (d, ¹ J_{CF} = 249.5 Hz), 139.4, 131.2, 129.8 (d, ³ J_{CF} = 8.8 Hz), 129.0, 128.0, 125.8, 115.0 (d, ² J_{CF} = 21.6 Hz), 62.8, 53.3, 36.4

HRMS (C₁₆H₁₇FNO₂) [M+H⁺] requires 274.1243, found [M+H⁺] 274.1241

m.p. 138 – 139 °C

Compound 130. (*S*)-*tert*-butyl (2-((1-hydroxy-3-phenylpropan-2-yl)amino)-2-oxoethyl)carbamate



Synthesised according to General Experimental Procedure J at rt (Table 17, Entry 19, Page 80) using Boc-glycine methyl ester (249 μL , 1.42 mmol, 1 equiv) and (*S*)-(-)-2-amino-3-phenyl-1-propanol (215 mg, 1.42 mmol, 1 equiv), and purified by flash column chromatography (6% methanol/DCM) to afford the title compound as a white solid (329 mg, 75%).

Synthesised according to General Experimental Procedure O (Table 26, Entry 15, Page 112) using Boc-glycine methyl ester (249 μL , 1.42 mmol, 1 equiv) and (*S*)-(-)-2-amino-3-phenyl-1-propanol (215 mg, 1.42 mmol, 1 equiv), and purified by flash column chromatography (6% methanol/DCM) to afford the title compound as a white solid (289 mg, 66%).

ν_{max} (neat): 3416, 3237, 3065, 2980, 2936, 1690, 1661, 1547 cm^{-1}

^1H NMR (500 MHz, CDCl_3): δ 7.32 – 7.29 (m, 2H, 2 x ArH), 7.25 – 7.21 (m, 3H, 3 x ArH), 6.42 (d, 1H, NH, $J = 6.5$ Hz), 5.19 (s, 1H, NH), 4.20 – 4.18 (m, 1H, CH), 3.76 – 3.68 (m, 3H, 3 x CH), 3.57 (dd, 1H, CH, $J = 11.3, 5.3$ Hz), 2.88 (dd, 2H, CH_2 , $J = 7.3, 2.8$ Hz), 1.45 (s, 9H, 3 x CH_3), 1H missing (exchangeable)

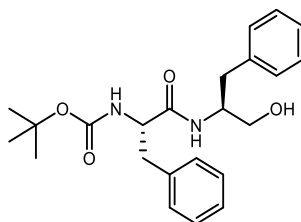
^{13}C NMR (126 MHz, DMSO): δ 168.8, 155.7, 139.0, 129.1, 128.1, 125.9, 77.9, 62.2, 52.4, 43.2, 36.5, 28.2

HRMS ($\text{C}_{16}\text{H}_{25}\text{N}_2\text{O}_4$) [$\text{M}+\text{H}^+$] requires 309.1809, found [$\text{M}+\text{H}^+$] 309.1810

m.p. 137 – 138 $^\circ\text{C}$

Consistent with previously reported data⁷⁴

Compound 131. tert-butyl ((S)-1-(((S)-1-hydroxy-3-phenylpropan-2-yl)amino)-1-oxo-3-phenylpropan-2-yl)carbamate



Synthesised according to General Experimental Procedure J at rt (Table 17, Entry 20, Page 80) using Boc-phenylalanine methyl ester (397 mg, 1.42 mmol, 1 equiv) and (*S*)-(-)-2-amino-3-phenyl-1-propanol (215 mg, 1.42 mmol, 1 equiv), and purified by flash column chromatography (5% methanol/DCM) to afford the title compound as a white solid (452 mg, 80%).

ν_{\max} (neat): 3333, 3296, 2928, 2866, 1686, 1657, 1524 cm^{-1}

^1H NMR (500 MHz, CDCl_3): δ 7.32 – 7.26 (m, 5H, 5 x ArH), 7.23 – 7.20 (m, 3H, 3 x ArH), 7.13 – 7.12 (m, 2H, 2 x ArH), 6.02 (s, 0.18H, NH, minor diastereomer), 5.90 (s, 0.82H, NH, major diastereomer), 5.04 (s, 1H, NH), 4.27 – 4.22 (m, 1H, CH), 4.10 – 4.08 (m, 1H, CH), 3.48 – 3.41 (m, 2H, 2 x CH), 3.09 – 2.95 (m, 2H, 2 x CH), 2.81 – 2.70 (m, 2H, 2 x CH), 1.42 (s, 7.56H, 3 x CH_3 , major diastereomer), 1.41 (s, 1.44 H, 3 x CH_3 , minor diastereomer), 1H missing (exchangeable)

^{13}C NMR (126 MHz, DMSO): δ 171.1, 155.0, 139.0, 138.1, 129.1, 128.0, 127.9, 126.1, 125.9, 78.0, 62.1, 55.8, 52.2, 37.8, 36.4, 28.1, 1C missing (overlapping peaks)

HRMS ($\text{C}_{23}\text{H}_{31}\text{N}_2\text{O}_4$) [$\text{M}+\text{H}^+$] requires 399.2270, found [$\text{M}+\text{H}^+$] 399.2274

m.p. 129 – 130 $^\circ\text{C}$

dr = 86:14 as determined by chiral HPLC

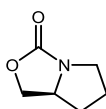
Experimental - Characterisation Data for Isolated Products

Synthesised according to General Experimental Procedure O (Table 26, Entry 16, Page 112) using Boc-phenylalanine methyl ester (397 mg, 1.42 mmol, 1 equiv) and (*S*)-(-)-2-amino-3-phenyl-1-propanol (215 mg, 1.42 mmol, 1 equiv), and purified by flash column chromatography (5% methanol/DCM) to afford the title compound as a white solid (237 mg, 42%).

$^1\text{H NMR}$ (500 MHz, CDCl_3): δ 7.33 – 7.28 (m, 5H, 5 x ArH), 7.27 – 7.20 (m, 3H, 3 x ArH), 7.13 – 7.12 (m, 2H, 2 x ArH), 5.85 (s, 1H, NH), 5.02 (s, 1H, NH), 4.26 – 4.25 (m, 1H, CH), 4.09 – 4.08 (m, 1H, CH), 3.49 – 3.41 (m, 2H, 2 x CH), 3.05 – 2.95 (m, 2H, 2 x CH), 2.81 – 2.71 (m, 2H, 2 x CH), 1.42 (s, 9H, 3 x CH_3), 1H missing (exchangeable)

dr = 98:2 as determined by chiral HPLC

Compound 146. (*S*)-tetrahydropyrrolo[1,2-*c*]oxazol-3(*1H*)-one



Synthesised according to General Experimental Procedure L (Scheme 42, Page 88) using (*S*)-(+)-2-(hydroxymethyl)pyrrolidine (140 μL , 1.42 mmol, 1 equiv), and purified by flash column chromatography (2% methanol/DCM) to afford the title compound as a yellow oil (125 mg, 69%).

ν_{max} (neat): 2974, 2911, 1738, 1481 cm^{-1}

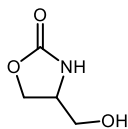
$^1\text{H NMR}$ (400 MHz, CDCl_3): δ 4.45 (dd, 1H, CH, $J = 8.9, 7.9$ Hz), 4.10 (dd, 1H, CH, $J = 8.9, 3.6$ Hz), 3.88 – 3.81 (m, 1H, CH), 3.60 – 3.53 (m, 1H, CH), 3.13 – 3.08 (m, 1H, CH), 2.07 – 1.97 (m, 2H, 2 x CH), 1.93 – 1.83 (m, 1H, CH), 1.46 – 1.36 (m, 1H, CH)

$^{13}\text{C NMR}$ (101 MHz, CDCl_3): δ 161.8, 67.8, 59.5, 45.8, 30.7, 25.7

HRMS ($\text{C}_6\text{H}_{10}\text{NO}_2$) [$\text{M}+\text{H}^+$] requires 128.0706, found [$\text{M}+\text{H}^+$] 128.0704

Consistent with previously reported data¹⁵⁰

Compound 148. 4-(hydroxymethyl)oxazolidin-2-one



Synthesised according to General Experimental Procedure L (Scheme 42, Page 88) using 2-aminopropane-1,3-diol (215 mg, 1.42 mmol, 1 equiv), and purified by flash column chromatography (4% methanol/DCM) to afford the title compound as a yellow oil (144 mg, 87%).

ν_{max} (neat): 3331, 3242, 2933, 2878, 1722, 1418 cm^{-1}

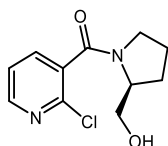
^1H NMR (500 MHz, DMSO): δ 7.57 (s, 1H, NH), 4.94 (t, 1H, OH, $J = 5.4$ Hz), 4.30 (t, 1H, CH, $J = 8.6$ Hz), 4.05 (dd, 1H, CH, $J = 8.5, 5.0$ Hz), 3.78 – 3.71 (m, 1H, CH), 3.37 – 3.35 (m, 2H, CH₂)

^{13}C NMR (126 MHz, DMSO): δ 159.1, 64.4, 62.7, 53.2

HRMS (C₄H₈NO₃) [M+H⁺] requires 118.0499, found [M+H⁺] 118.0496

Consistent with previously reported data¹⁵¹

Compound 149. (S)-(2-chloropyridin-3-yl)(2-(hydroxymethyl)pyrrolidin-1-yl)methanone



Synthesised according to General Experimental Procedure J at rt (Scheme 43, Page 89) using methyl 2-chloronicotinate (185 μL , 1.42 mmol, 1 equiv) and (S)-(+)-2-(hydroxymethyl)pyrrolidine (140 μL , 1.42 mmol, 1 equiv), and purified by flash column chromatography (6% methanol/DCM) to afford the title compound as a pale yellow oil (297 mg, 87%).

Experimental - Characterisation Data for Isolated Products

Synthesised according to General Experimental Procedure J at 40 °C (Scheme 43, Page 89) using methyl 2-chloronicotinate (185 μL , 1.42 mmol, 1 equiv) and (*S*)-(+)-2-(hydroxymethyl)pyrrolidine (140 μL , 1.42 mmol, 1 equiv), and purified by flash column chromatography (6% methanol/DCM) to afford the title compound as a pale yellow oil (334 mg, 98%).

Synthesised according to General Experimental Procedure O (Table 26, Entry 12, Page 112) using methyl 2-chloronicotinate (185 μL , 1.42 mmol, 1 equiv) and (*S*)-(+)-2-(hydroxymethyl)pyrrolidine (140 μL , 1.42 mmol, 1 equiv), and purified by flash column chromatography (6% methanol/DCM) to afford the title compound as a pale yellow oil (208 mg, 61%).

ν_{max} (neat): 3375, 2949, 2878, 1612, 1582 cm^{-1}

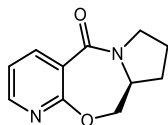
^1H NMR (500 MHz, CDCl_3): δ 8.44 (dd, 1H, ArH, $J = 4.8, 1.8$ Hz), δ 7.69 (dd, 1H, ArH, $J = 7.5, 2.0$ Hz), δ 7.32 (dd, 1H, ArH, $J = 7.5, 5.0$ Hz), δ 4.38 – 4.33 (m, 1H, CH), δ 3.82 – 3.77 (m, 2H, 2 x CH), δ 3.31 – 3.26 (m, 2H, 2 x CH), δ 2.21 – 2.14 (m, 1H, CH), δ 1.96 – 1.89 (m, 1H, CH), δ 1.87 – 1.80 (m, 1H, CH), δ 1.79 – 1.71 (m, 1H, CH), 1H missing (exchangeable)

^{13}C NMR (126 MHz, DMSO): δ 169.6, 153.5, 152.6, 143.9, 111.5, 108.1, 68.2, 60.4, 49.2, 29.4, 22.4

HRMS ($\text{C}_{11}\text{H}_{14}\text{ClN}_2\text{O}_2$) [$\text{M}+\text{H}^+$] requires 241.0738, found [$\text{M}+\text{H}^+$] 241.0737

Consistent with previously reported data¹¹⁸

Compound 150. (*S*)-8,9,9a,10-tetrahydropyrido[3,2-*f*]pyrrolo[2,1-*c*][1,4]oxazepin-5(*7H*)-one



To a round-bottomed flask containing (*S*)-(2-chloropyridin-3-yl)(2-(hydroxymethyl)pyrrolidin-1-yl)methanone (**149**, 226 mg, 0.94 mmol, 1 equiv) and THF (10 mL) was added sodium hydride (28 mg, 1.18 mmol, 1.25 equiv). The reaction mixture was heated at 80 °C for 15 h then filtered and concentrated to a residue that was purified by flash column chromatography (4% methanol/DCM) to afford the title compound as a white solid (186 mg, 97%).

ν_{\max} (neat): 3261, 2955, 2926, 1618, 1560 cm^{-1}

^1H NMR (500 MHz, CDCl_3): δ 8.64 (dd, 1H, ArH, $J = 7.5, 2.0$ Hz), 8.38 (dd, 1H, ArH, $J = 4.5, 2.0$ Hz), 7.12 (dd, 1H, ArH, $J = 7.8, 4.8$ Hz), 4.63 (d, 1H, CH, $J = 12.0$ Hz), 4.14 (dd, 1H, CH, $J = 12.0, 8.5$ Hz), 4.03 (q, 1H, CH, $J = 8.0$ Hz), 3.84 – 3.72 (m, 2H, CH_2), 2.31 – 2.25 (m, 1H, CH), 2.07 – 2.01 (m, 1H, CH), 1.96 – 1.88 (m, 1H, CH), 1.74 – 1.66 (m, 1H, CH)

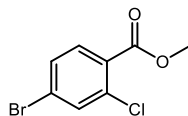
^{13}C NMR (126 MHz, DMSO): δ 162.0, 160.5, 151.3, 142.9, 118.3, 116.5, 73.3, 56.9, 48.0, 28.6, 22.2

HRMS ($\text{C}_{11}\text{H}_{13}\text{N}_2\text{O}_2$) [$\text{M}+\text{H}^+$] requires 205.0972, found [$\text{M}+\text{H}^+$] 205.0969

m.p. 143 – 144 °C

Consistent with previously reported data¹¹⁸

Compound 151. methyl 4-bromo-2-chlorobenzoate



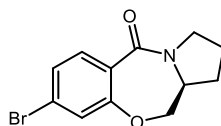
To a round-bottomed flask containing MeOH (25 mL) at 0 °C was added acetyl chloride (1.8 mL, 25.4 mmol, 2 equiv) and the reaction mixture was stirred at 0 °C for 10 min. A solution of 4-bromo-2-chlorobenzoic acid (3 g, 12.7 mmol, 1 equiv) in MeOH (25 mL) was added dropwise. The reaction mixture was heated at 100 °C for 7 h then neutralised with NaHCO₃ and concentrated under vacuum. The residue was dissolved in DCM, washed with water, passed through a hydrophobic frit, and concentrated under vacuum to afford the title compound as a colourless liquid (2.76 g, 87%).

ν_{max} (neat): 3092, 2951, 1730, 1578, 1553, 1468, 1431, 1369 cm⁻¹

¹H NMR (500 MHz, CDCl₃): δ 7.71 (d, 1H, ArH, J = 8.5 Hz), 7.63 (d, 1H, ArH, J = 2.0 Hz), 7.45 (dd, 1H, ArH, J = 8.5, 2.0 Hz), 3.92 (s, 3H, CH₃)

¹³C NMR (126 MHz, CDCl₃): δ 165.3, 135.0, 133.9, 132.7, 130.0, 128.8, 126.6, 52.6

Compound 152. (S)-8-bromo-2,3,11,11a-tetrahydrobenzo[f]pyrrolo[2,1-c][1,4]oxazepin-5(1H)-one



To a round-bottomed flask containing (S)-(4-bromo-2-chlorophenyl)(2-(hydroxymethyl)pyrrolidin-1-yl)methanone (**126**, 960 mg, 3 mmol, 1 equiv) and DMF (3 mL) at 0 °C was added NaH (144 mg, 6 mmol, 2 equiv). The reaction mixture was heated at 120 °C for 15 h then quenched with 2M HCl. The reaction mixture was diluted with water, extracted with DCM, passed through a hydrophobic frit, and concentrated to a residue that was purified by flash column chromatography (50% EtOAc/hexanes) to afford the title compound as a white solid (592 mg, 70 %).

Experimental - Characterisation Data for Isolated Products

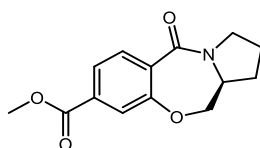
ν_{\max} (neat): 2982, 2870, 1614, 1589, 1429 cm^{-1}

^1H NMR (500 MHz, CDCl_3): δ 7.93 (d, 1H, ArH, $J = 8.5$ Hz), 7.23 (dd, 1H, ArH, $J = 8.5$, 2.0 Hz), 7.18 (d, 1H, ArH, $J = 2.0$ Hz), 4.42 (dd, 1H, CH, $J = 11.5$, 2.0 Hz), 4.08 (dd, 1H, CH, $J = 11.5$, 9.5 Hz), 3.97 – 3.92 (m, 1H, CH), 3.82 – 3.72 (m, 2H, 2 x CH), 2.26 – 2.20 (m, 1H, CH), 2.07 – 1.99 (m, 1H, CH), 1.97 – 1.90 (m, 1H, CH), 1.74 – 1.66 (m, 1H, CH)

^{13}C NMR (126 MHz, CDCl_3): δ 164.5, 156.3, 133.9, 126.5, 125.7, 123.9, 122.5, 75.8, 56.9, 48.1, 29.0, 23.1

HRMS ($\text{C}_{12}\text{H}_{13}^{79}\text{BrNO}_2$) $[\text{M}+\text{H}^+]$ requires 282.0124, found $[\text{M}+\text{H}^+]$ 282.0124

Compound 153. (*S*)-methyl 5-oxo-1,2,3,5,11,11a-hexahydrobenzo[*f*]pyrrolo[2,1-*c*][1,4]oxazepine-8-carboxylate



To a microwave vial containing (*S*)-8-bromo-2,3,11,11a-tetrahydrobenzo[*f*]pyrrolo[2,1-*c*][1,4]oxazepin-5(1*H*)-one (**152**, 100 mg, 0.35 mmol, 1 equiv) and MeCN/MeOH (1:1, 4 mL) was added $\text{Mo}(\text{CO})_6$ (92 mg, 0.35 mmol, 1 equiv), *trans*-bis(acetato)bis[*o*-(di-*o*-tolylphosphino) benzyl]dipalladium(II) (33 mg, 0.035 mmol, 0.1 equiv), tri-*tert*-butylphosphonium tetrafluoroborate (20 mg, 0.07 mmol, 0.2 equiv) and DBU (79 μL , 0.525 mmol, 1.5 equiv). The reaction mixture was heated at 150 $^\circ\text{C}$ for 30 min then concentrated under vacuum. The reaction was repeated with a further 3 batches then combined, dissolved in DCM, washed with 2M HCl, water, and brine, passed through a hydrophobic frit, and concentrated to a residue that was purified by flash column chromatography (40% EtOAc/hexanes) to afford the title compound as an off-white solid (57 mg, 62%).

ν_{\max} (neat): 2951, 2880, 1722, 1609 cm^{-1}

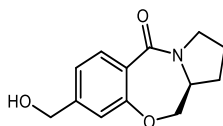
Experimental - Characterisation Data for Isolated Products

^1H NMR (500 MHz, CDCl_3): δ 8.07 (d, 1H, ArH, $J = 8.0$ Hz), 7.72 (dd, 1H, ArH, $J = 8.5$, 1.5 Hz), 7.66 (d, 1H, ArH, $J = 1.0$ Hz), 4.41 (dd, 1H, CH, $J = 11.5$, 2.5 Hz), 4.11 – 4.07 (m, 1H, CH), 3.96 – 3.94 (m, 1H, CH), 3.92 (s, 3H, CH_3), 3.78 – 3.75 (m, 2H, 2 x CH), 2.24 – 2.17 (m, 1H, CH), 2.06 – 2.00 (m, 1H, CH), 1.97 – 1.90 (m, 1H, CH), 1.73 – 1.66 (m, 1H, CH)

^{13}C NMR (126 MHz, CDCl_3): δ 166.2, 164.6, 155.4, 134.1, 132.4, 128.2, 123.1, 122.6, 76.2, 56.6, 52.5, 47.8, 28.7, 23.1

HRMS ($\text{C}_{14}\text{H}_{16}\text{NO}_4$) [$\text{M}+\text{H}^+$] requires 262.1074, found [$\text{M}+\text{H}^+$] 262.1074

Compound 154. (*S*)-8-(hydroxymethyl)-2,3,11,11a-tetrahydrobenzo[*f*]pyrrolo[2,1-*c*][1,4]oxazepin-5(1*H*)-one



To an oven-dried round-bottomed flask containing LiAlH_4 (20 mg, 0.54 mmol, 2 equiv) and THF (3 mL) at 0°C was added a solution of (*S*)-methyl 5-oxo-1,2,3,5,11,11a-hexahydrobenzo[*f*]pyrrolo[2,1-*c*][1,4]oxazepine-8-carboxylate (**153**, 70 mg, 0.27 mmol, 1 equiv) in THF (3 mL). The reaction mixture was stirred at room temperature for 5 h then quenched with 2M HCl. Saturated potassium sodium tartrate (2 mL) was added and the reaction mixture was extracted with DCM, passed through a hydrophobic frit, and concentrated under vacuum to afford the title compound as a colourless oil (34 mg, 54%).

ν_{max} (neat): 3370, 2968, 2922, 2876, 1622 cm^{-1}

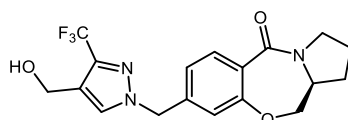
^1H NMR (500 MHz, CDCl_3): δ 8.02 (d, 1H, ArH, $J = 8.0$ Hz), 7.06 (dd, 1H, ArH, $J = 8.0$, 1.5 Hz), 7.00 (s, 1H, ArH), 4.70 (s, 2H, CH_2), 4.39 (dd, 1H, CH, $J = 11.0$, 2.5 Hz), 4.05 (dd, 1H, CH, $J = 11.5$, 9.5 Hz), 3.95 – 3.90 (m, 1H, CH), 3.78 – 3.74 (m, 2H, 2 x CH), 2.23 – 2.17 (m, 1H, CH), 2.05 – 1.97 (m, 1H, CH), 1.95 – 1.88 (m, 1H, CH), 1.72 – 1.65 (m, 1H, CH), 1H missing (exchangeable)

Experimental - Characterisation Data for Isolated Products

^{13}C NMR (126 MHz, CDCl_3): δ 165.4, 156.0, 146.4, 132.7, 123.0, 120.7, 118.8, 75.9, 64.6, 56.9, 47.9, 28.9, 23.2

HRMS ($\text{C}_{13}\text{H}_{16}\text{NO}_3$) [$\text{M}+\text{H}^+$] requires 234.1125, found [$\text{M}+\text{H}^+$] 234.1126

Compound 155. *(S)*-8-((4-(hydroxymethyl)-3-(trifluoromethyl)-1H-pyrazol-1-yl)methyl)-2,3,11,11a-tetrahydrobenzo[*f*]pyrrolo[2,1-*c*][1,4]oxazepin-5(1*H*)-one



To a round-bottomed flask containing *(S)*-8-(hydroxymethyl)-2,3,11,11a-tetrahydrobenzo[*f*]pyrrolo[2,1-*c*][1,4]oxazepin-5(1*H*)-one (**154**, 13 mg, 0.06 mmol, 1 equiv) and DCM (3 mL) was added thionyl chloride (22 μL , 0.3 mmol, 5 equiv). The reaction mixture was stirred at room temperature for 2 h then concentrated under vacuum and azeotroped with DCM. (3-(Trifluoromethyl)-1H-pyrazol-4-yl)methanol (12.5 mg, 0.06 mmol, 1 equiv), K_2CO_3 (41 mg, 0.3 mmol, 5 equiv) and DMF (3 mL) were added and the reaction mixture was heated at 60 $^\circ\text{C}$ for 16 h then concentrated under vacuum. The reaction mixture was dissolved in EtOAc, washed with water, dried over MgSO_4 , filtered and concentrated to a residue that was purified by reversed phase HPLC (0 – 80 % MeCN/water) to afford the title compound as an off-white solid (6 mg, 26%).

ν_{max} (neat): 3416, 3404, 2990, 1636, 1430 cm^{-1}

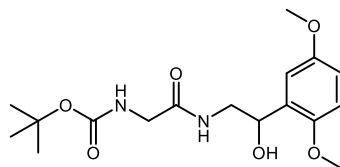
^1H NMR (400 MHz, DMSO): δ 7.07 (d, 1H, ArH, $J = 8.4$ Hz), 7.01 (s, 1H, ArH), 6.20 (dd, 1H, ArH, $J = 8.4, 1.8$ Hz), 6.08 (d, 1H, ArH, $J = 1.6$ Hz), 4.56 (s, 2H, CH_2), 3.76 (s, 2H, CH_2), 3.60 (dd, 1H, CH, $J = 11.6, 2.6$ Hz), 3.29 (dd, 1H, CH, $J = 11.6, 9.6$ Hz), 3.16 – 3.09 (m, 1H, CH), 2.87 (t, 2H, CH_2 , $J = 6.8$ Hz), 1.44 – 1.35 (m, 1H, CH), 1.26 – 1.15 (m, 1H, CH), 1.15 – 1.06 (m, 1H, CH), 0.95 – 0.87 (m, 1H, CH), 1H missing (exchangeable)

^{13}C NMR (126 MHz, CDCl_3): δ 164.8, 156.1, 141.0 (q, $^3J_{\text{CF}} = 6.3$ Hz), 140.2, 140.1 (q, $^2J_{\text{CF}} = 28.6$ Hz), 133.4, 131.1, 130.7, 122.5 (q, $^1J_{\text{CF}} = 273.2$ Hz), 121.6, 120.2, 75.8, 56.9, 56.1, 55.1, 48.0, 28.9, 23.1

Experimental - Characterisation Data for Isolated Products

HRMS (C₁₈H₁₉F₃N₃O₃) [M+H⁺] requires 382.1375, found [M+H⁺] 382.1375

Compound 157. *tert*-butyl (2-((2-(2,5-dimethoxyphenyl)-2-hydroxyethyl)amino)-2-oxoethyl)carbamate



Synthesised according to General Experimental Procedure J at 40 °C (Scheme 45, Page 91) using Boc-glycine methyl ester (249 μL, 1.42 mmol, 1 equiv) and 2-amino-1-(2,5-dimethoxyphenyl)ethanol (280 mg, 1.42 mmol, 1 equiv), and purified by flash column chromatography (4% methanol/DCM) to afford the title compound as a colourless oil (354 mg, 70%).

ν_{max} (neat): 3312, 2976, 2934, 1692, 1659, 1495 cm⁻¹

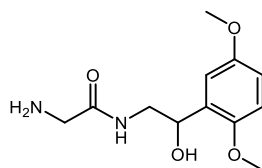
¹H NMR (500 MHz, CDCl₃): δ 7.00 (d, 1H, ArH, *J* = 2.5 Hz), 6.79 – 6.73 (m, 3H, 2 x ArH + NH), 5.46 (br. s, 1H, NH), 5.00 (dd, 1H, CH, *J* = 8.0, 3.0 Hz), 3.78 – 3.75 (m, 5H, CH₃ + 2 x CH₂), 3.74 (s, 3H, CH₃), 3.72 – 3.67 (m, 1H, CH), 3.40 – 3.35 (m, 1H, CH), 1.42 (s, 9H, 3 x CH₃), 1H missing (exchangeable)

¹³C NMR (126 MHz, CDCl₃): δ 170.9, 156.3, 154.0, 150.5, 130.8, 113.4, 113.1, 111.6, 80.4, 69.4, 56.0, 55.9, 45.7, 44.4, 28.4

HRMS (C₁₇H₂₇N₂O₆) [M+H⁺] requires 355.1869, found [M+H⁺] 355.1870

¹H NMR consistent with previously reported data¹⁵²

Compound 158. 2-amino-N-(2-(2,5-dimethoxyphenyl)-2-hydroxyethyl)acetamide



To a vial containing *tert*-butyl (2-((2-(2,5-dimethoxyphenyl)-2-hydroxyethyl)amino)-2-oxoethyl)carbamate (**157**, 91 mg, 0.26 mmol, 1 equiv) and methanol (1 mL) was added HCl/methanol (3 M, 250 μ L). The reaction mixture was stirred at room temperature for 2 h then concentrated to a residue that was purified by strong cation exchange chromatography to afford the title compound as a colourless oil (49 mg, 75%).

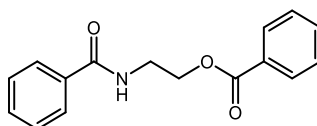
ν_{max} (neat): 3304, 2932, 2833, 1649, 1533, 1493 cm^{-1}

^1H NMR (500 MHz, MeOD): δ 7.12 (d, 1H, ArH, $J = 3.0$ Hz), 6.92 (d, 1H, ArH, $J = 8.5$ Hz), 6.85 (dd, 1H, ArH, $J = 9.0, 3.0$ Hz), 5.15 (dd, 1H, CH, $J = 7.5, 4.0$ Hz), 3.89 – 3.84 (m, 4H, $\text{CH}_3 + \text{CH}$), 3.81 (s, 3H, CH_3), 3.60 (dd, 1H, CH, $J = 13.5, 4.0$ Hz), 3.42 – 3.37 (m, 2H, 2 x CH), 4H missing (exchangeable)

^{13}C NMR (126 MHz, MeOD): δ 175.6, 155.4, 151.9, 132.9, 114.0, 113.9, 112.7, 68.4, 56.5, 56.2, 46.6, 45.1

HRMS ($\text{C}_{12}\text{H}_{19}\text{N}_2\text{O}_4$) [$\text{M}+\text{H}^+$] requires 255.1339, found [$\text{M}+\text{H}^+$] 255.1338

Compound 173. 2-benzamidoethyl benzoate



By-product formed during synthesis of *N*-(2-hydroxyethyl)benzamide according to General Experimental Procedure N (Table 25, Reaction 12, Page 111) using methyl benzoate (178 μ L, 1.42 mmol, 1 equiv), ethanolamine (86 μ L, 1.42 mmol, 1 equiv) and K_3PO_4 (60 mg, 0.28 mmol, 0.2 equiv) at 80 $^\circ\text{C}$, and purified by flash column chromatography (5% methanol/DCM) to afford the title compound as a white solid (23 mg, 6%).

Experimental - Characterisation Data for Isolated Products

ν_{\max} (neat): 3387, 1697, 1643, 1518, 1483 cm^{-1}

^1H NMR (500 MHz, CDCl_3): δ 8.05 (dd, 2H, 2 x ArH, $J = 8.3, 1.3$ Hz), 7.79 – 7.78 (m, 2H, 2 x ArH), 7.56 (tt, 1H, ArH, $J = 7.5, 1.5$ Hz), 8.05 (tt, 1H, ArH, $J = 7.5, 1.5$ Hz), 7.45 – 7.39 (m, 4H, 4 x ArH), 6.89 (br. s, 1H, NH), 4.54 (t, 2H, CH_2 , $J = 5.3$ Hz), 3.85 (q, 2H, CH_2 , $J = 5.5$ Hz)

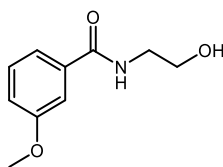
^{13}C NMR (126 MHz, CDCl_3): δ 167.9, 167.1, 134.4, 133.4, 131.7, 129.8, 128.7, 128.6, 127.1, 63.9, 39.9, 1C missing (overlapping peaks)

HRMS ($\text{C}_{16}\text{H}_{16}\text{NO}_3$) [$\text{M}+\text{H}^+$] requires 270.1125, found [$\text{M}+\text{H}^+$] 270.1124

m.p. 97 – 99 $^\circ\text{C}$

Consistent with previously reported data¹⁵³

Compound 174. *N*-(2-hydroxyethyl)-3-methoxybenzamide



Synthesised according to General Experimental Procedure O (Table 26, Entry 3, Page 112) using methyl 3-methoxybenzoate (206 μL , 1.42 mmol, 1 equiv) and ethanolamine (86 μL , 1.42 mmol, 1 equiv), and purified by flash column chromatography (5% methanol/DCM) to afford the title compound as a pale yellow oil (202 mg, 73%).

ν_{\max} (neat): 3314, 2943, 2882, 2835, 1632, 1580, 1537 cm^{-1}

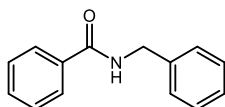
^1H NMR (500 MHz, CDCl_3): δ 7.37 (t, 1H, ArH, $J = 1.8$ Hz), 7.33 – 7.29 (m, 2H, 2 x ArH), 7.21 (br. s, 1H, NH), 7.03 (dq, 1H, ArH, $J = 8.0, 1.3$ Hz), 3.91 (br. s, 1H, OH), 3.81 – 3.79 (m, 5H, $\text{CH}_3 + \text{CH}_2$), 3.59 (q, 2H, CH_2 , $J = 5.2$ Hz)

Experimental - Characterisation Data for Isolated Products

^{13}C NMR (126 MHz, CDCl_3): δ 168.7, 159.9, 135.7, 129.7, 119.1, 117.8, 112.6, 61.9, 55.5, 43.0

HRMS ($\text{C}_{10}\text{H}_{14}\text{NO}_3$) [$\text{M}+\text{H}^+$] requires 196.0968, found [$\text{M}+\text{H}^+$] 196.0966

Compound 56. *N*-benzylbenzamide



Synthesised according to General Experimental Procedure S (Table 33, Reaction 35, Page 127) using methyl benzoate (178 μL , 1.42 mmol, 1 equiv) and benzylamine (155 μL , 1.42 mmol, 1 equiv), and purified by flash column chromatography (1% methanol/DCM) to afford the title compound as a white solid (258 mg, 86%).

To an oven-dried sealed Schlenk tube containing 2,2,2-trifluoroethylbenzoate (**200**, 290 mg, 1.42 mmol, 1 equiv) and THF (700 μL) was added benzylamine (155 μL , 1.42 mmol, 1 equiv). The reaction mixture was stirred at 90 $^\circ\text{C}$ for 22 h then diluted with EtOAc (10 mL), washed with water (3 x 10 mL), passed through a hydrophobic frit, and concentrated to a residue that was purified by flash column chromatography (1% methanol/DCM) to afford the title compound as a white solid (233 mg, 77%)

ν_{max} (neat): 3356, 3092, 3036, 2932, 1636, 1560, 1261 cm^{-1}

^1H NMR (400 MHz, DMSO): δ 9.06 (t, 1H, NH, $J = 5.9$ Hz), 7.91 – 7.88 (m, 2H, 2 x ArH), 7.54 (dt, 1H, ArH, $J = 7.2, 1.9$ Hz), 7.50 – 7.45 (m, 2H, 2 x ArH), 7.36 – 7.30 (m, 4H, 4 x ArH), 7.27 – 7.22 (m, 1H, ArH), 4.48 (d, 2H, CH_2 , $J = 6.0$ Hz)

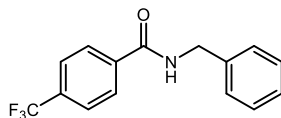
^{13}C NMR (101 MHz, DMSO): δ 166.2, 139.7, 134.3, 131.2, 128.3, 128.2, 127.2, 127.1, 126.7, 42.6

HRMS ($\text{C}_{14}\text{H}_{14}\text{NO}$) [$\text{M}+\text{H}$] requires 212.1070, found [$\text{M}+\text{H}$] 212.1069

m.p. 108 – 110 $^\circ\text{C}$

Consistent with previously reported data⁴⁸

Compound 177. *N*-benzyl-4-(trifluoromethyl)benzamide



Synthesised according to General Experimental Procedure S (Table 34, Entry 2, Page 128) using methyl 4-(trifluoromethyl)benzoate (229 μL , 1.42 mmol, 1 equiv) and benzylamine (155 μL , 1.42 mmol, 1 equiv), and purified by flash column chromatography (1% methanol/DCM) to afford the title compound as a white solid (377 mg, 95%).

ν_{max} (neat): 3356, 3092, 3036, 2932, 1641, 1549, 1310, 1155 cm^{-1}

^1H NMR (400 MHz, DMSO): δ 9.29 (t, 1H, NH, $J = 6.0$ Hz), 8.09, (d, 2H, ArH, $J = 8.0$ Hz), 7.87 (d, 2H, ArH, $J = 8.0$ Hz), 7.35 – 7.32 (m, 4H, 4 x ArH), 7.28 – 7.23 (m, 1H, ArH), 4.50 (d, 2H, CH₂, $J = 6.0$ Hz)

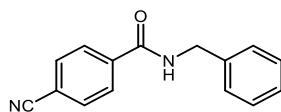
^{13}C NMR (101 MHz, DMSO): δ 165.0, 139.2, 138.0, 131.1 (q, $^2J_{\text{CF}} = 32.1$ Hz), 128.2, 128.1, 127.2, 126.7, 125.3 (q, $^3J_{\text{CF}} = 3.6$ Hz), 124.0 (q, $^1J_{\text{CF}} = 273.3$ Hz), 42.7

HRMS (C₁₅H₁₃F₃NO) [M+H] requires 280.0944, found [M+H] 280.0943

m.p. 165 – 167 °C

Consistent with previously reported data³⁸

Compound 178. *N*-benzyl-4-cyanobenzamide



Synthesised according to General Experimental Procedure S (Table 34, Entry 3, Page 128) using methyl 4-cyanobenzoate (229 mg, 1.42 mmol, 1 equiv) and benzylamine (155 μ L, 1.42 mmol, 1 equiv), and purified by flash column chromatography (100% DCM) to afford the title compound as a white solid (201 mg, 60%).

ν_{max} (neat): 3310, 3092, 3036, 2932, 2837, 2210, 1643, 1560 cm^{-1}

^1H NMR (400 MHz, DMSO): δ 9.28 (t, 1H, NH, $J = 5.8$ Hz), 8.05 – 8.03 (m, 2H, 2 x ArH), 7.98 – 7.96 (m, 2H, 2 x ArH), 7.34 – 7.31 (m, 4H, 4 x ArH), 7.28 – 7.23 (m, 1H, ArH), 4.50 (d, 2H, CH_2 , $J = 6.0$ Hz)

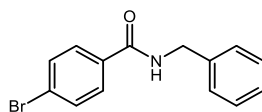
^{13}C NMR (101 MHz, DMSO): δ 164.8, 139.1, 138.3, 132.4, 128.3, 128.1, 127.2, 126.8, 118.3, 113.6, 42.8

HRMS ($\text{C}_{15}\text{H}_{13}\text{N}_2\text{O}$) $[\text{M}+\text{H}]$ requires 237.1022, found $[\text{M}+\text{H}]$ 237.1023

m.p. 119 – 122 $^{\circ}\text{C}$

Consistent with previously reported data¹⁵⁴

Compound 179. N-benzyl-4-bromobenzamide



Synthesised according to General Experimental Procedure S (Table 34, Entry 4, Page 128) using methyl 4-bromobenzoate (305 mg, 1.42 mmol, 1 equiv) and benzylamine (155 μ L, 1.42 mmol, 1 equiv), and purified by flash column chromatography (1% methanol/DCM) to afford the title compound as a white solid (358 mg, 87%).

ν_{max} (neat): 3298, 3092, 3063, 2932, 2837, 1641, 1560 cm^{-1}

^1H NMR (400 MHz, DMSO): δ 9.10 (t, 1H, NH, $J = 5.8$ Hz), 7.84 (dt, 2H, 2 x ArH, $J = 8.8, 2.2$ Hz), 7.69 (dt, 2H, 2 x ArH, $J = 8.8, 2.2$ Hz), 7.35 – 7.30 (m, 4H, 4 x ArH), 7.28 – 7.22 (m, 1H, ArH), 4.47 (d, 2H, CH_2 , $J = 6.0$ Hz)

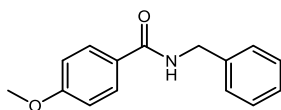
^{13}C NMR (126 MHz, DMSO): δ 165.2, 139.4, 133.4, 131.3, 129.4, 128.3, 127.2, 126.8, 124.9, 42.6

HRMS ($\text{C}_{14}\text{H}_{13}^{79}\text{BrNO}$) [M+H] requires 290.0175, found [M+H] 290.0177

m.p. 169 – 170 $^{\circ}\text{C}$

Consistent with previously reported data¹⁵⁴

Compound 180. *N*-benzyl-4-methoxybenzamide



Synthesised according to General Experimental Procedure S (Table 34, Entry 5, Page 128) using methyl 4-methoxybenzoate (236 mg, 1.42 mmol, 1 equiv) and benzylamine (155 μ L, 1.42 mmol, 1 equiv), and purified by flash column chromatography (2% methanol/DCM) to afford the title compound as a white solid (140 mg, 41%).

ν_{max} (neat): 3254, 3092, 3036, 2932, 2837, 1630, 1028 cm^{-1}

^1H NMR (500 MHz, DMSO): δ 8.88 (t, 1H, NH, $J = 6.1$ Hz), 7.88 (dt, 2H, 2 x ArH, $J = 9.0, 2.4$ Hz), 7.34 – 7.30 (m, 4H, 4 x ArH), 7.25 – 7.21 (m, 1H, ArH), 7.00 (dt, 2H, 2 x ArH, $J = 8.5, 2.5$ Hz), 4.47 (d, 2H, CH₂, $J = 6.0$ Hz), 3.81 (s, 3H, CH₃)

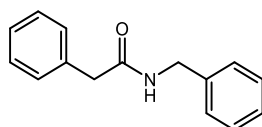
^{13}C NMR (126 MHz, DMSO): δ 165.6, 161.6, 139.9, 129.0, 128.2, 127.1, 126.6, 126.5, 113.5, 55.3, 42.5

HRMS (C₁₅H₁₆NO₂) [M+H] 242.1176, found [M+H] 242.1173

m.p. 70 – 72 $^{\circ}\text{C}$

Consistent with previously reported data³⁸

Compound 181. *N*-benzyl-2-phenylacetamide



Synthesised according to General Experimental Procedure S (Table 34, Entry 6, Page 128) using methyl 2-phenylacetate (200 μ L, 1.42 mmol, 1 equiv) and benzylamine (155 μ L, 1.42 mmol, 1 equiv), and purified by flash column chromatography (40% ethyl acetate/pet. ether 40–60 $^{\circ}$) to afford the title compound as a white solid (288 mg, 90%).

Experimental - Characterisation Data for Isolated Products

ν_{\max} (neat): 3283, 3092, 3036, 2932, 1636, 1547, 1431 cm^{-1}

^1H NMR (400 MHz, DMSO): δ 8.53 (t, 1H, NH, $J = 4.8$ Hz), 7.32 – 7.27 (m, 6H, 6 x ArH), 7.24 – 7.20 (m, 4H, 4 x ArH), 4.27 (d, 2H, CH_2 , $J = 6.0$ Hz), 3.48 (s, 2H, CH_2)

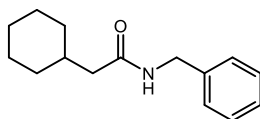
^{13}C NMR (101 MHz, DMSO): δ 170.0, 139.4, 136.4, 129.0, 128.2, 128.1, 127.2, 126.7, 126.3, 42.3, 42.1

HRMS ($\text{C}_{15}\text{H}_{16}\text{NO}$) $[\text{M}+\text{H}]$ requires 226.1226, found $[\text{M}+\text{H}]$ 226.1224

m.p. 126 – 129 $^{\circ}\text{C}$

Consistent with previously reported data⁴⁸

Compound 182. *N*-benzyl-2-cyclohexylacetamide



Synthesised according to General Experimental Procedure S (Table 34, Entry 7, Page 128) using methyl 2-cyclohexylacetate (233 μL , 1.42 mmol, 1 equiv) and benzylamine (155 μL , 1.42 mmol, 1 equiv), and purified by flash column chromatography (1% methanol/DCM) to afford the title compound as a white solid (263 mg, 80%).

ν_{\max} (neat): 3067, 3030, 2920, 2849, 1636, 1553 cm^{-1}

^1H NMR (400 MHz, DMSO): δ 8.26 (t, 1H, NH, $J = 5.4$ Hz), 7.33 – 7.29 (m, 2H, 2 x ArH), 7.24 – 7.20 (m, 3H, 3 x ArH), 4.25 (d, 2H, CH_2 , $J = 6.0$ Hz), 2.01 (d, 2H, CH_2 , $J = 7.0$ Hz), 1.71 – 1.58 (m, 6H, 6 x CH), 1.25 – 1.08 (m, 3H, 3 x CH), 0.95 – 0.86 (m, 2H, 2 x CH)

^{13}C NMR (101 MHz, CDCl_3): δ 173.7, 137.9, 129.0, 128.1, 128.0, 44.9, 44.2, 35.7, 33.3, 26.3, 26.2

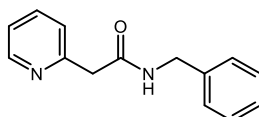
Experimental - Characterisation Data for Isolated Products

HRMS (C₁₅H₂₂NO) [M+H] requires 232.1696, found [M+H] 232.1695

m.p. 137 – 138 °C

Consistent with previously reported data¹⁵⁵

Compound 183. *N*-benzyl-2-(pyridin-2-yl)acetamide



Synthesised according to General Experimental Procedure S (Table 34, Entry 8, Page 128) using methyl 2-(pyridin-2-yl)acetate (219 μ L, 1.42 mmol, 1 equiv) and benzylamine (155 μ L, 1.42 mmol, 1 equiv), and purified by flash column chromatography (2% methanol/DCM) to afford the title compound as a white solid (276 mg, 86%).

ν_{max} (neat): 3265, 3061, 3028, 2924, 2874, 1633, 1539, 1454 cm^{-1}

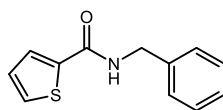
¹H NMR (400 MHz, DMSO): δ 8.58 (t, 1H, NH, $J = 5.2$ Hz), 8.48 (ddd, 1H, ArH, $J = 4.8, 1.8, 1.0$ Hz), 7.73 (td, 1H, ArH, $J = 7.6, 2.0$ Hz), 7.36 – 7.29 (m, 3H, 3 x ArH), 7.27 – 7.21 (m, 4H, 4 x ArH), 4.29 (d, 2H, CH₂, $J = 6.0$ Hz), 3.68 (s, 2H, CH₂)

¹³C NMR (101 MHz, DMSO): δ 169.1, 156.3, 148.8, 139.4, 136.4, 128.2, 127.2, 126.7, 123.7, 121.7, 44.9, 42.2

HRMS (C₁₄H₁₅N₂O) [M+H] requires 227.1179, found [M+H] 229.1175

m.p. 121 – 123 °C

Compound 184. *N*-benzylthiophene-2-carboxamide



Synthesised according to General Experimental Procedure S (Table 34, Entry 9, Page 128) using ethyl thiophene-2-carboxylate (191 μL , 1.42 mmol, 1 equiv) and benzylamine (155 μL , 1.42 mmol, 1 equiv), and purified by flash column chromatography (100% DCM) to afford the title compound as a white solid (234 mg, 76%).

ν_{max} (neat): 3356, 3092, 3036, 2932, 2838, 1620, 1541, 1301 cm^{-1}

^1H NMR (500 MHz, DMSO): δ 9.03 (t, 1H, NH, $J = 5.5$ Hz), 7.81 (dd, 1H, ArH, $J = 3.5, 1.0$ Hz), 7.75 (dd, 1H, ArH, $J = 5.0, 1.0$ Hz), 7.35 – 7.30 (m, 4H, 4 x ArH), 7.26 – 7.23 (m, 1H, ArH), 7.16 – 7.14 (m, 1H, ArH), 4.45 (d, 2H, CH_2 , $J = 6.0$ Hz)

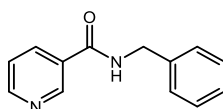
^{13}C NMR (126 MHz, DMSO): δ 161.1, 139.9, 139.5, 130.8, 128.3, 128.1, 127.9, 127.2, 126.8, 42.4

HRMS ($\text{C}_{12}\text{H}_{12}\text{NOS}$) $[\text{M}+\text{H}]$ requires 218.0634, found $[\text{M}+\text{H}]$ 218.0634

m.p. 125 – 127 $^{\circ}\text{C}$

Consistent with previously reported data¹⁵⁶

Compound 185. *N*-benzylnicotinamide



Synthesised according to General Experimental Procedure S (Table 34, Entry 10, Page 128) using methyl nicotinate (195 mg, 1.42 mmol, 1 equiv) and benzylamine (155 μL , 1.42 mmol, 1 equiv), and purified by flash column chromatography (2% methanol/DCM) to afford the title compound as a white solid (202 mg, 67%).

Experimental - Characterisation Data for Isolated Products

ν_{\max} (neat): 3281, 3092, 2932, 2837, 1632, 1541 cm^{-1}

^1H NMR (400 MHz, DMSO): δ 9.23 (t, 1H, NH, $J = 5.6$ Hz), 9.06 (dd, 1H, ArH, $J = 2.4, 0.8$ Hz), 8.71 (dd, 1H, ArH, $J = 4.8, 1.6$ Hz), 8.25 – 8.22 (m, 1H, ArH), 7.51 (ddd, 1H, ArH, $J = 8.0, 4.8, 0.8$ Hz), 7.36 – 7.31 (m, 4H, 4 x ArH), 7.28 – 7.23 (m, 1H, ArH), 4.51 (d, 2H, CH_2 , $J = 6.0$ Hz)

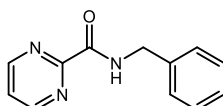
^{13}C NMR (101 MHz, DMSO): δ 164.8, 151.9, 148.4, 139.3, 135.0, 129.8, 128.3, 127.3, 126.9, 123.5, 42.6

HRMS ($\text{C}_{13}\text{H}_{13}\text{N}_2\text{O}$) $[\text{M}+\text{H}]$ requires 213.1022, found $[\text{M}+\text{H}]$ 213.1019

m.p. 79 – 80 $^{\circ}\text{C}$

Consistent with previously reported data¹⁵⁷

Compound 186. *N*-benzylpyrimidine-2-carboxamide



Synthesised according to General Experimental Procedure S (Table 34, Entry 11, Page 128) using methyl pyrimidine-2-carboxylate (196 mg, 1.42 mmol, 1 equiv) and benzylamine (155 μL , 1.42 mmol, 1 equiv), and purified by flash column chromatography (100% DCM) to afford the title compound as a yellow solid (200 mg, 66%).

ν_{\max} (neat): 3356, 3092, 3063, 2932, 2837, 1680, 1537, 1408 cm^{-1}

^1H NMR (400 MHz, DMSO): δ 9.41 (t, 1H, NH, $J = 5.2$ Hz), 8.97 (d, 2H, 2 x ArH, $J = 4.8$ Hz), 7.68 (t, 1H, ArH, $J = 4.8$ Hz), 7.36 – 7.30 (m, 4H, 4 x ArH), 7.26 – 7.22 (m, 1H, ArH), 4.50 (d, 2H, CH_2 , $J = 6.4$ Hz)

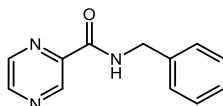
^{13}C NMR (101 MHz, DMSO): δ 162.6, 158.2, 157.7, 139.3, 128.3, 127.3, 126.8, 123.0, 42.6

Experimental - Characterisation Data for Isolated Products

HRMS (C₁₂H₁₂N₃O) [M+H] requires 214.0975, found [M+H] 214.0975

m.p. 108 – 110 °C

Compound 187. *N*-benzylpyrazine-2-carboxamide



Synthesised according to General Experimental Procedure S (Table 34, Entry 12, Page 128) using methyl pyrazine-2-carboxylate (196 mg, 1.42 mmol, 1 equiv) and benzylamine (155 μ L, 1.42 mmol, 1 equiv), and purified by flash column chromatography (1% methanol/DCM) to afford the title compound as a white solid (194 mg, 64%).

ν_{max} (neat): 3356, 3092, 3036, 2926, 1668, 1514 cm^{-1}

¹H NMR (500 MHz, DMSO): δ 9.47 (t, 1H, NH, $J = 6.0$ Hz), 9.20 (d, 1H, ArH, $J = 1.5$ Hz), 8.88 (d, 1H, ArH, $J = 2.5$ Hz), 8.74 (dd, 1H, ArH, $J = 2.5, 1.5$ Hz), 7.35 – 7.30 (m, 4H, 4 x ArH), 7.25 – 7.22 (m, 1H, ArH), 4.51 (d, 2H, CH₂, $J = 6.5$ Hz)

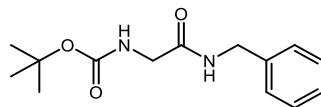
¹³C NMR (126 MHz, DMSO): δ 163.0, 147.5, 144.8, 143.6, 143.4, 139.2, 128.2, 127.3, 126.8, 42.3

HRMS (C₁₂H₁₂N₃O) [M+H] requires 214.0975, found [M+H] 214.0974

m.p. 119 – 120 °C

Consistent with previously reported data¹⁵⁸

Compound 188. *tert*-butyl (2-(benzylamino)-2-oxoethyl)carbamate



Synthesised according to General Experimental Procedure S (Table 34, Entry 13, Page 128) using Boc-glycine methyl ester (249 μ L, 1.42 mmol, 1 equiv) and benzylamine (155 μ L, 1.42 mmol, 1 equiv), and purified by flash column chromatography (2% methanol/DCM) to afford the title compound as a white solid (285 mg, 76%).

ν_{\max} (neat): 3314, 3092, 2932, 2926, 1703, 1655 cm^{-1}

^1H NMR (400 MHz, CDCl_3): δ 7.34 – 7.30 (m, 2H, 2 x ArH), 7.28 – 7.25 (m, 3H, 3 x ArH), 6.95 (br. s, 1H, NH), 5.53 (t, 1H, NH, $J = 5.4$ Hz), 4.43 (d, 2H, CH_2 , $J = 5.6$ Hz), 3.81 (d, 2H, CH_2 , $J = 5.2$ Hz), 1.43 (s, 9H, 3 x CH_3)

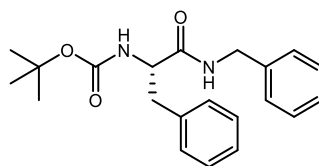
^{13}C NMR (101 MHz, CDCl_3): δ 169.6, 156.3, 138.1, 128.9, 127.9, 127.7, 44.7, 43.6, 28.5, 1C missing (overlapping peaks)

HRMS ($\text{C}_{14}\text{H}_{21}\text{N}_2\text{O}_3$) $[\text{M}+\text{H}]$ requires 265.1547, found $[\text{M}+\text{H}]$ 265.1551

m.p. 65 – 67 $^\circ\text{C}$

Consistent with previously reported data⁴⁰

Compound 189. (S)-tert-butyl (1-(benzylamino)-1-oxo-3-phenylpropan-2-yl)carbamate



Synthesised according to General Experimental Procedure S (Table 34, Entry 14, Page 128) using Boc-L-phenylalanine methyl ester (397 mg, 1.42 mmol, 1 equiv), benzylamine (155 μL , 1.42 mmol, 1 equiv), and trifluoroethanol (20 μL , 0.28 mmol, 0.2 equiv), and purified by flash column chromatography (1% methanol/DCM) to afford the title compound as a white solid (211 mg, 42%).

ν_{max} (neat): 3067, 3030, 2926, 1714, 1661, 1528, 1161 cm^{-1}

^1H NMR (400 MHz, DMSO): δ 8.38 (t, 1H, NH, $J = 5.8$ Hz), 7.30 – 7.18 (m, 9H, 9 x ArH), 6.94 (d, 1H, ArH, $J = 8.4$ Hz), 4.28 (d, 2H, CH_2 , $J = 6.0$ Hz), 4.23 – 4.17 (m, 1H, CH), 3.17 (d, 1H, CH, $J = 5.2$ Hz), 2.96 (dd, 1H, CH, $J = 13.6, 5.2$ Hz), 2.78 (dd, 1H, CH, $J = 13.6, 10.0$ Hz), 1.31 (s, 9H, 3 x CH_3)

^{13}C NMR (126 MHz, DMSO): δ 171.6, 155.2, 139.3, 138.1, 129.2, 128.1, 128.0, 127.0, 126.6, 126.1, 78.0, 55.9, 42.0, 37.5, 28.1

HRMS ($\text{C}_{21}\text{H}_{27}\text{N}_2\text{O}_3$) [M+H] requires 355.2016, found [M+H] 355.2017

m.p. 143 – 145 $^\circ\text{C}$

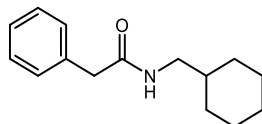
ee = 8% as determined by chiral HPLC

Synthesised according to General Experimental Procedure T (Table 35, Entry 3, Page 132) using Boc-L-phenylalanine methyl ester (397 mg, 1.42 mmol, 1 equiv), benzylamine (155 μL , 1.42 mmol, 1 equiv), and 4-(trifluoromethyl)phenol (45 mg, 0.28 mmol, 0.2 equiv), and purified by flash column chromatography (1% methanol/DCM) to afford the title compound as a white solid (191 mg, 38%).

Experimental - Characterisation Data for Isolated Products

ee = 65% as determined by chiral HPLC

Compound 190. *N*-(cyclohexylmethyl)-2-phenylacetamide



Synthesised according to General Experimental Procedure S (Table 34, Entry 15, Page 128) using methyl 2-phenylacetate (200 μ L, 1.42 mmol, 1 equiv) and cyclohexylmethanamine (185 μ L, 1.42 mmol, 1 equiv), and purified by flash column chromatography (100% DCM) to afford the title compound as a white solid (210 mg, 64%).

ν_{max} (neat): 3356, 3084, 3063, 2932, 2926, 1641, 1560 cm^{-1}

^1H NMR (400 MHz, DMSO): δ 7.95 (t, 1H, NH, $J = 4.8$ Hz), 7.31 – 7.18 (m, 5H, 5 x ArH), 3.39 (s, 2H, CH_2), 2.89 (t, 2H, CH_2 , $J = 6.4$ Hz), 1.65 – 1.59 (m, 5H, 5 x CH), 1.41 – 1.32 (m, 1H, CH), 1.21 – 1.07 (m, 3H, 3 x CH), 0.88 – 0.79 (m, 2H, 2 x CH)

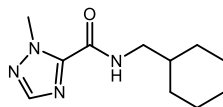
^{13}C NMR (101 MHz, DMSO): δ 169.9, 136.6, 128.9, 128.1, 126.2, 44.9, 42.4, 37.4, 30.3, 26.0, 25.3

HRMS ($\text{C}_{15}\text{H}_{22}\text{NO}$) $[\text{M}+\text{H}]$ requires 232.1696, found $[\text{M}+\text{H}]$ 232.1695

m.p. 115 – 117 $^{\circ}\text{C}$

Consistent with previously reported data¹⁵⁹

Compound 191. *N*-(cyclohexylmethyl)-1-methyl-1*H*-1,2,4-triazole-5-carboxamide



Synthesised according to General Experimental Procedure S (Table 34, Entry 16, Page 128) using methyl 1-methyl-1*H*-1,2,4-triazole-5-carboxylate (200 mg, 1.42 mmol, 1 equiv) and cyclohexylmethanamine (185 μ L, 1.42 mmol, 1 equiv), and purified by flash column chromatography (1% methanol/DCM) to afford the title compound as a colourless oil (253 mg, 80%).

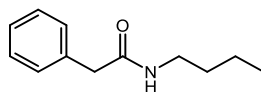
ν_{\max} (neat): 3356, 2932, 2851, 1674, 1543, 1481 cm^{-1}

^1H NMR (500 MHz, DMSO): δ 8.78 (t, 1H, NH, $J = 5.8$ Hz), 8.03 (s, 1H, ArH), 4.12 (s, 3H, CH_3), 3.08 (t, 2H, CH_2 , $J = 6.5$ Hz), 1.67 – 1.65 (m, 4H, 4 x CH), 1.61 – 1.52 (m, 2H, 2 x CH), 1.20 – 1.11 (m, 3H, 3 x CH), 0.93 – 0.87 (m, 2H, 2 x CH)

^{13}C NMR (126 MHz, DMSO): δ 157.0, 149.4, 146.4, 44.7, 37.6, 37.2, 30.3, 26.0, 25.3

HRMS ($\text{C}_{11}\text{H}_{19}\text{N}_4\text{O}$) [$\text{M}+\text{H}$] requires 223.1553, found [$\text{M}+\text{H}$] 223.1555

Compound 192. *N*-butyl-2-phenylacetamide



Synthesised according to General Experimental Procedure S (Table 34, Entry 17, Page 128) using methyl 2-phenylacetate (200 μ L, 1.42 mmol, 1 equiv) and *n*-butylamine (140 μ L, 1.42 mmol, 1 equiv), and purified by flash column chromatography (1% methanol/DCM) to afford the title compound as a white solid (102 mg, 38%).

ν_{\max} (neat): 3071, 2959, 2940, 1626, 1577, 1454 cm^{-1}

Experimental - Characterisation Data for Isolated Products

^1H NMR (400 MHz, DMSO): δ 7.96 (t, 1H, NH, $J = 6.0$ Hz), 7.31 – 7.20 (m, 5H, 5 x ArH), 3.38 (s, 2H, CH₂), 3.03 (q, 2H, CH₂, $J = 6.4$ Hz), 1.41 – 1.34 (m, 2H, CH₂), 1.30 – 1.21 (m, 2H, CH₂), 0.85 (t, 3H, CH₃, $J = 7.2$ Hz)

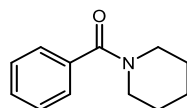
^{13}C NMR (101 MHz, CDCl₃): δ 171.1, 135.3, 129.7, 129.3, 127.6, 44.2, 39.6, 31.8, 20.2, 13.9

HRMS (C₁₂H₁₈NO) [M+H] requires 192.1383, found [M+H] 192.1381

m.p. 86 – 87 °C

Consistent with previously reported data³⁷

Compound 193. phenyl(piperidin-1-yl)methanone



Synthesised according to General Experimental Procedure S (Table 34, Entry 18, Page 128) using methyl benzoate (178 μL , 1.42 mmol, 1 equiv) and piperidine (140 μL , 1.42 mmol, 1 equiv), and purified by flash column chromatography (1% methanol/DCM) to afford the title compound as a yellow oil (207 mg, 77%).

ν_{max} (neat): 2936, 2926, 2837, 1626, 1427 cm^{-1}

^1H NMR (400 MHz, DMSO): δ 7.44 – 7.42 (m, 3H, 3 x ArH), 7.37 – 7.34 (m, 2H, 2 x ArH), 3.57 (br. s, 2H, 2 x CH), 3.26 (br. s, 2H, 2 x CH), 1.61 – 1.60 (m, 2H, 2 x CH), 1.48 (br. s, 4H, 4 x CH)

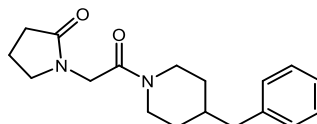
^{13}C NMR (101 MHz, CDCl₃): δ 170.4, 136.6, 129.5, 128.5, 126.9, 48.9, 43.2, 26.6, 25.7, 24.7

HRMS (C₁₂H₁₆NO) [M+H] requires 190.1226, found [M+H] 190.1225

Experimental - Characterisation Data for Isolated Products

Consistent with previously reported data¹⁶⁰

Compound 194. 1-(2-(4-benzylpiperidin-1-yl)-2-oxoethyl)pyrrolidin-2-one



Synthesised according to General Experimental Procedure S (Table 34, Entry 19, Page 128) using methyl 2-(2-oxopyrrolidin-1-yl)acetate (197 μL , 1.42 mmol, 1 equiv) and 4-benzylpiperidine (250 μL , 1.42 mmol, 1 equiv), and purified by flash column chromatography (1% methanol/DCM) to afford the title compound as a colourless oil (269 mg, 63%).

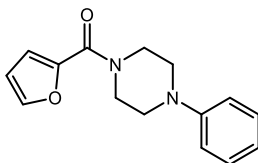
ν_{max} (neat): 3306, 3036, 2932, 2918, 1682, 1645, 1452, 1287 cm^{-1}

^1H NMR (500 MHz, DMSO): δ 7.30 – 7.27 (m, 2H, 2 x ArH), 7.20 – 7.16 (m, 3H, 3 x ArH), 4.28 (d, 1H, CH, $J = 13.0$ Hz), 4.10 – 4.05 (m, 1H, CH), 3.99 – 3.95 (m, 1H, CH), 3.77 (d, 1H, CH, $J = 13.5$ Hz), 3.46 – 3.32 (m, 2H, 2 x CH), 3.17 (d, 1H, CH, $J = 5.5$ Hz), 2.94 – 2.89 (m, 1H, CH), 2.52 (s, 2H, 2 x CH), 2.22 (t, 2H, CH_2 , $J = 8.0$ Hz), 1.96 – 1.90 (m, 2H, 2 x CH), 1.79 – 1.70 (m, 1H, CH), 1.58 (d, 2H, CH_2 , $J = 13.0$), 1.10 (qd, 1H, CH, $J = 12.4$, 3.9 Hz), 0.99 (qd, 1H, CH, $J = 12.3$, 4.1 Hz)

^{13}C NMR (101 MHz, CDCl_3): δ 175.7, 165.7, 139.9, 129.2, 128.5, 126.2, 48.1, 45.3, 44.4, 43.0, 42.5, 38.2, 32.5, 31.7, 30.6, 18.1

HRMS ($\text{C}_{18}\text{H}_{25}\text{N}_2\text{O}_2$) $[\text{M}+\text{H}]$ requires 301.1911, found $[\text{M}+\text{H}]$ 301.1909

Compound 195. furan-2-yl(4-phenylpiperazin-1-yl)methanone



Synthesised according to General Experimental Procedure S (Table 34, Entry 20, Page 128) using methyl furan-2-carboxylate (152 μL , 1.42 mmol, 1 equiv) and 1 phenylpiperazine (217 μL , 1.42 mmol, 1 equiv), and purified by flash column chromatography (2% methanol/DCM) to afford the title compound as an orange oil (233 mg, 64%).

ν_{max} (neat): 3092, 3036, 2932, 2837, 1620, 1485, 1229 cm^{-1}

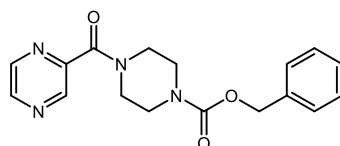
^1H NMR (500 MHz, DMSO): δ 7.86 (d, 1H, ArH, $J = 1.5$ Hz), 7.25 – 7.22 (m, 2H, 2 x ArH), 7.03 (d, 1H, ArH, $J = 3.5$ Hz), 6.97 – 6.96 (m, 2H, 2 x ArH), 6.81 (t, 1H, ArH, $J = 7.3$ Hz), 6.64 (dd, 1H, ArH, $J = 3.5, 2.0$ Hz), 3.81 (br. s, 4H, 4 x CH), 3.20 (t, 4H, 4 x CH, $J = 5.3$ Hz)

^{13}C NMR (126 MHz, DMSO): δ 158.3, 150.7, 147.0, 144.8, 129.0, 119.3, 115.8, 115.7, 111.3, 48.5, 40.1

HRMS ($\text{C}_{15}\text{H}_{17}\text{N}_2\text{O}_2$) [M+H] requires 256.1285, found [M+H] 256.1286

Consistent with previously reported data¹⁶¹

Compound 196. benzyl 4-(pyrazine-2-carbonyl)piperazine-1-carboxylate



Synthesised according to General Experimental Procedure S (Table 34, Entry 21, Page 128) using methyl pyrazine-2-carboxylate (196 mg, 1.42 mmol, 1 equiv) and benzyl piperazine-1-carboxylate (274 μ L, 1.42 mmol, 1 equiv), and purified by flash column chromatography (100% DCM) to afford the title compound as an off-white solid (167 mg, 36%).

ν_{\max} (neat): 3084, 3044, 3026, 2912, 2862, 1697, 1632, 1433, 1423, 1225 cm^{-1}

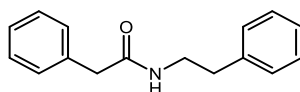
^1H NMR (400 MHz, CDCl_3): δ 8.99 (d, 1H, ArH, $J = 1.2$ Hz), 8.66 (d, 1H, ArH, $J = 2.4$ Hz), 8.54 (s, 1H, ArH), 7.40 – 7.31 (m, 5H, 5 x ArH), 5.17 (s, 2H, CH_2), 3.82 (s, 2H, CH_2), 3.67 – 3.65 (m, 4H, 2 x CH_2), 3.60 – 3.58 (m, 2H, CH_2)

^{13}C NMR (101 MHz, CDCl_3): δ 165.5, 155.4, 149.1, 146.2, 145.8, 142.6, 136.5, 128.8, 128.5, 128.3, 67.8, 47.2, 44.4, 43.8, 42.6

HRMS ($\text{C}_{17}\text{H}_{19}\text{N}_4\text{O}_3$) $[\text{M}+\text{H}]$ requires 327.1452, found $[\text{M}+\text{H}]$ 327.1453

m.p. 108 – 110 $^{\circ}\text{C}$

Compound 197. *N*-phenethyl-2-phenylacetamide



Synthesised according to General Experimental Procedure S (Table 34, Entry 22, Page 128) using methyl 2-phenylacetate (200 μ L, 1.42 mmol, 1 equiv) and 2-phenylethan-1-amine (179 μ L, 1.42 mmol, 1 equiv), and purified by flash column chromatography (2% methanol/DCM) to afford the title compound as a white solid (228 mg, 67%).

ν_{\max} (neat): 3298, 3084, 3063, 2932, 2837, 1668, 1537 cm^{-1}

Experimental - Characterisation Data for Isolated Products

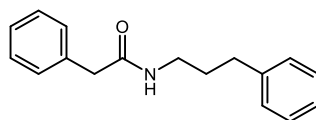
^1H NMR (400 MHz, DMSO): δ 8.10 (t, 1H, NH, $J = 5.0$ Hz), 7.30 – 7.25 (m, 4H, 4 x ArH), 7.22 – 7.15 (m, 6H, 6 x ArH), 3.37 (s, 2H, CH₂), 3.27 (q, 2H, CH₂, $J = 7.2$ Hz), 2.70 (t, 2H, CH₂, $J = 7.3$ Hz)

^{13}C NMR (101 MHz, DMSO): δ 169.9, 139.4, 136.4, 128.9, 128.6, 128.2, 128.1, 126.2, 126.0, 42.4, 40.2, 35.0

HRMS (C₁₆H₁₈NO) [M+H] requires 240.1383, found [M+H] 240.1382

m.p. 96 – 98 °C

Compound 198. 2-phenyl-N-(3-phenylpropyl)acetamide



Synthesised according to General Experimental Procedure S (Table 34, Entry 23, Page 128) using methyl 2-phenylacetate (200 μL , 1.42 mmol, 1 equiv) and 3-phenylpropan-1-amine (202 μL , 1.42 mmol, 1 equiv), and purified by flash column chromatography (2% methanol/DCM) to afford the title compound as a white solid (252 mg, 70%).

ν_{max} (neat): 3356, 3092, 2932, 2837, 1632, 1560, 1452 cm^{-1}

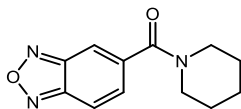
^1H NMR (400 MHz, DMSO): δ 8.05 (t, 1H, NH, $J = 5.0$ Hz), 7.31 – 7.19 (m, 7H, 7 x ArH), 7.18 – 7.14 (m, 3H, 3 x ArH), 3.40 (s, 2H, CH₂), 3.05 (q, 2H, CH₂, $J = 6.5$ Hz), 2.54 (t, 2H, CH₂, $J = 7.8$ Hz), 1.68 (quintet, 2H, CH₂, $J = 7.4$ Hz)

^{13}C NMR (101 MHz, DMSO): δ 170.0, 141.7, 136.6, 128.9, 128.3, 128.2, 126.3, 125.7, 42.5, 38.2, 32.5, 30.9, 1C missing (overlapping peaks)

HRMS (C₁₇H₂₀NO) [M+H] requires 254.1539, found [M+H] 254.1539

m.p. 84 – 85 °C

Compound 199. *tert*-butyl 4-((2-phenylacetamido)methyl)piperidine-1-carboxylate



Synthesised according to General Experimental Procedure S (Table 34, Entry 24, Page 128) using methyl benzo[*c*][1,2,5]oxadiazole-5-carboxylate (253 mg, 1.42 mmol, 1 equiv) and piperidine (140 μ L, 1.42 mmol, 1 equiv), and purified by flash column chromatography (1% methanol/DCM) to afford the title compound as an orange solid (196 mg, 60%).

ν_{max} (neat): 3103, 3073, 3047, 2921, 2857, 1629, 1619, 1446, 1258 cm^{-1}

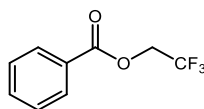
^1H NMR (400 MHz, CDCl_3): δ 7.91 (dd, 1H, ArH, $J = 9.0, 1.0$ Hz), 7.85 (app. t, 1H, ArH, $J = 1.0$ Hz), 7.44 (dd, 1H, ArH, $J = 9.2, 1.2$ Hz), 3.75 (s, 2H, CH_2), 3.40 (s, 2H, CH_2), 1.73 (s, 4H, 2 x CH_2), 1.60 (s, 2H, CH_2)

^{13}C NMR (101 MHz, CDCl_3): δ 167.6, 148.9, 148.8, 139.7, 131.0, 117.5, 114.6, 48.9, 43.5, 26.8, 25.7, 24.6

HRMS ($\text{C}_{12}\text{H}_{14}\text{N}_3\text{O}_2$) [$\text{M}+\text{H}$] requires 232.1081, found [$\text{M}+\text{H}$] 232.1080

m.p. 94 – 95 $^\circ\text{C}$

Compound 200. 2,2,2-trifluoroethyl benzoate



To a round-bottomed flask containing 2,2,2-trifluoroethanol (0.7 mL, 10 mmol, 1 equiv) and triethylamine (1.7 mL, 12 mmol, 1.2 equiv) was added benzoyl chloride (1.7 mL, 15 mmol, 1.5 equiv). The reaction mixture was stirred at 60 $^\circ\text{C}$ for 15 h then concentrated under vacuum. The residue was diluted with EtOAc (20 mL), washed with NaHCO_3 (20 mL) and brine (20 mL), dried over Na_2SO_4 , and concentrated to a residue that was purified by flash column chromatography (10% ethyl acetate/pet. ether 40–60 $^\circ$) to afford the title compound as a colourless liquid (2.00 g, 98%).

Experimental - Characterisation Data for Isolated Products

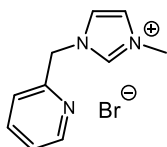
ν_{\max} (neat): 3061, 3028, 2924, 2874, 1736, 1254, 1163 cm^{-1}

^1H NMR (400 MHz, CDCl_3): δ 8.11 – 8.09 (m, 2H, 2 x ArH), 7.63 (tt, 1H, ArH, $J = 7.4, 1.5$ Hz), 7.51 – 7.47 (m, 2H, 2 x ArH), 4.72 (q, 2H, CH_2 , $J = 8.4$ Hz)

^{13}C NMR (101 MHz, CDCl_3): δ 165.2, 134.1, 130.2, 128.8, 128.6, 123.4 (q, $^1J_{\text{CF}} = 278.3$ Hz), 61.0 (q, $^2J_{\text{CF}} = 36.9$ Hz)

Consistent with previously reported data¹⁶²

Compound 209. 1-methyl-3-(pyridin-2-ylmethyl)-1*H*-imidazol-3-ium bromide



Bromomethylpyridine hydrobromide (5 g, 19.8 mmol, 1.2 equiv) was neutralised by dropwise addition of sat. NaHCO_3 , extracted with Et_2O , dried over MgSO_4 , and added to a solution of methylimidazole (1.3 mL, 1.65 mmol, 1 equiv) in 1,4-dioxane (50 mL). Et_2O was removed under vacuum and the reaction mixture was heated at 120 $^\circ\text{C}$ for 16 h then concentrated under vacuum to afford the title compound as a brown oil (3.4 g, 81%).

ν_{\max} (neat): 3401, 3366, 3293, 3051, 1628, 1595, 1572, 1437, 1169 cm^{-1}

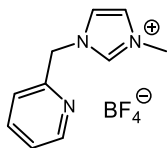
^1H NMR (400 MHz, DMSO): δ 9.22 (s, 1H, ArH), 8.56 – 8.54 (m, 1H, ArH), 7.88 (td, 1H, ArH, $J = 7.6, 1.9$ Hz), 7.75 (app. t, 1H, ArH, $J = 1.8$ Hz), 7.69 (app. t, 1H, ArH, $J = 1.6$ Hz), 7.48 (d, 1H, ArH, $J = 8.0$ Hz), 7.39 (dd, 1H, ArH, $J = 4.8, 0.9$ Hz), 5.55 (s, 2H, CH_2), 3.89 (s, 3H, CH_3)

^{13}C NMR (126 MHz, DMSO): 153.6, 149.6, 137.6, 137.3, 123.7, 123.1, 122.6, 52.9, 35.9, 1C missing (overlapping peaks)

HRMS ($\text{C}_{10}\text{H}_{12}\text{N}_3$) [M^+] requires 174.1026, found [M^+] 174.1022

Consistent with previously reported data⁹⁷

Compound 210. 1-methyl-3-(pyridin-2-ylmethyl)-1*H*-imidazol-3-ium tetrafluoroborate



To a round bottomed flask containing 1-methyl-3-(pyridin-2-ylmethyl)-1*H*-imidazol-3-ium bromide (**209**, 1 g, 3.9 mmol, 1 equiv) in DCM (10 mL) was added silver tetrafluoroborate (760 mg, 3.9 mmol, 1 equiv). The reaction mixture was stirred at rt for 16 h then filtered. The filtrate was concentrated under vacuum to afford the title compound as a sandy solid (265 mg, 26%).

ν_{\max} (neat): 3165, 3125, 3113, 1634, 1593, 1566, 1441 cm^{-1}

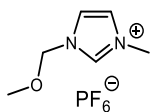
^1H NMR (400 MHz, $\text{DMSO-}d_6$): δ 9.21 (s, 1H, ArH), 8.56 – 8.54 (m, 1H, ArH), 7.89 (td, 1H, ArH, $J = 7.8, 1.9$ Hz), 7.76 (app. t, 1H, ArH, $J = 1.8$ Hz), 7.71 (app. t, 1H, ArH, $J = 1.8$ Hz), 7.48 (d, 1H, ArH, $J = 7.6$ Hz), 7.42 – 7.39 (m, 1H, ArH), 5.56 (s, 2H, CH_2), 3.88 (s, 3H, CH_3)

^{13}C NMR (101 MHz, DMSO): δ 153.6, 149.6, 137.5, 137.3, 123.7, 123.6, 123.1, 122.5, 53.0, 35.8

HRMS ($\text{C}_{10}\text{H}_{12}\text{N}_3$) [M^+] requires 174.1026, found [M^+] 174.1024

m.p. 184 – 186 $^\circ\text{C}$

Compound 212. 3-(methoxymethyl)-1-methyl-1*H*-imidazol-3-ium hexafluorophosphate



To a round bottomed flask containing chloromethyl methyl ether (1.4 mL, 18 mmol, 1.5 equiv), *N,N*-dimethylaniline (2.3 mL, 18 mmol, 1.5 equiv) and DCM (20 mL) at 0 °C was added 1-methylimidazole (0.97 mL, 12 mmol, 1 equiv) dropwise. The reaction mixture was stirred at rt for 16 h then concentrated under vacuum. The crude reaction mixture was purified by SCX, concentrated under vacuum then redissolved in water (20 mL). A solution of ammonium hexafluorophosphate (3 g, 18 mmol, 1.5 equiv) was added and the reaction mixture was stirred at rt for 16 h. The reaction mixture was diluted with water, extracted with DCM, dried over MgSO₄, filtered, and concentrated under vacuum to afford the title compound as a white solid (777 mg, 23%).

ν_{\max} (neat): 3318, 3161, 1651, 1416 cm⁻¹

¹H NMR (400 MHz, CDCl₃): δ 10.57 (s, 1H, ArH), 7.70 (app. t, 1H, ArH, $J = 1.6$ Hz), 7.63 (app. t, 1H, ArH, $J = 1.8$ Hz), 5.71 (s, 2H, CH₂), 4.09 (s, 3H, CH₃), 3.40 (s, 3H, CH₃)

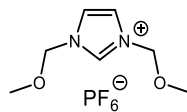
¹³C NMR (101 MHz, CDCl₃): δ 138.3, 124.2, 121.6, 80.2, 57.8, 36.9

HRMS (C₆H₁₁N₂O) [M⁺] requires 127.0866, found [M⁺] 127.0863

m.p. 171 – 174 °C

Consistent with previously reported data¹⁶³

Compound 214. 1,3-bis(methoxymethyl)-1*H*-imidazol-3-ium hexafluorophosphate



To a round bottomed flask containing chloromethyl methyl ether (2.8 mL, 37 mmol, 2.5 equiv), *N,N*-dimethylaniline (4.7 mL, 37 mmol, 2.5 equiv) and DCM (20 mL) at 0 °C was added imidazole (1 g, 15 mmol, 1 equiv). The reaction mixture was stirred at rt for 16 h then concentrated under vacuum. The crude reaction mixture was purified by SCX, concentrated under vacuum then redissolved in water (20 mL). A solution of ammonium hexafluorophosphate (3.6 g, 22 mmol, 1.5 equiv) was added and the reaction mixture was stirred at rt for 30 min. The resulting precipitate was collected by filtration, washed with water, and dried under vacuum to afford the title compound as a white solid (1.5 g, 34%).

ν_{\max} (neat): 3159, 3121, 3100, 1614, 1557, 1107 cm^{-1}

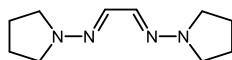
^1H NMR (400 MHz, DMSO): δ 9.54 (t, 1H, ArH, $J = 1.4$ Hz), 7.94 (d, 2H, ArH, $J = 1.6$ Hz), 5.56 (s, 4H, 2 x CH_2), 3.35 (s, 6H, 2 x CH_3)

^{13}C NMR (101 MHz, MeOD): δ 136.1, 123.7, 121.8, 82.0, 58.1

HRMS ($\text{C}_7\text{H}_{13}\text{N}_2\text{O}_2$) [M^+] requires 157.0972, found [M^+] 157.0969

m.p. 118 – 120 °C

Compound 219. (*N,N'E,N,N'E*)-*N,N'*-(ethane-1,2-diylidene)bis(pyrrolidin-1-amine)



To a round-bottomed flask containing pyrrolidin-1-amine hydrochloride (500 mg, 4.08 mmol, 2.2 equiv), glyoxal solution (40 wt.% in water, 213 μL , 1.85 mmol, 1 equiv) and MeOH (10 mL) was added Et_3N (566 μL , 4.08 mmol, 2.2 equiv). The reaction mixture was stirred at room temperature for 16 h. The reaction mixture was quenched with NaHCO_3 , extracted with EtOAc, dried over MgSO_4 , filtered, and concentrated to afford the title compound as a yellow solid (282 mg, 87%).

ν_{max} (neat): 2968, 2875, 2824, 1538, 1456, 1337 cm^{-1}

^1H NMR (400 MHz, CDCl_3): δ 7.05 (s, 2H, 2 x CH), 3.25 (t, 8H, 4 x CH_2 , $J = 6.7$ Hz), 1.82 – 2.02 (m, 8H, 4 x CH_2)

^{13}C NMR (101 MHz, CDCl_3): δ 134.7, 51.2, 23.6

HRMS ($\text{C}_{10}\text{H}_{18}\text{N}_4$) [$\text{M}+\text{H}^+$] requires 195.1604, found [$\text{M}+\text{H}^+$] 195.1603

m.p. 131 – 132 $^\circ\text{C}$

Consistent with previously reported data¹⁶⁴

7 References

- 1 A. K. Ghose, V. N. Viswanadhan and J. J. Wendoloski, *J. Comb. Chem.*, 1999, **1**, 55–68.
- 2 G. L. Patrick, *An Introduction to Medicinal Chemistry*, Oxford University Press, Oxford, UK, 4th edn., 2009.
- 3 S. D. Roughley and A. M. Jordan, *J. Med. Chem.*, 2011, **54**, 3451–3479.
- 4 T. W. J. Cooper, I. B. Campbell and S. J. F. MacDonald, *Angew. Chem. Int. Ed.*, 2010, **49**, 8082–8091.
- 5 C. A. G. N. Montalbetti and V. Falque, *Tetrahedron*, 2005, **61**, 10827–10852.
- 6 H. H. Bosshard, R. Mory, M. Schmid and H. Zollinger, *Helv. Chim. Acta.*, 1959, **42**, 1653–1658.
- 7 H. L. Rayle and L. Fellmeth, *Org. Proc. Res. Dev.*, 1999, **3**, 172–176.
- 8 J. B. Lee, *J. Am. Chem. Soc.*, 1966, **88**, 3440–3441.
- 9 D. C. Lenstra, F. P. J. T. Rutjes and J. Mecinović, *Chem. Commun.*, 2014, **50**, 5763–5766.
- 10 J. P. Adams, C. M. Alder, I. Andrews, A. M. Bullion, M. Campbell-Crawford, M. G. Darcy, J. D. Hayler, R. K. Henderson, C. A. Oare, I. Pendrak, A. M. Redman, L. E. Shuster, H. F. Sneddon and M. D. Walker, *Green Chem.*, 2013, **15**, 1542–1549.
- 11 A. El-Faham and F. Albericio, *Chem. Rev.*, 2011, **111**, 6557–6602.
- 12 J. C. Sheehan and G. P. Hess, *J. Am. Chem. Soc.*, 1955, **77**, 1067–1068.
- 13 L. A. Carpino, *J. Am. Chem. Soc.*, 1993, **115**, 4397–4398.
- 14 W. König and R. Geiger, *Chem. Ber.*, 1970, **103**, 788–798.
- 15 K. D. Wehrstedt, P. A. Wandrey and D. Heitkamp, *J. Hazard. Mat.*, 2005, **126**, 8082–8091.
- 16 R. Subirós-Funosas, R. Prohens, R. Barbas, A. El-Faham and F. Albericio, *Chem. Eur. J.*, 2009, **15**, 9394–9403.
- 17 E. Valeur and M. Bradley, *Chem. Soc. Rev.*, 2009, **38**, 606–631.
- 18 B. M. Trost, *Science*, 1991, **254**, 1471–1477.
- 19 L. A. Carpino, H. Imazumi, A. El-Faham, F. J. Ferrer, C. Zhang, Y. Lee, B. M. Foxman, P. Henklein, C. Hanay, C. Mügge, H. Wenschuh, J. Klose, M. Beyermann and M. Bienert, *Angew. Chem. Int. Ed.*, 2002, **41**, 441–445.
- 20 A. El-Faham, R. Subirós Funosas, R. Prohens and F. Albericio, *Chem. Eur. J.*, 2009, **15**, 9404–9416.

References

- 21 A. El-Faham and F. Albericio, *Org. Lett.*, 2007, **9**, 4475–4477.
- 22 G. Gawne, G. W. Kenner and R. C. Sheppard, *J. Am. Chem. Soc.*, 1969, **91**, 5669–5671.
- 23 J. Coste, D. Le-Nguyen and B. Castro, *Tetrahedron Lett.*, 1990, **31**, 205–208.
- 24 J. Coste, E. Frerot and P. Jouin, *J. Org. Chem.*, 1994, **59**, 2437–2446.
- 25 D. J. C. Constable, P. J. Dunn, J. D. Hayler, G. R. Humphrey, J. L. Leazer, Jr., R. J. Linderman, K. Lorenz, J. Manley, B. A. Pearlman, A. Wells, A. Zaks and T. Y. Zhang, *Green Chem.*, 2007, **9**, 411–420.
- 26 V. R. Pattabiraman and J. W. Bode, *Nature*, 2011, **480**, 471–479.
- 27 R. M. Lanigan and T. D. Sheppard, *Eur. J. Org. Chem.*, 2013, 7453–7465.
- 28 K. Ishihara, S. Ohara and H. Yamamoto, *J. Org. Chem.*, 1996, **61**, 4196–4197.
- 29 C. Wang, H.-Z. Yu, Y. Fu and Q.-X. Guo, *Org. Biomol. Chem.*, 2013, **11**, 2140–2146.
- 30 T. Marcelli, *Angew. Chem. Int. Ed.*, 2010, **49**, 6840–6843.
- 31 R. M. Al-Zoubi, O. Marion and D. G. Hall, *Angew. Chem. Int. Ed.*, 2008, **47**, 2876–2879.
- 32 A. J. J. Lennox and G. C. Lloyd-Jones, *Chem. Soc. Rev.*, 2014, **43**, 412–443.
- 33 N. Gernigon, R. M. Al-Zoubi and D. G. Hall, *J. Org. Chem.*, 2012, **77**, 8386–8400.
- 34 T. Maki, K. Ishihara and H. Yamamoto, *Tetrahedron*, 2007, **63**, 8645–8657.
- 35 R. Latta, G. Springsteen and B. Wang, *Synthesis*, 2001, 1611–1613.
- 36 K. Arnold, A. S. Batsanov, B. Davies and A. Whiting, *Green Chem.*, 2008, **10**, 124–134.
- 37 P. Starkov and T. D. Sheppard, *Org. Biomol. Chem.*, 2011, **9**, 1320–1323.
- 38 R. M. Lanigan, P. Starkov and T. D. Sheppard, *J. Org. Chem.*, 2013, **78**, 4512–4523.
- 39 B. S. Jursic and Z. Zdravkovski, *Synth. Commun.*, 1993, **23**, 2761–2770.
- 40 C. L. Allen, A. R. Chhatwal and J. M. J. Williams, *Chem. Commun.*, 2012, **48**, 666–668.
- 41 J. D. Wilson and H. Weingarten, *Can. J. Chemistry*, 1970, **48**, 983–986.
- 42 H. Lundberg, F. Tinnis and H. Adolfsson, *Chem. Eur. J.*, 2012, **18**, 3822–3826.
- 43 H. Lundberg, F. Tinnis and H. Adolfsson, *Synlett*, 2012, **23**, 2201–2204.
- 44 C. L. Allen and J. M. J. Williams, *Chem. Soc. Rev.*, 2011, **40**, 3405–3415.
- 45 A. Basha, M. Lipton and S. M. Weinreb, *Tetrahedron Lett.*, 1977, **48**, 4171–4174.

References

- 46 A. Novak, L. D. Humphreys, M. D. Walker and S. Woodward, *Tetrahedron Lett.*, 2006, **47**, 5767–5769.
- 47 C. Han, J. P. Lee, E. Lobkovsky and J. A. Porco, *J. Am. Chem. Soc.*, 2005, **127**, 10039–10044.
- 48 H. Morimoto, R. Fujiwara, Y. Shimizu, K. Morisaki and T. Ohshima, *Org. Lett.*, 2014, **16**, 2018–2021.
- 49 B. C. McLellan, G. D. Corder and S. H. Ali, *Minerals*, 2013, **3**, 304–317.
- 50 C. Gunanathan, Y. Ben-David and D. Milstein, *Science*, 2007, **317**, 790–792.
- 51 J. Zhang, G. Leitus, Y. Ben-David and D. Milstein, *J. Am. Chem. Soc.*, 2005, **127**, 10840–10841.
- 52 N. D. Schley, G. E. Dobereiner and R. H. Crabtree, *Organometallics*, 2011, **30**, 4174–4179.
- 53 E. Sindhuja, R. Ramesh, S. Balaji and Y. Liu, *Organometallics*, 2014, **33**, 4269–4278.
- 54 Y. Zhang, C. Chen, S. C. Ghosh, Y. Li and S. H. Hong, *Organometallics*, 2010, **29**, 1374–1378.
- 55 C. Chen, Y. Zhang and S. H. Hong, *J. Org. Chem.*, 2011, **76**, 10005–10010.
- 56 A. J. A. Watson, A. C. Maxwell and J. M. J. Williams, *Org. Lett.*, 2009, **11**, 2667–2670.
- 57 K. Shimizu, K. Ohshima and A. Satsuma, *Chem. Eur. J.*, 2009, **15**, 9977–9980.
- 58 European Medicines Agency,
www.ema.europa.eu/ema/pages/includes/document/open_document.jsp?webContentId=WC500003586, Date Accessed: February 2015.
- 59 D. W. C. MacMillan, *Nature*, 2008, **455**, 304–308.
- 60 A. Erkkila, I. Majander and P. M. Pihko, *Chem. Rev.*, 2007, **107**, 5416–5470.
- 61 S. Mukherjee, J. W. Yang, S. Hoffmann and B. List, *Chem. Rev.*, 2007, **107**, 5471–5569.
- 62 A. G. Doyle and E. N. Jacobsen, *Chem. Rev.*, 2007, **107**, 5713–5743.
- 63 D. Enders, O. Niemeier and A. Henseler, *Chem. Rev.*, 2007, **107**, 5606–5655.
- 64 N. Marion, S. Díez-González and S. P. Nolan, *Angew. Chem. Int. Ed.*, 2007, **46**, 2988–3000.
- 65 L. Benhamou, E. Chardon, G. Lavigne, S. Bellemin-Laponnaz and V. César, *Chem. Rev.*, 2011, **111**, 2705–2733.
- 66 G. W. Nyce, J. A. Lamboy, E. F. Connor, R. M. Waymouth and J. L. Hedrick, *Org. Lett.*, 2002, **4**, 3587–3590.

References

- 67 G. A. Grasa, R. M. Kissling and S. P. Nolan, *Org. Lett.*, 2002, **4**, 3583–3586.
- 68 G. A. Grasa, T. Guveli, R. Singh and S. P. Nolan, *J. Org. Chem.*, 2003, **68**, 2812–2819.
- 69 R. Singh, R. M. Kissling, M.-A. Letellier and S. P. Nolan, *J. Org. Chem.*, 2004, **69**, 209–212.
- 70 Y. Suzuki, K. Muramatsu, K. Yamauchi, Y. Morie and M. Sato, *Tetrahedron*, 2006, **62**, 302–310.
- 71 R. C. Samanta, S. De Sarkar, R. Fröhlich, S. Grimme and A. Studer, *Chem. Sci.*, 2013, **4**, 2177–2184.
- 72 A. J. Arduengo, R. Krafczyk and R. Schmutzler, *Tetrahedron*, 1999, **55**, 14523–14534.
- 73 S. De Sarkar, S. Grimme and A. Studer, *J. Am. Chem. Soc.*, 2010, **132**, 1190–1191.
- 74 M. Movassaghi and M. A. Schmidt, *Org. Lett.*, 2005, **7**, 2453–2456.
- 75 M. A. Schmidt, P. Müller and M. Movassaghi, *Tetrahedron Lett.*, 2008, **49**, 4316–4318.
- 76 S. De Sarkar and A. Studer, *Org. Lett.*, 2010, **12**, 1992–1995.
- 77 R. Breslow, *J. Am. Chem. Soc.*, 1958, **80**, 3719–3726.
- 78 H. U. Vora and T. Rovis, *J. Am. Chem. Soc.*, 2007, **129**, 13796–13797.
- 79 P.-C. Chiang, Y. Kim and J. W. Bode, *Chem. Commun.*, 2009, 4566–4568.
- 80 X. Yang and V. B. Birman, *Org. Lett.*, 2009, **11**, 1499–1502.
- 81 C. Sabot, K. A. Kumar, S. Meunier and C. Mioskowski, *Tetrahedron Lett.*, 2007, **48**, 3863–3866.
- 82 M. K. Kiesewetter, M. D. Scholten, N. Kirn, R. L. Weber, J. L. Hedrick and R. M. Waymouth, *J. Org. Chem.*, 2009, **74**, 9490–9496.
- 83 F. J. Weiberth, Y. Yu, W. Subotkowski and C. Pemberton, *Org. Proc. Res. Dev.*, 2012, **16**, 1967–1969.
- 84 R. B. Merrifield, *J. Am. Chem. Soc.*, 1963, **85**, 2149–2154.
- 85 R. B. Merrifield, *Science*, 1965, **150**, 178–185.
- 86 W. C. Chan and P. D. White, *Fmoc Solid Phase Peptide Synthesis*, Oxford University Press, Oxford, UK, 1st edn., 2000.
- 87 P. E. Dawson, T. W. Muir, I. Clark-Lewis and S. B. Kent, *Science*, 1994, **266**, 776–779.
- 88 E. C. B. Johnson and S. B. H. Kent, *J. Am. Chem. Soc.*, 2006, **128**, 6640–6646.
- 89 L. Z. Yan and P. E. Dawson, *J. Am. Chem. Soc.*, 2001, **123**, 526–533.

References

- 90 Q. Wan and S. J. Danishefsky, *Angew. Chem. Int. Ed.*, 2007, **46**, 9248–9252.
- 91 R. E. Thompson, X. Liu, N. Alonso-Garcia, P. J. B. Pereira, K. A. Jolliffe and R. J. Payne, *J. Am. Chem. Soc.*, 2014, **136**, 8161–8164.
- 92 X. Li, H. Y. Lam, Y. Zhang and C. K. Chan, *Org. Lett.*, 2010, **12**, 1724–1727.
- 93 B. L. Nilsson, L. L. Kiessling and R. T. Raines, *Org. Lett.*, 2000, **2**, 1939–1941.
- 94 E. Saxon, J. I. Armstrong and C. R. Bertozzi, *Org. Lett.*, 2000, **2**, 2141–2143.
- 95 S. P. Andrews and M. Ladlow, *J. Org. Chem.*, 2003, **68**, 5525–5533.
- 96 Sigma-Aldrich, <http://www.sigmaaldrich.com/united-kingdom>.
- 97 L. N. Appelhans, D. Zuccaccia, A. Kovacevic, A. R. Chianese, J. R. Miecznikowski, A. Macchioni, E. Clot, O. Eisenstein and R. H. Crabtree, *J. Am. Chem. Soc.*, 2005, **127**, 16299–16311.
- 98 H. K. Hall Jr, *J. Am. Chem. Soc.*, 1957, **79**, 5441–5444.
- 99 D. H. Ripin and D. A. Evans, http://evans.harvard.edu/pdf/evans_pka_table.pdf.
- 100 N. Caldwell, C. Jamieson, I. Simpson and T. Tuttle, *Org. Lett.*, 2013, **15**, 2506–2509.
- 101 R. Schwesinger and H. Schlemper, *Angew. Chem. Int. Ed.*, 1987, **26**, 1167–1169.
- 102 R. Carlson, *Design and Optimisation in Organic Synthesis*, Elsevier, Amsterdam, 2nd edn., 1992.
- 103 R. Carlson and J. E. Carlson, *Org. Proc. Res. Dev.*, 2005, **9**, 680–689.
- 104 P. M. Murray, S. N. G. Tyler and J. D. Moseley, *Org. Proc. Res. Dev.*, 2013, **17**, 40–46.
- 105 R. Carlson, T. Lundstedt and C. Albano, *Acta. Chem. Scand.*, 1985, **39B**, 79–91.
- 106 W. L. F. Armarego and C. L. L. Chai, *Purification of Laboratory Chemicals*, Elsevier Inc., Oxford, UK, 6th edn., 2009.
- 107 Stat-Ease Inc, *Design Expert Version 8*, 2010.
- 108 N. Caldwell, P. S. Campbell, C. Jamieson, F. Potjewyd, I. Simpson and A. J. B. Watson, *J. Org. Chem.*, 2014, **79**, 9347–9354.
- 109 P. S. Campbell, *Final Year Thesis, University of Strathclyde*, 2014.
- 110 R. M. Beesley, C. K. Ingold and J. F. Thorpe, *J. Chem. Soc. Trans.*, 1915, **107**.
- 111 P. Garg and M. D. Milton, *Tetrahedron Lett.*, 2013, **54**, 7074–7077.
- 112 D. A. Evans, G. Helmchen and M. Ruping, in *Asymmetric Synthesis*, 2007, pp. 3–9.

References

- 113 D. A. Evans, J. Bartoli and T. L. Shih, *J. Am. Chem. Soc.*, 1981, **103**, 2127–2129.
- 114 D. A. Evans, M. D. Ennis and D. J. Mathre, *J. Am. Chem. Soc.*, 1982, **104**, 1737–1739.
- 115 D. A. Evans, K. T. Chapman, D. T. Hung and A. T. Kawaguchi, *Angew. Chem. Int. Ed.*, 1987, **26**, 1184–1186.
- 116 R. Bursi, G. Erdemli, R. Campbell, M. M. Hutmacher, T. Kerbusch, D. Spanswick, R. Jeggo, K. R. Nations, P. Dogterom, J. Schipper and M. Shahid, *Psychopharmacology*, 2011, **218**, 713–724.
- 117 S. J. A. Grove, C. Jamieson, J. K. F. Maclean, J. A. Morrow and Z. Rankovic, *J. Med. Chem.*, 2010, **53**, 7271–7279.
- 118 A. G. Schultz, L. Flood and J. P. Springer, *J. Org. Chem.*, 1986, **51**, 838–841.
- 119 N. Caldwell, J. E. Harms, K. M. Partin and C. Jamieson, *ACS Med. Chem. Lett.*, 2015, **6**, 392–396.
- 120 O. Oldenburg, A. Kribben, D. Baumgart, T. Philipp, R. Erbel and M. V. Cohen, *Curr. Opin. Pharmacol.*, 2002, **2**, 740–747.
- 121 A. A. Armstrong and L. M. Amzel, *J. Am. Chem. Soc.*, 2003, **125**, 14596–14602.
- 122 E. V. Anslyn and D. A. Dougherty, *Modern Physical Organic Chemistry*, University Science, Sausalito, CA, 2006.
- 123 ACD/Labs, *www.acdlabs.com*, Date Accessed: March 2013.
- 124 R. K. Henderson, C. Jiménez-González, D. J. C. Constable, S. R. Alston, G. G. A. Inglis, G. Fisher, J. Sherwood, S. P. Binks and A. D. Curzons, *Green Chem.*, 2011, **13**, 854–862.
- 125 R. K. Henderson, A. P. Hill, A. M. Redman and H. F. Sneddon, *Green Chem.*, 2015, **17**, 945–949.
- 126 K. Alfonsi, J. Colberg, P. J. Dunn, T. Fevig, S. Jennings, T. A. Johnson, H. P. Kleine, C. Knight, M. A. Nagy, D. A. Perry and M. Stefaniak, *Green Chem.*, 2008, **10**, 31–36.
- 127 P. T. Anastas and J. C. Warner, *Green Chemistry: Theory and Practice*, Oxford University Press, New York, 1998.
- 128 N. Caldwell, C. Jamieson, I. Simpson and A. J. B. Watson, *ACS Sustainable Chem. Eng.*, 2013, **1**, 1339–1344.
- 129 A. Takagaki, K. Iwatani, S. Nishimura and K. Ebitani, *Green Chem.*, 2010, **12**, 578–581.
- 130 T. Jin, S. Zhang and T. Li, *Green Chem.*, 2002, **4**, 32–34.
- 131 V. Antonucci, J. Coleman, J. B. Ferry, N. Johnson, M. Mathe and J. P. Scott, *Org. Proc. Res. Dev.*, 2011, **15**, 939–941.
- 132 K. Watanabe, N. Yamagiwa and Y. Torisawa, *Org. Proc. Res. Dev.*, 2007, **11**, 251–258.

References

- 133 M. Winterberg, E. Schulte-Korne, U. Peters and F. Nierlich, *Ullmann's Encyclopedia of Industrial Chemistry*, Wiley-VCH, Hoboken, NJ, 2010.
- 134 A. D. Curzons, D. J. C. Constable, D. N. Mortimer and V. L. Cunningham, *Green Chem.*, 2001, **3**, 1–6.
- 135 N. Caldwell, C. Jamieson, I. Simpson and A. J. B. Watson, *Chem. Commun.*, 2015, **51**, 9495–9498.
- 136 L. Jiang, A. Davison, G. Tennant and R. Ramage, *Tetrahedron*, 1998, **54**, 14233–14254.
- 137 E. Wezenberg, R. J. Verkes, G. S. F. Ruigt, W. Hulstijn and B. G. C. Sabbe, *Neuropsychopharmacol.*, 2007, **32**, 1272–1283.
- 138 T. Ohshima, Y. Hayashi, K. Agura, Y. Fujii, A. Yoshiyama and K. Mashima, *Chem. Commun.*, 2012, **48**, 5434–5436.
- 139 M. J. Frisch, G. W. Trucks, H. B. Schlegel, G. E. Scuseria, M. A. Robb, J. R. Cheeseman, G. Scalmani, V. Barone, B. Mennucci, G. A. Petersson, H. Nakatsuji, M. Caricato, X. Li, H. P. Hratchian, A. F. Izmaylov, J. Bloino, G. Zheng, J. L. Sonnenberg, M. Hada, M. Ehara, K. Toyota, R. Fukuda, J. Hasegawa, M. Ishida, T. Nakajima, Y. Honda, O. Kitao, H. Nakai, T. Vreven, J. A. Montgomery, J. E. Peralta, F. Ogliaro, M. Bearpark, J. J. Heyd, E. Brothers, K. N. Kudin, V. N. Staroverov, R. Kobayashi, J. Normand, K. Raghavachari, A. Rendell, J. C. Burant, S. S. Iyengar, J. Tomasi, M. Cossi, N. Rega, J. M. Millan, M. Klene, J. E. Knox, J. B. Cross, V. Bakken, C. Adamo, J. Jaramillo, R. Gomperts, R. E. Stratmann, O. Yazyev, A. J. Austin, R. Cammi, C. Pomelli, J. W. Ochterski, R. L. Martin, K. Morokuma, V. G. Zakrzewski, G. A. Voth, P. Salvador, J. J. Dannenberg, S. Dapprich, A. D. Daniels, O. Farkas, J. B. Foresman, J. V. Ortiz, J. Cioslowski and D. J. Fox, *Gaussian 09, Revision A.02*, Gaussian Inc., Wallingford, CT, 2009.
- 140 D. E. Ward and S. G. Pardeshi, *J. Org. Chem.*, 2010, **75**, 5170–5177.
- 141 V. Gierz, C. Maichle-Mossmer and D. Kunz, *Organometallics*, 2012, **31**, 739–747.
- 142 R. H. Wiley, *J. Macromol. Chem.*, 1987, **24**, 1183–1190.
- 143 R. S. Varma and K. P. Naicker, *Tetrahedron Lett.*, 1999, **40**, 6177–6180.
- 144 B. R. Kim, H.-G. Lee, S.-B. Kang, G. H. Sung, J.-J. Kim, J. K. Park, S.-G. Lee and Y.-J. Yoon, *Synthesis*, 2012, **44**, 42–50.
- 145 M. Pech and K. H. Nierhaus, *Chem. Biol.*, 2008, **15**, 485–492.
- 146 PureSolv MD 5, <http://www.solventpurification.co.uk/md/>.
- 147 A. Winkel and R. Wilhelm, *Tetrahedron Asymm.*, 2009, **20**, 2344–2350.
- 148 I. Kuriyama, N. Asano, I. Kato, K. Ikeda, M. Takemura, H. Yoshida, K. Sakaguchi and Y. Mizushina, *Bioorg. Med. Chem.*, 2005, **13**, 2187–2196.
- 149 Y. Kita, Y. Nishii, T. Higuchi and K. Mashima, *Angew. Chem. Int. Ed.*, 2012, **51**, 5723–5726.

References

- 150 Y. Imada, Y. Mitsue, K. Ike, K. Washizuka and S.-I. Murahashi, *Bull. Chem. Soc. Jpn.*, 1996, **69**, 2079–2090.
- 151 T. J. Donohoe, M. J. Chughtai, D. J. Klauber, D. Griffin and A. D. Campbell, *J. Am. Chem. Soc.*, 2006, **128**, 2514–2515.
- 152 A. K. Ray, H. Patel and M. R. Patel, *United States Patent US6201153B1*, 2001.
- 153 M. Nechab, D. N. Kumar, C. Philouze, C. Einhorn and J. Einhorn, *Angew. Chem. Int. Ed.*, 2007, **46**, 3080–3083.
- 154 A. D. Kosal, E. E. Wilson and B. L. Ashfeld, *Angew. Chem. Int. Ed.*, 2012, **51**, 12036–12040.
- 155 M. K. Gupta, Z. Li and T. S. Snowden, *Org. Lett.*, 2014, **16**, 1602–1605.
- 156 T. Ueda, H. Konishi and K. Manabe, *Org. Lett.*, 2013, **15**, 5370–5373.
- 157 B. N. Atkinson, A. R. Chhatwal, H. V. Lomax, J. W. Walton and J. M. J. Williams, *Chem. Commun.*, 2012, **48**, 11626–11628.
- 158 U. Ragnarsson, L. Grehn, H. L. S. Maia and L. S. Monteiro, *J. Chem. Soc. Perkin Trans. 1*, 2002, 97–101.
- 159 B. Kang, Z. Fu and S. H. Hong, *J. Am. Chem. Soc.*, 2013, **135**, 11704–11707.
- 160 S. Zhou, K. Junge, D. Addis, S. Das and M. Beller, *Angew. Chem. Int. Ed.*, 2009, **48**, 9507–9510.
- 161 D. S. MacMillan, J. Murray, H. F. Sneddon, C. Jamieson and A. J. B. Watson, *Green Chem.*, 2013, **15**, 596–600.
- 162 S. Gowrisankar, H. Neumann and M. Beller, *Angew. Chem. Int. Ed.*, 2011, **50**, 5139–5143.
- 163 Q. Liu, M. H. A. Janssen, F. Van Rantwijk and R. A. Sheldon, *Green Chem.*, 2005, **7**, 39–42.
- 164 T. Mino, Y. Shirae, Y. Sasai, M. Sakamoto and T. Fujita, *J. Org. Chem.*, 2006, **71**, 6834–6839.